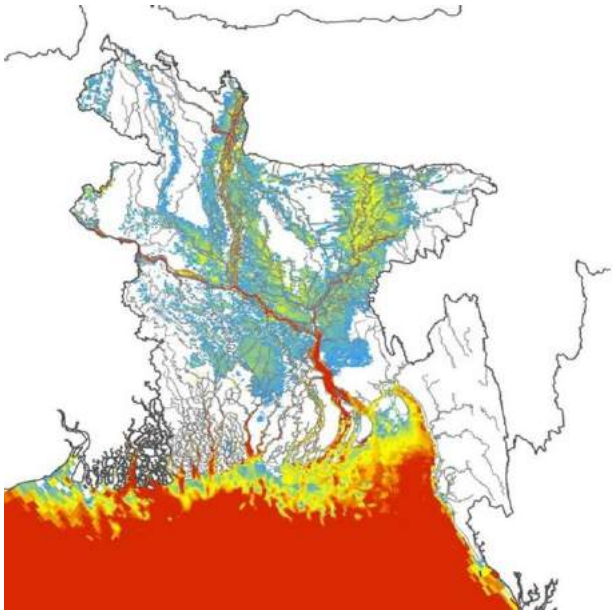

Research on Sediment Distribution and Management in South-West Region of Bangladesh

WARPO TEAM

Md. Aminul Haque
Md. Jahid Hossain
Md. Jamal Haider
Md. Anwar Hossain
Shuvro Bhowmick
Md. Sakib Mahdi Aziz

BUET TEAM

Anisul Haque
Quamrul Ahsan
Md. Munsur Rahman
Sadmina Razzaque
Anika Tahsin
Imran Hossain Newton
Delowar Hossain
Afroza Akther
Mohona Debnath

Draft Final Report

November 2021

Table of Contents

CHAPTER FOUR

Sediment Management Practices in the GBM Delta

List of Figures

List of Tables

EXECUTIVE SUMMARY

In this study we applied Bangladesh Delta Model (BDM) to study sediment transport process and sediment management options in GBM delta. BDM is developed within the Delft3D numerical model framework. Three components of BDM are applied in this study – flow, morphology, and storm surge. Flow model of BDM is calibrated by simulating time series of water level in 43 water level stations and comparing the results with the available measured data in 29 water level stations for the year 2017. Except in most of the tidal water level stations in the coast, statistical performance of the model in other water level stations shows that BDM is performing either 'very good' or 'good' or 'satisfactory'. Water level data in most of the tidal stations are 3-hourly manually measured data. These data do not represent tidal phase and amplitude correctly. This leads to 'unsatisfactory' model performance in these locations. Calibration of morphology model of BDM is made by comparing model simulated time series Suspended Sediment Concentration (SSC) with the measurement, and also by comparing the model simulated spatiotemporal distribution of suspended sediment concentration with the satellite image for the year 2017. Except a slight phase shift of peak values of SSC, time series comparison between the BDM and measurement shows smaller error bars for the rest of the season. Comparison of spatiotemporal distribution of SSC between the BDM and the satellite image along the major rivers and along the coast shows that BDM can reasonably simulate main physical features of SSC distribution, keeping in mind that satellite images represent only the surface SSC distribution while model simulations represent depth average SSC distribution. For flow model validation of BDM, comparison between model and measurement is made in 23 available measuring water level stations out of 40 simulating stations. Performance of BDM during flow model validation against water level is almost similar to the calibration performance of the model. Validation of flow model of BDM is also made by comparing model simulated areal extent of land inundation with similar data available from satellite image during 1998 flood. The result shows that BDM simulates 27.6% of land is inundated during 1998 flood against 29.1% land inundation value calculated from satellite image. For morphology model validation, BDM simulated sedimentation depths in 4 locations of Sundarban region during an average flood and extreme flood is compared with the measurement from secondary source which was conducted during March to October 2008. Considering the uncertainty of mismatch of time between the model and the measurement, BDM performance appears to be reasonable.

Past studies reveals that sediment transport processes in the GBM delta have not yet been studied as an integrated system. In this study we discuss the sediment transport processes in the GBM delta by applying BDM. This makes it possible to understand the process not as a piecemeal approach, but within an integrated systems where sediments are entered in riverine systems and after transporting, depositing, and eroding through rivers, estuaries, and floodplains eventually discharges to the ocean. During this journey, sediments encounter embankments and polders in different locations of its path. We considered impacts of these interventions in the transport processes of sediments. After the sediments discharge into the oceans, part of these sediments re-

enter into the estuarine systems. We also consider this process in BDM simulation. We use proxy parameters to study impact of cyclone in sediment transport process. For the first time, we tried to study impact of swatch of no ground in the transport processes.

The results show that tides arrive almost at the same time along the west and east coasts. Flood tide current slows down along the Lower Meghna estuary due to the impact of freshwater. Relatively higher current along the mouth of the estuaries of the western coast during the flood tide causes ocean sediments to enter inside the western estuarine systems. Sources of these ocean sediments are Lower Meghna estuary which propagates along the continental shelf during the ebb tide and later re-enter into the system during the flood tide. Just at the beginning of the ebb tide in the ocean, there is a flow disaggregation line, and a zone of stagnation occurs. This zone has significant impact on the sedimentation all along the estuary mouths in creating zone of turbidity maximum

Cyclonic wind suddenly increases the flood flow velocity (hydrodynamic shock) compared to without cyclone scenario. As sediment flux is related to water velocity, increased water velocity creates increased sediment flux for the same sediment concentration. So, for a similar sediment regime, cyclonic event creates increased sediment flux. This will drive increased volume of sediments to re-enter into the estuarine systems through increased flood flow velocity created by cyclone. We can see visible impact of wind only along the Lower Meghna mouth, but not along the other locations of the coast. Cyclone impact is also significant in this location. This is mainly due to large Meghna flow associated by wide estuary mouth. Location of Meghna mouth is at the right side of cyclone track which made impact of this cyclone maximum in this location. This increased flux will drive increased volume of sediments through the Lower Meghna mouth. This south-westerly current will drive the sediments from the turbidity maximum region to the swatch of no ground and may be a probable cause of sediment accumulation inside the swatch of no ground. The results show gradual increase of bed shear stress along the estuary mouths when the forcing increases from tide, tide & wind, and tide & cyclone depicting the increased sediment flux during cyclonic events. As cyclone is a short duration, season dependent but high intensity incident, cyclone generated sediment transport will not create a long duration impact on sedimentation in the region.

We applied BDM to compute sediment dispersion zone in the ocean. We used dispersion of conservative substance in the ocean to delineate this zone. Following the dilation line of the conservative substance, dispersion path of sediments is identified. The results show that high concentration sediments is confined within the continental shelf. Sediments from the Lower Meghna estuary is mainly distributed within this zone. Deep ocean has very low sediment concentration.

Vertical distribution of the dilution zone representing sediment concentration close to the coast from the 3D model simulation shows that high sediment concentration is confined within the first 50m depth of the ocean from MSL of the ocean surface. Deeper part of the swatch of no ground is within low sediment concentration zone. This shows in normal tidal environment (not cyclonic

condition), sediments from either the eastern or the western oceanic circulations do not enter deep into the submarine canyon.

To determine sediment movement path along the coast, sediment is released from the main inflow systems and its movement is traced all along its travel path. The sediment movement path shows that the sediments from the Ganges-Brahmaputra-Meghna systems discharges into the Bay of Bengal through the Lower Meghna mouth, turn clockwise, part of the sediments deposit in the ocean and the rest of the sediments re-enter into the western estuarine systems. On the swatch of no ground sediment movement path is deflected and by-passed the swatch of no ground region. This shows that in normal tide condition, sediments from the Lower Meghna system may not be directly depositing inside the canyon. This situation will prevail for tide & wind condition also but may change during tide & cyclone condition depending on the cyclone track and strength. The driving force behind this recirculation is fluvial flow from upstream rivers, tide in the ocean, and Coriolis force due to earth rotation. Wind (normal wind and cyclonic wind) acts an additional force behind this re-circulation.

Flooding in the delta brings the sediments on the floodplains and thus cause floodplain sedimentation. So, it is important to understand the flooding process in the delta particularly during monsoon. We applied BDM to simulate flooding caused by fluvial and tidal flows. When only land inundated area due to riverine flood is considered, the 1998 flood shows 27% to 29% of the country was inundated during 1998 flood. This is the effective inundated area which is relevant for flood management, and which also contributes to the floodplain sedimentation.

Floodplain sedimentation in the delta surface is an important determinant of delta sustainability against sea level rise and offsetting waterlogging created due to polders. To understand the flooding and sedimentation processes in different flooding and intervened conditions, we performed four numerical experiments. The four numerical experiments performed are (1) Intervened stage in average flood condition (2) Intervened stage in extreme flood condition (3) Natural stage in average flood condition (4) Natural state in extreme flood condition.

We can see that in the intervened state, due to increased sediment inflows in the system from 400 MT in average flood condition to 1243 MT in extreme flood condition, total retained sediment volume in the delta floodplain increases from 315 MT (79% of total inflow sediments) to 820 MT (66% of total inflow sediments). When sedimentation on the delta surface is considered, coastal floodplain gets special attention due to relatively low elevation of the coastal land which is susceptible to inundation due to sea level rise. We can see that sedimentation volume in the coastal floodplain increases from 192 MT (48% of total inflow sediments) in average flood condition to 517 MT (42% of total inflow sediments) in extreme flood condition. Here, for both total retained sediment volume and coastal floodplain retained volume, sediment volume increases in extreme flood condition compared to average flood condition. But its percentage share decreases due to relatively large increase of total sediment inflows in extreme flood condition. It is seen that sedimentation depth on the delta surface during intervened condition varies between 0.57mm to

9.85mm depending on the flood condition and floodplain location. It is found from the literature that the relative sea level rise (RSLR) in GBM delta is approximately 5.0 mm/year by considering average yearly sea level rise and subsidence. We can see that in average flood condition, sedimentation depth on the delta surface is less than 5.0 mm/year only in NW, NE, and EHT regions, and in extreme flood condition only in NE and SE regions have sedimentation depth less than 5.0 mm. For all other regions except these, sedimentation depth is greater than 5.0 mm/year showing potential sedimentation on the delta surface in the intervened state for all flood conditions which will offset the threat of inundation of GBM delta. The 2 regions (NW and NE) are relatively higher elevation non-coastal regions which are not susceptible to inundation due to sea level rise. Although sedimentation rate in EHT region is relatively low during average flood condition (4.84mm), we can see a very high rate of sedimentation in this region for extreme flood condition (9.85mm). The maximum sedimentation depth on delta surface is found in SE region (8.31mm) during average flood condition and in SC region (8.56mm) during extreme flood condition (we are not considering high sedimentation in EHT region during extreme flood condition as mentionable, because the high value of sedimentation in this region occurs mainly along the low elevation mud flats along the coast).

Similar to the intervened states, sedimentation in the natural states also follow the inundation pattern on the floodplains. With similar sediment inflow volumes for both the flooding conditions, increased inundated (and thus sedimented) areas cause increased sediment volumes on the delta surface. In average flood condition, sediment volume on the floodplains in the natural state increase to 342 MT compared to 315 MT in intervened state (about 9% increase). In extreme flood condition, this increase is 967 MT in natural state from 820 MT in intervened state (about 18% increase). This additional volumes of sediments on the delta surface are mainly in the coastal region and contributes to delta building process. When coastal floodplains are considered, we can see that in average flood condition, increase in natural state is 214 MT compared to 192 MT in intervened condition (about 12% increase). In extreme flood condition, these values are 626 MT in natural state from 517 MT in intervened state (about 21% increase).

Except in SE region, sedimentation thickness for all other regions have increased in extreme flood condition compared to average flood condition. This means if new sedimented area appears due to increased flooding with relatively lower depth, average sedimentation thickness decreases. So, the decreased sedimentation thickness does not mean that less sedimentation has occurred in that place. This is the reason of decreased sedimentation thickness in SE region due to increased flooding in extreme flood condition. We have earlier seen this incident for the same region (SE region) in the intervened state. For average flood condition, the RSLR value of 5.0 mm/year is seen to be lower in all the regions except NW, NE of the non-coastal region and EHT of the coastal region. Land elevations of NW and NE regions are relatively high, and these two regions are not susceptible to be inundated by sea level rise. The part of the EHT which is sedimented is low elevation mud flat. Although sedimentation is this part of EHT is relatively low (3.63 mm) in average flood condition, we can see a very high rate of sedimentation (12.81mm) during extreme

flood condition. A similar pattern in EHT region was found for intervened condition. Except EHT, we can see a high rate of increase of sedimentation in SC region in natural state when flood condition changes from average to extreme (5.14mm is increased to 8.25mm). We also found similar trend in this region for intervened state also (6.01mm increased to 8.56mm). When sedimentation volume is considered, we can see increased sedimentation volume in all the regions when flood condition changes from average to extreme. This is obvious, because sediment inflow has increased from 400 MT in average flood condition to 1243 MT in extreme flood condition. Regarding percentage share of these sediments, we found SW region (Sundarban dependent region) has the maximum share (27.3%) in average flood condition, and SC region (non-poldered region in intervened state) has the maximum share (27.3%) in extreme flood condition.

We can see that change in physical state of the system from intervened state to natural state increase the sedimented area by 18-19% for entire delta and 30-31% for the coastal region, while change in flood condition from average to extreme condition increase the sedimented area by 83-84% for the entire delta and 92-93% for the coastal region. So, GBM delta in its present state (intervened state) is sufficiently capable to accommodate increased sedimented area only due to change in flood condition. In our case, change in flood condition from average to extreme condition means increase in sediment inflows from 400 MT to 1243 MT. Changing physical state of the system means removing the existing embankments / polders from the system which is not realistic and not implementable. But if we can ensure more sediment inflows to the system in the delta through transboundary negotiation and proper sediment management, we can ensure delta sustainability without any further intervention.

The results show that due to change in flood condition from average to extreme, average increase of sedimentation depth on delta surface for intervened state is 0.93mm and for natural state is 2.04mm. On the other hand, if we change the physical state of the system from intervened to natural keeping the flood condition same (and thus keeping the sediment inflow to the system same), average sedimentation depth on the delta surface decreases to 0.48mm in average flood but increases to 0.63mm in extreme flood conditions. The decrease of sedimentation depth is caused by extended sedimented area while total sediment inflows remain the same (because flood condition is same but physical state is changed). These results show that in terms of sedimentation depth on the delta surface, we will get advantage by changing delta state form intervened state to natural state. We have seen to get advantage in terms of sedimented area when flood condition is changed from average to extreme. So, in terms of delta sustainability, maximum advantage will be achieved if flood condition is changed from average to extreme and physical state of delta is changed from intervened to natural state.

In our case, change in flood condition from average to extreme condition means increase in sediment inflows from 400 MT to 1243 MT (210%). Changing physical state of the system means removing the existing polders from the system. In intervened state, increasing sediment inflows by 210% increases the sedimented area on floodplains by 83%, sediment volume by 160%, and sedimentation depth on the delta surface by 1.15-1.54mm. The corresponding increase for natural

state is 84% for the sedimented area, 183% for sediment volume, and 4.28-7.07mm for sedimentation depth. This shows that by increasing sediment inflows, sedimented area and volume on the floodplains can be largely increased. But we get comparatively little advantage in terms of sedimented area and volume by changing the physical state of the system from intervened to natural (83% & 160% in intervened state, and 84% & 183% in natural state). But for sedimentation depth, we can see remarkable increase for the similar increase of sediment inflows (1.15-1.54mm to 4.28-7.07mm).

Changing physical state of the system by removing all the polders from the system is not realistic and not implementable. But the similar impact can be achieved by adopting different sediment management practices (for example different form of controlled flooding including TRM). On the other hand, we can ensure sustained sediment inflows to the system in the delta through transboundary negotiation and proper sediment management. So, delta sustainability can be ensured by ensuring required sediment inflows from outside of the delta and by appropriate sediment management inside of the delta.

A special note should be mentioned about the SC region. At present there is no polder in the SC region. Compared to the total GBM delta surface, the share of SC region is: total inundated area which is also sedimented area is 9%, sediment retained on the floodplain 21.4-27.3%, sediment volume retained 94-340 MT, and sedimentation depth 5.14-8.56mm. This shows overall importance of SC region compared to the entire delta when delta sustainability is considered. Any intervention (directly or indirectly) on SC region that restricts sedimentation in SC region will seriously affect the delta sustainability.

The present sediment practices in the GBM delta are (1) TRM (2) Cross-dam and (3) Dredging. In this study, we concentrated on two sediment management practices in the region – cross-dam and dredging. Instead of studying local impacts of these two sediment management practices, we used a system approach by applying BDM to study the system impact.

EDP proposed 18 probable cross dam locations in the coast. Out of these 18 probable locations, in this study, system impacts of 13 of these cross-dams are studied. In addition, system impact of Noakhali-Urir char cross-dam planned by BWDB is also studied.

Due to 13 cross-dams, impact on water level at two locations shows changes in tidal amplitude along Meghna Estuary. We can see more impact close to Meghna Estuary mouth compared to inside of the estuary. This change in tidal amplitude will change the tidal hydrodynamics of the system and may lead to a long-term hydro-morphodynamic change in the region.

Sedimentation in the cross-dam location reclaims the land and reduces the cross-section area. Due to trapped sediments in the cross-dam location, sediment supply from the zone of turbidity maximum decreases. This may lead to riverbed erosion in the western estuarine systems. This impact of cross-dam is significant. If cross-dam locations are intelligently selected, then reduced sediment supply (due to trapped sediment in cross-dam location) in the western estuarine systems

may act positively to increase conveyance capacity of the rivers in the south-west region. This will act to reduce waterlogging problem in the region.

Cross-dam reduces the channel depth. Due to reduced channel depth, water level close to reclaimed land increases. This leads to increased flood inundation in locations close to the cross-dam locations. Due to construction of 13 cross-dams, we can see increased flooding in unprotected low-elevation intertidal mud flats in the EHT region. Increased flooding is also observed in the unprotected regions of Sandwip, Urir Char, Noakhali, Hatiya, Bhola, and surrounding island.

Cross-dams decreases peak monsoon velocity in the vicinity of cross-dam locations. This reduces sediment transport capacity in these locations and cause increased sedimentation. This accelerates the process of land reclamation. But the at the same time, increases the increased inundation depth during peak monsoon. The decreased velocity zone is also observed along the Meghna Estuary and in the deep ocean region. This will increase unwanted sedimentation in these locations. However, there are few locations that includes Sandwip channel and downstream of the Meghna mouth where peak monsoon velocity will increase. This will increase sediment transport capacity in these regions.

Due to 13 cross-dams, we can see decreased sediment concentration in the turbidity maximum region and increased sedimentation in the western estuarine systems. So, there is a possibility of increased bed erosion for the estuaries in the western region which will improve waterlogging problem in this region. Combined operation of cross-dam and TRM may accelerate improving the channel conveyance capacities. But at the same time, may decrease the land building process.

The changes of yearly distribution of sedimentation parameters shows that impact of 13 cross-dams do not affect the non-tidal part of the delta. Due to the trapped sediments as a result of 13 cross-dams, total retained sediments on the delta floodplain reduces by -0.4%. The maximum reduction occurs in SC region. The impact of 13 cross-dams shows that due to construction of these cross-dams, sedimentation volume on SC region will decrease by 0.7% associated with a 0.26mm reduction of sedimentation depth. This will have a long-term negative impact on delta sustainability. We also see that these 13 cross-dams increase the retained sedimentation volume on SE and EHT regions with a corresponding increase of sedimentation depth of 0.64mm on SE region and decrease of 0.15mm on EHT region. Increase of sedimentation depth on SE region is concentrated in Sandwip-Urir Char and other cross-dam influenced region of the delta. On the other hand, sedimentation depth on EHT decreases although the sedimentation volume is increased. This happens because larger area of EHT which is mainly low-elevation intertidal zone is sedimented with 0.2% increase of sedimentation volume.

The intensity and extent of impact of sedimentation on delta surface of Urir Char cross-dam is much less than 13 cross-dams. Contrary to the 13 cross-dam, we do not see any noticeable decrease of sedimentation depth in Sundarban region for the Urir Char cross-dam. Similar to 13 cross-dam, Urir Char cross-dam has no effect on non-tidal delta surface and also on SC region. Due to Urir Char cross-dam, sedimentation volume on the delta surface reduces to 0.1 MT which is 0.008% of

the total inflow sediments. This value is insignificant compared to the 13 cross-dam. Similar to 13 cross-dams, we can see decrease of sedimentation volume in SC region due to Urir Char cross-dam also (decrease by 1.1 MT) which is 0.088% with respect to total inflow sediments. The sedimentation depth in the SC region also decreases by 0.20mm due to Urir Char cross-dam compared to 0.26mm decrease due to 13 cross-dams. Although sedimentation volume in SE region (the region where Urir Char is located) increases by 1 MT, sedimentation depth in SE region decreases by 0.18mm. This happens due to larger area of SE is sedimented due to construction of Urir Char cross-dam. This shows that sedimentation rate in Urir Char region will be higher if 13 cross-dams are constructed instead of Urir Char cross-dam only.

If we summarize the positive and negative impacts of cross-dam, this will make it possible for an overall assessment of performance of cross-dam as a sediment management practice. Positive impacts of cross-dam are: (1) reclaim land in the cross-dam location where sediment concertation is high (2) increase river conveyance in other regions caused by reduced sediment supply due to trapped sediments in the cross-dam location. If this region is within the zone of waterlogging, this will act positively to reduce waterlogging problem in the region. The negative impacts of cross-dam are (1) change the tidal amplitude in the influenced zone which may lead to a long-term hydro-morphodynamic change in the region (2) increases the inundation in the unprotected land close to the cross-dam (3) decreases sediment transport capacity in other regions which are within the influence zone of the cross-dam and causes unwanted sedimentation in those locations (4) reduces retained sediment volume and sedimentation depth on the delta surface and act against delta sustainability. If we make a trade-off between positive impacts and negative impacts of cross-dam, we can see that in terms of effective use of sediment resource which will serve both local purpose and overall delta sustainability – cross-dam alone is not an effective sediment management practice.

Dredging is the most common and frequently conducted sediment management practice in this region. Dredging is done mainly to improve channel conveyance for navigational purposes, to reduce flood extent, and to guide the river to an expected course. To study simultaneous system impacts of dredging on major river systems, we made numerical experiments by synthetically conducting dredging in two reaches of Jamuna-Brahmaputra River and two reaches of Ganges River. The results show that most part of the dredged section is filled within one year of dredging operation. Among the dredged reaches, the maximum filling rate (134% and 244%) of dredged depth is observed in the reaches of Brahmaputra-Jamuna River. This rate is higher than the filling rate of the dredged reaches of the Ganges River (100% and 178%). This shows that the filling rate depends on the sediment flux of the dredged river.

Dredging reduces the flooding extent by decreasing flood depth in an extended region of the delta. A negative impact on inundation (increased inundation depth) is visible in the downstream reaches of the dredged section. Dredging reduces inundation depth in the floodplains. The water volume on these floodplains is carried by the increased conveyance of the dredged section. But when the same volume of water reaches at the downstream section, it overflows because the conveyance of

the downstream reaches is inadequate to carry the extra volume of water coming from the floodplains. This result shows that dredging is indeed effective in reducing the inundation depth and flooding extent. But at the same time, adverse effect may result in the reaches where river conveyance is insufficient to carry the extra volume of water coming from the floodplains.

Dredging reduces sediment transport capacity of the river in the dredged sections. As total inflow of sediment flux in the system remains unchanged, the reduced sediment transport capacity in the dredged section will cause sedimentation in the dredged reaches and new dredging is required to maintain the dredged depth.

As dredging reduces flooding extent in the floodplains, the sediments which were supposed to be deposited over the floodplain are transported to the downstream reaches. These additional sediments, in addition to sediments coming from the river-bed due to increased bed shear stress in upstream and downstream reaches of dredged reaches increase the sediment concentration in the downstream reach of the dredged sections.

The changed yearly sedimentation depth on the delta surface shows a decreased sedimentation depth on the delta floodplains from where we have earlier seen an improved inundation condition due to dredging. In these locations we have also seen decreased transport capacity associated with decreased suspended sediment concentration. The increased conveyance of the dredged section decreases its transport capacity. The sediments which were supposed to be deposited over the floodplains are now deposited in the dredged section causing a rapid filling of the dredged section. This process eventually results a decreased sedimentation volume and sedimentation depth over the delta surface which are flood free due to dredging.

Due to dredging, 48 MT of sediment volume in the delta floodplain will be decreased which is 3.9% of total inflow sediment volume. In terms of sediment volume on the delta surface, change in coastal floodplain is positive which shows an increase of 4 MT of sediments on the delta surface (0.3% of total inflow sediments in the system). We can see maximum negative impacts on NE and NC regions. These regions are directly benefited in terms of inundation reduction. Sedimentation volume in the NE region is decreased by 20 MT (1.6% of total inflow volume) with a corresponding decrease of sedimentation depth of 1.0mm. For the NC region, these values are 33 MT (2.7% of total inflow sediments) and 0.3mm respectively. For the coastal region, the changes are positive. The maximum increase of sedimentation depth is for the SW region (0.9mm) followed by SC (0.2mm) and SE regions (0.3mm). The corresponding increase of sedimentation volume in SW region is 7 MT, and for the SE region it is 1 MT. In the SC region, the increase in sedimentation depth (0.2mm) is associated with a decrease of sedimentation volume of 4 MT. This means in the dredged state of delta, increased volume of sediments in the SC region is distributed in a reduced inundated area compared to the non-dredged state. The positive impact on the coastal region is due to the increased suspended sediments in the coastal ocean which comes in the system from the excess sediments which were supposed to be deposited on the delta floodplains.

We investigated system impacts due to the dredging in Hari River. Hari River is located in the SW region. But the impact of dredging in the Hari River is seen to be felt in the entire coast except the EHT region. However, there is no impact in the non-tidal part of the delta. As mentioned before, when dredging reduces flood inundation in the floodplains, it also reduces sedimentation depth in the floodplain. On the other hand, TRM also reduces flood inundation, but at the same time increases the sedimentation depth in the connected beels. So, this will increase the average sedimentation depth in the floodplains. This is the advantage of TRM over dredging. Due to Hari River dredging, total sediment volume on the delta surface reduces by 0.2 MT which is 0.016% of total sediment inflow to the system. This reduction of sediment volume is entirely in the coastal zone. In the coastal zone, maximum reduction of sedimentation depth on the delta surface is for SC region (0.2mm) followed by SW and SE regions (0.1mm each). Corresponding sediment volume reductions are 0.1 MT for the SC region, and 0.05 MT each for the SW and SE region. We can see that dredging in the Hari River reduces the sedimentation depth in SW region where the Hari River is located. This dredging also reduces sedimentation depth on the SC region which is an important region for the delta sustainability.

BDM is applied to study the sedimentation process in the Payra port channel. A fine-scale Payra port model is constructed within the BDM. It is found that sedimentation in the dredged channel is significantly higher than the channel in natural state. With the increase of dredging depth, sedimentation increases at a faster rate. Sedimentation process in the Payra port channel depends on the upstream flow conditions of the riverine systems. Sediment supply from upstream depends on the sediment inflow during the monsoon. Increased sediment inflow from upstream generally increases the sedimentation in the channel. Although high flow from upstream also causes erosion of the channel at few sections. Depending on the sediment inflow pattern, sedimentation in a specific monsoon month can be higher than yearly sedimentation volume. Sedimentation patterns at different sections of channel are different. The channel filling rate for the shallow channel varies 35% - 50% with sedimentation depths 1.6m – 1.9m. For deeper channel, these values are 31% - 34% and 4.8m – 5.2m. High strength cyclone during post-monsoon season that makes landfall at the west side of the channel (for example cyclone Sidr) cause additional sedimentation in the channel. A similar but low strength cyclone (for example cyclone Amphan) during pre-monsoon season has little impact on sedimentation in the channel. Depending on the dredged channel depth, a strong cyclone can cause extra filling of the channel by 11% - 28% with sedimentation depths 0.50m – 0.90m.

CHAPTER ONE
Introduction

1.1 Background of the Study

When the research project was intuited in June 2019, both the title and objectives of the research were confined in the south-west region of Bangladesh. With the progress of research on sediment management for the south-west region in the country, it was observed that the sedimentation in south-west region is part of an integrated processes of flow and sediment transport from the inland river systems, erosion-deposition in the inland rivers and floodplain, transport of these sediments in the estuaries and coastal floodplains, discharge of sediments to the ocean, deposition of sediment in marine environment, transport of sediment with the oceanic processes and re-entry of part of these sediments into the estuarine systems. Any sediment management practice implemented in this system becomes an integral part of this complex system. So, to study effectiveness and impacts of any specific sediment management practice or combination of different practices in any region of the GBM delta including the south-west region – the entire system need be considered in an integrated way. The only way to make this integrated system is to construct a seamless model setup that will combine the entire system in a single modelling framework.

1.2 Past Studies on Sediment Management in GBM Delta

Most of the past studies in GBM delta related to sediment management focused on Tidal River Management or TRM. To solve the long-standing problems of waterlogging in the region, the Khulna-Jessore drainage rehabilitation project known as KJDRP was implemented during 1994-2002. Later, a popular concept based on generations of indigenous water management practices, formally known as Tidal River Management (TRM), was adopted. TRM allows natural movement of sediment with tidal water into a beel which is called tidal basin and allows deposition of sediment in the beel. Although TRM is a process-based sediment management practice, but its impact is dominantly local. Moreover, the implementation process of TRM creates social conflict as during TRM a certain part of the area (including the beel area) become water-logged for a long time. Amit et al. (2013) suggested an 'embankment option' coupled with TRM which will allow construction of embankment along both banks of the main channel and then cutting the embankment sequentially from upstream to downstream to ensure gradual sedimentation of beels. TRM is technically proved to be successful in solving water-logging problem (Khadim et al., 2013) but its success is limited due to multiple social problems (Karim and Mondal, 2017). Gain et al., 2017 proposed a transdisciplinary approach to solve these social problems which indirectly indicates complexity of the situation within the community. The benefits of TRM concept were assessed by Al Masud and Islam (2018) by satellite data analysis and noticed that the TRM concept have reduced waterlogging up to 4243 ha of land in August 2011 compared to 2006 in Hari-Teka and Bhadra basins. Hence, the total agricultural land was increased by 3005 ha of land in 2011 (during TRM operation) as compared to 2006. The vegetation was also improved by 2851 ha of

land in the floodplain. A geo-spatial analysis by Hussain et al. (2018) denoted that during TRM implementation in Pakhimara Beel at Tala upazila of Satkhira district, about 5090 acres of agricultural land and about 729 acres of homestead land was water-logged. To increase the efficiency of TRM, a single embankment cut is proposed (Talchabhadel et al., 2018). Adnan et al., (2018) proposed 106 beels that can be used as TRM sites. They claimed that implementation of TRM in these 106 sites will reduce probability of flooding by 35%. They accepted the reality that agriculture need to be stopped in these locations during implementation of the TRM but argued that this will be compensated later by additional agricultural production when flooding will be reduced. Seijgera et al., (2019) mentioned that TRM is very different from mainstream engineering strategies related to tidal rivers and polders. They stressed for reconceptualization of TRM by focusing on restored tidal rivers, flora, and fauna. Gain et al., (2019) after accepting the potential of TRM, proposed an institutional framework for effective implementation of TRM. Islam et al., (2020) proposed a different approach of TRM operation which will be operated only during the monsoon. They argued that although this approach will result 20-30% less sedimentation, it will be socially more acceptable. In two recent papers by the same research group (Islam et al., 2021a; Islam et al, 2021b) arrived similar conclusion with the additional information where they mentioned that TRM operation in the beels close to the sea and western part of the coast will retain more sediments. They also recommended compartmentalization of large beels. They also found that sedimentation in the tide dominated region is 28 times higher than the river and mixed regions.

There are only few studies available where sediment management issue is mentioned other than the TRM. Cross-dam is a well-known sediment management practice which is used for land reclamation in off-shore region (EDP, 2007). Jakobsen et al. (2002) warned about construction of cross-dam in the north of Sandwip which, in their opinion, will change the residual circulation pattern in the region. Sarker et al. (2011) discussed the potentials of cross dam as sediment management option that will reclaim land. They stressed the fact the success of cross dam depends on the sediment supply from the upstream. In their opinion, the 1950 Assam earthquake resulted enormous volume of wash load to the GBM systems that ultimately accumulated high volume of suspended sediment in the mouth of Meghna estuary. The volume of sediments generated from that earthquake has already started to decrease. So, impacts of cross dam as a land reclamation method may not be effective in future as it was visible in the past. Construction of cross dam will not increase net accretion, rather it will connect water locked islands with the mainland. Sarker et al. (2011) warned that additional accreted land around cross dam may initiate erosion in other parts of the estuary. But in their study, there was no specific impact assessment of cross dams. Rogers and Overeem (2017) with the measured sedimentation thickness in few locations in south and south-central region in the coast revealed the important role of polders on sediment management. They showed that secondary and tertiary channels as well as the engineered irrigation canals that penetrate the polders are effective in sediment distribution in the floodplain. These findings should be considered in any sediment management options in the coastal region. Angamuthu et al., (2018) showed that cross-dams can achieve their local goal of land accretion but will not accomplish net land in delta scale. This role of cross-dam was also mentioned by Sarker et al. (2011). Hale et al. (2019) measured water and sediment flux in Shibsha River and two if its bifurcations. They showed

the importance of seasonality that should be considered in any sediment management strategy in the region. Their findings showed excess sediment in the north of the Shibsha system which, in their opinion, can be utilized to inject sediment in poldered area by using TRM like methodology. The seasonality issue is later explored by three consecutive papers by a group of researchers (Islam et al., 2020; Islam et al., 2021a; Islam et al, 2021b).

Dredging is another known sediment management practice in the south-west region. Studies are available where focus was to determine the most cost-effective dredged route for navigational purpose (Alim et al., 2016; Rahim et al., 2016). The impact of dredging of Hari River is studied by WARPO and BUET (2019) and the result show that sedimentation in the main river indeed increases the waterlogging. Dredging in the main river improves the waterlogging condition in the area which are within the drainage zone of the river. Local impact of dredging in Gorai River was studied by Rahman and Younus (2016) and Jamuna River was studied by Rahman et al. (2021). In both the studies, the authors have shown increased sedimentation in the dredged section.

It should be mentioned here that all the previous studies related to sediment management mentioned above focused only on the local effect. Impacts on integrated river-estuary-coast-ocean-floodplain systems for the entire GBM delta within Bangladesh was not considered by any of the past studies. The present study focused on this research gap.

1.3 Objectives of the Study

Analyzing the past studies in the previous section, it is seen that sediment management studies in the GBM delta so far focused mainly on TRM. There were few studies in the past where sedimentation processes in the delta are studied. As specific sediment management strategy, few studies are available related to cross dam. We know that dredging is the most common sediment management strategy (TRM is also a natural dredging of the tidal river related to the process) in this part of the delta. But we found no detail impact study on dredging which is visible in beyond the immediate vicinity of the dredged zone. There is at all no study conducted so far to understand the delta system impact of commonly practiced sediment management options. The main reason for this is lack of an integrated delta modeling system that can relate all the river-estuary-floodplain-wetland-polder-embankment-ocean systems in a single framework. This is a visible research gap to study any sediment management option in GBM delta. To fill this research gap, the objective of the research is set as:

1. Development of an integrated modeling framework for the GBM delta.
2. Application of the integrated modeling framework to study
    a. Sediment transport processes in the GBM delta
    b. Sediment management options in the GBM delta
3. Prepare a sediment management manual for the GBM delta

Based on the application of the integrated modeling framework in the GBM delta, an additional objective is set to prepare a sediment management manual for the GBM delta.

1.4 Organization of the Report

This report has five chapters. *Chapter One* presents the background of the study and related past studies on sediment management in the GBM delta. After identifying the research gap based on the past studies, objectives of the research are set. *Chapter Two* presents details of BDM setup including calibration and validation of the model. This chapter describes the domain of BDM, bathymetry, topography, and boundary conditions of the model. Calibration and validation of BDM is presented separately for the flow model and the morphology model. *Chapter Three* describes BDM applications to analyze sediment transport processes in the GBM delta. The sediments in the delta are transported with fluvial flow and tidal flow. Wind and cyclones play an important role in these transport processes. In describing the transport processes, sediment dispersion zone and re-circulation zone in the ocean are identified. As sedimentation in the floodplain is related to flooding, inundation in floodplains due to flooding is described. Sedimentation in floodplains of the delta is described by analyzing results of 8 numerical experiments. *Chapter Four* concentrates on BDM application to synthesize different sediment management options in the delta. Two sediment management options are analyzed – cross-dam and dredging. System impacts of these two sediment management options are presented in this chapter. Two cross-dam options are selected to study systems impacts – EDP proposed 13 cross-dams and BWDB planned Urir Char cross-dam. Three dredging options are described in this chapter – dredging in Brahmaputra-Jamuna and Ganges, dredging in Hari River and dredging in Payra port navigation channel. *Chapter Five* presents the conclusions of the study. Sediment management manual for the GBM delta is added as an *Appendix* of the report after the reference chapter.

CHAPTER TWO
Bangladesh Delta Model (BDM)

2.1 Introduction

During this research project time frame (June 2019 to December 2021), an integrated modeling framework is developed which is named as Bangladesh Delta Model (from hereafter we will term it as BDM). BDM is based on Delft3D and constitutes four modules of Delft3D modeling suite (Deltares, 2014) (1) hydrodynamic model, (2) morphology model, (3) salinity model, and (4) storm surge model. The Delft3D has a long track record of using in different environments, such as, oceans, coastal oceans, estuarine and river systems all over the world (Thanh et al., 2019; Sandbach et al., 2018; Hu et al., 2018; Salehi, 2018; Li et al. 2018; Bennett et al., 2018; Al Azad et al., 2018). This model has been used in many applications in Bangladesh as well (Haque, et al., 2016, for hydrodynamic model, WARPO and BUET, 2019, for morphology model, Akter et al., 2019 for salinity model and Al Azad et al., 2018 and Haque et al., 2018 for storm surge model). BDM integrates the entire processes of ocean, coast, Sundarban, polders, canal network, estuaries, inland rivers of different scales, embankments, wetlands, beels and haors. The model domain is extended southward to the Bay of Bengal down to Sri Lanka & Thailand coast and northward to the inflow points of transboundary rivers. The extended southern boundary enables the model to capture the cyclone genesis in the Bay of Bengal and the extended northern boundary enables the model to receive the inflows coming from outside the geographical boundary of the country.

2.2 Domain and Grid of BDM

The details of the BDM domain and the grid is shown in Figure 2.1. Relatively coarser grids are used in the ocean (12km x 35km) compared to the land (200m x 300m). As the tidal wave scale in the Bay of Bengal is several hundred kilometers, we do not need fine grid in the ocean part. Instead, the high-resolution grid in the land can capture details of land features. Separate grid maps for different regions of the country are shown in Figure 2.2. To capture the Pabna town protection embankment (Mujib Badh), we have used Domain Decomposition (DD) to resolve part of the NW region surrounding the Ganges River (Figure 2.3) in finer resolution (30m x 30m). The DD is also used to model the Payra port navigation channel dredging.

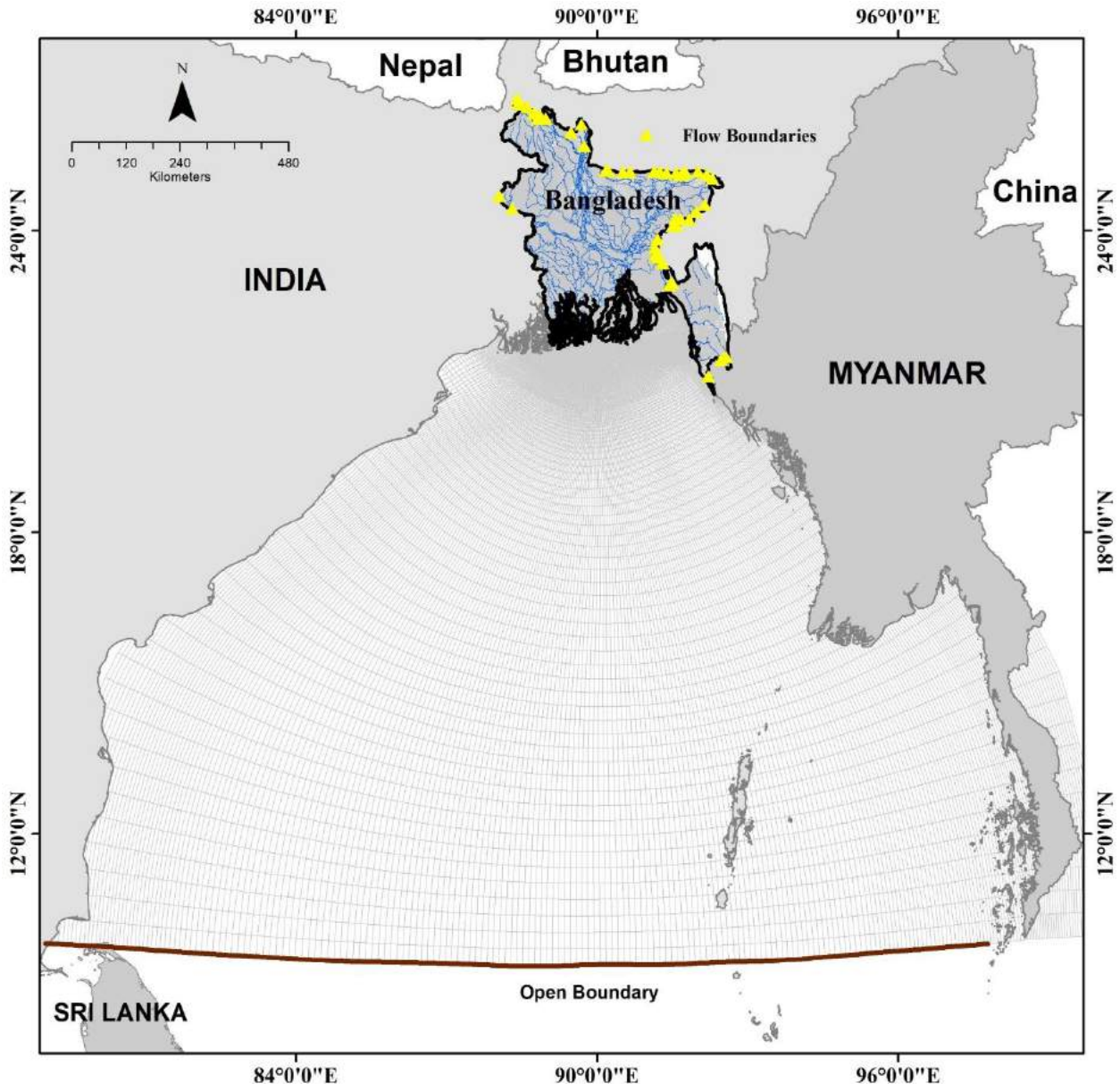

Figure 2.1: *Domain and grid of BDM. The BDM domain covers the entire Bangladesh with all the rivers, estuaries, and their floodplains. The yellow circles show the locations of upstream boundaries, and the dark brown curve line shows the location of downstream boundary of BDM. The transition of grid resolution from coarse to fine is visible in the figure. Due to relatively finer grids, the grids inside the land territory are not clearly visible in the figure. The zoomed view of grids in the land territories are shown in Figure 2.2.*

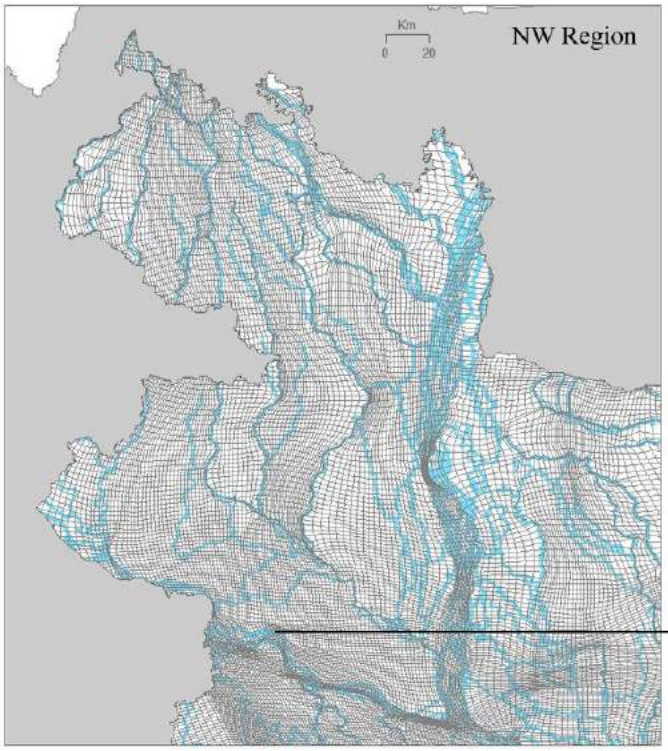

Fine Grid Resolution

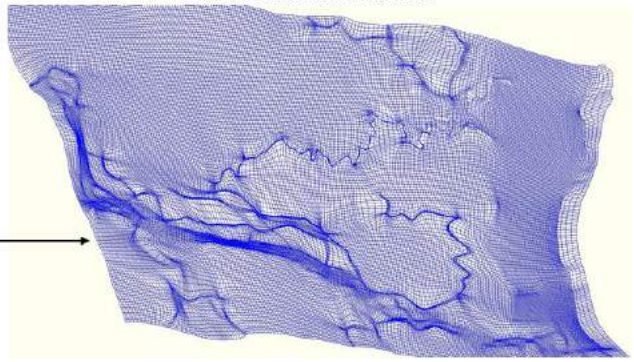

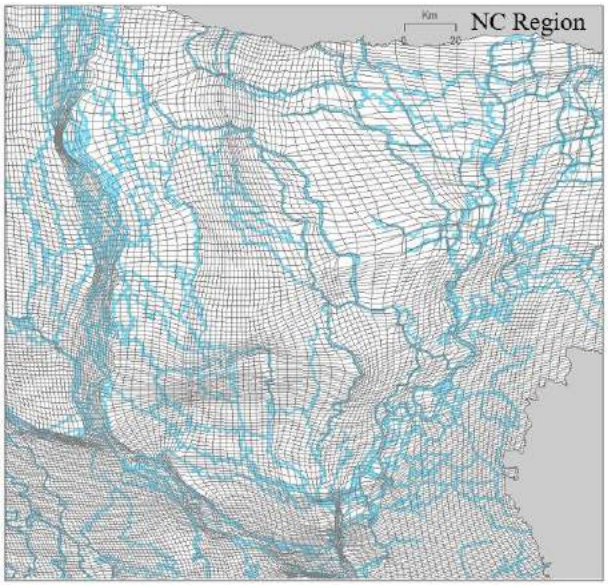

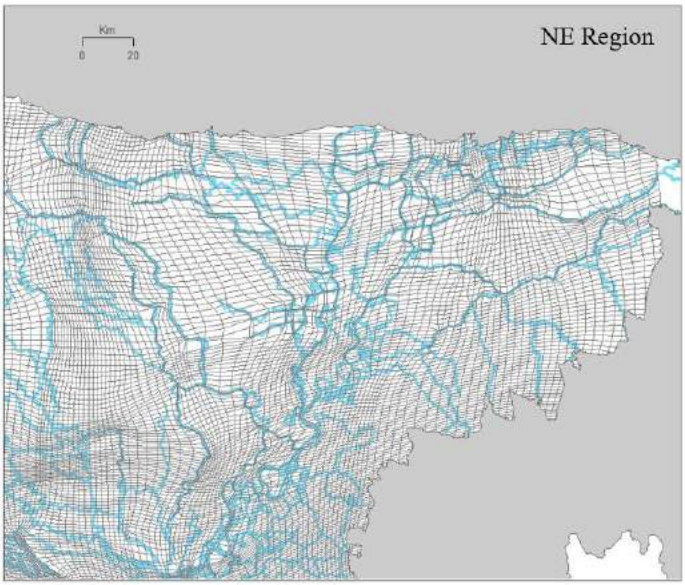

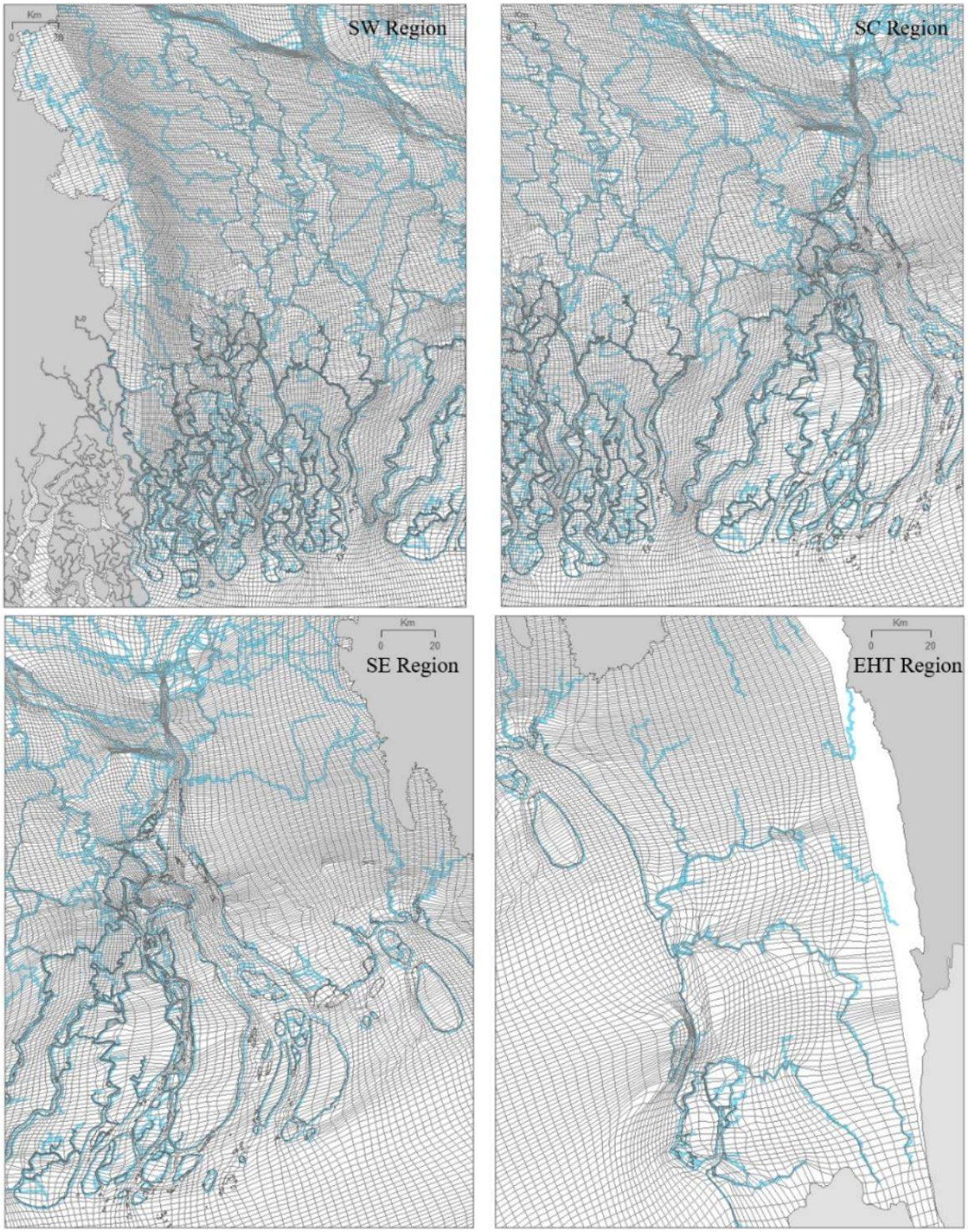

Figure 2.2: *Separate grid maps for North-West (NW), North-Central (NC), North-East (NE), South-West (SW), South-Central (SC), South-East (SE), and Eastern Hill Tracks (EHT) regions. The figure also shows the finer resolution of the grid near Pabna Town to capture the details of Pabna Town Protection Embankment (Mujib Badh).*

2.3 Bathymetry and Topography of BDM

The inland ground topography (Figure 2.3) is provided from the National Water Resources Data base (NWRD) DEM of the Water Resources Planning Organization (WARPO) of Bangladesh. This DEM was generated from the FINNMAP Land Survey of 1991, and the National DEM is from FAP19 (IWM, 2009). The horizontal resolution of this DEM is 50m × 50m prepared from 300m × 300m resolution data. Field validation from locations in coastal Bangladesh shows that this DEM has a vertical accuracy of ±50cm (unpublished data, 2019). Ocean bathymetry (Figure 2.3) is provided from the open access General Bathymetric Chart of the Oceans (GEBCO) (https://www.gebco.net/). For the river bathymetry, combinations of secondary and primary data were used. Secondary data were collated from the Bangladesh Water Development Board (BWDB), while primary data were collected at 294 locations in the rivers/estuaries of the coastal zone of Bangladesh (Nicholls et al, 2018). These primary data were collected using Echotrac CV100 echo-sounder surveys in the dry seasons of 2015 and 2017 at a vertical accuracy of ±1cm (https://www.comm-tec.com/prods/mfgs/odom/manuals/ohsi_um040001_etcv100_um.pdf).

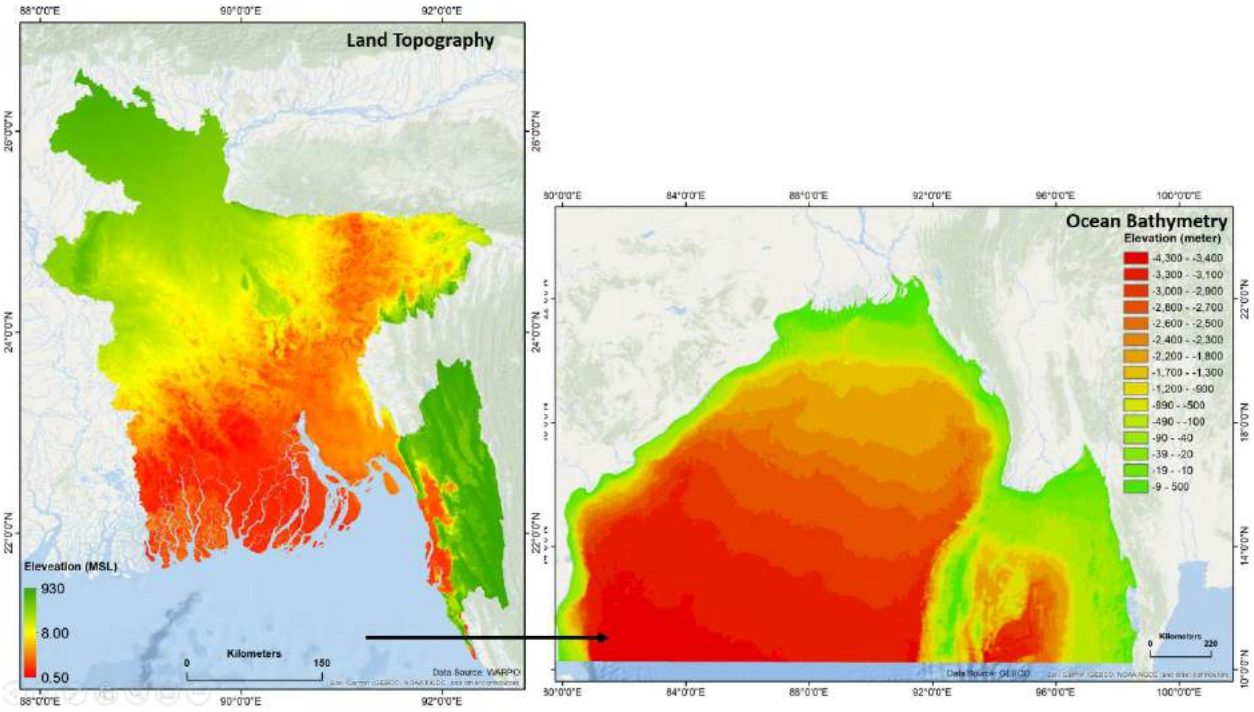

Figure 2.3: *Inland ground topography and ocean bathymetry that are used in BDM. The source of inland ground topography data is DEM available in NWRD of WARPO. The source of ocean bathymetry is open-source data from General Bathymetric Chart of the Oceans (GEBCO).*

2.4 Boundary Conditions of BDM

Two types of boundaries are used in the model. Open boundary at the southern end of the model domain where temporal variation of water level is imposed and river flow input at the northern end of the model domain (Figure 2.1). Western coast of the open boundary is Sri Lanka and eastern coast is Thailand. These southern boundary locations are selected to encompass the genesis of cyclones in the Bay of Bengal. For Sri Lanka coast, times series of water level is provided at water level station Colombo and for Thailand coast, time series of water level is provided at water level station Ko Taphao Noi (Figure 2.4). The time series data of these water levels are collected from global source (https://uhslc.soest.hawaii.edu/).

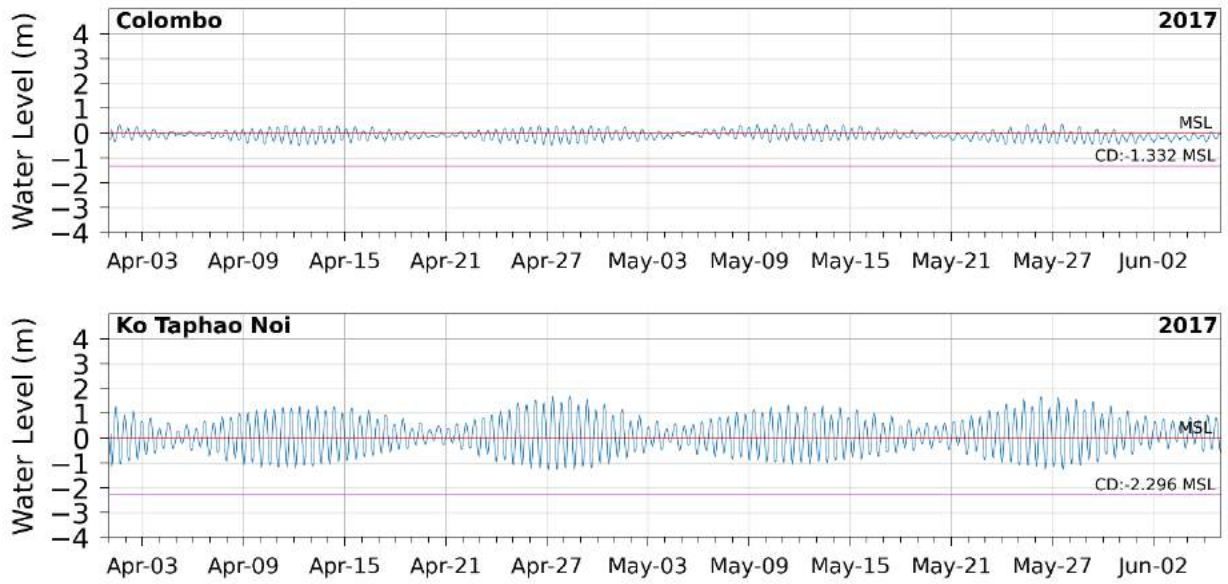

Figure 2.4: *Water level data at two open boundary locations Colombo of Sri Lanka and Ko Taphao Noi of Thailand. Snapshot of data are shown for early April to early June 2017. The Chart Datum (CD) at Bangladesh coast is shown in the figure to have an idea about the difference of water level at the boundary location and at the coast.*

For upstream flow boundary, out of 54 transboundary rives, BDM uses measured discharge data from BWDB at 44 flow boundary locations (Figure 2.5). For the rest of the transboundary rivers, measured discharge data are not available and data are provided by assuming the discharge based on BWDB (2011).

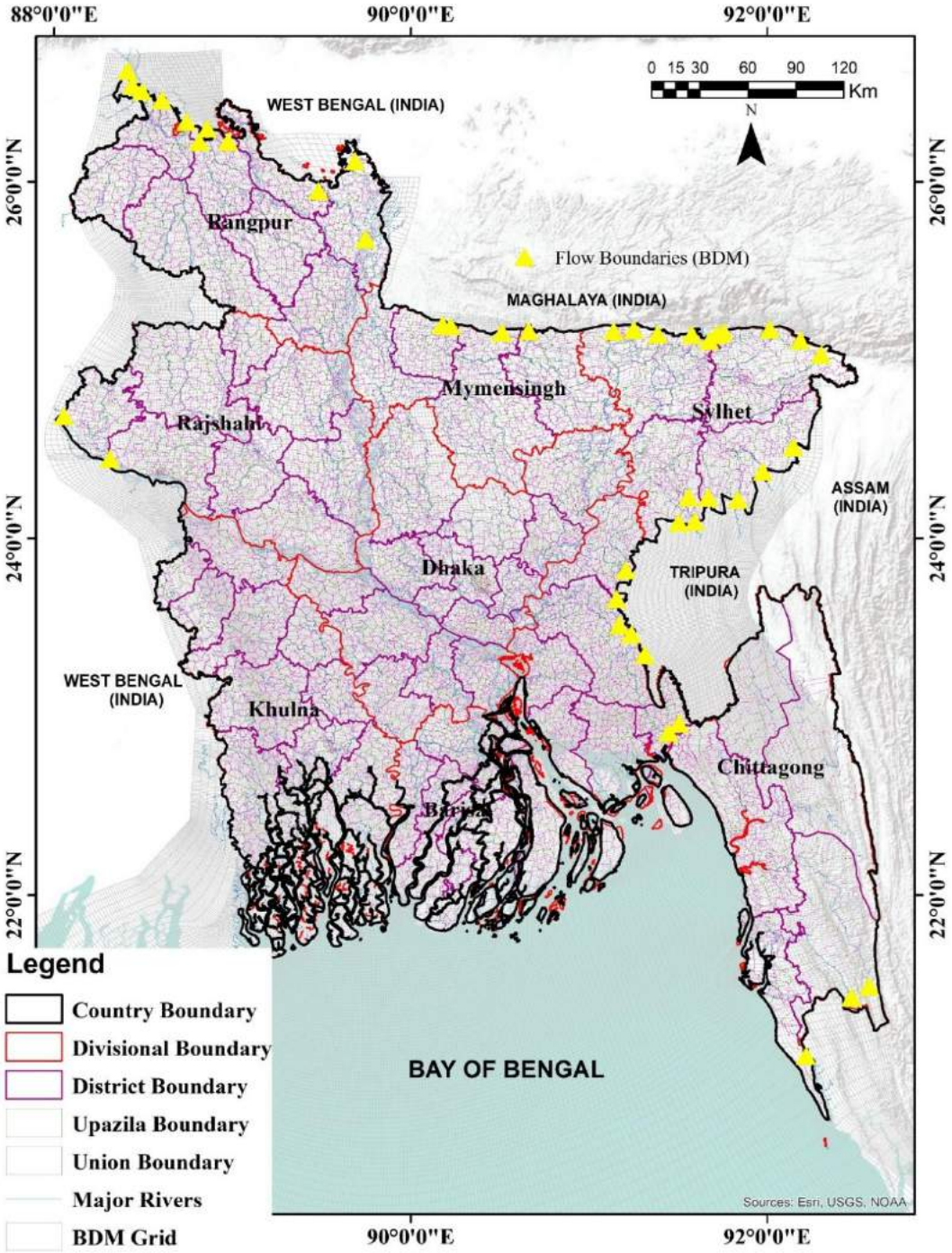

Figure 2.5: *Locations of upstream flow boundaries in the BDM grid. The yellow marked signs show the locations of flow boundaries. The figure also shows BDM grid inside Bangladesh territory with all the administrative boundaries and major rivers.*

2.5 BDM Calibration

In this study, we applied the flow and morphology models of BDM. In this section, we will present the calibration results of BDM for flow and morphology models. Flow model of BDM is calibrated against water levels in 43 measuring stations for the year 2017. Source of data for the water levels are: Bangladesh Water Development Board (BWDB), Bangladesh Inland Water Transport Authority (BIWTA), and Bangladesh Navy (BN). Data durations for BWDB and BIWTA data are for 1 year (year 2017), whereas data duration for BN data is for 1 month (May 19 to June 21, 2017). The selected 43 water level stations cover the inland non-tidal water level, coastal tidal water level, and marine tidal water level stations. The locations of water level stations for the model calibration are shown in Figure 2.6.

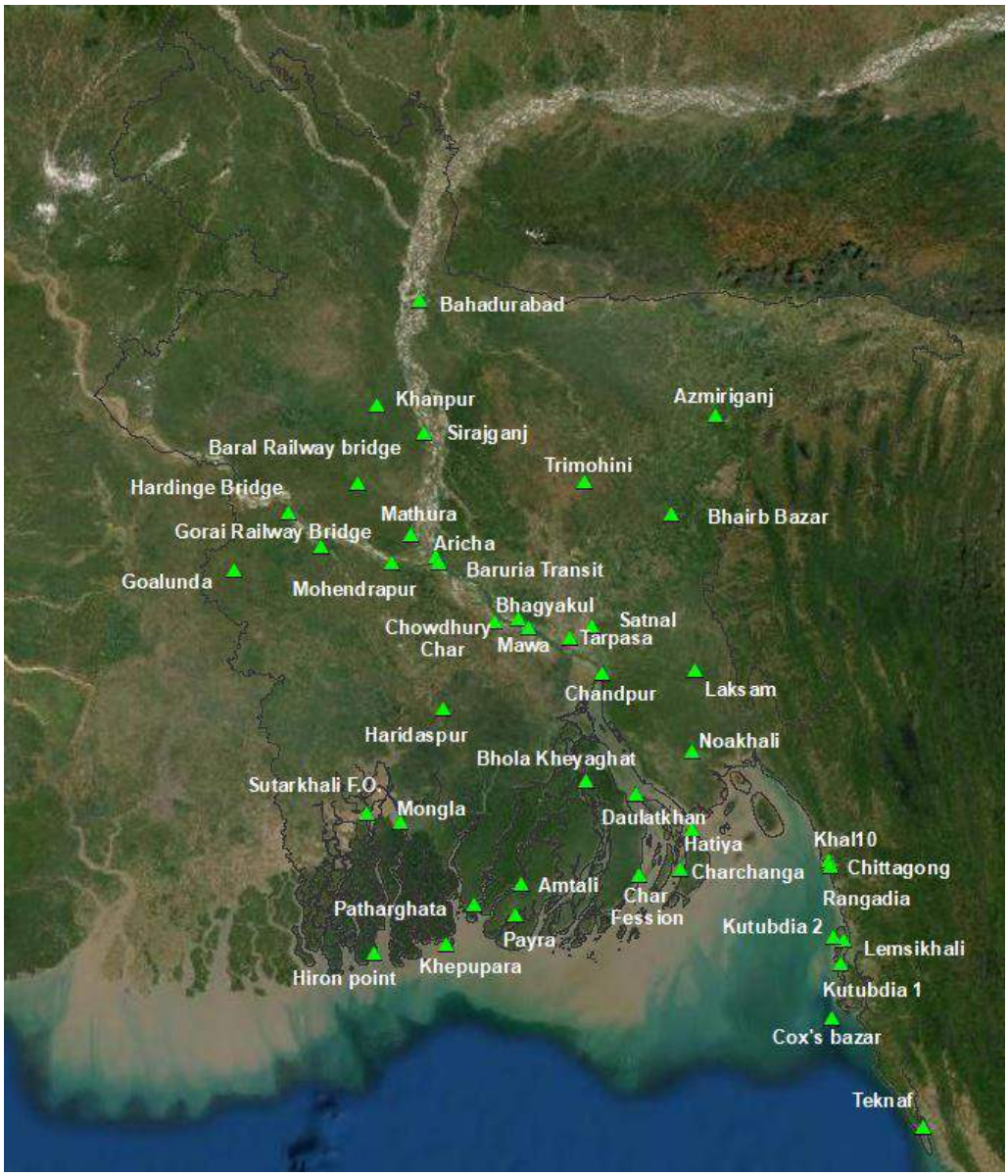

Figure 2.6: Location of water level stations used for BDM flow model calibration.

2.5.1 Flow model calibration

Calibration locations in 43 water level stations for BDM simulation is shown in Figure 2.6 and results are shown in Figure 2.7. Out of these 43 locations, measured data are available in 29 locations. In the locations where measured data are not available, only the BDM simulation results are shown. A statistical evaluation is made for the model performance and the results are shown at the bottom of each comparison results. The statistical evaluation criteria which are used to evaluate qualitative performance of the model is described in Table 2.1:

Table 2.1: Statistical evaluation criteria used for BDM calibration

Statistics	Very Good	Good	Satisfactory	Unsatisfactory	Reference
R^2	$0.80 < R^2 \leq 1.00$	$0.70 < R^2 \leq 0.80$	$0.60 < R^2 \leq 0.70$	$R^2 \leq 0.60$	(Duda et al. 2012)
NSE	$0.75 < NSE \leq 1.00$	$0.65 < NSE \leq 0.75$	$0.50 < NSE \leq 0.65$	$NSE \leq 0.50$	(Moriasi et al. 2007)
RSR	$0.00 \leq RSR \leq 0.50$	$0.50 < RSR \leq 0.60$	$0.60< RSR \leq 0.70$	$RSR > 0.70$	(Moriasi et al. 2007)

Out of the total 29 stations compared between BDM and measured data (Figure 2.7), statistical evaluation shows model performance varies either as ‘very good’ or as ‘good’ or as ‘satisfactory’ in 11 stations. On the other hand, in 18 stations, statistical evaluation shows that model performance is ‘unsatisfactory’. It is to be noted that out of these 18 stations, only 8 stations belong to the inland non-tidal water level stations and the rest 10 stations belong to the coastal tidal water level stations. Data source for most of the tidal stations is BWDB where only 3 hourly manual measured data is available. From these 3 hourly data, it is impossible to detect the details of the tidal phases and amplitudes in the measured data. This leads to ‘unsatisfactory’ performance of the model when compared with the measured data. Data source of 3 ocean tidal water level stations (Rangadia, Kutubdia 1, and Kutubdia 2) is Bangladesh Navy. Data from these 3 stations are continuous hourly measured data. Statistical comparison between BDM and measured data in these 3 stations show ‘very good’ performance of the model.

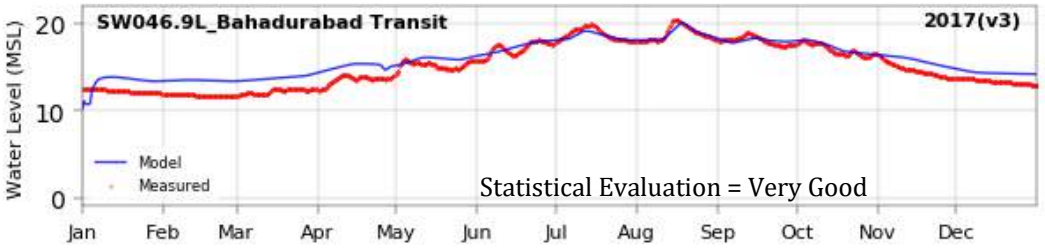

R^2 = 0.954, NSE=0.84, RMSE = 1.03, MSE = 1.06, MAE = 0.85, PBIAS = -4.44, RSR = 0.4

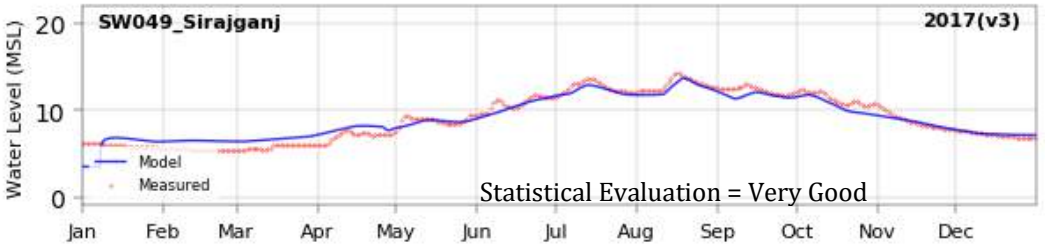

R^2 = 0.936, NSE=0.92, RMSE = 0.78, MSE = 0.62, MAE = 0.63, PBIAS = 0.54, RSR = 0.28

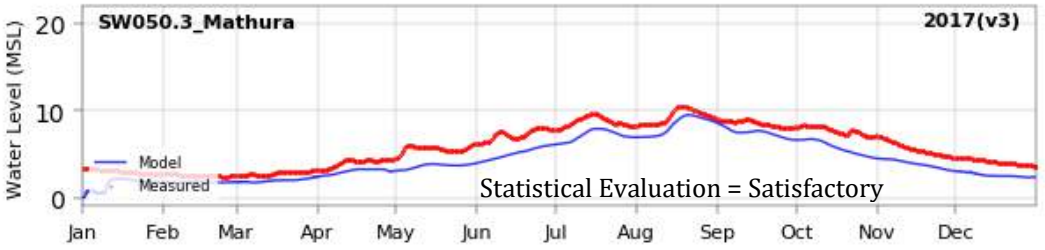

R^2 = 0.942, NSE=0.57, RMSE = 1.59, MSE = 2.52, MAE = 1.48, PBIAS = 25.41, RSR = 0.66

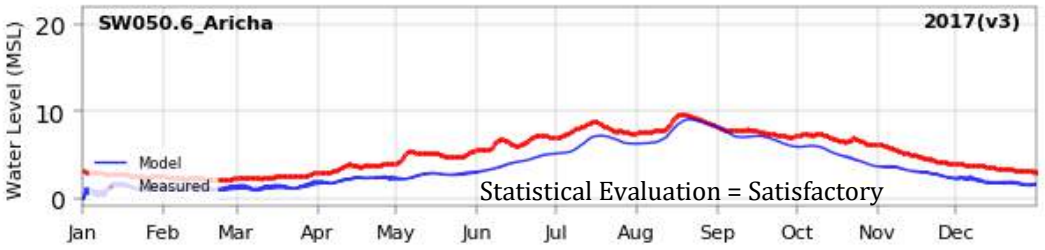

R^2 = 0.93, NSE=0.43, RMSE = 1.68, MSE = 2.82, MAE = 1.56, PBIAS = 30.19, RSR = 0.76

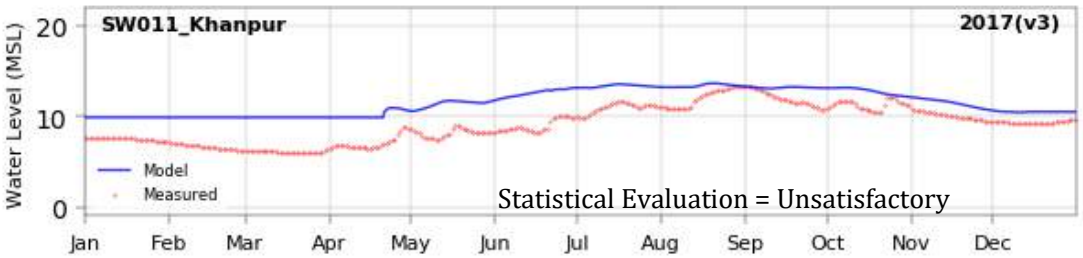

R^2 = 0.773, NSE=-0.53, RMSE = 2.59, MSE = 6.72, MAE = 2.35, PBIAS = -25.6, RSR = 1.24

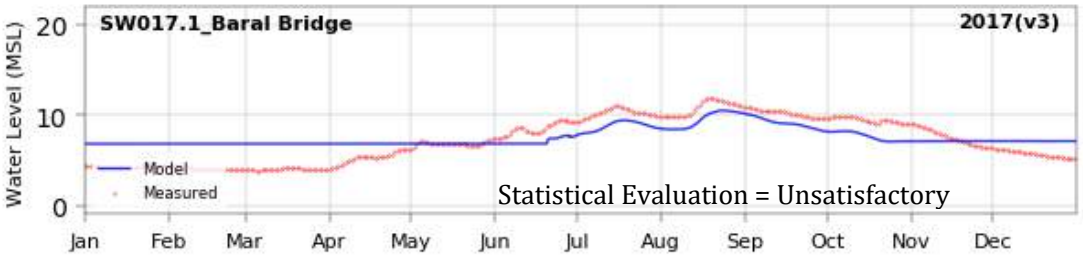

R^2 = 0.667, NSE=0.49, RMSE = 1.79, MSE = 3.22, MAE = 1.6, PBIAS = -3.56, RSR = 0.71

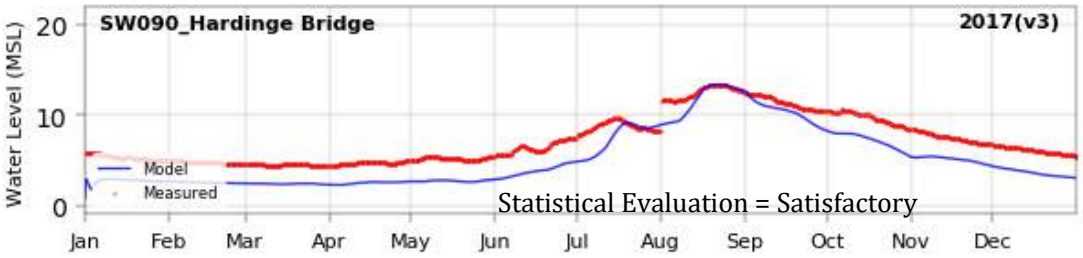

R^2 = 0.952, NSE=0.3, RMSE = 2.25, MSE = 5.07, MAE = 2.11, PBIAS = 28.79, RSR = 0.84

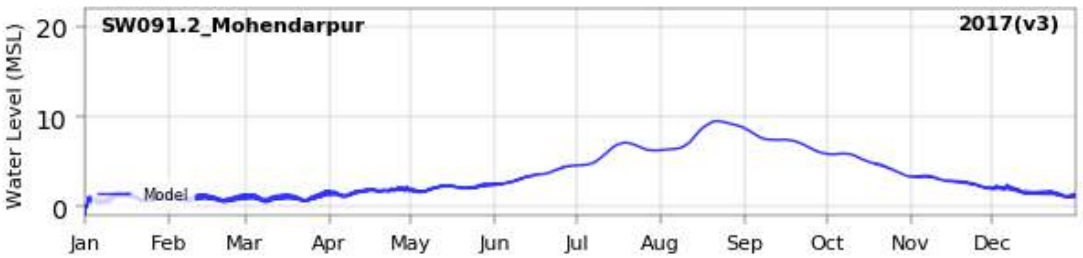

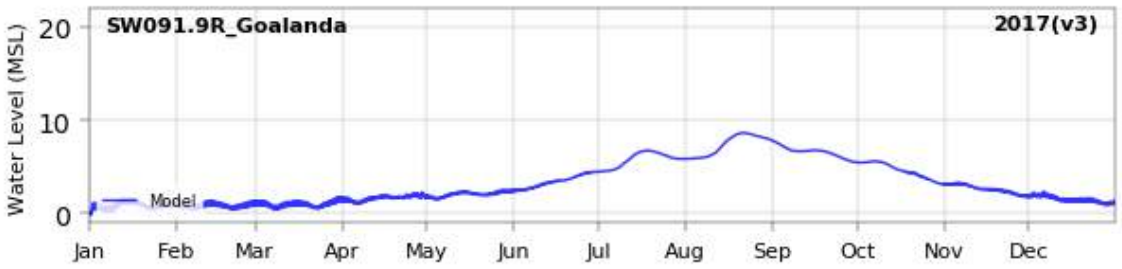

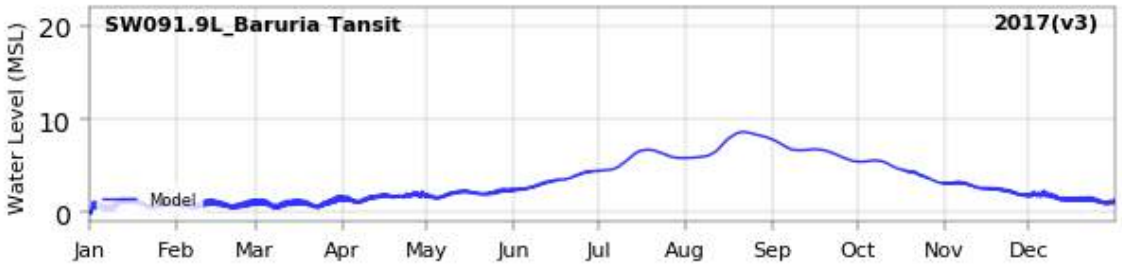

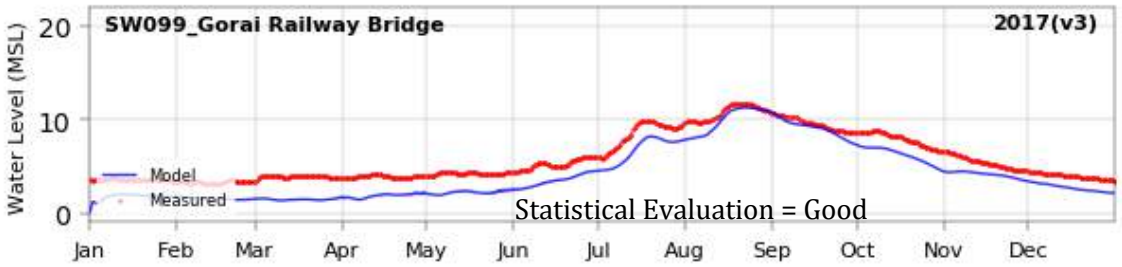

R^2 = 0.972, NSE=0.54, RMSE = 1.74, MSE = 3.02, MAE = 1.63, PBIAS = 27.73, RSR = 0.67

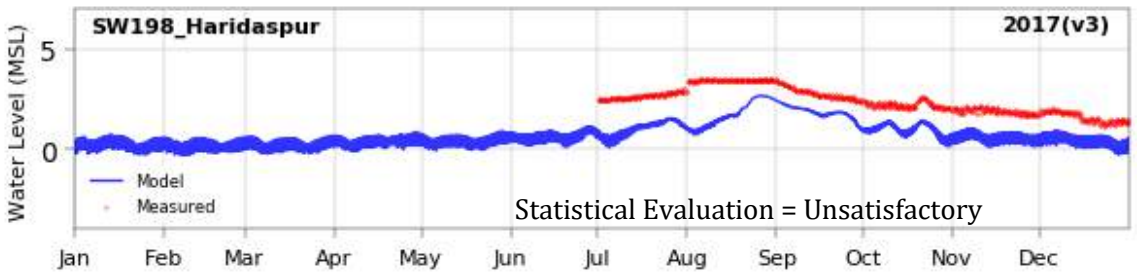

R^2 = 0.636, NSE=-3.83, RMSE = 1.39, MSE = 1.92, MAE = 1.32, PBIAS = 54.31, RSR = 2.2

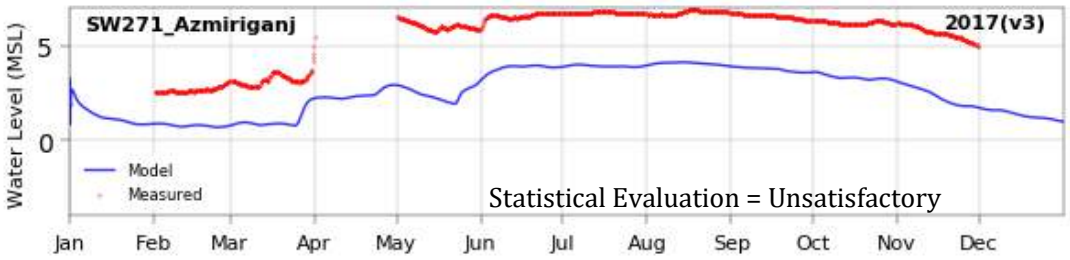

R^2 = 0.891, NSE=-2.77, RMSE = 2.84, MSE = 8.07, MAE = 2.79, PBIAS = 49.53, RSR = 1.94

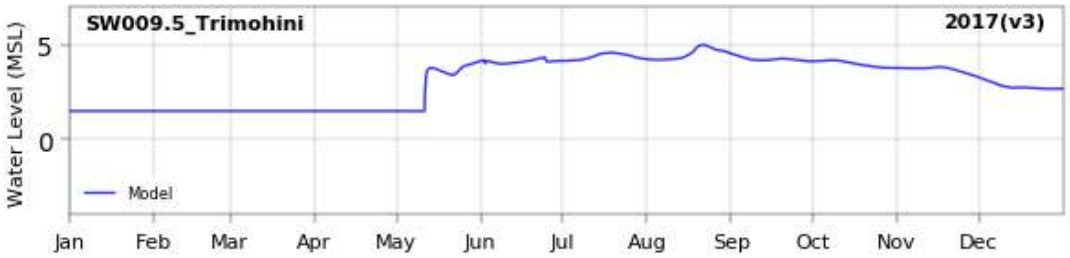

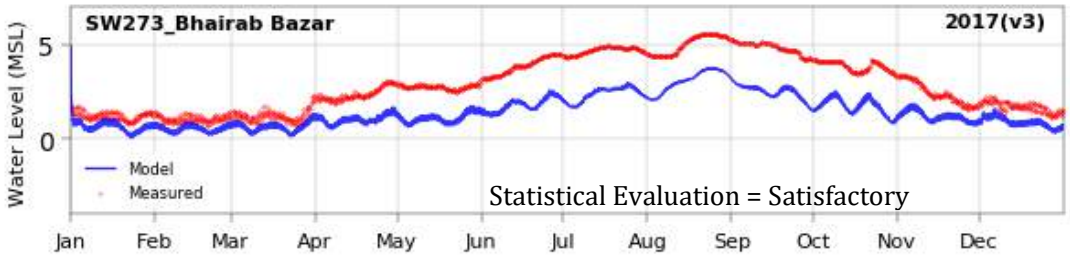

R^2 = 0.879, NSE=-0.28, RMSE = 1.65, MSE = 2.72, MAE = 1.49, PBIAS = 50.54, RSR = 1.13

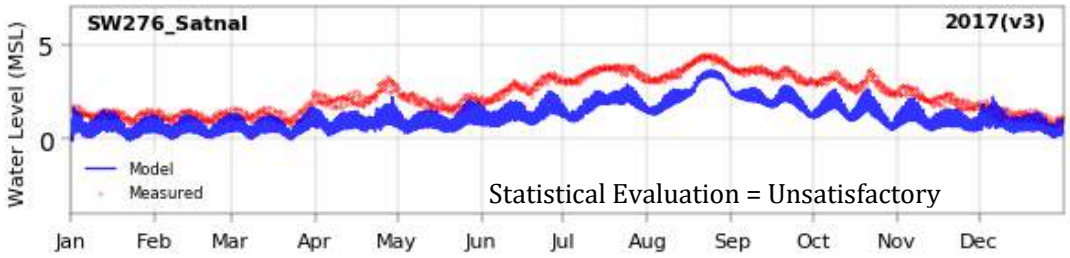

R^2 = 0.678, NSE=-0.66, RMSE = 1.25, MSE = 1.56, MAE = 1.13, PBIAS = 47.94, RSR = 1.29

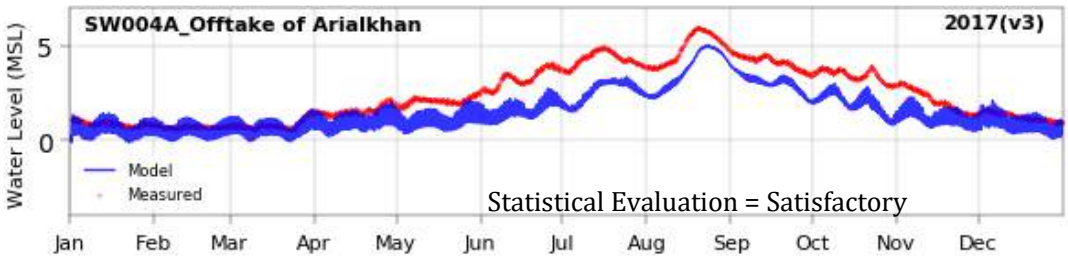

Statistical Evaluation = Satisfactory

R^2 = 0.818, NSE=0.42, RMSE = 1.11, MSE = 1.24, MAE = 0.93, PBIAS = 36.51, RSR = 0.76

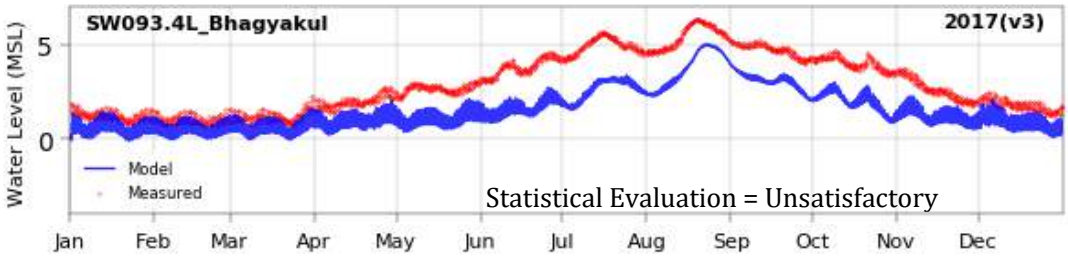

Statistical Evaluation = Unsatisfactory

R^2 = 0.822, NSE=0.03, RMSE = 1.53, MSE = 2.35, MAE = 1.36, PBIAS = 45.48, RSR = 0.99

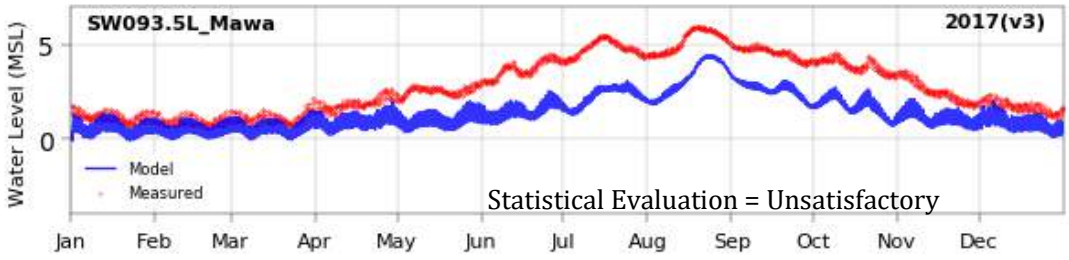

Statistical Evaluation = Unsatisfactory

R^2 = 0.788, NSE=-0.14, RMSE = 1.62, MSE = 2.62, MAE = 1.41, PBIAS = 49.11, RSR = 1.07

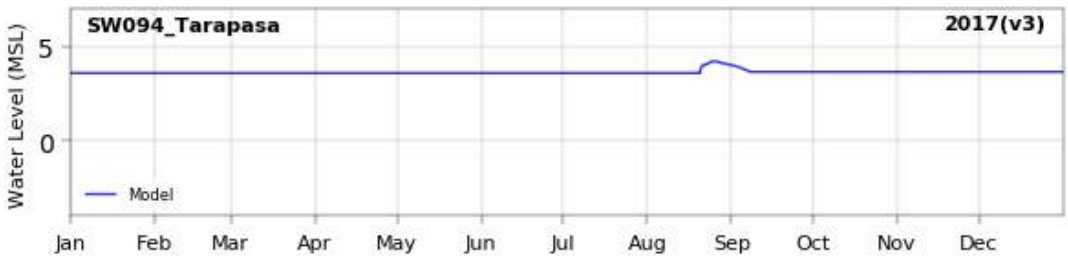

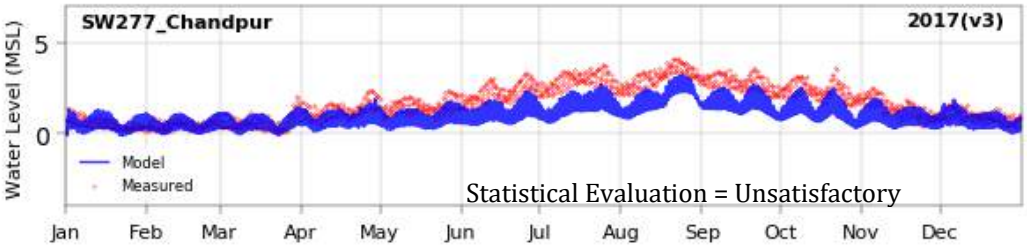

R^2 = 0.518, NSE=0.04, RMSE = 0.99, MSE = 0.97, MAE = 0.81, PBIAS = 40.84, RSR = 0.98

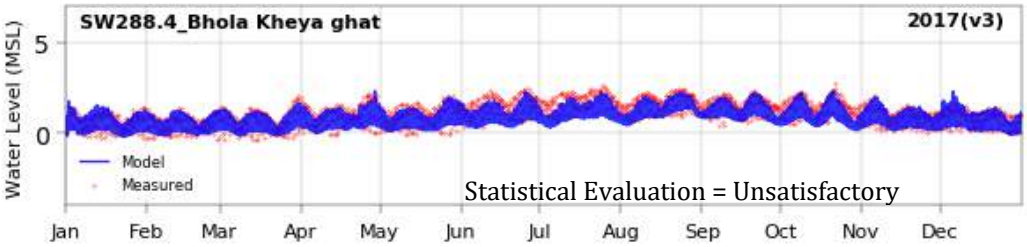

R^2 = 0.169, NSE=-0.15, RMSE = 0.67, MSE = 0.45, MAE = 0.58, PBIAS = 24.97, RSR = 1.07

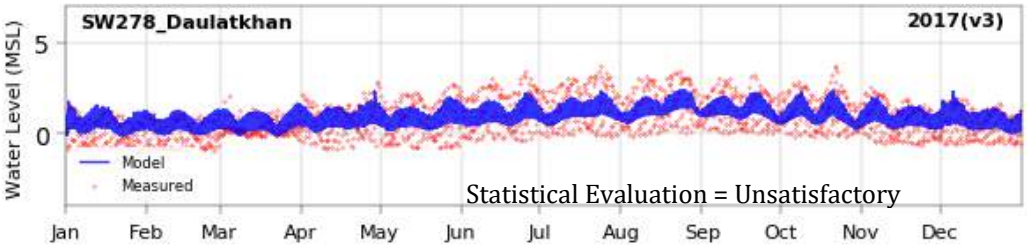

R^2 = 0.175, NSE=0.16, RMSE = 0.89, MSE = 0.79, MAE = 0.73, PBIAS = -8.33, RSR = 0.91

R^2 = 0.0, NSE=-0.58, RMSE = 2.22, MSE = 4.92, MAE = 1.43, PBIAS = -27.78, RSR = 1.26

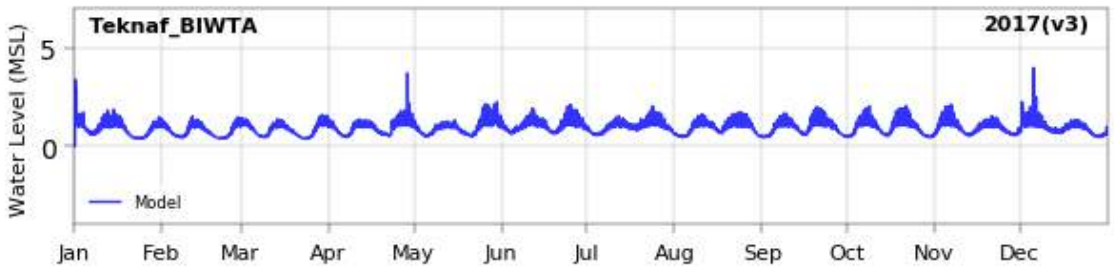

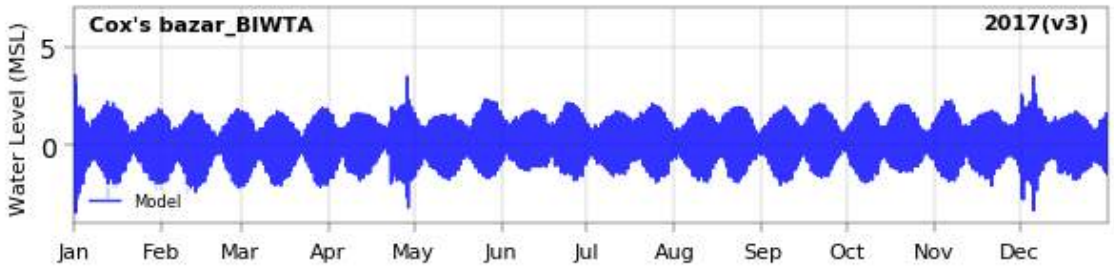

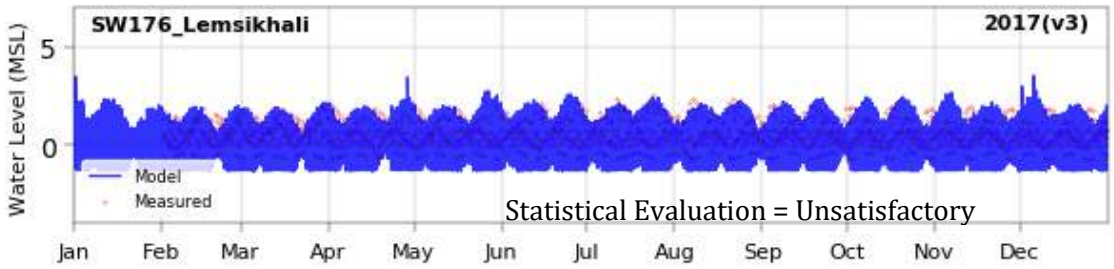

Statistical Evaluation = Unsatisfactory

R^2 = 0.063, NSE=-2.24, RMSE = 1.14, MSE = 1.29, MAE = 0.92, PBIAS = 47.03, RSR = 1.8

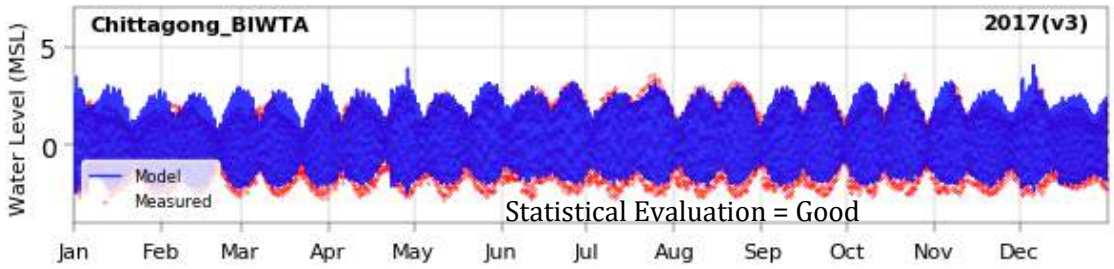

Statistical Evaluation = Good

R^2 = 0.777, NSE=0.76, RMSE = 0.7, MSE = 0.49, MAE = 0.59, PBIAS = -828.65, RSR = 0.49

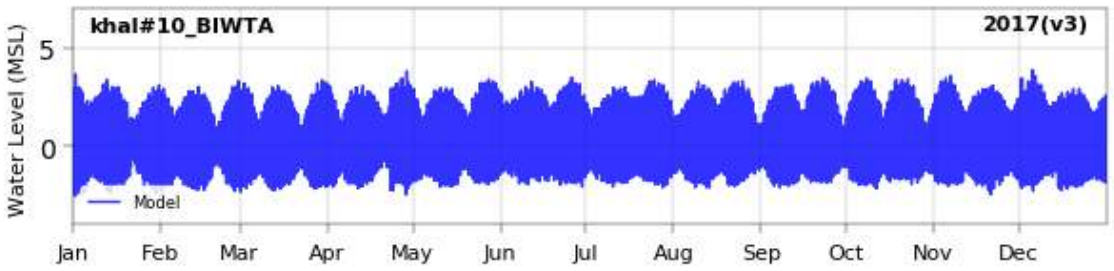

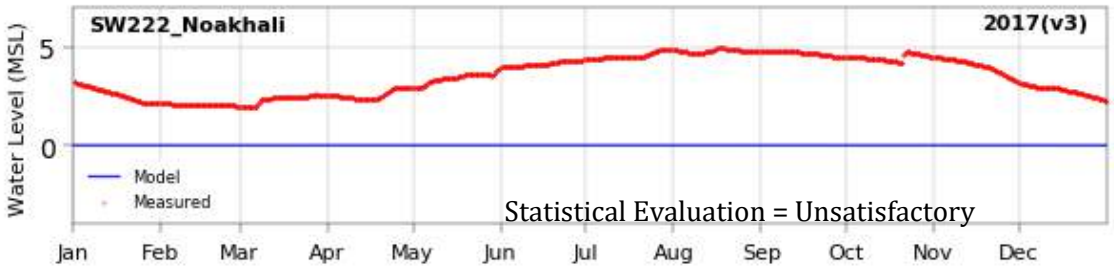

Statistical Evaluation = Unsatisfactory

R^2 = 0.038, NSE=-12.81, RMSE = 3.69, MSE = 13.64, MAE = 3.56, PBIAS = 99.99, RSR = 3.71

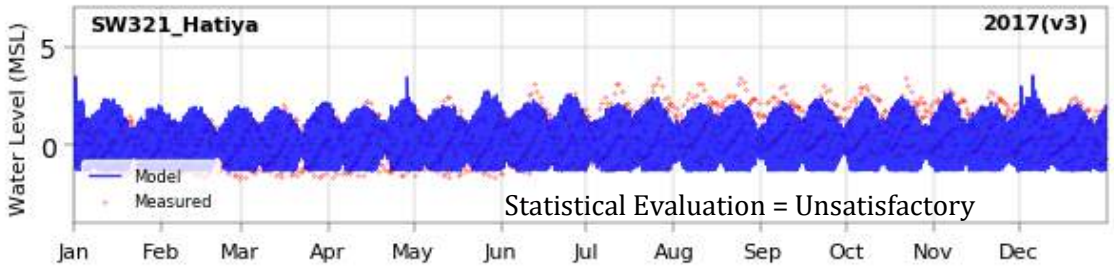

Statistical Evaluation = Unsatisfactory

R^2 = 0.591, NSE=-2.62, RMSE = 2.05, MSE = 4.19, MAE = 1.79, PBIAS = 46.62, RSR = 1.9

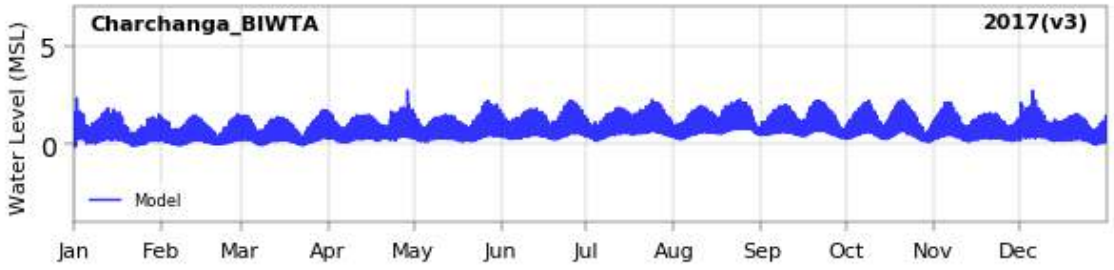

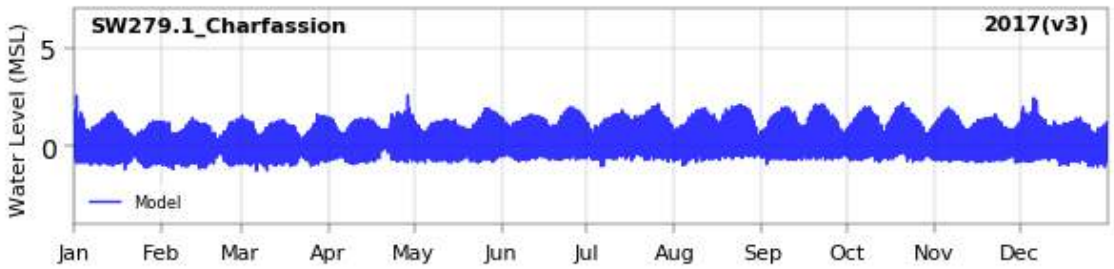

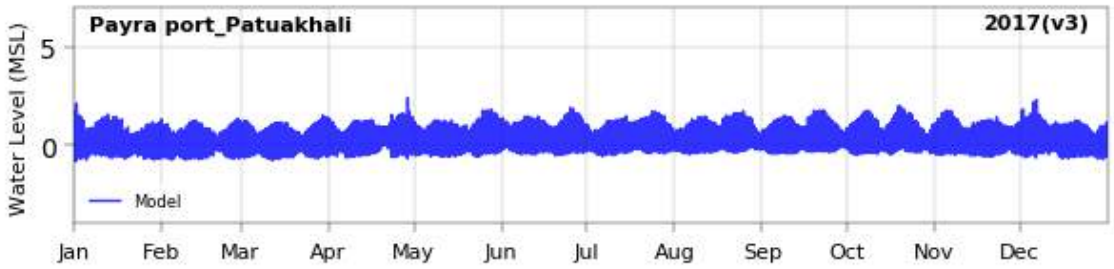

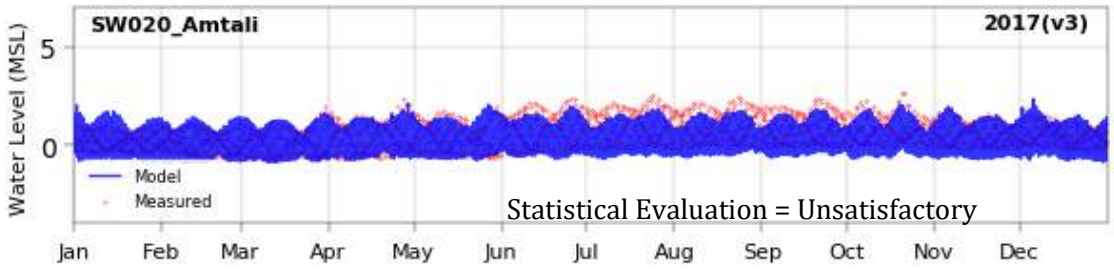

R^2 = 0.136, NSE=-0.26, RMSE = 0.77, MSE = 0.59, MAE = 0.66, PBIAS = 46.84, RSR = 1.12

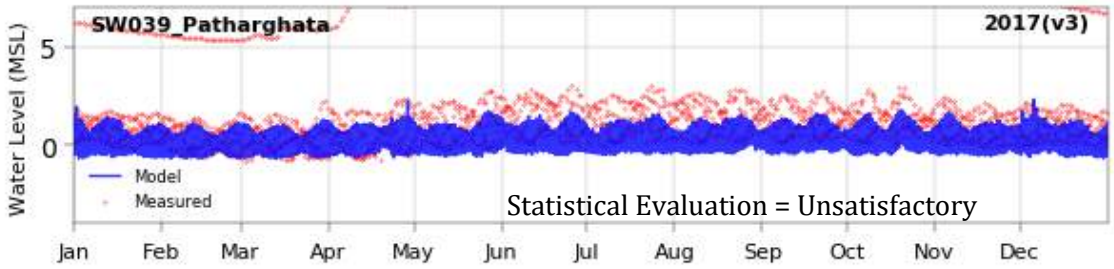

R^2 = 0.011, NSE=-0.32, RMSE = 3.63, MSE = 13.2, MAE = 2.0, PBIAS = 85.11, RSR = 1.15

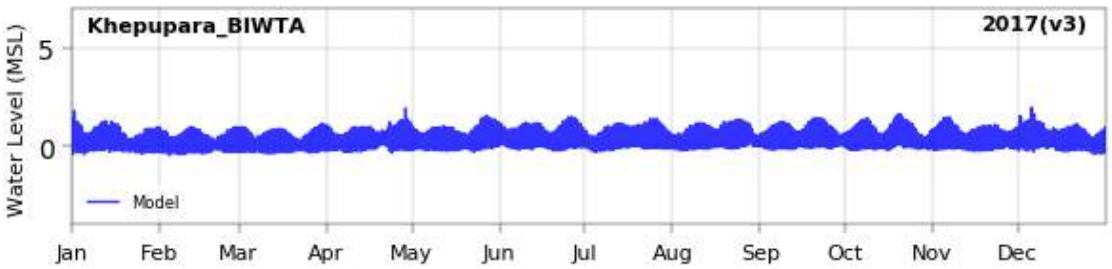

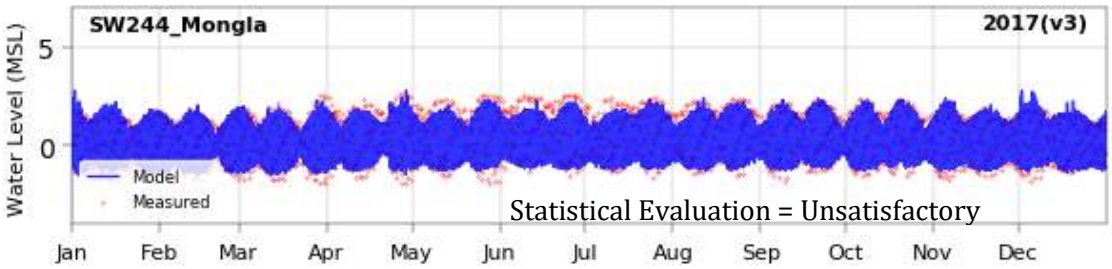

R^2 = 0.013, NSE=-0.83, RMSE = 1.57, MSE = 2.45, MAE = 1.36, PBIAS = 27.61, RSR = 1.35

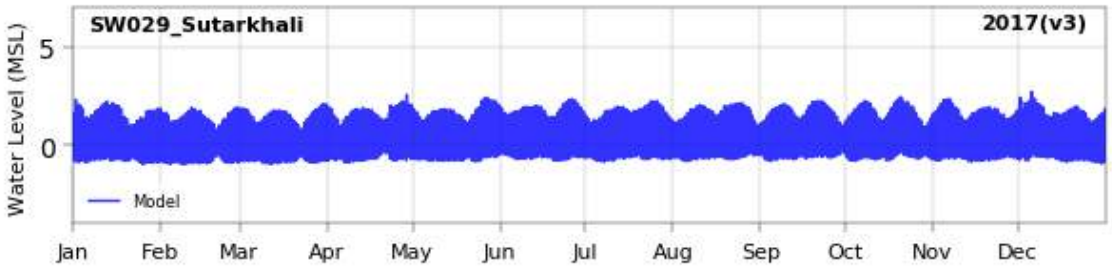

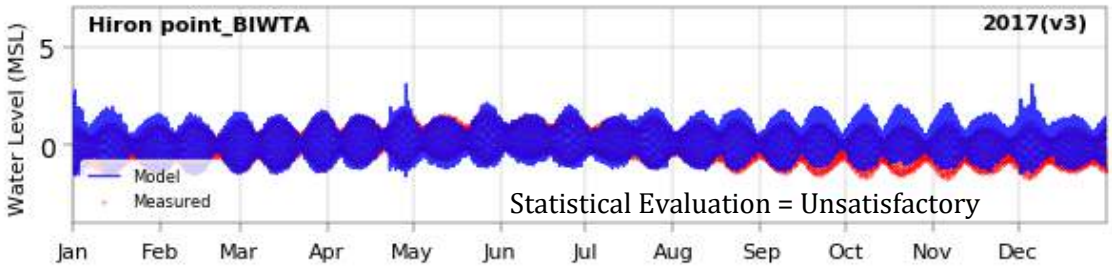

R^2 = 0.283, NSE=-0.19, RMSE = 0.76, MSE = 0.57, MAE = 0.62, PBIAS = 151872.81, RSR = 1.09

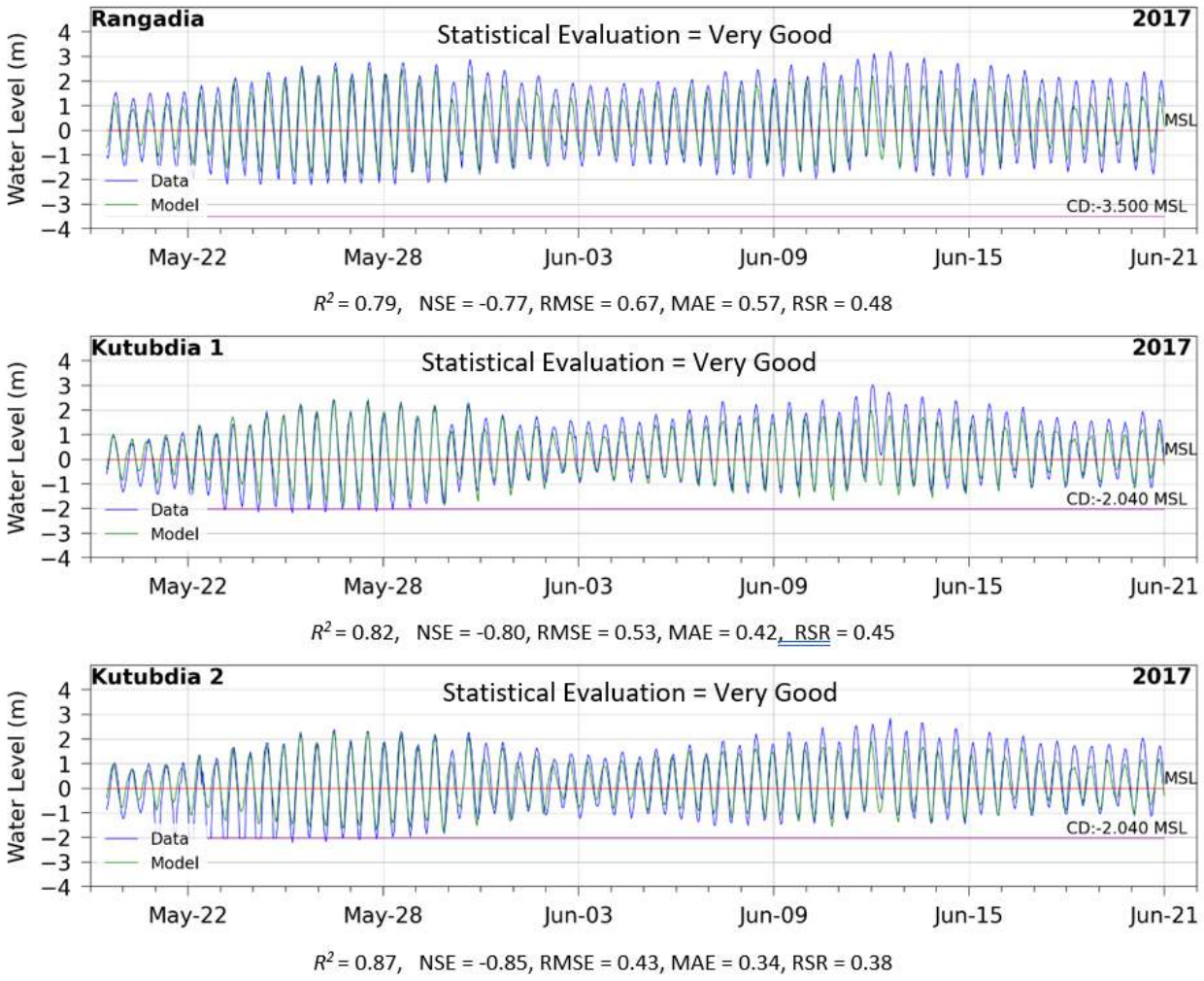

Figure 2.7: *Calibration of BDM shows comparison between measured data and BDM. Total 43 water level stations are selected for comparison of which measured data is available for 29 stations. The statistical evaluation criteria below each figure are used to determine qualitative performance of the model. The qualitative performance of the model is shown for each of the calibration results. In 3 water level simulation stations (SW094, SW058A, SW222), BDM simulates zero water level for the entire year. Locations of these stations could not be correctly determined from the available information. So, these stations are located on the land part of the model domain. We did not use any assumption about these locations because it might give a wrong information.*

2.5.2 Morphology model calibration

Morphology model is calibrated against measured sediment concentration data in one location and against spatiotemporal distribution of suspended sediment concentration along the major rivers, estuaries, coast, and ocean.

Time series comparison between the model and measurement is shown in Figure 2.8. To average out the temporal fluctuation of SSC, a 7-day moving average values of SSC are shown for

comparison along with error bars. Statistical comparison between the model and the measurement is shown by the error bars. Temporal distribution of error bars shows a reasonable performance of the model except slight phase shift of the peak values of SSC.

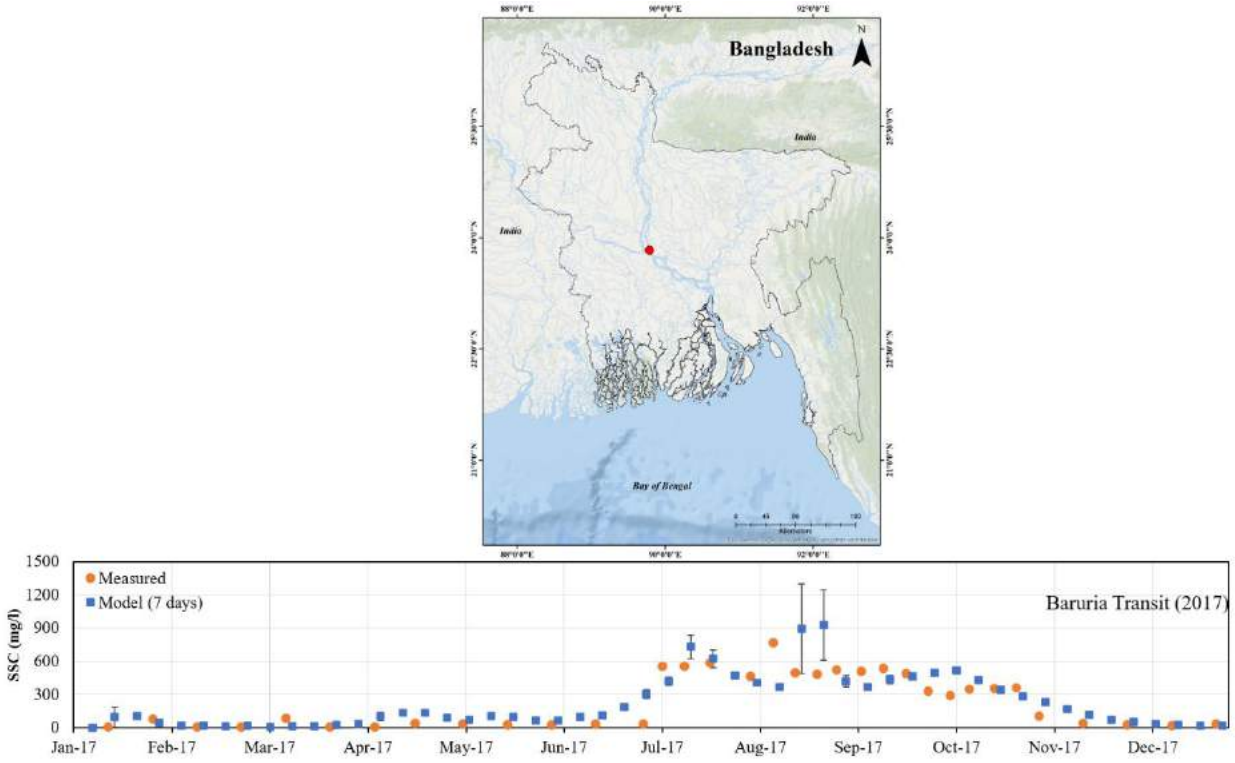

Figure 2.8: *Comparison between the model and the measured Suspended Sediment Concentration (SSC) for the year 2017 at station Baruria Transit in Padma River. This specific location represents total SSC coming from the Ganges and the Brahmaputra-Jamuna rivers. The error bar shows slight phase shift of peak value of SSC of the model from the measurement which leads to overprediction of the model during the initial phase of recession stage of SSC.*

Calibration is also performed against spatiotemporal distribution of suspended sediment concentration obtained from satellite image for the year 2017. Sediment concentration is calculated from regression analysis using bands reflectance of the sentinel images and measured concentration. Spatiotemporal sediment concentration behaviors of Ganges, Brahmaputra-Jamuna and Padma rivers and the mixing patterns of sediments at the confluence and coastal zone are studied. For calibration of the satellite image, sediment concentration data is collected from BWDB at 3 stations – Bahadurabad of Brahmaputra-Jamuna, Harding Bridge of Ganges and Baruria Transit of Padma. We have found good correlation between bands reflectance from the water bodies and measured sediment concentrations. All images are analyzed by Python programming language supported by Google earth engine.

In this study, Sentinel satellite images are used. The spatial resolution of the sentinel is 10 meters, and the revisit time is 5 days. Here, we have used seven bands out of 12 spectral bands. Google earth engine, a cloud based computational platform is used to extract the band reflectance from sentinel satellite images. For regression analysis we have selected the images based on the sediment sample collection time. The image and the sample collection date are not matched in most of the cases. So, we considered forward or backward three days from the sample collection day. Total 49 matched samples are found from 2017 to 2018.

Out layer data was omitted from the measured sediment concentration. Cohesive sediment concentration is added with non-cohesive sediment concentration to get the total sediment concentration. Ninety percentile data is considered for this analysis.

From the raw satellite image, we get atmospheric reflection because there is cloud, cloud shadow and different types of gasses in the atmosphere. Atmospheric correction is done to get earth surface reflectance. Water vapor, ozone, aerosol, and land elevation data are collected during image collection time from earth engine database to correct sentinel image reflectance. Python 6S module is used for complex calculation that removes atmospheric gaseous components. After all correction, bands reflectance data are extracted manually from atmospheric corrected images for Bahadurabad, Harding Bridge and Baruria Transit stations. Figure 2.9 shows the difference between raw image and corrected image.

Figure 2.9: *Difference between raw image and corrected image. The corrected image is later used to extract the SSC data. The extracted SSC data represents only the surface sediment concentration.*

Linear and polynomial regression analysis are done to establish the correlation between the water surface reflectance and measured sediment concentration. Single and multiple bands are used. For single band linear regression, two types of data are used. Type 1 is single bands and type 2 is ratio of two bands. Regression analysis types used in this study is shown in Figure 2.10.

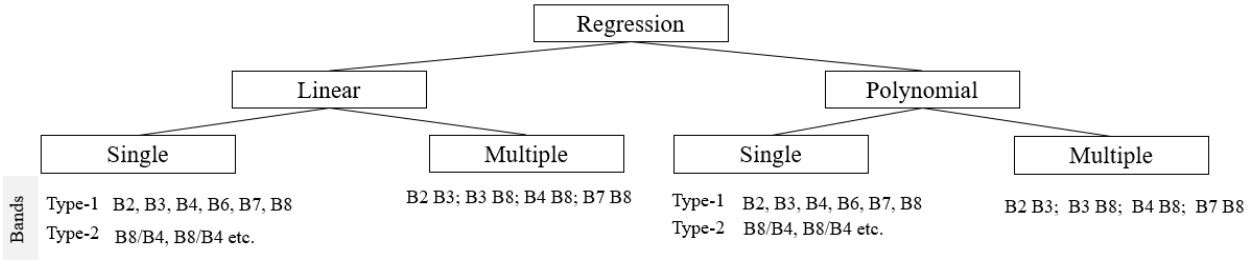

Figure 2.10: *Regression analysis for image processing. Different bands used in the analysis are also shown.*

From the above methods, we got the best result from the multiple linear regression analysis using the bands B3 and B8. The equation and R^2 value are given below.

$$Y = B3*-0.19 + B8*1.56$$

And $R^2 = 0.79$

Comparisons of spatial distribution of suspended sediment concentration between the BDM simulation and the satellite image at different time of the year 2017 are shown in Figure 2.11.

(a) BDM Comparison against Satellite Image of SSC for Brahmaputra-Jamuna-Ganges – 12 April 2017

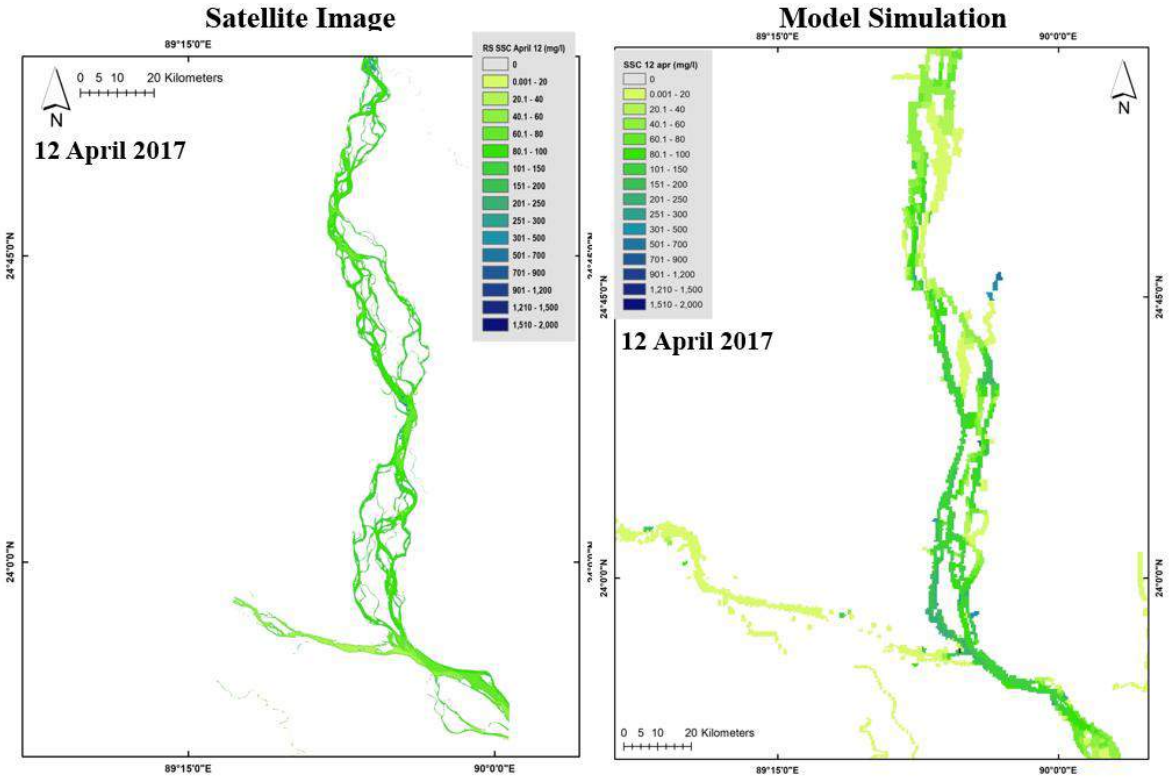

(b) BDM Comparison against Satellite Image of SSC for Brahmaputra-Jamuna-Ganges – 2 May 2017

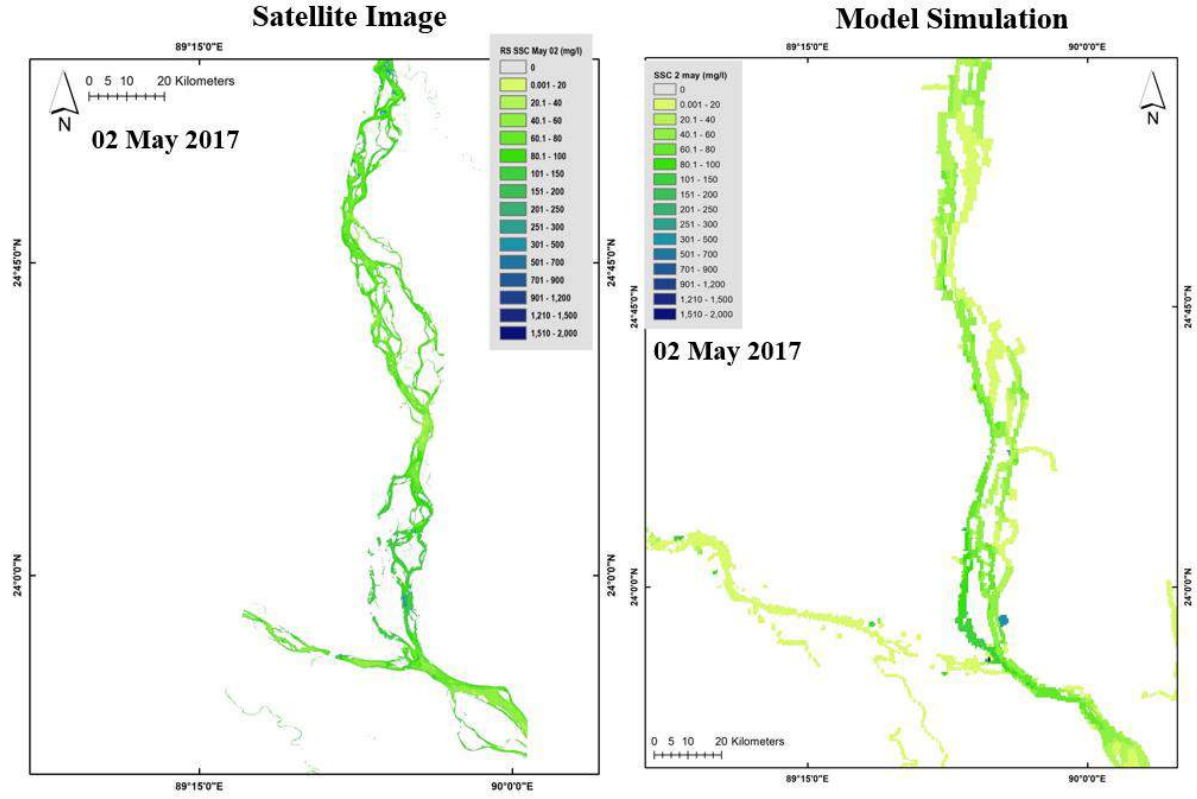

(c) BDM Comparison against Satellite Image of SSC for Brahmaputra-Jamuna-Ganges – 24 September 2017

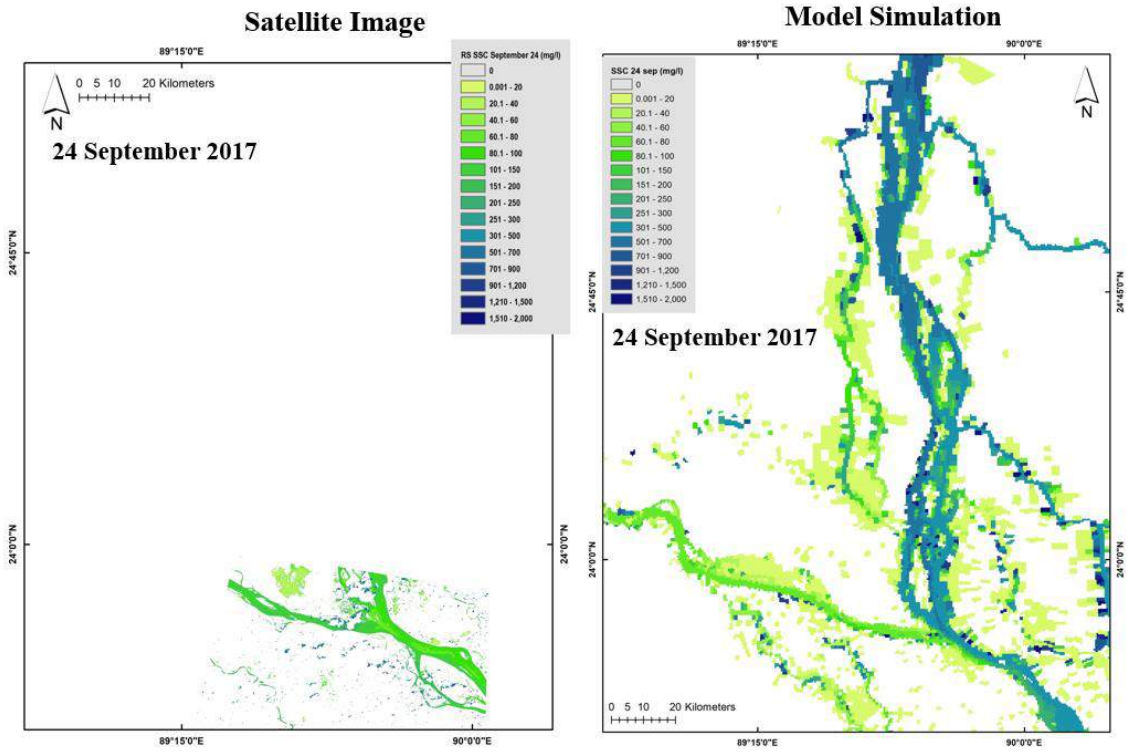

(d) BDM Comparison against Satellite Image of SSC for Brahmaputra-Jamuna-Ganges – 17 October 2017

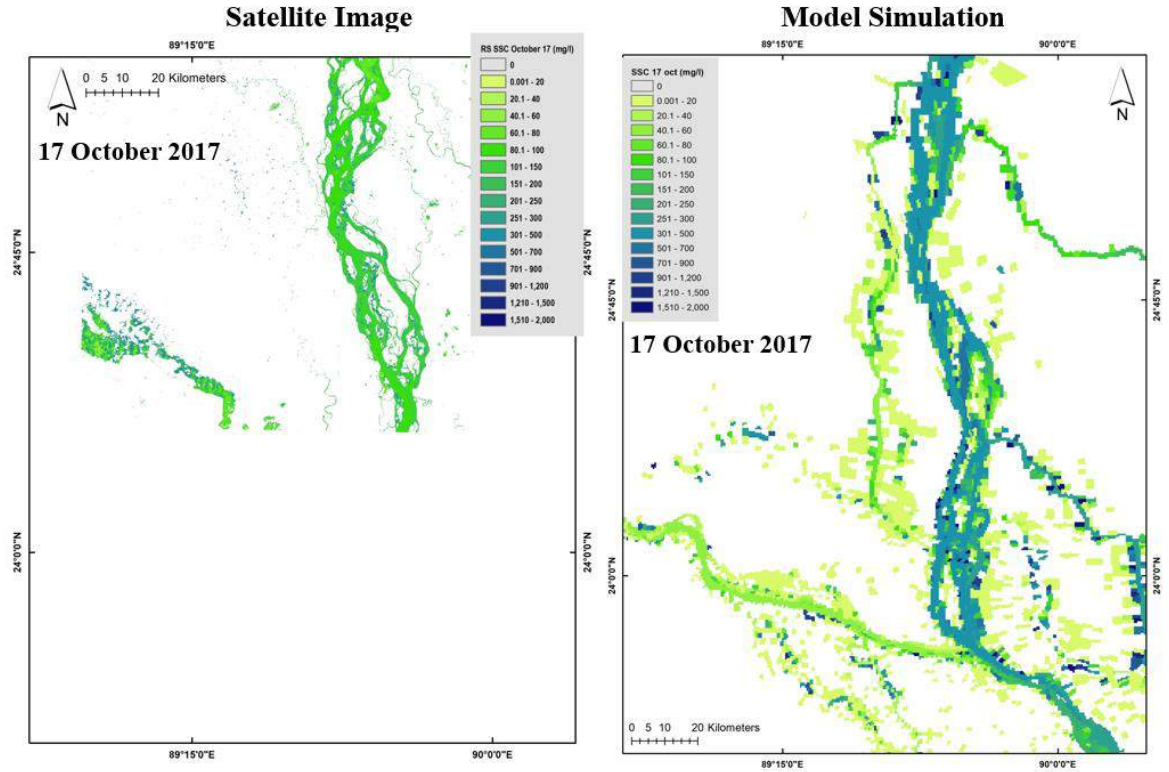

(e) BDM Comparison against Satellite Image of SSC for Coastal Region – 12 April 2017

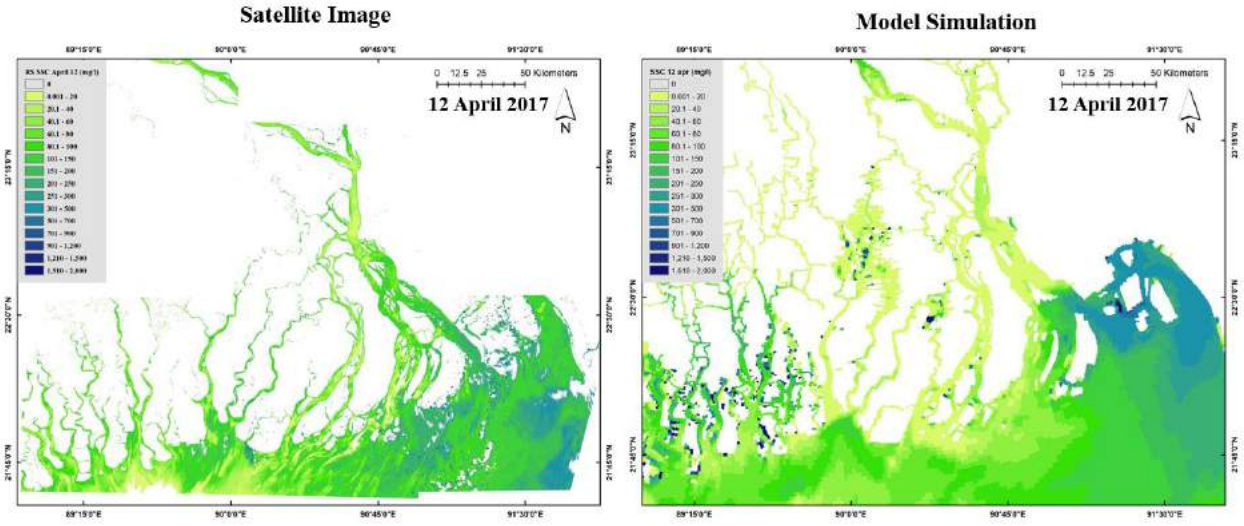

(f) BDM Comparison against Satellite Image of SSC for Coastal Region – 2 May 2017

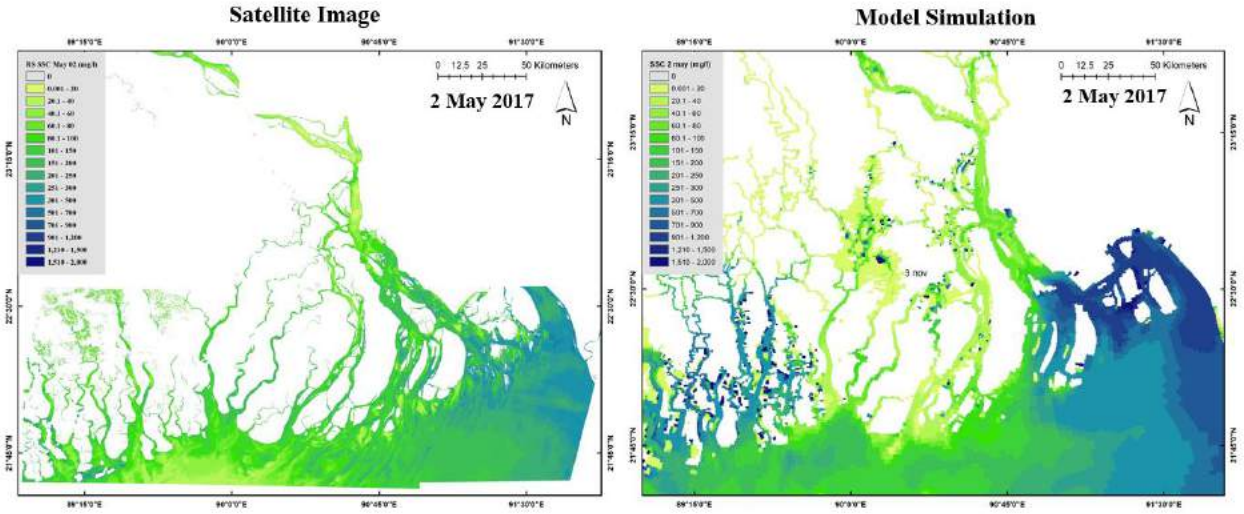

(g) BDM Comparison against Satellite Image of SSC for Coastal Region – 24 September 2017

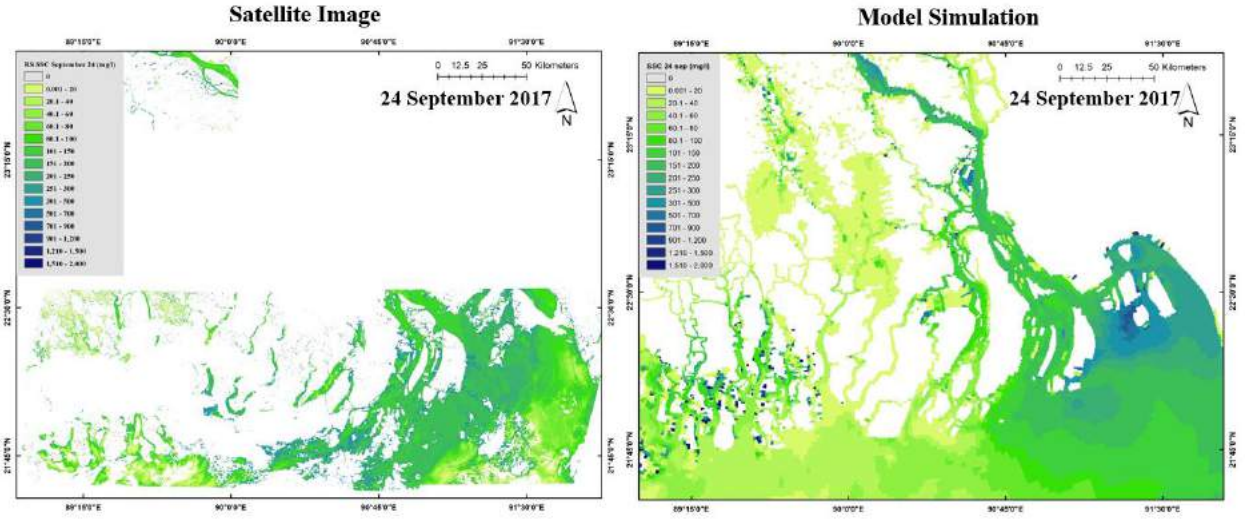

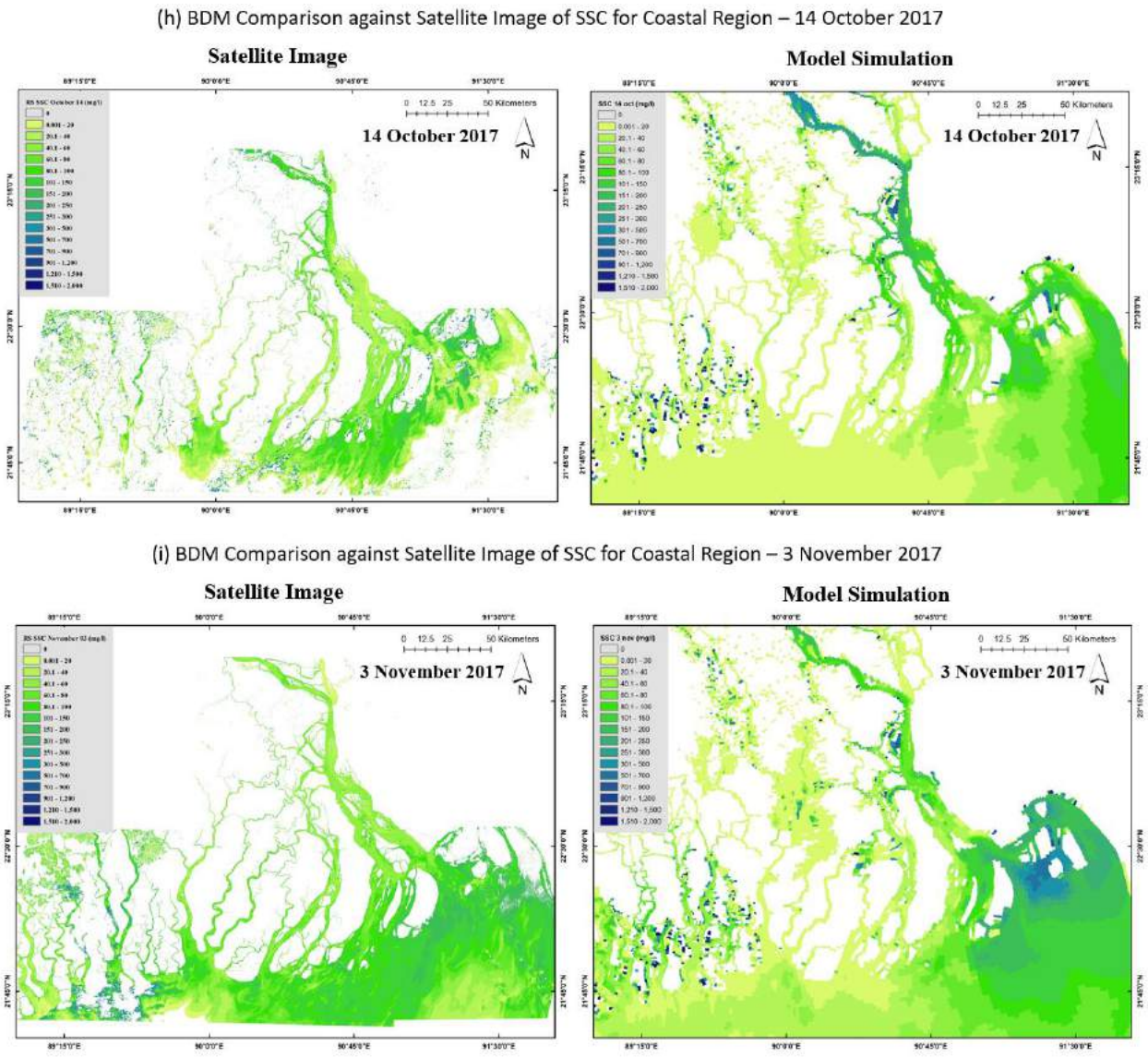

Figure 2.11: *Calibration of BDM. Comparison of spatial distribution of suspended sediment concentration in the months of March, April, May, September, October, and November of 2017 in different locations of the rivers, estuaries, and ocean in different dates (a-d) along the Ganges, Brahmaputra-Jamuna, and Padma rivers (e-i) along the coastal region and ocean.*

Figures 6(a-d) show the comparison between image and BDM along the Ganges, Brahmaputra-Jamuna, and Padma rivers and Figures 6(e-i) show the comparison for the coastal region. Satellite images show SSC distribution only in surface layer of a water body. On the other hand, model simulation shows depth averaged SSC which contains sediment concentration values over the depths of the water body. BDM reasonably reproduced spatiotemporal distribution of SSC in the system specially the zone of turbidity maximum in the Lower Meghna Estuary (Sarker et al., 2011). The BDM also simulates the fact that sediment concentration remains high both in dry season and

in monsoon in the north-eastern part of the Sandwip channel (Sarker et al., 2011). The important feature of higher SSC along the Sandwip-Urir char region is well simulated. This sediment ultimately is building land in the region. The process of sediments transporting through the Ganges, Brahmaputra-Jamuna, Padma, and Lower Meghna rivers is also well reproduced. Sediments from the major river systems transport to the Bay of Bengal and later re-enters into the system through Coriolis and tidal forcing. Seasonal variability of sediment concentration along this propagation path is well simulated by BDM.

2.6 BDM Validation

After completion of calibration, BDM is validated with the same parameters that were used during model calibration. For flow model validation, we selected the year 2019 to compare BDM simulated water level against measured water level and year 1998 to compare BDM simulated inundation map against inundation map from satellite image. For morphology model validation, we used sediment depth data in floodplain from secondary sources in few locations of Sundarban region and compare these with BDM simulation.

2.6.1 Flow model validation

For flow model validation, water level comparison is made against 40 water level stations which are same as calibration stations minus 3 stations (Rangadia, Kutubdia-1, Kutubdia-2) (Figure 2.6). Out of these 40 stations, measured data are available in 23 locations. Source of measured data for the water levels are: Bangladesh Water Development Board (BWDB) and Bangladesh Inland Water Transport Authority (BIWTA). The selected 40 water level stations cover both the non-tidal and tidal water level stations in inland and in coastal areas.

Qualitative performance of the model validation is done by using statistical evaluation criteria as we did for model calibration (Table 2.1). For validation, out of 23 measuring stations where measured data are available, we found statistical evaluation of the model performance as either ‘very good’ or as ‘good’ or as ‘satisfactory’ for 11 stations and evaluation of the rest 12 stations shows ‘unsatisfactory’ model performance. Out of these 12 ‘unsatisfactory’ model performance stations, only 2 stations belong to non-tidal water level stations and the rest 10 stations belong to the tidal water level stations. Most of these 10 tidal water level stations belong to BWDB where measured data are from 3 hourly manual measuring stations. It is not possible to detect the real tidal phase and amplitude from these 3 hourly data. This makes statistical evaluation of the model for these stations as ‘unsatisfactory’.

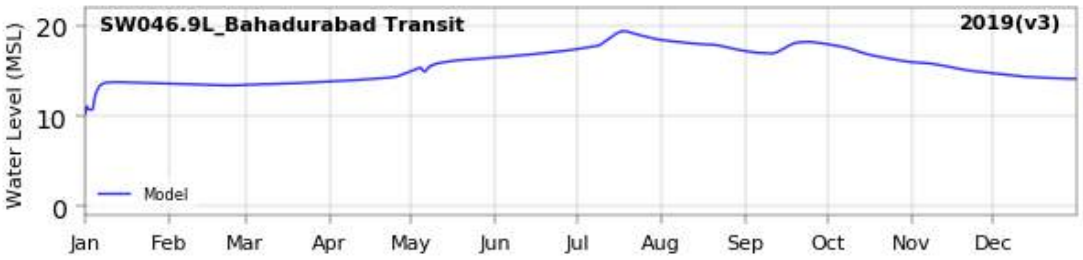

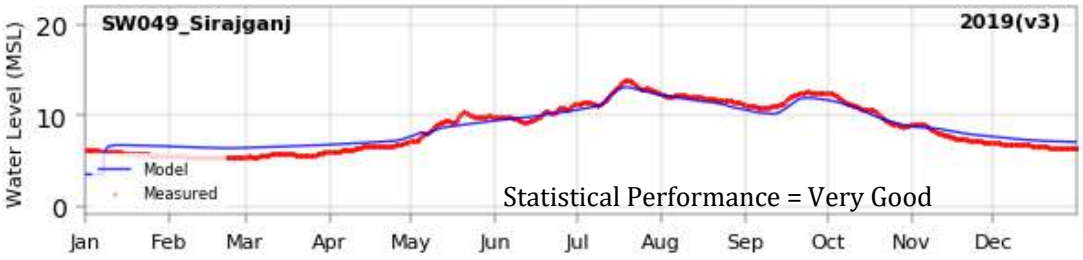

R^2 = 0.937, NSE=0.92, RMSE = 0.75, MSE = 0.57, MAE = 0.64, PBIAS = -1.09, RSR = 0.29

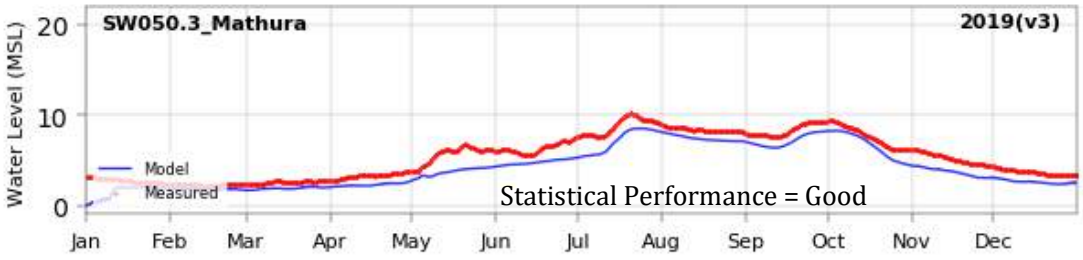

R^2 = 0.948, NSE=0.7, RMSE = 1.35, MSE = 1.81, MAE = 1.22, PBIAS = 22.54, RSR = 0.55

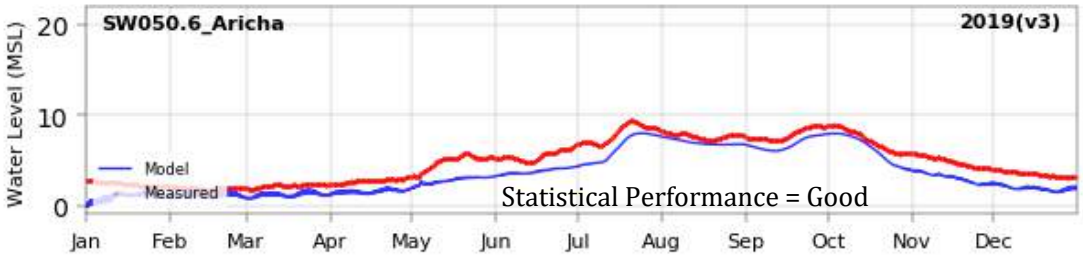

R^2 = 0.949, NSE=0.61, RMSE = 1.47, MSE = 2.15, MAE = 1.36, PBIAS = 27.69, RSR = 0.63

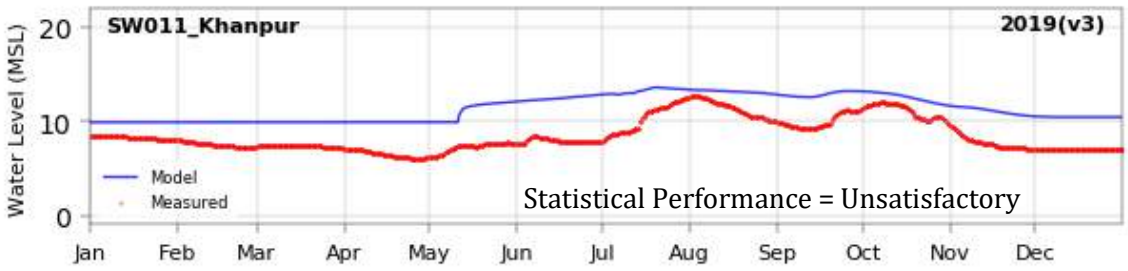

R^2 = 0.644, NSE=-1.94, RMSE = 3.03, MSE = 9.17, MAE = 2.84, PBIAS = -33.22, RSR = 1.72

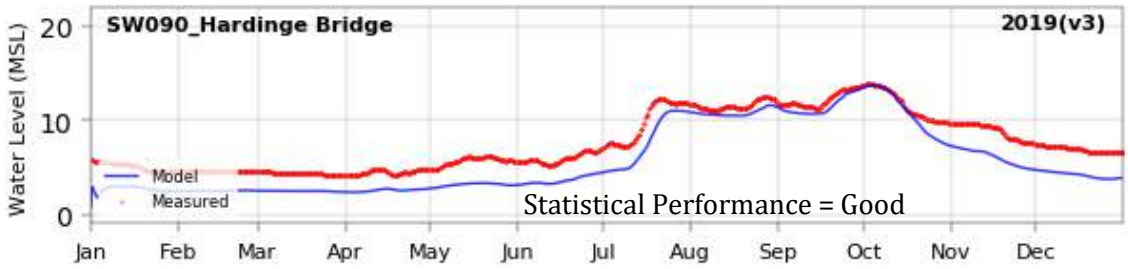

R^2 = 0.967, NSE=0.52, RMSE = 2.13, MSE = 4.52, MAE = 1.95, PBIAS = 25.6, RSR = 0.69

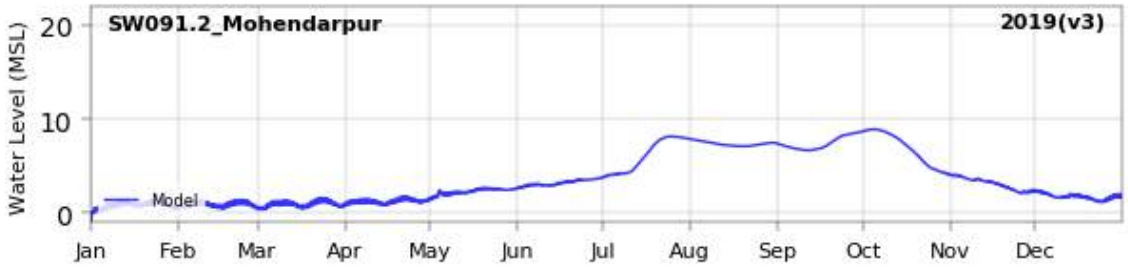

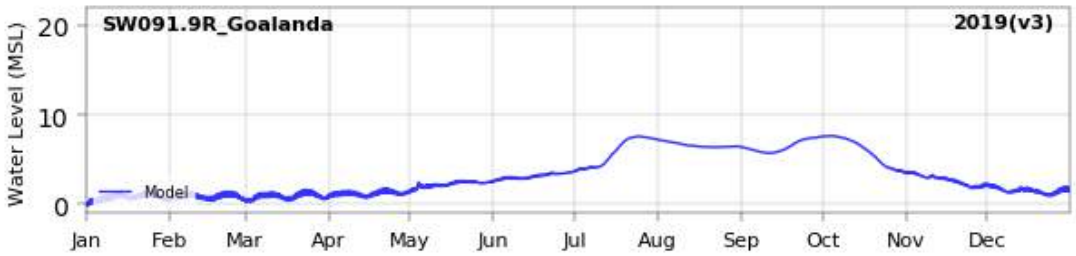

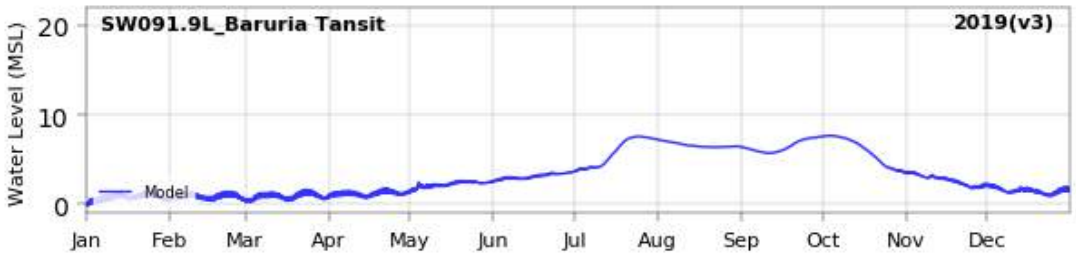

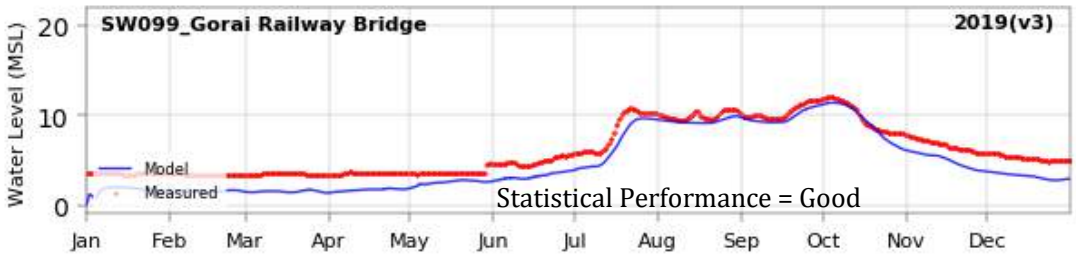

R^2 = 0.98, NSE=0.69, RMSE = 1.58, MSE = 2.51, MAE = 1.46, PBIAS = 23.86, RSR = 0.55

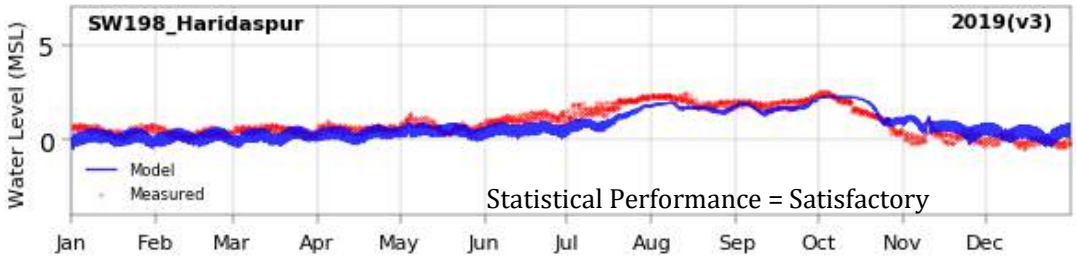

R^2 = 0.641, NSE=0.55, RMSE = 0.5, MSE = 0.25, MAE = 0.42, PBIAS = 20.86, RSR = 0.67

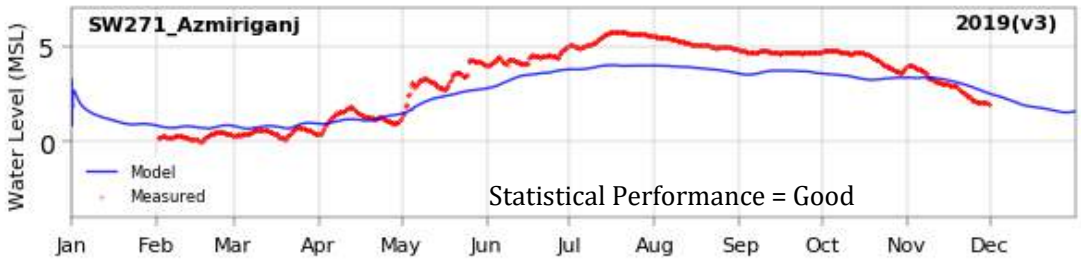

R^2 = 0.936, NSE=0.73, RMSE = 0.97, MSE = 0.93, MAE = 0.84, PBIAS = 18.91, RSR = 0.52

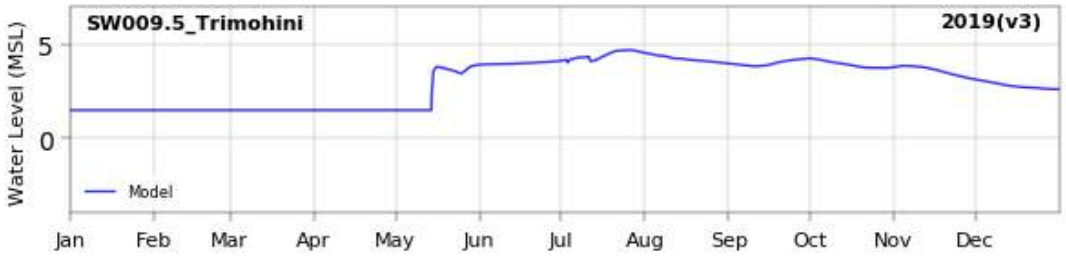

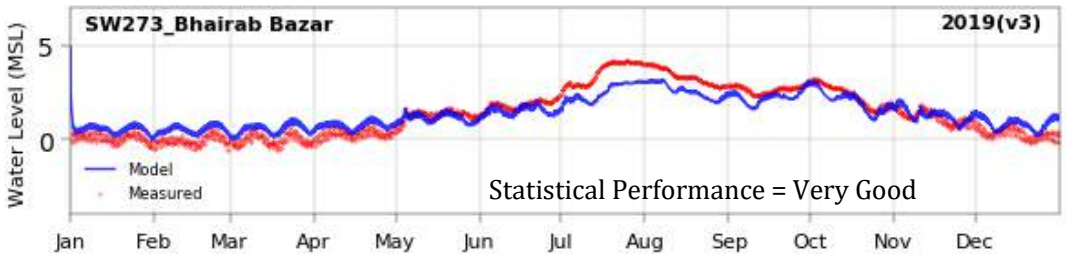

R^2 = 0.914, NSE=0.8, RMSE = 0.59, MSE = 0.35, MAE = 0.51, PBIAS = 3.39, RSR = 0.45

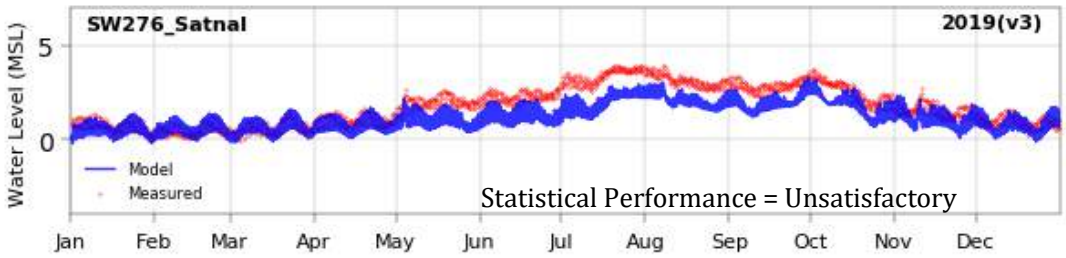

R^2 = 0.647, NSE=0.28, RMSE = 0.89, MSE = 0.79, MAE = 0.75, PBIAS = 34.64, RSR = 0.85

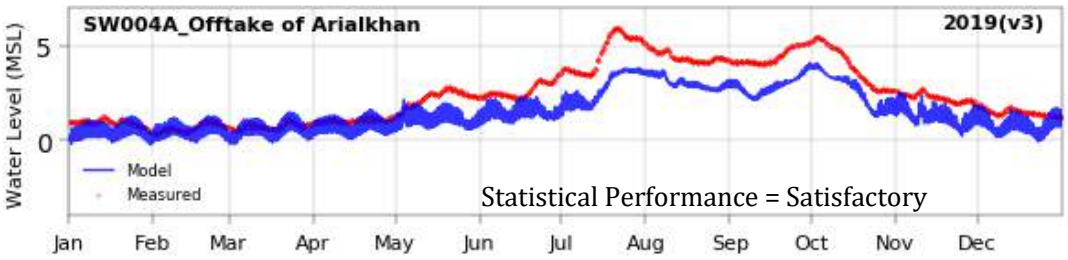

R^2 = 0.869, NSE=0.46, RMSE = 1.13, MSE = 1.29, MAE = 0.96, PBIAS = 37.27, RSR = 0.73

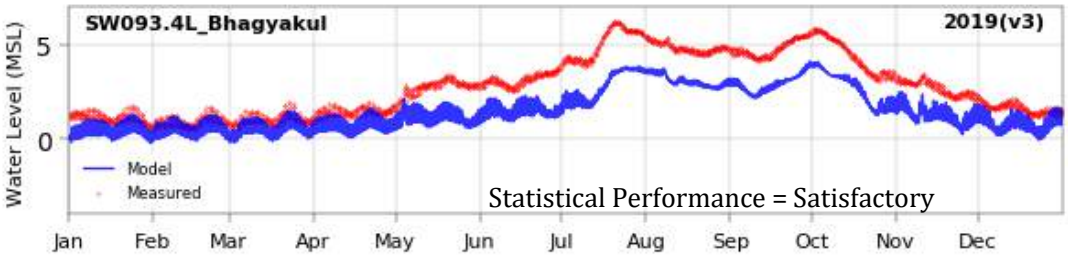

R^2 = 0.872, NSE=0.2, RMSE = 1.44, MSE = 2.08, MAE = 1.27, PBIAS = 44.14, RSR = 0.9

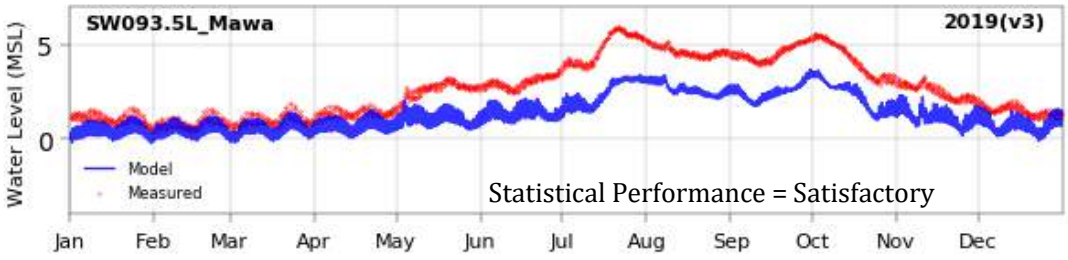

R^2 = 0.848, NSE=0.05, RMSE = 1.51, MSE = 2.29, MAE = 1.3, PBIAS = 47.65, RSR = 0.97

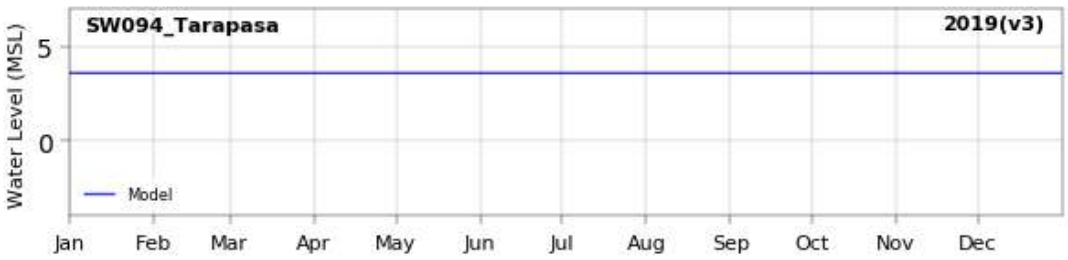

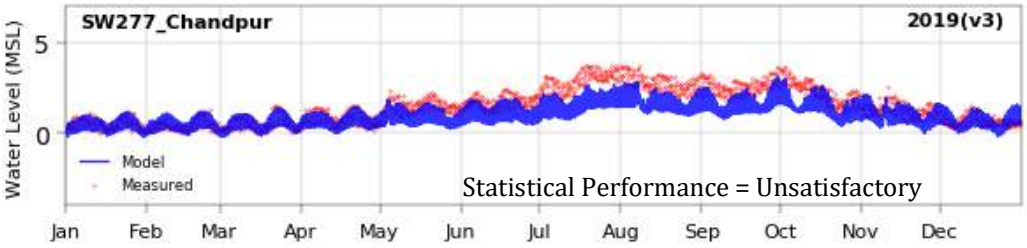

R^2 = 0.512, NSE=0.19, RMSE = 0.88, MSE = 0.77, MAE = 0.71, PBIAS = 36.0, RSR = 0.9

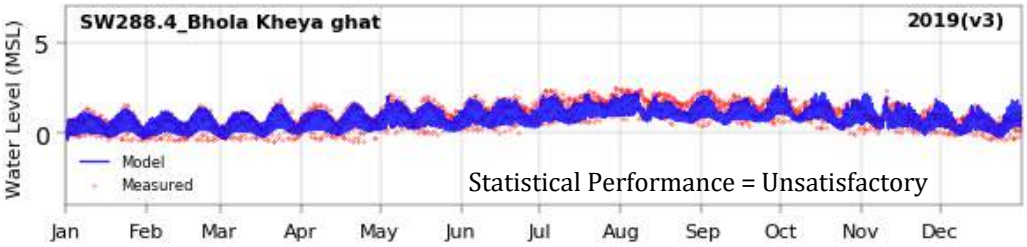

R^2 = 0.113, NSE=-0.13, RMSE = 0.72, MSE = 0.51, MAE = 0.61, PBIAS = 17.68, RSR = 1.06

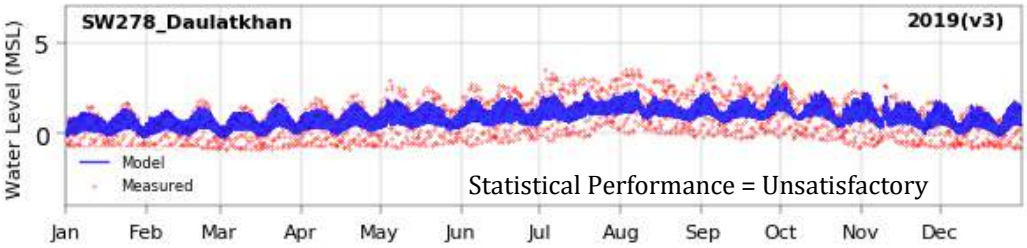

R^2 = 0.108, NSE=0.06, RMSE = 0.98, MSE = 0.97, MAE = 0.82, PBIAS = -19.16, RSR = 0.97

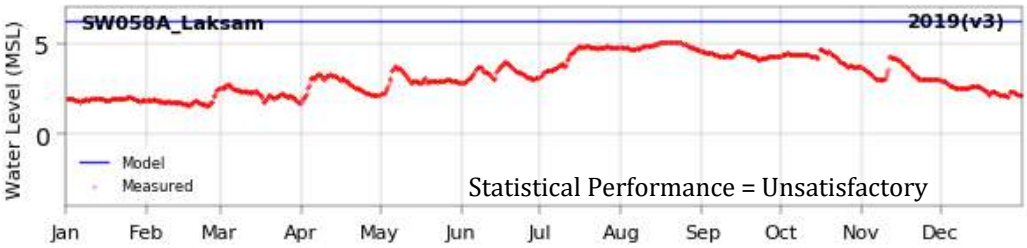

R^2 = 0.0, NSE=-8.04, RMSE = 3.13, MSE = 9.82, MAE = 2.95, PBIAS = -91.07, RSR = 3.01

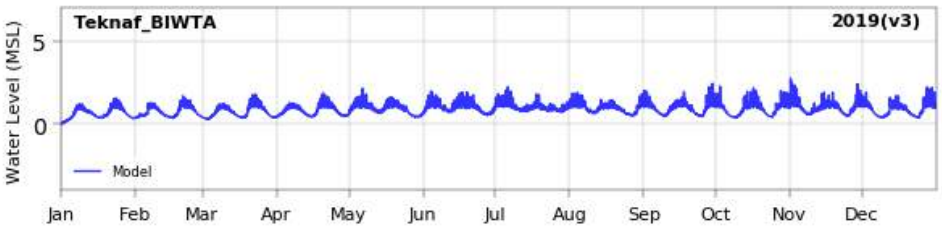

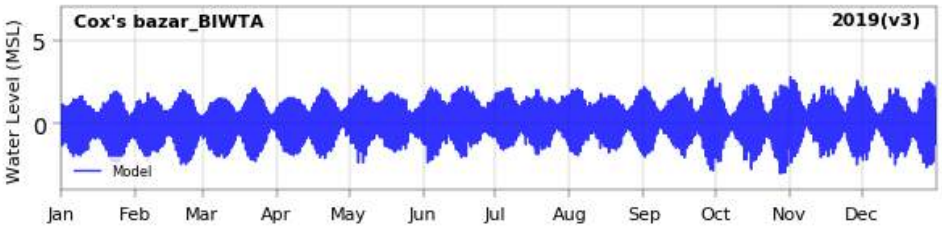

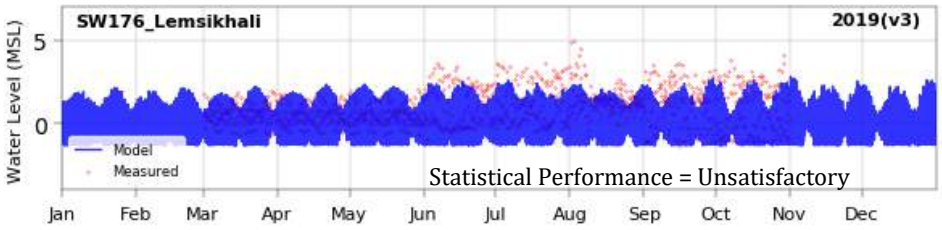

R^2 = 0.068, NSE=-1.88, RMSE = 1.8, MSE = 3.24, MAE = 1.49, PBIAS = 65.54, RSR = 1.7

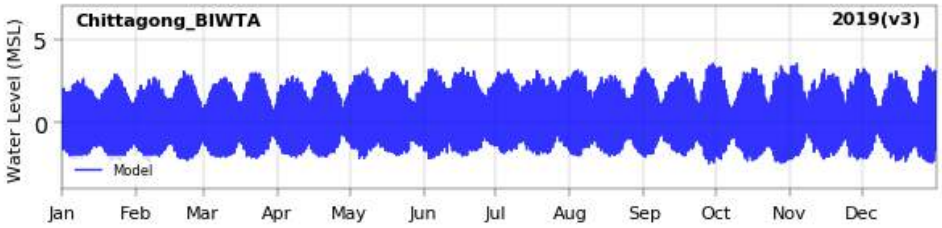

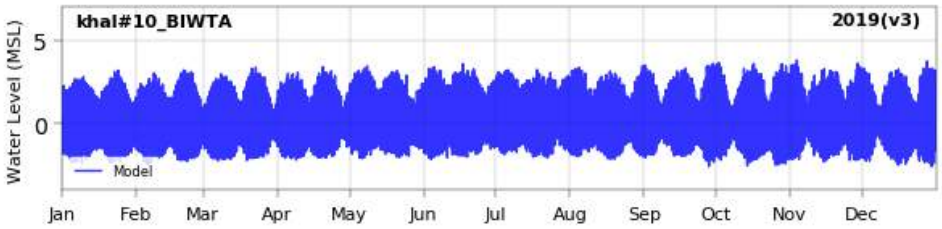

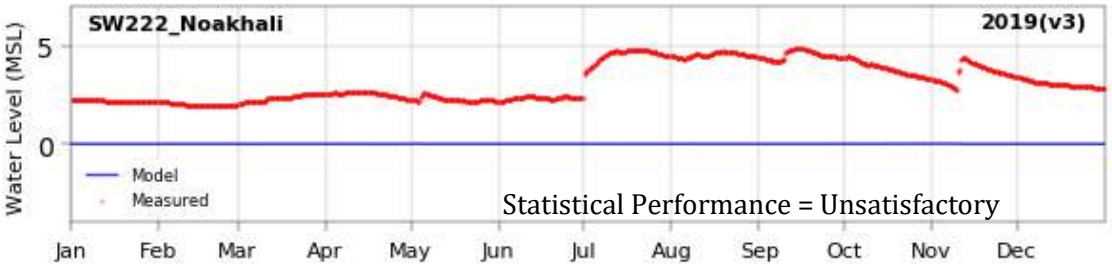

Statistical Performance = Unsatisfactory

R^2 = 0.051, NSE=-10.36, RMSE = 3.31, MSE = 10.98, MAE = 3.16, PBIAS = 99.98, RSR = 3.37

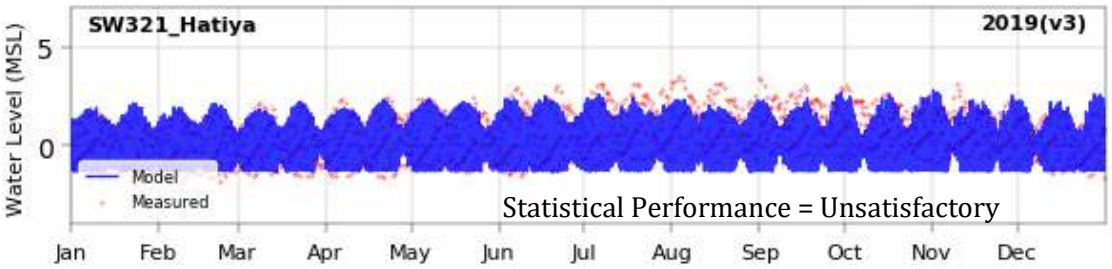

Statistical Performance = Unsatisfactory

R^2 = 0.353, NSE=-2.21, RMSE = 1.97, MSE = 3.86, MAE = 1.68, PBIAS = 50.67, RSR = 1.79

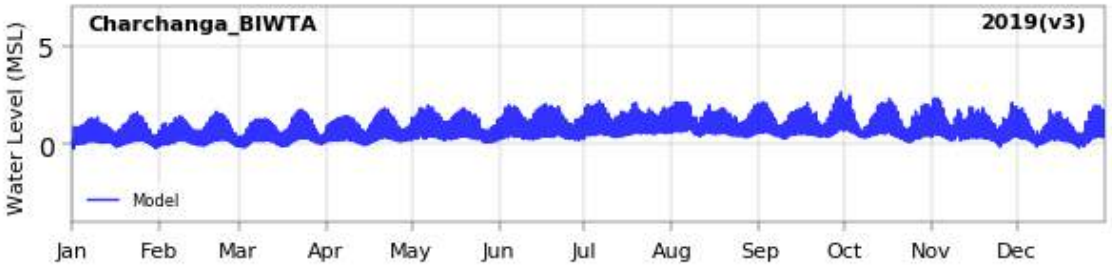

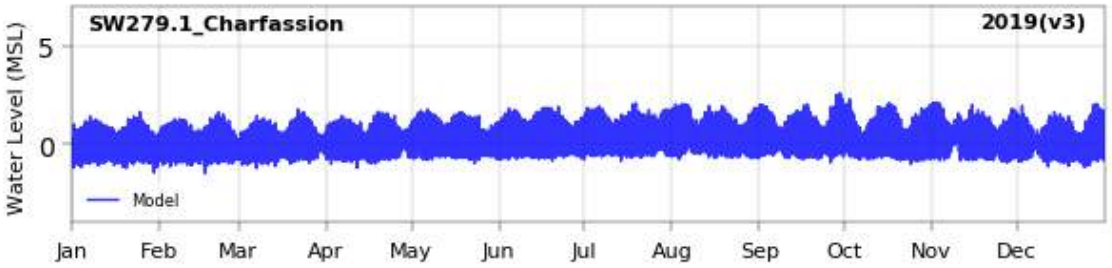

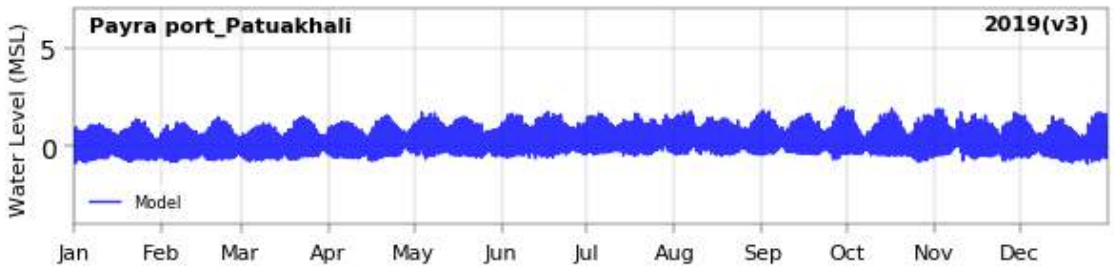

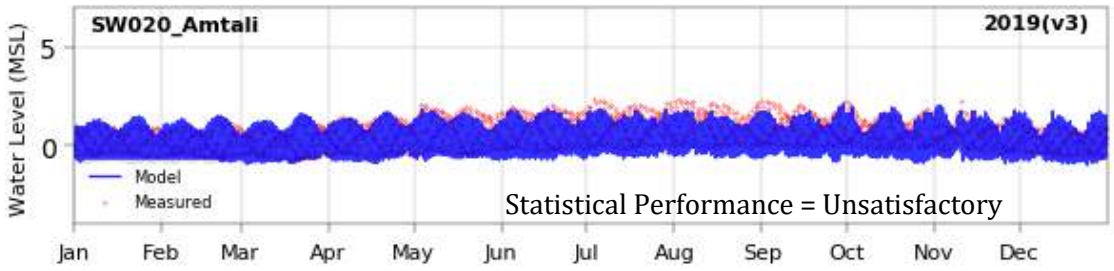

R^2 = 0.068, NSE=-0.47, RMSE = 0.81, MSE = 0.65, MAE = 0.69, PBIAS = 47.37, RSR = 1.21

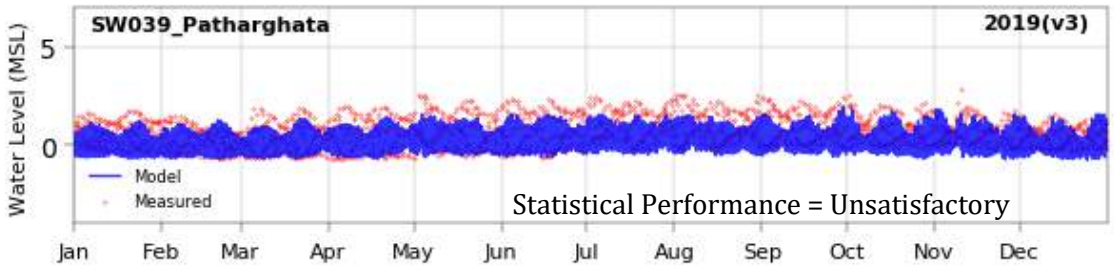

R^2 = 0.012, NSE=-0.53, RMSE = 0.93, MSE = 0.87, MAE = 0.79, PBIAS = 56.31, RSR = 1.24

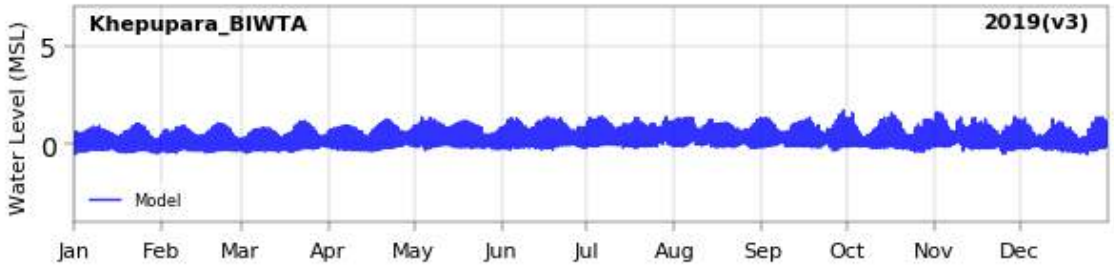

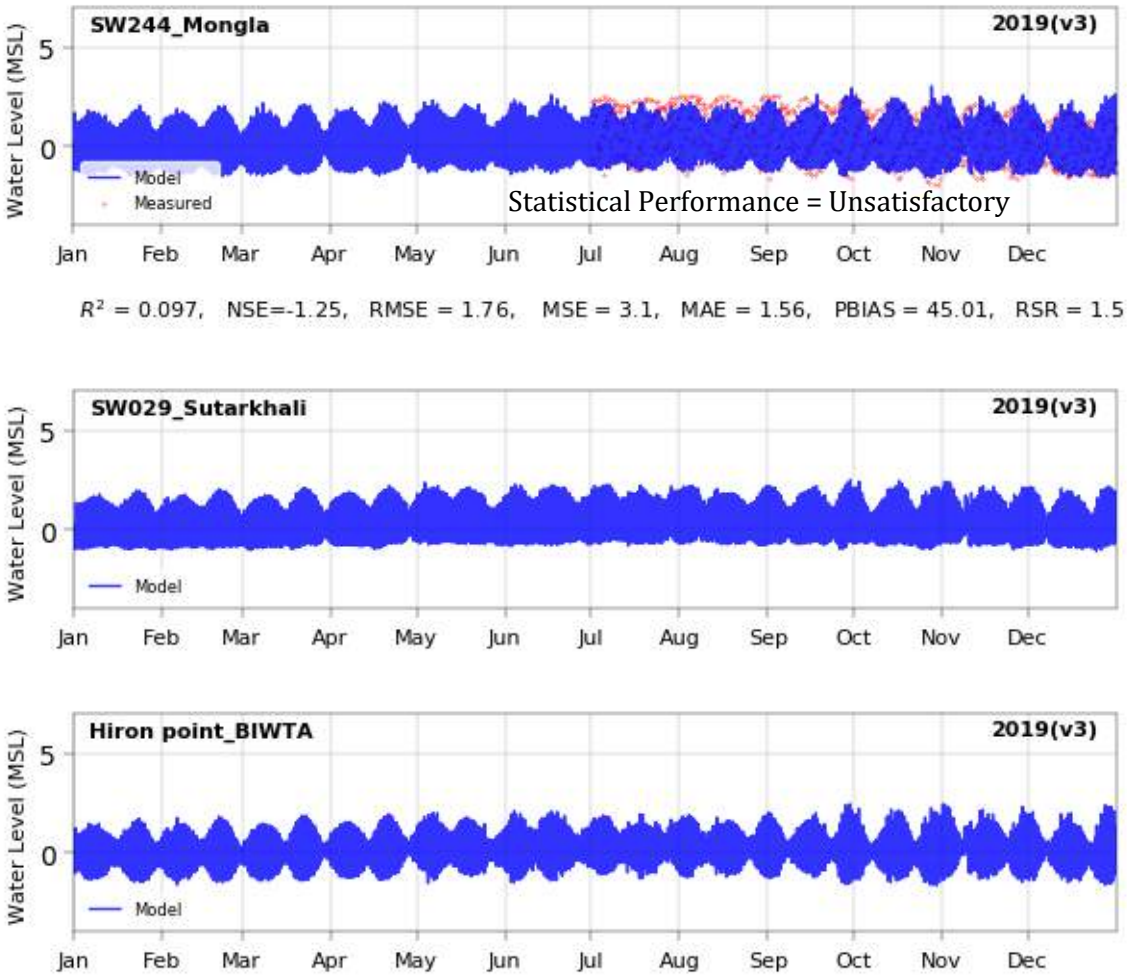

Figure 2.12: *Validation of BDM shows comparison between measured data and BDM. Total 40 water level stations are selected for comparison of which measured data is available for 23 stations. The statistical evaluation criteria below each figure are used to determine qualitative performance of the model. The qualitative performance of the model is shown for each of the validation results. Like calibration results, the exact locations of 3 stations (SW094, SW058A, SW222) could not be identified. Inside the model domain, these 3 stations fall in the land and simulates zero water levels.*

The second validation of flow component of BDM is made by comparing the areal extent of flood inundation generated by the model with the areal extent of flood inundation available from satellite image for 1998 flood. The selected date for comparison is September 10, 1998. This is the date when peak of the three major rivers (Ganges, Brahmaputra-Jamuna, and Meghna) synchronized (Haque and Nichols, 2018). Comparison result is shown in Figure 2.13.

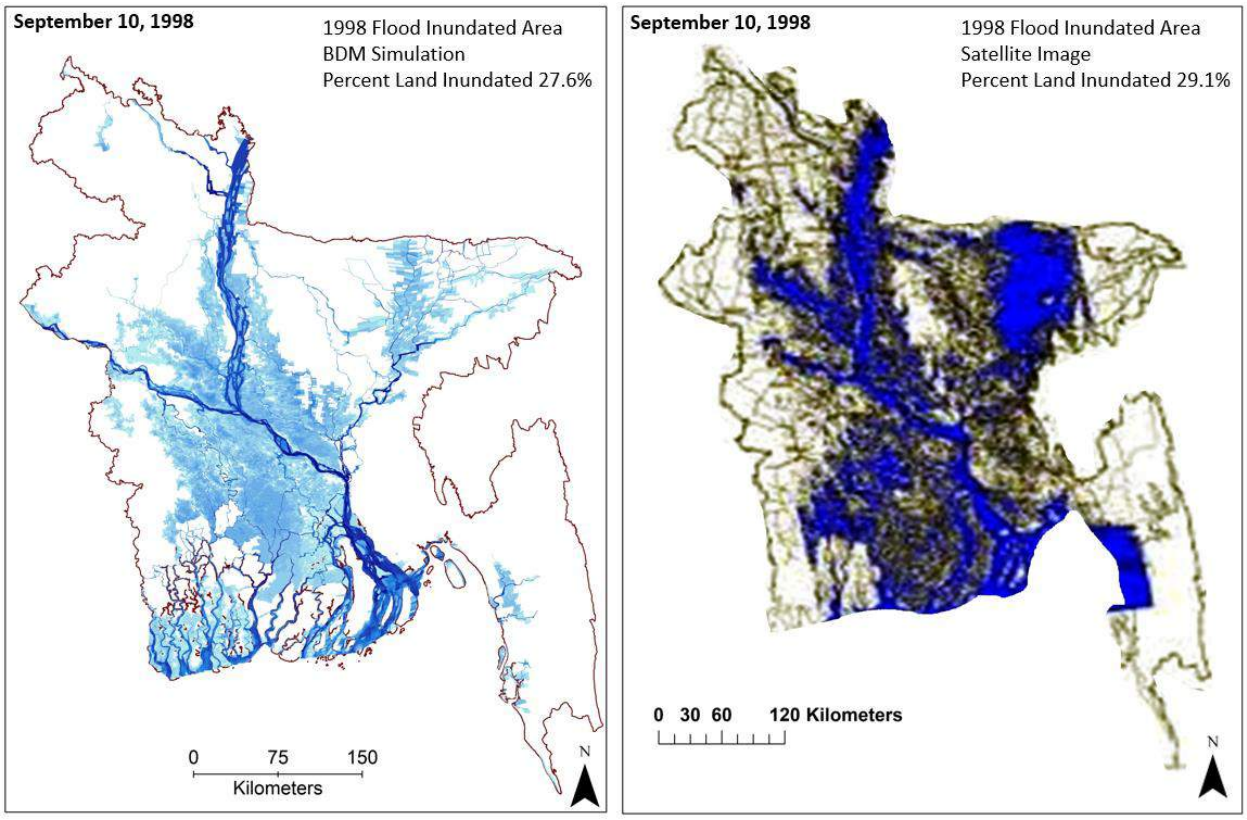

Figure 2.13: *Comparison between areal extent of 1998 flood inundation generated by simulation of BDM and that available from satellite image. The map is prepared for September 10, 1998, the date which is supposed to be the day when peak synchronization of three major rivers occurred. The figure also shows calculated land inundation area from the model and the image.*

For comparison of areal extent of flood inundation, we restrict ourselves only to lands which are inundated due to flood. To do this, we excluded all the perennial water bodies (rivers, haors, beels, wetlands) from calculation of inundated area. The percent land inundated area is calculated with respect to total land area of the country. The comparison shows BDM calculated land inundation extent is 27.6% of the total land area of the country against 29.1% of inundated land area calculated from the satellite image.

2.6.2 Morphology model validation

For morphology model validation, we compared BDM simulated sedimentation depth on the floodplain with available sedimentation depth data from secondary source. Rogers et al. (2013) measured sedimentation depth in 4 locations in the Sundarban region during March to October 2008. The measurement locations by Rogers et al. (2013) are shown in Figure 2.14.

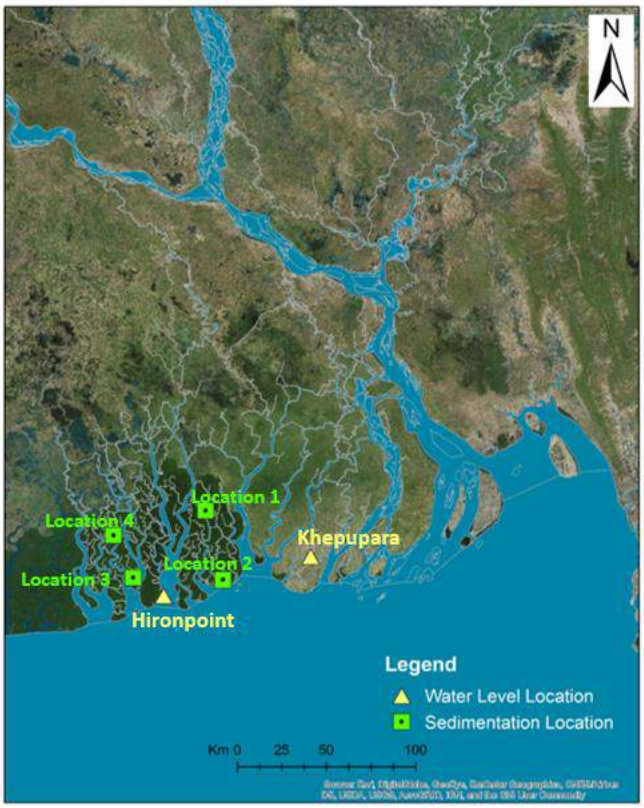

Figure 2.14: *Measurement locations of sedimentation depth by Rogers et al. (2013). The figure also shows two water level station locations from BIWTA to give an idea about the region where sediment thickness is measured.*

The measurement period by Rogers et al. (2013) was March to October 2008, which is the monsoon period. We do not have all the boundary condition data for BDM simulation for a one-to-one comparison with the measurement. Instead, we assume that the flood condition of the year 2008 is in between the average flood condition and extreme flood condition. As sedimentation in the floodplain depends on the upstream sediment supply which in turn depends on the flood condition, so if we can simulate a flood condition which is in between the flood condition of 2008, we will be able to compare the model simulated floodplain sedimentation depth with the sedimentation depth of 2008. To define average flood year and extreme flood year, we did frequency analysis to determine representative flood year for a return period of 2.33 years which

can be defined as average flood year and a flood year with a return period of 200 years which can be defined as extreme flood year. With this definition, year 2000 is found as the average flood year and year 1998 is found as the extreme flood year. All required boundary data are available for the years 2000 and 1998 for BDM simulations. We then execute the BDM for these two representative years and compared the floodplain sedimentation depth simulated by BDM for the entire year with the measurement by Rogers et al. (2013) during the monsoon (March-October) of 2008 in the 4 measurement locations (Figure 2.14). In this way, instead of a one-to-one comparison, it was possible to determine a range of sedimentation depth in these 4 locations and compare this with the measurement. The comparison is shown in Table 2.2.

Table 2.2: Comparison between floodplain sedimentation depth of BDM and measured data.

Location	Sedimentation Depth (mm)		
	Measurement March-October 2008 Rogers et al. (2013)	BDM January-December 2000 BDM	BDM January-December 1998 BDM
1	9.2	2.8	7.0
2	9.3	0.0	4.8
3	11.2	3.4	8.0
4	9.6	9.8	11.4

From Table 2.2 it is found that in 3 locations (locations 1, 2, and 3), measured sedimentation depths show higher values than the ranges of sedimentation depths simulated by BDM. It should be noted here that Rogers et al. (2013) made their measurement during 8 months of the year (March to October), whereas BDM simulates yearly sedimentation depths (January to December). It is likely that within their measurement period, Rogers et al. (2013) did not cover the late recession stage of flood in the region which causes erosion in floodplains. Yearly sedimentation depths in the floodplains account for this erosion phase also.

2.7 Calibration and Validation Summary of BDM

In this chapter, we present the results of calibration and validation of BDM for both the flow model and the morphology model. Flow model of BDM is calibrated by simulating time series of water level in 43 water level stations and comparing the results with the available measured data in 29 water level stations for the year 2017. Except in most of the tidal water level stations in the coast, statistical performance of the model in other water level stations shows that BDM is performing either ‘very good’ or ‘good’ or ‘satisfactory’. Water level data in most of the tidal stations are 3-hourly manually measured data. These data do not represent tidal phase and amplitude correctly. This leads to ‘unsatisfactory’ model performance in these locations. Calibration of morphology model of BDM is made by comparing model simulated time series Suspended Sediment Concentration (SSC) with the measurement and, also by comparing the model simulated spatiotemporal distribution of suspended sediment concentration with the satellite image for the

year 2017. Except a slight phase shift of peak values of SSC, time series comparison between the BDM and measurement shows smaller error bars for the rest of the season. Comparison of spatiotemporal distribution of SSC between the BDM and the satellite image along the major rivers and along the coast shows that BDM can reasonably simulate main physical features of SSC distribution including the turbidity maximum region, keeping in mind that satellite images represent only the surface SSC distribution while model simulations represent depth average SSC distribution. For flow model validation of BDM, comparison between model and measurement is made in 23 available measuring water level stations out of 40 simulating stations. Performance of BDM during flow model validation against water level is almost similar to calibration performance of the model. Validation of flow model of BDM is also made by comparing model simulated areal extent of land inundation with similar data available from satellite image during 1998 flood. The result shows that BDM simulates 27.6% of land is inundated during 1998 flood against 29.1% land inundation value calculated from satellite image. For morphology model validation, BDM simulated sedimentation thickness in 4 locations of Sundarban region during an average flood and extreme flood is compared with the measurement made by Rogers et al. (2013) which was conducted during March to October 2008. Considering the uncertainty of mismatch of time between the model and the measurement, BDM performance appears to be reasonable.

CHAPTER THREE
Sediment Transport Processes in the GBM delta

3.1 Introduction

The river systems within Bangladesh carry water and sediment discharges coming from the GBM basins and associated rivers (see Figure 3.1).

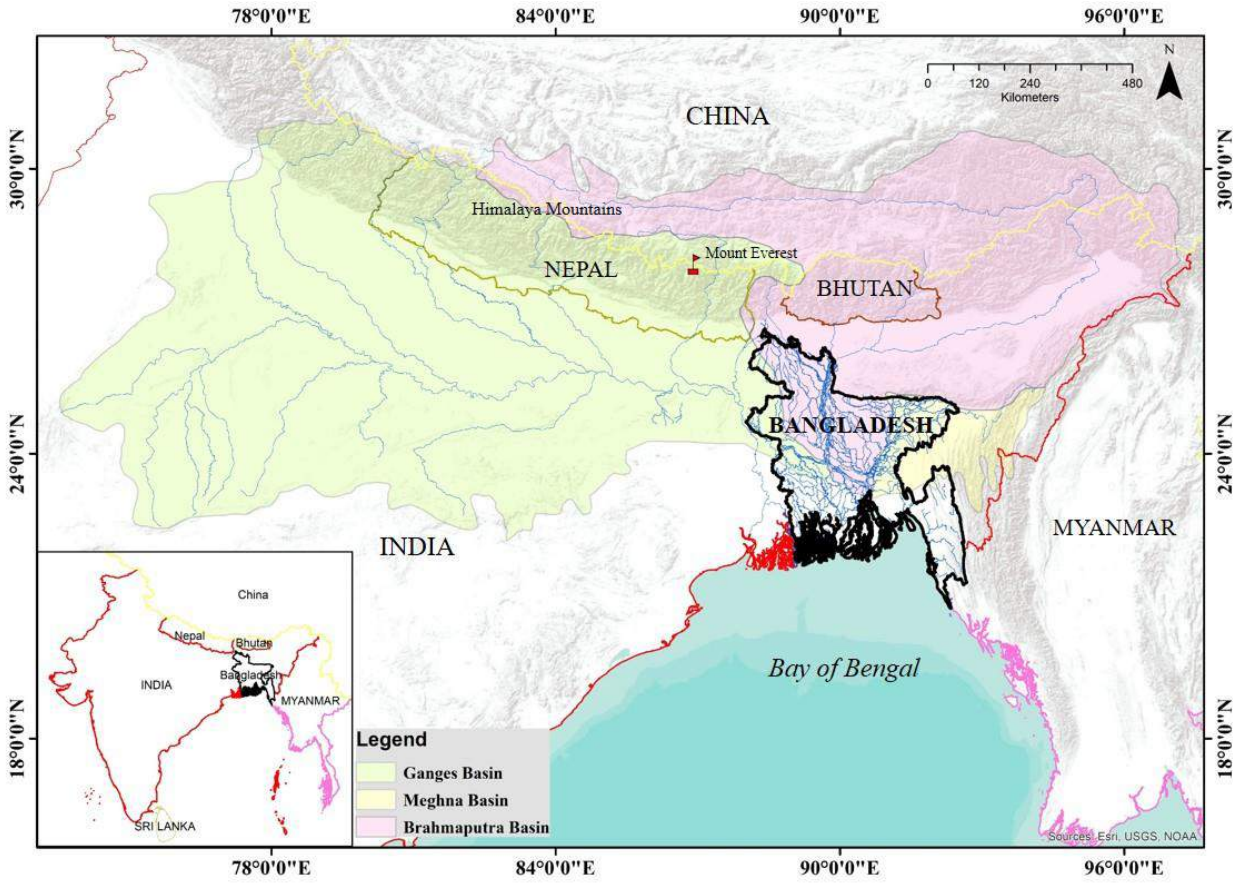

Figure 3.1: *GBM basins and its river systems. The figure shows the boundaries of Ganges, Brahmaputra and Meghna basins. The entire traverse paths of Ganges River, Brahmaputra River and Meghna River outside and inside of GBM delta of Bangladesh part is also seen.*

Sediment discharge in the GBM delta is the highest (Coleman, 1969) and water discharge is the third highest in the world, only after Amazon and Congo Rivers (Milliman, 1991). Before going to discuss the transport processes of these huge volume of water and sediments within the deltaic environment, we tried to explore the relevant studies so far been conducted in this issue. Rahman et al. (2018) made an extensive study to determine total amount of sediment load coming into the region. The study shows that total incoming sediments through the Ganges-Brahmaputra-Upper

Meghna systems is around 500 million ton/year. This value is less than half the values of incoming sediments mentioned in all other earlier studies. In an earlier study (WARPO, 2016), it was found that total incoming sediments to the system is around 1050 million ton/year which is more than double the values calculated my Rahman et al. (2018). All these results show degrees of uncertainty still prevailing on the estimate of actual value of incoming sediments to the region. Once entered the river systems, these sediments ultimately transport to the ocean after depositing/eroding in the river-estuary-floodplain systems. The clockwise oceanic circulation of these sediments causes re-entry of sediments through the mouths of large number of western estuaries in the south-west region (Haque et al., 2016). It is believed that this circulation is impacted by frequent cyclones in the region and may drive these sediments inside the swatch of no ground (Kudrass et al., 2018). Goodbred and Kuehl (2000) mentioned that one third of the sediment carried by the rivers is deposited on the floodplain and tidal plain, one third is trapped in sub-aqueous delta causing vertical accretion and lateral progression of the delta, and the remaining sediment is probably transported to the ocean. Polders in the coastal area restricts the floodplain deposition inside the poldered area causing the reduced elevation of land in these areas compared to riverbed level which ultimately results waterlogging (WARPO and BUET, 2019). The situation can be aggravated due to subsidence of the delta (Brown and Nicholls, 2015). The evidence of limited measurements in the delta floodplain showed enough potential of existing sedimentation on the delta surface to combat against waterlogging, subsidence, and sea level rise (Rogers and Overeem, 2017). Seasonality is another important parameter that determines sediment balance in the delta (Hale et al., 2019). Not only seasonality, it is found from the measured data that suspended sediment concentration in the Meghna Estuary also varies within the neap-spring cycle (Zhong-hua et al., 2021). Akter et al. (2021) applied Delft3D model mostly in the coastal floodplain of the country by covering major river systems. They found that about 22% of total incoming sediments are deposited in the coastal floodplain. They did not consider the non-coastal floodplains in their application domain. They mentioned that nearly 78% of the sediments goes out of the system through the estuarine systems. These oceanic sediments contribute nearly 5% of the global riverine discharge of solid phase of sediments out of which contribution of heavy metal varies between 5% to 10% (Dietrich et al., 2020). The average concentration of most of these heavy metals are above the threshold levels of contamination (Rahman et al., 2020). This quality aspect of sediments in the delta may have some influence on the Oxygen Minimum zone (OMZ) in the Bay of Bengal (Sridevi and Sharma, 2020; Ahsan and Haque, 2020).

The above discussion on past studies reveals that sediment transport processes in the GBM delta has not yet been studied as an integrated system. In this chapter we will discuss the sediment transport processes in the GBM delta by applying BDM. This will make it possible to understand the process not as a piecemeal approach, but within an integrated systems where sediments are entered in riverine systems and after transporting, depositing, and eroding through rivers, estuaries, and floodplains eventually discharges to the ocean. During this journey, sediments encounter embankments and polders in different locations of its path. We considered impacts of these interventions in the transport processes of sediments. After the sediments discharge into the

oceans, part of these sediments re-enter into the estuarine systems. We also consider this process in BDM simulation. We use proxy parameters to study impact of cyclone in sediment transport process. For the first time, we tried to study impact of swatch of no ground in the transport processes.

3.2 Sediment Transport with the Fluvial Flow

As shown in Figure 3.1, after generating in the GBM basins, sediments in the Bangladesh part of the GBM delta enters through the main river systems – Ganges, Brahmaputra-Jamuna, and Upper Meghna. The sediments enter in the region with fluvial flood and after travelling through all the river and estuarine systems, discharges to the ocean. During fluvial flood, floodplains of the country are inundated with sediment laden water causing sediments to be deposited on and eroded from the floodplains. During this flooding process, sedimentation and erosion also occur within the river and estuarine beds. The entire process of fluvial flooding in the delta simulated by BDM is shown in Figure 3.2. The figure shows the snapshots of inundation scenarios during dry season, rising stage of flood, peak of monsoon, and recession stage. The sediments enter in the system with the flood water.

As shown in Figure 3.2, during the dry season, there is almost no sediment supply from the upstream system as flooding has not yet started. Rising stage of flood in this region is generally June. During the rising stage of flood, sediment laden water starts to enter from the inflow river systems inside the delta. The eastern haor system is normally flooded before June which is visible in the inundation scenario. This system is not flooded with the major river systems which carry the bulk volume of sediment inflows. During peak monsoon, we can see the maximum flooding scenarios when delta floodplains are inundated. This flood water transports the sediments in the entire river-estuary-floodplain systems. The inundation in the coastal zone is caused by compound flooding driven by fluvial and tidal processes. Inundation in the coastal zone starts during the peak monsoon season and continues till the recession stage. So, fluvial sediments start to transport in the coastal zone from the peak monsoon. The sediments which enter the floodplains during the peak flood starts to deposit on the floodplain during the recession stage. Marine sediments are normally transported to the coastal zone (mainly in the Sundarban region) during the recession stage of the flood and during early dry season when sediments from the ‘turbidity maximum’ zone (Sarker et al., 2011) re-enters into the system through the estuary mouth. Embankments and polders restrict sedimentation inside the protected region. These protected regions are visible in the right bank of Brahmaputra-Jamuna (due to Brahmaputra right embankment), in the northern part of Ganges (due to Mujib badh), and in the polders part of the coastal region. Flooding in the monsoon also cause erosion in the sedimented part of the delta surface mainly due to the high flow velocity during the recession phase of the flood when sediment concentration in the flood water decreases. Erosion also occurs in the coastal region during the ebb phase of the tide in the dry season when tidal range increases due to decreased upstream flow.

Cyclone in the delta occurs during the pre- and post-monsoon season. In terms of sediment transport, post-monsoon cyclone plays important role compared to pre-monsoon cyclone. We will discuss the impact of cyclone in a separate section.

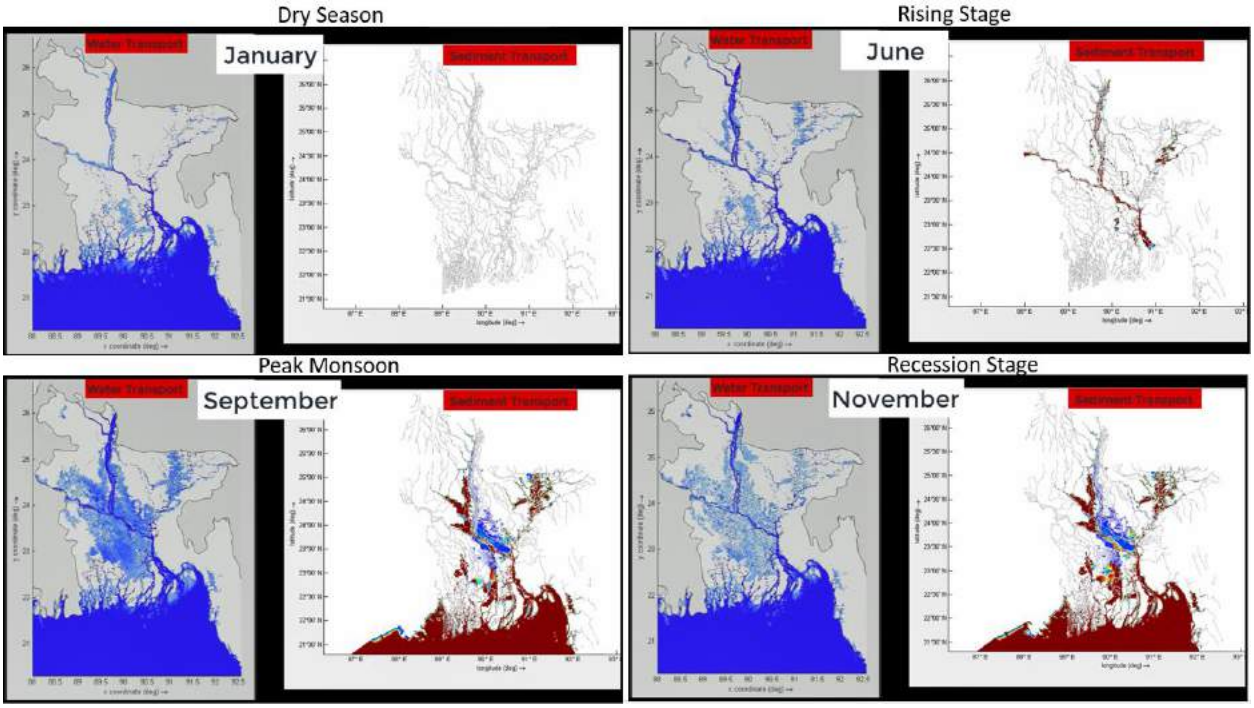

Figure 3.2: *Water and sediment transport along the river-estuary-floodplain systems in the Bangladesh part of GBM delta. The transport scenarios are generated from the BDM simulation of 1998 flood. BDM simulation considers all the river-estuary systems of the delta which is visible in the figure. The figure shows snapshots of transport situation during four representative time of the season – dry season, rising stage of flood, flood during peak monsoon, and during recession stage. The blue color in the water transport figure shows inundation extent and depth, the brown and blue colors in the sediment transport figure shows sediment concentration magnitudes.*

3.3 Sediment Transport with the Tidal Flow

As discussed in the previous section, sediments after entering the river systems of the GBM delta propagates along the river-estuary-floodplain systems and finally discharges into the ocean. In the ocean, the sediments encounter tide and cyclone. Tide is a regular phenomenon with short term (daily) and long term (fortnightly and above) variability. Sediments after discharged into the ocean from the riverine-estuarine systems encounter this tide. The oceanic phase of the sediment transport and overall sedimentation in the delta is affected by the tides.

BDM simulation of the daily tide generation process in the ocean and the coast is shown in Figure 3.3. High tide generated in the deep ocean propagates all along the Bay of Bengal and reaches to west and east coast almost at the same time. At the time when high tide reaches the coast, low tide

starts its journey and eventually reaches the coast. The process repeats itself to generate daily variation of tide.

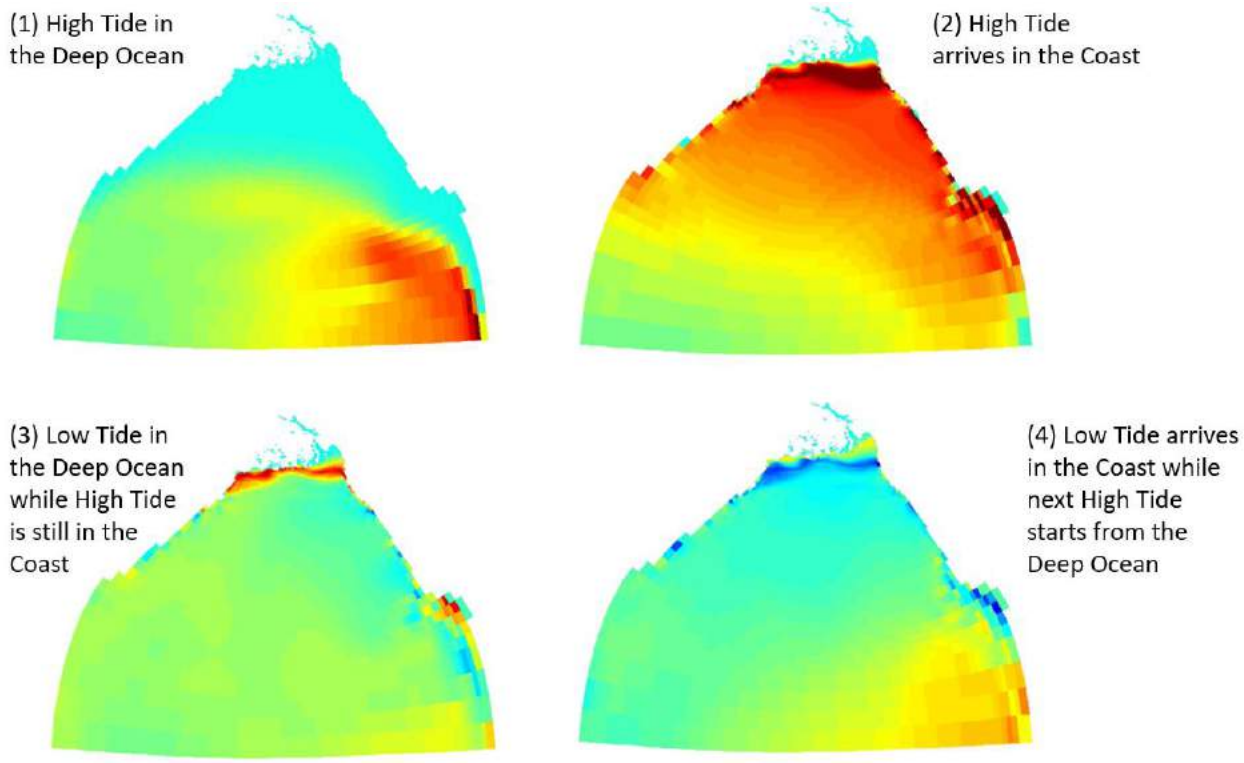

Figure 3.3: *Daily tide generation in the ocean and the coast. The figure shows four snapshots of tide generation process in the ocean that travels towards the coast.*

The sediments in the ocean and coast are driven by tidal current. BDM simulated flood and ebb tidal currents in the Bay of Bengal towards the Bangladesh coast is shown in Figure 3.4. The figures also show location of swatch of no ground in the Bay.

The results show that tides arrive almost at the same time along the west and east coasts. Flood tide current slows down along the Lower Meghna estuary due to the impact of freshwater. Relatively higher current along the mouth of the estuaries of the western coast during the flood tide causes ocean sediments to enter inside the western estuarine systems. Sources of these ocean sediments are Lower Meghna estuary which propagates along the continental shelf during the ebb tide and later re-enter into the system during the flood tide. Just at the beginning of the ebb tide in the ocean, there is a flow disaggregation line, and a zone of stagnation occurs (Figure 3.4, ebb tide current). This zone has significant impact on the sedimentation all along the estuary mouths in creating zone of turbidity maximum (Sarker et al., 2011).

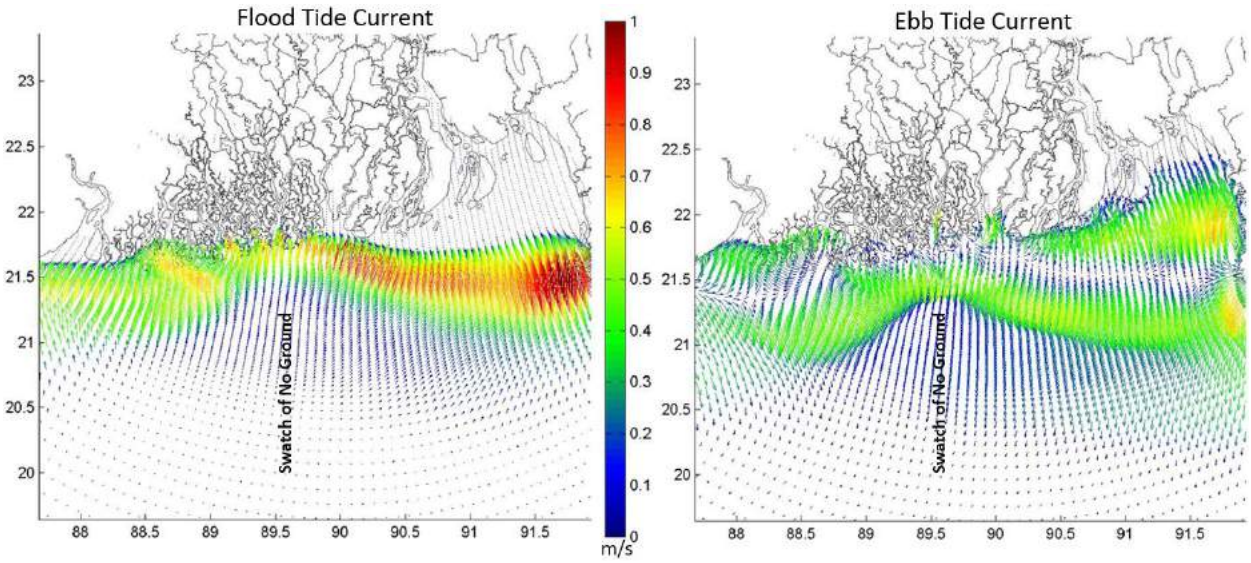

Figure 3.4: *Simulated flood and ebb currents in the Bay of Bengal. The location of swatch of no ground is also shown in the figure. A zone of flow disaggregation is seen in the ebb tide current which plays an important role in sedimentation in the coast.*

Swatch of no ground is a submarine canyon in the ocean floor (Figure 3.5). It spans around 1,738 km^2. The floor is about 5km to 7km wide with a southward continuation of about 2,000 km. At the edge of the shelf, the depth is about 1,200m. Both the flood and ebb currents move faster along the swatch of no ground (Figure 3.5). The swatch of no ground acts like a separate channel on the ocean and divides the entire oceanic circulation into two distinct parts – eastern circulation and western circulation. Eastern circulation is dominated by the Lower Meghna flow, and the western circulation is dominated by the flows from the Indian coast. Due to the separation zone created by the channel on the swatch of no ground, it appears that the sediments from the Lower Meghna system may be diverted (see Figure 3.12) and may not be able to directly deposit in the swatch of no ground (Figure 3.11), although the situation may change during cyclones (Kudrass et al., 2018). This needs further analysis before any conclusion.

Figure 3.5: *Location of swatch of no ground in the Bay of Bengal.*

3.4 Impacts of Wind and Cyclone on Transport of Sediment

The main driving forces determining the transport processes in the Meghna estuary are (Jakobsen et al., 2002): bathymetry, hydrology of the adjacent watershed (river discharge), oceanographic condition outside the estuary (tides), and meteorological conditions (wind and cyclone). In our results for sediment transport process in the delta we have so far considered bathymetry (section 2.3), river discharge (section 3.2), and tides (section 3.3). In this section we will discuss the impacts of wind and cyclone. In the Bay of Bengal, south-westerly monsoon wind blows with a speed of 4-5 m/s during June to September, and north-easterly wind of 1.5-3 m/s blows during December to February (Jakobsen et al., 2002). To show the impact of wind in transport process, BDM simulation of tidal current without and with south-westerly wind in a typical day in June 2018 is shown in Figure 3.6.

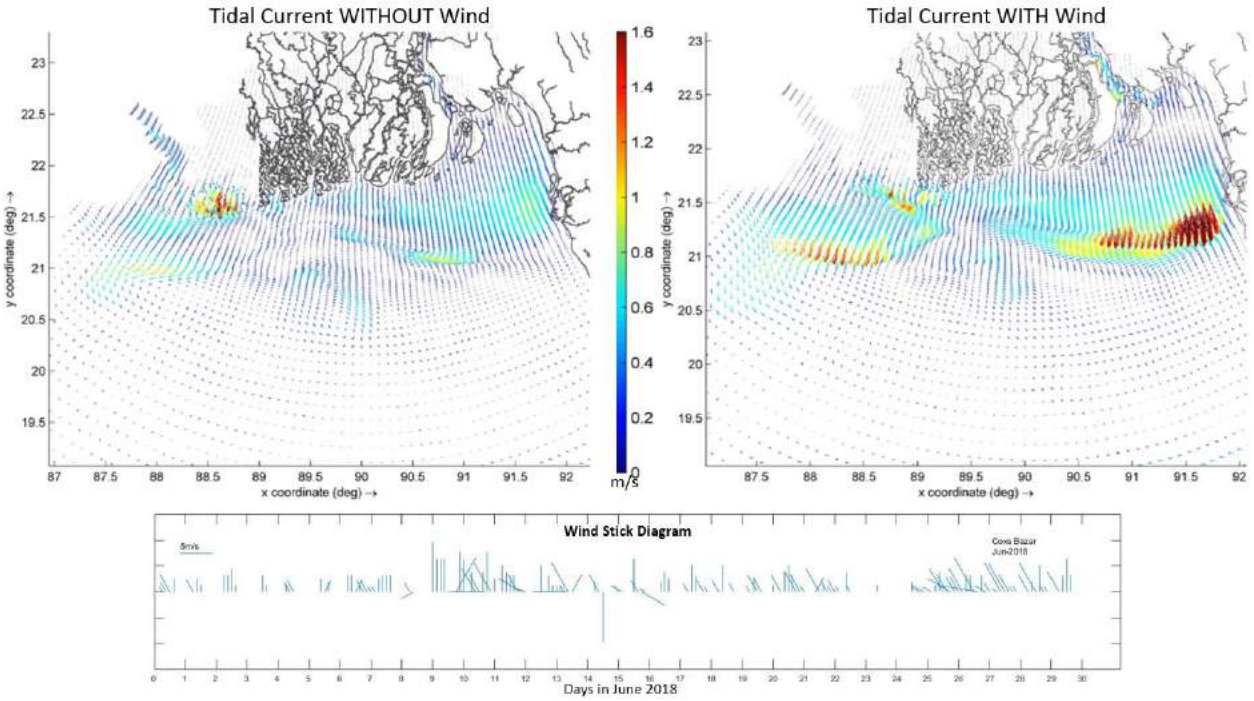

Figure 3.6: *Tidal current in the ocean for with and without south-westerly monsoon wind. The figure shows a typical day in June 2018. The wind stick diagram in Cox's Bazar station in the coast is also shown.*

Although Jakobsen et al. (2002) did not recognize wind as a significant driving force on tidal current in this region, we found it otherwise. South-westerly wind increases the tidal current during the flood phase of the tide which will increase the sediment flux along the coast.

We did not find any study in the past related to transport process during the cyclone time. Kudrass et al. (2018) with the evidence from characteristics of sedimentary deposit inside swatch of no ground anticipated the significant impact of cyclone on transport of sediment in the region during the cyclone time. We made tidal current simulation during the cyclone time by applying BDM and

compared the situation for with and without cyclone condition (Figure 3.7). As a representative cyclone we select cyclone Sidr which made landfall in Bangladesh coast on November 15, 2007, at 1800 hrs. The result shows this specific incident (Figure 3.7).

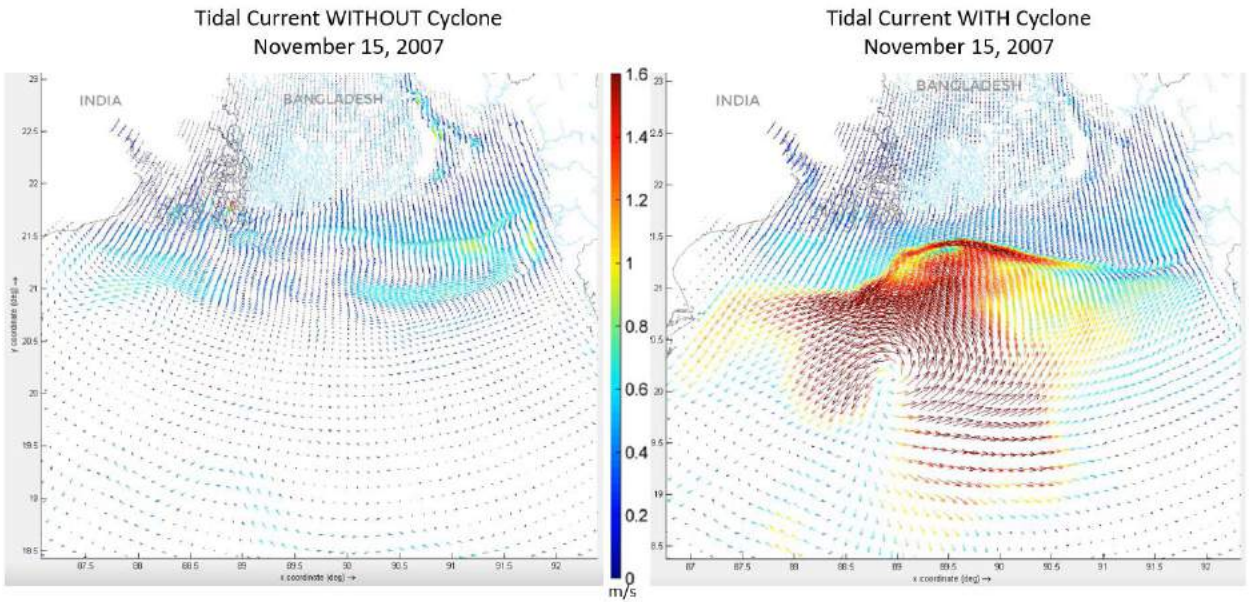

Figure 3.7: *Tidal current in the ocean for with and without cyclone condition. Cyclone Sidr is selected as a representative cyclone. The result shows the specific condition at the time of landfall. The left figure shows the case without cyclone and the right figure shows the case with cyclone.*

Cyclones create hydrodynamic shock (sudden increase of velocity) in the system. It is generally believed that large volume of sediments re-enter into the estuarine systems during a cyclonic event. The results in Figure 3.7 show that cyclonic wind suddenly increase the flood flow velocity (hydrodynamic shock) compared to *without cyclone* scenario. As sediment flux is related to water velocity, increased water velocity creates increased sediment flux for the same sediment concentration. So, for a similar sediment regime, cyclonic event creates increased sediment flux. This will drive increased volume of sediments to re-enter into the estuarine systems through increased flood flow velocity created by cyclone.

We already mentioned about the increased flux due to wind and cyclone effects. To demonstrate this, flux in four different sections of the coast is calculated for 3 different conditions – tide only, tide & wind, and tide & cyclone (Figure 3.8). We can see visible impact of wind only along the Lower Meghna mouth, but not along the other locations of the coast. Cyclone impact is also significant in this location. This is mainly due to large Meghna flow associated with wide estuary mouth. Location of Meghna mouth is at the right side of cyclone track which made impact of this cyclone maximum in this location. This increased flux will drive increased volume of sediments through the Lower Meghna mouth. In this region, the normal wind direction in November is north-easterly (Jakobsen et al., 2002) which means towards the ocean. So, this wind creates flux in a

direction away from the coast (Figure 3.8) and will not drive additional sediments to enter in the estuary. Wind speed during this time of the year is low compared to south-westerly monsoon wind (Jakobsen et al., 2002). So, we see very little impact of wind during this time of the year (Figure 3.8). But this condition will be changed during south-westerly monsoon wind. We have earlier seen visible wind effect during south-westerly monsoon wind (see Figure 3.6) which also creates visible flux in the direction of the coast (results not shown) and will drive additional sediments in the estuarine systems. On the other hand, cyclone wind speed is several times stronger than the normal wind speed, is always directed toward the coast, and accordingly increased volume of flux and its direction changes toward the coast during cyclone. The cyclone in this region creates a south-westerly current due to anticlockwise rotation of cyclone. This south-westerly current will drive the sediments from the turbidity maximum region (Sarker et al., 2011) to the swatch of no ground and may be a probable cause of sediment accumulation inside the swatch of no ground (Kudrass et al., 2018). The location and amount of sediment flux depends on the cyclone landfall location, cyclone time (pre- or post-monsoon), and cyclone strength.

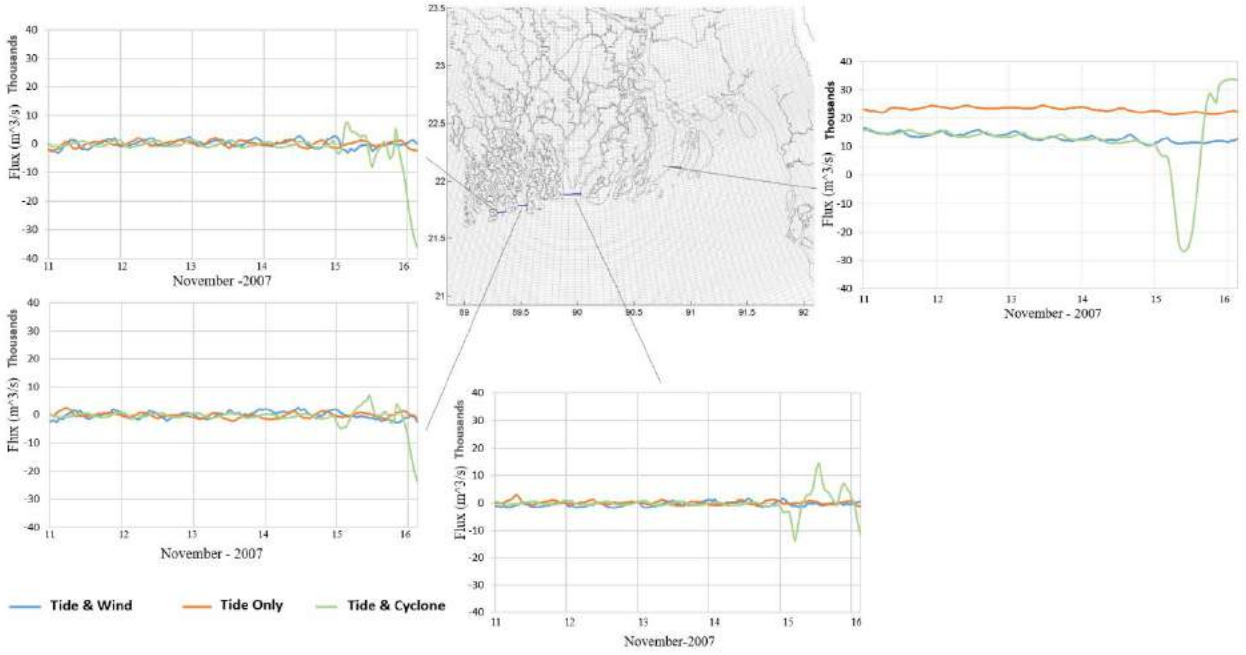

Figure 3.8: *Flux along selected sections along the coast for three different driving forces: tide & wind, tide only and tide & cyclone. The results show fluxes due to cyclone Sidr during the landfall time on November 15, 2007, at 1800 hrs. We calculated fluxes along three regions along the coast – west, central, and east. Cyclone Sidr made landfall in the border of west and central region. In these figures negative flux indicates direction towards the coast and positive flux indicates flux towards the ocean. The wind in the figures is north-easterly wind during November which creates a positive flux towards the ocean direction.*

Bed shear force is the force which is responsible to initiate and transport bed materials. This force also generates bed sediments to come into suspension and increases the suspended sediment concentration. We applied BDM to compute bed shear stress in the ocean be for the 3 driving forces of sediment transport – tide, tide & wind, and tide & cyclone (Figure 3.9). The results show gradual increase of bed shear stress along the estuary mouths when the forcing increases from tide, tide & wind, and tide & cyclone depicting the increased sediment flux during cyclonic events. The wind in these figures represents north-easterly wind during November directed towards the ocean which is much weaker than the south-westerly monsoon wind during June to October. The generated bed shear stress thus is not representative of maximum bed shear stress due to tide & wind. Nevertheless, the bed shear stress due to tide & cyclone is the maximum in this region. As cyclone is a short duration, season dependent but high intensity incident, cyclone generated sediment transport will not create a long-term impact on sedimentation in the region.

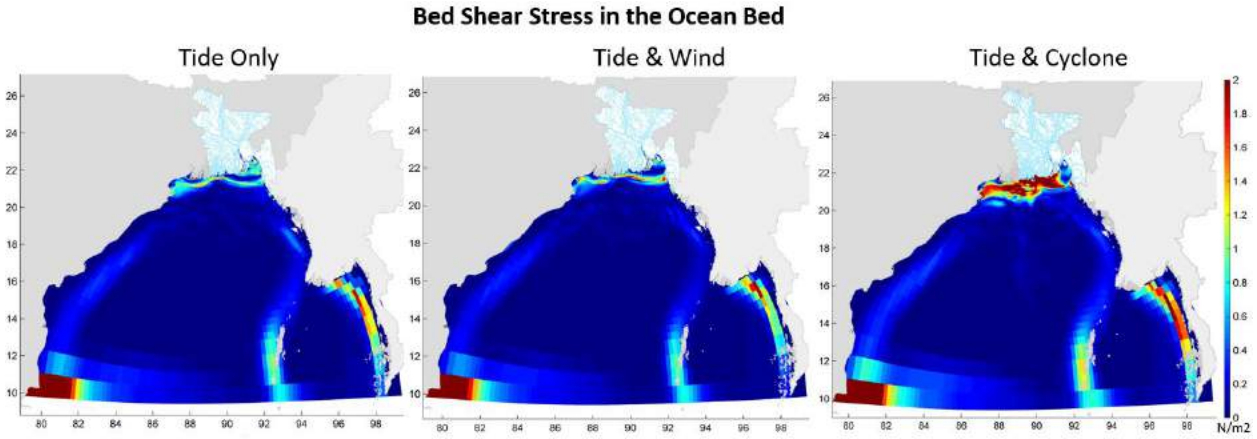

Figure 3.9: *Bed shear stress along the ocean floor for 3 driving forces of sediment transport – tide, tide & wind, tide & cyclone. To make the tidal phase similar for the 3 drivers, the generated bed shear stresses are shown for November 15, 2007, at 1800 hrs, which is the time of landfall of cyclone Sidr.*

3.5 Sediment Dispersion Zone in the Ocean

We applied BDM to compute sediment dispersion zone in the ocean. We used dispersion of conservative substance in the ocean to delineate this zone. Following the dilation line of the conservative substance, dispersion path of sediments is identified (Figure 3.10). The higher the dilution, the higher is the sediment concentration. With this definition, the zone close to the coast (near dispersion zone with maximum dilution) has the maximum sediment concentration. Sediment concertation decreases as we go deeper into the ocean (far dispersion zone). The results show that high concentration sediments in the near dispersion zone is confined within the continental shelf. Sediments from the Lower Meghna estuary is mainly distributed within this zone. Deep ocean (far dispersion zone) has very low sediment concentration. This means that

sediment concentration in the deep ocean is low. This also shows that assumption of a low sediment concentration in the deep ocean is valid (WARPO and BUET, 2019). In between the high sediment concentration zone and low sediment concentration, there is a narrow middle zone with medium sediment concentration where transition between high and low sediment concentration occurs. In the east coast, sediments from Lower Meghna propagates a long distance up to the coast of Thailand. In the west coast, sediments are propagated along the east coast of India. This simulation does not consider all the sediment sources from India, Sri Lanka, Myanmar, and Thailand.

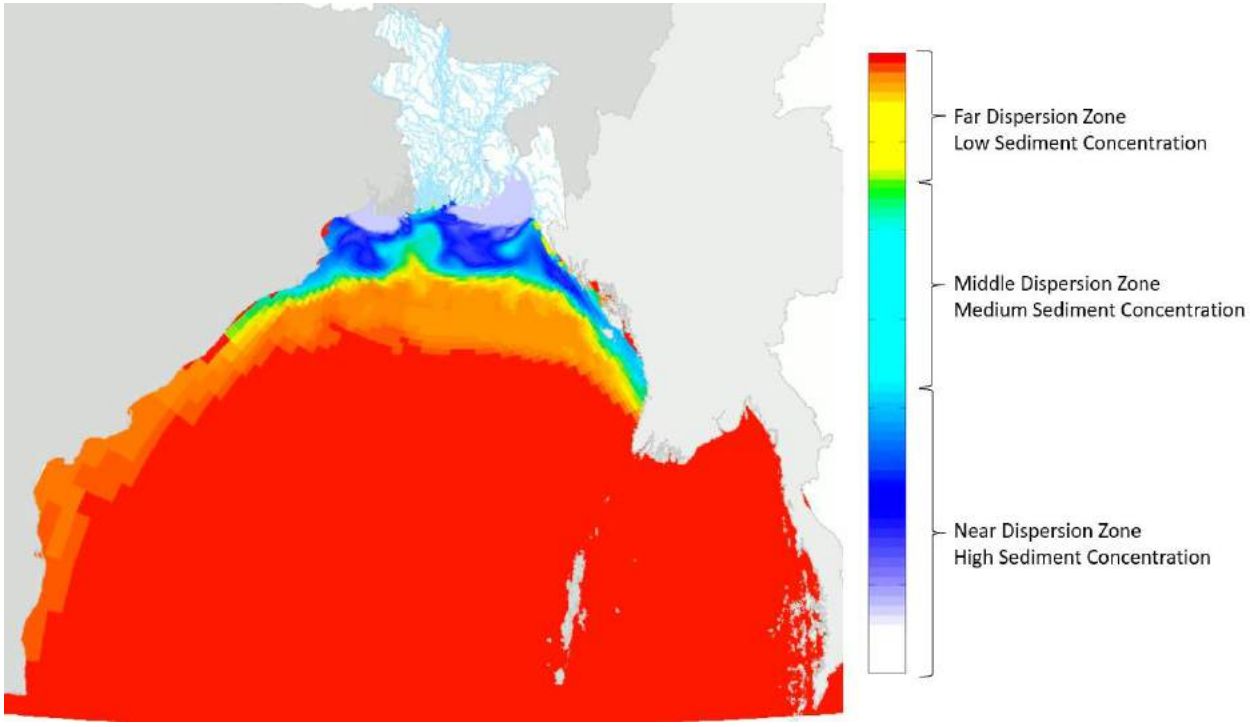

Figure 3.10: *BDM simulation of sediment dispersion zone in Bay of Bengal. The dispersion zone is identified based on dilution of conservative substance. Concentration of conservative substance is used to delineate the three dispersion zones – near, middle, and far. Sediment concentration is high in near dispersion zone, medium in middle dispersion zone, and low in far dispersion zone.*

Vertical distribution of the dilution zone representing sediment concentration close to the coast from the 3D model simulation shows that high sediment concentration is confined within the first 50m depth of the ocean from MSL of the ocean surface (Figure 3.11). Deeper part of the swatch of no ground is within low sediment concentration zone. This shows in normal tidal environment (not cyclonic condition), sediments from either the eastern or the western oceanic circulations do not enter deep into the submarine canyon. More study is needed to explore this vertical distribution pattern due to seasonal variations including the cyclones.

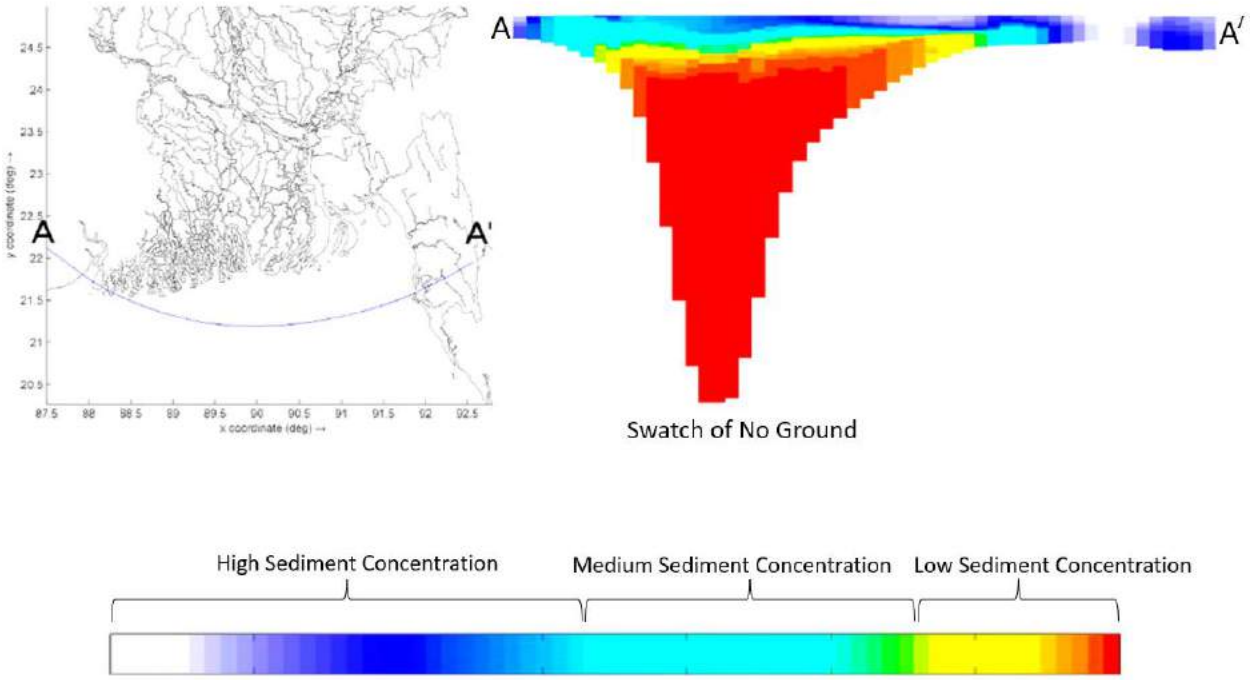

Figure 3.11: *Vertical distribution of sediment concentration zones. The cross section along the coast is drawn along the horizontal section AA′ shown in the left image. The line AA′ passes through the swatch of no ground. This makes it possible to show the vertical structure of sediment concentration zone inside the swatch of no ground.*

3.6 Sediment Re-circulation in the Ocean

To determine sediment movement path along the coast, sediment is released from the main inflow systems and its movement is traced all along its travel path (Figure 3.12). The sediment movement path shows that the sediments from the Ganges-Brahmaputra-Meghna systems discharges into the Bay of Bengal through the Lower Meghna mouth, turn clockwise, part of the sediments deposit in the ocean and the rest of the sediments re-enter into the western estuarine systems. On the swatch of no ground sediment movement path is deflected and by-passed the swatch of no ground region. This shows that in normal tide condition, sediments from the Lower Meghna system may not be directly depositing inside the canyon. This simulation is done by considering tide only condition. This situation will prevail for tide & wind condition also but may change during tide & cyclone condition depending on the cyclone track and strength. The driving force behind this recirculation is fluvial flow from upstream rivers, tide in the ocean, and Coriolis force due to earth rotation. Wind (normal wind and cyclonic wind) creates an additional force behind this re-circulation.

In terms of sedimentation in the GBM delta, this re-circulation plays a very important role. Most of the sediments in the western estuarine systems and its related floodplains are re-entering into the system due to this re-circulation. The upstream freshwater connectivity of these systems is

severely restricted due to flow reduction in Ganges during dry season as a result of Farakka barrage in the Indian part of the delta. This re-circulation drives the sediments to the western system from the turbidity maximum zone in the Lower Meghna Estuary (Sarker et al., 2011). Sediment transport due to this re-circulation plays a dominant role in delta building process and accelerating sedimentation in the unprotected part of the delta.

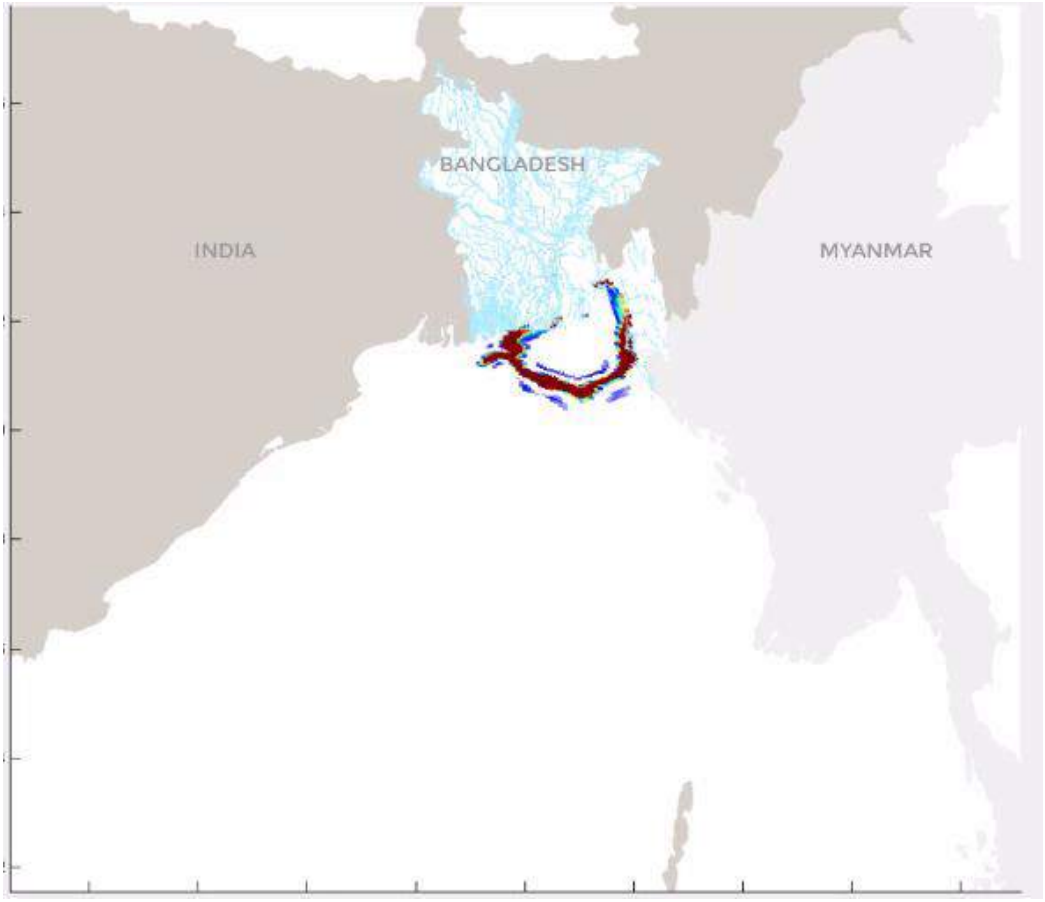

Figure 3.12: *BDM simulation showing sediment movement path along the coast. The red color shows high sediment concentration, green and blue colors show relatively low sediment concentration.*

3.7 Flooding in the Delta

Flooding in the delta brings the sediments on the floodplains and thus cause floodplain sedimentation. So, it is important to understand the flooding process in the delta particularly during monsoon. We applied BDM to simulate flooding caused by fluvial and tidal flows. Flooded area of the country for 1998 flood is calculated from simulated inundation map by BDM (Figure 3.13). Total percentage of land inundated area with respect to the entire land area of the country is also shown in the figure.

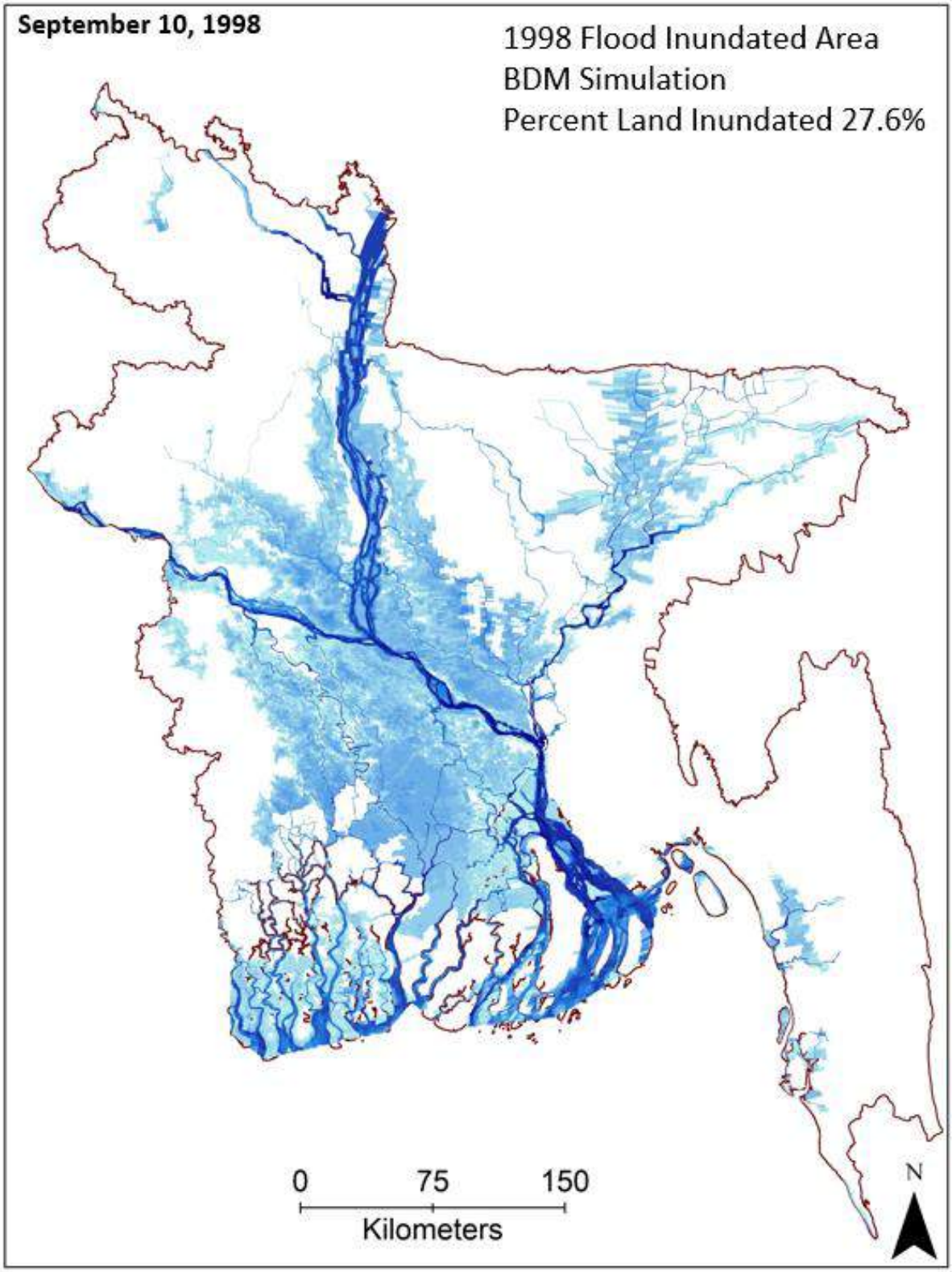

Figure 3.13: *Inundation map for 1998 flood generated by BDM simulation. The figure also shows percent land inundation with respect to total land area of the country. This calculation excludes all perennial water bodies, i.e., rivers, estuaries, ocean, wetlands, haors.*

To calculate inundated area shown in Figure 3.13, we followed two different methods:

Method-1

In this method, we have calculated the area inundated on 'land only'. In doing this, we have excluded the perennial water bodies (rivers, estuaries, ocean, wetlands, haors) from the inundated area calculation. So, inundated area percentage in method-1 represents the land area which is 'actually' inundated. This is a conservative estimate of inundated area during flood.

Method-2

In this method, we calculated the inundated area as 'total area' which is identified as the wetted area. This wetted area includes lands, rivers, estuaries, haors, beels, and other wetlands. We can expect inundated area calculated with this method will be larger than method-1. The useability of this method is – this is the actual 'wetted' area during the peak monsoon that includes land, river, haor, and other wetlands. The rest of the area of the country remains 'dry'.

Comparison of regional and country wide inundation area for 1998 flood between method-1 and method-2 is shown in Table 3.1.

Table 3.1: Comparison between method-1 and method-2 from BDM simulated regional and country wide flood inundation area for 1998 flood

	Region							
Methods	NW	NC	NE	SW	SC	SE	EHT	Total
Method-1 Area	6,044 km^2	7,120 km^2	308 km^2	8,815 km^2	11,735 km^2	1,152 km^2	807 km^2	35,981 km^2
Method-1 Percent w.r.t land area of country	4.6 %	5.5 %	0.23 %	6.8 %	9.0 %	0.9 %	0.6 %	27.6 %
Method-2 Area	9,813 km^2	10,804 km^2	3,071 km^2	11,259 km^2	16,605 km^2	1,530 km^2	1,313 km^2	54,395 km^2
Method-2 Percent w.r.t total area of country	6.6 %	7.3 %	2.1 %	7.6 %	11.2 %	1.0 %	0.9 %	36.6 %

Land area of country = 1,30,170 km^2, Water area of country = 18,290 km^2, Total area of country = 1,48,460 km^2 (source: 2020 CIA World Factbook https://www.cia.gov/the-world-factbook/countries/bangladesh/).

Results of Table 3.1 shows that inundated area largely varies with how the inundation is defined. In the most conservative approach (method-1), where inundated area is defined as the land area where impact of flooding is actually visible, we found 27.6% of the land with respect to land area

of the country is inundated during 1998 flood. With this criterion, the maximum flooding is found in south-central region (9.0%) where there is no flood control embankment (polder) and the minimum flooding is found in eastern hill tract (EHT) region (0.6%). On the other hand, if we follow a generalized approach (method-2) where inundated area includes all the perennial water bodies in addition to inundated area obtained from method-1, we found 36.6% of the area as inundated area with respect to total area of the country. The regional distribution in this method shows maximum inundation in south-central region is 11.2%, where we have included water area of Lower Meghna, and minimum inundation in the eastern hill tract (EHT) region (0.9%).

We have seen large variation of inundated area depending on the definition of inundation. To validate the inundated area obtained from BDM simulation (Table 3.1), we compared calculated inundated area from the BDM simulation with the available maps and reported inundated area from secondary sources. Available maps from secondary sources are satellite image of 1998 flood of Figure 3.14 and RADARSAT map of Figure 3.15 (Duti et al., 2017). For flooded area, BWDB calculated flooded area is 100,250 km^2 (BWDB, 1998) which is 67.5% of total country area. If only land area of the country is considered, this percentage becomes 77%. The total country area and land area of the country is used from the following data (source: 2020 CIA World Factbook https://www.cia.gov/the-world-factbook/countries/bangladesh/):

Land area = 130,170 km^2
Water area = 18,290 km^2
Total country area = 130,170 + 18,290 = 148,460 km^2

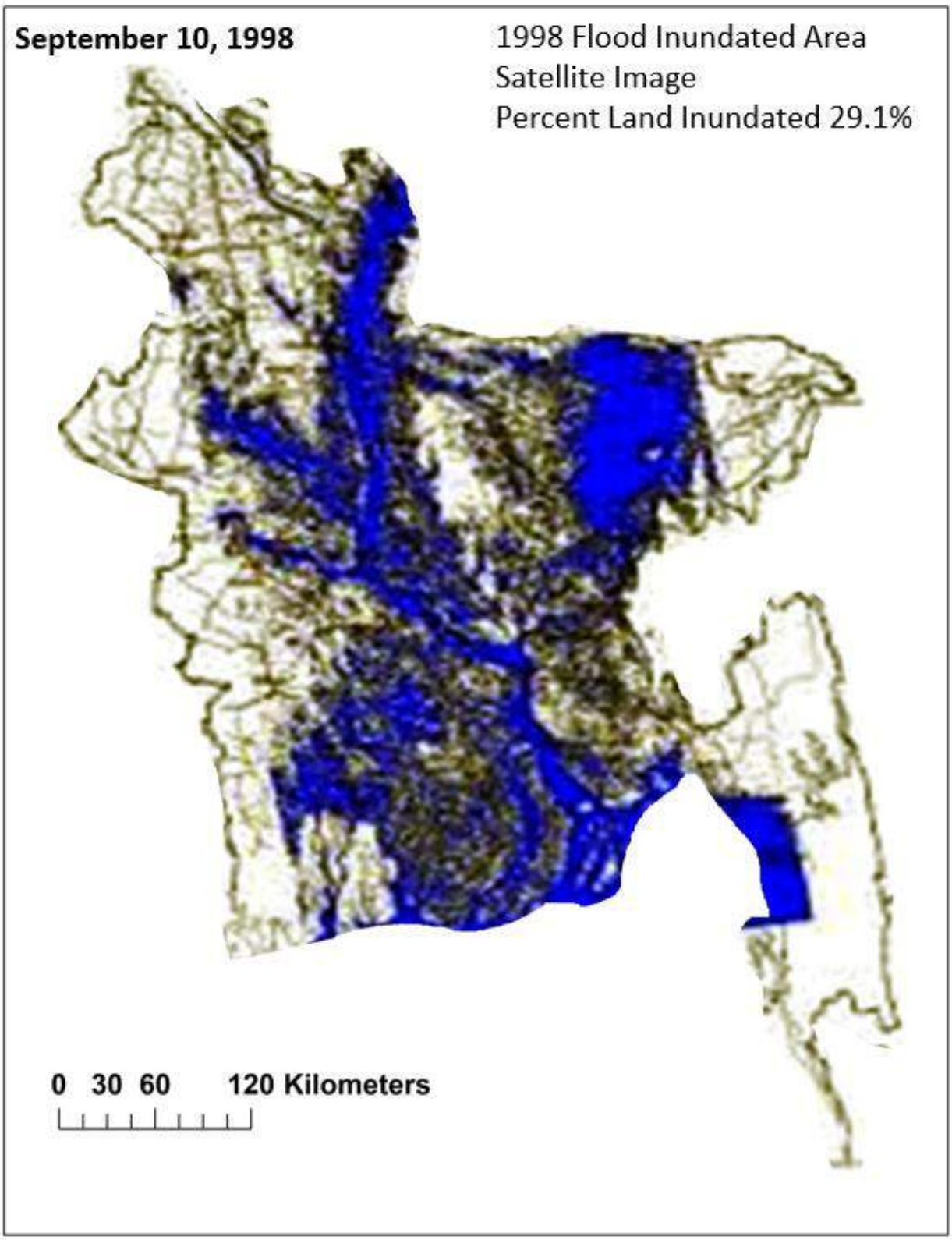

Figure 3.14: *Satellite image of 1998 flood. The image date of September 10 represents peak monsoon. The type of satellite for this image is unknown.*

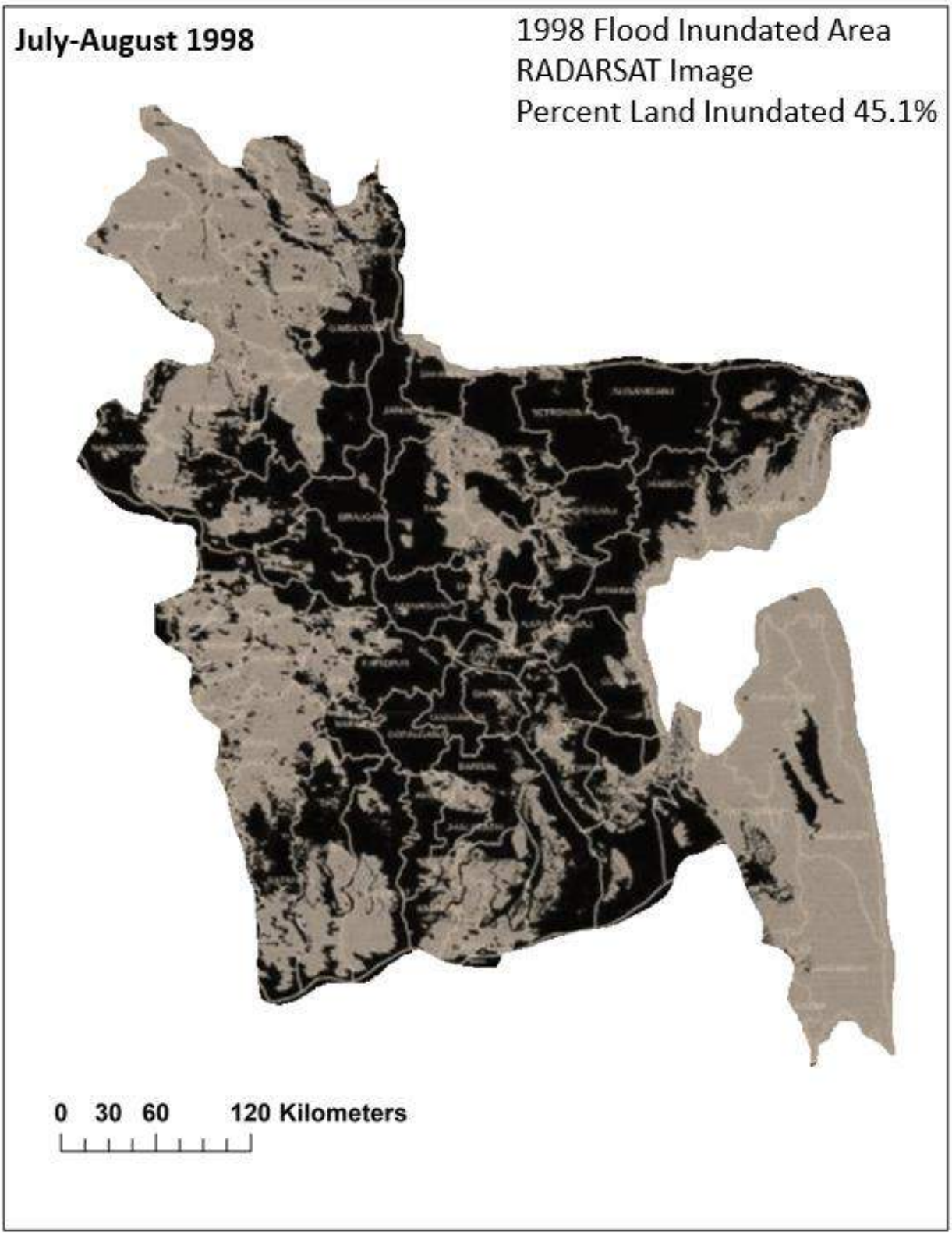

Figure 3.15: *RADARSAT image of 1998 flood (source: Duti et al., 2017). The image has no specific date rather it shows inundation condition in any date on July-August 1998. The inundation in this image shows both riverine and rainfall flooding.*

In literature, it is widely mentioned that 'two-third' of the country was inundated during 1998 flood (del Ninno, 2001). We did not find any literature on how BWDB calculated the inundated area of 100,250 km^2 (BWDB, 1998). To verify the 'two-third' statement, we calculated the inundated area from BDM, Figure 3.14, and Figure 3.15 by following 'land only' (method-1) approach and 'total wetted area' approach (method-2). The results are shown in Table 3.2. Inundated areas of BDM and Figure 3.14 are for September 10, 1998, whereas there is no actual date mentioned for the RADARSAT image of Figure 3.15 (Duti et al., 2017). The RADARSAT image appears to show inundation inside the polders in the coastal region during months of July-August. This is definitely not the riverine flood, because coastal region is flooded during the recession stage of the flood (September-October). So, the large inundated area showing in the RADARST image of Figure 3.15 is mainly due to rainfall. Both the BDM and the satellite image of Figure 3.14 do not consider this rainfall flooding.

Results of Table 3.2 shows that the inundated area from the RADARSAT image closely agrees with the BWDB (1998) mentioned percentage of inundation for the 1998 flood. Both the BDM and the satellite image of September 10, 1998 (Figure 3.14) do not show this extra inundated land and the inundation area from these two maps are lower than the RADARSAT image (Figure 3.15).

Table 3.2: Anomalies of calculated flood inundation area by different methods and from different sources.

	Source						
	BDM		Figure 3.14		Figure 3.15		BWDB (1998)
Inundation Calculation	Wetted Land	Wetted Total Area	Wetted Land	Wetted Total Area	Wetted Land	Wetted Total Area	
Area	35,981 km^2	54, 395 km^2	37,868 km^2	73,595 km^2	58,690 km^2	97, 835 km^2	1,00,250 km^2
Percent with respect to land area of country	27.6%	41.8%	29.1 %	56.5%	45.1 %	75.2 %	77.0%
Percent with respect to total area of country	24.2 %	36.6%	25.5 %	49.6 %	39.5%	65.9 %	67.5%

Land area of country = 1,30,170 km^2, Water area of country = 18,290 km^2, Total area country = 1,48,460 km^2 (source: 2020 CIA World Factbook https://www.cia.gov/the-world-factbook/countries/bangladesh/).

Comparison among BDM, satellite image (Figure 3.14), and RADARSAT image (Figure 3.15) is shown in Figure 3.16 and in Table 3.3. This comparison shows a close agreement of BDM with the satellite image (Figure 3.14). Inundated area of BDM is slightly above 5% of the inundated area calculated from the satellite image (Figure 3.14). There is a large deviation of calculated

inundated are of BDM from the RADARSAT image (63.1%). It should be mentioned here that both the BDM and the satellite image of Figure 3.14 do not consider rainfall flooding.

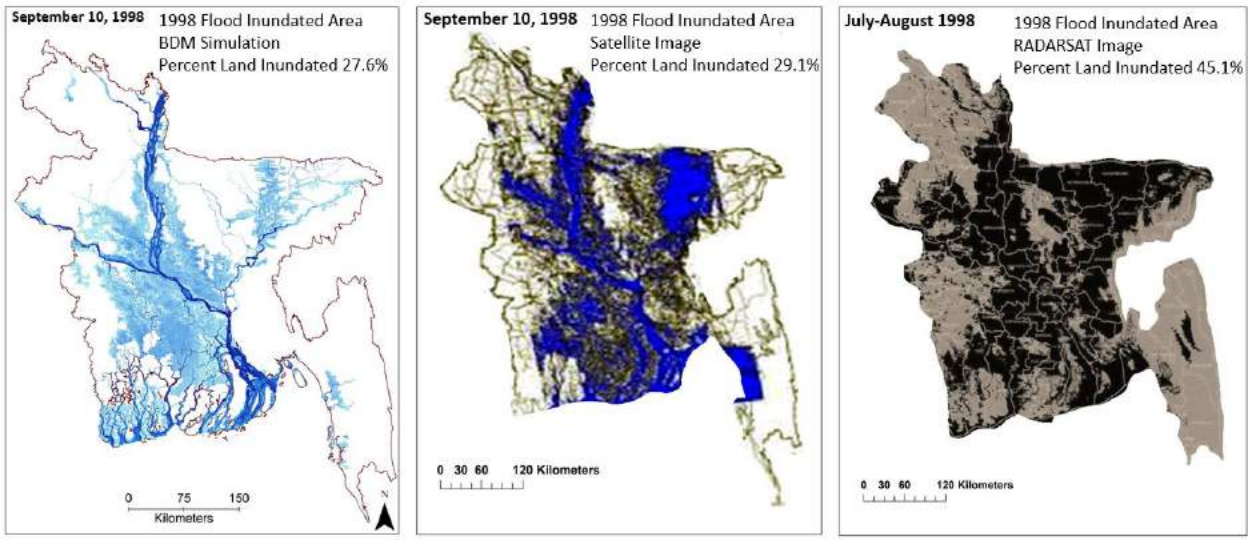

Figure 3.16: *Comparison of 1998 flood inundation area from 3 different sources. The BDM image (left image) and the satellite image (middle image) do not show rainfall inundation. The RADARSAT image (right image) shows inundation for both riverine and rainfall flooding.*

Inclusion of rivers, estuaries, haors, beels, and other wetlands within the definition of inundated area has no practical meaning and unrealistically increases the inundated area giving a false impression of severity of the flood. When only land inundated area due to riverine flood is considered, the 1998 flood shows 27% to 29% of the country was inundated during 1998 flood (see BDM and Satellite images of Figure 3.13, Figure 3.14, and Table 3.3). This is the effective inundated area which is relevant for flood management, and which also contributes to the floodplain sedimentation.

Table 3.3: Land inundation area of 1998 flood from different sources

Inundation Calculation	Source		
	BDM (Figure 3.13)	Satellite Image (Figure 3.14)	RADARSAT Image (Figure 3.15)
Inundated Area	35,981 km^2	37,868 km^2	58,690 km^2
Percent with respect to land area of country	27.6%	29.1%	45.1%
Percent deviation of BDM		5.2%	63.1%

To make compatible with the satellite images, all the flooding scenarios by BDM simulations shown so far shows the areal extent of flood. We also made flood simulation by BDM where flood depth information is also available. The flood depth map by BDM simulations shows water depths during peak of 1998 flood in land and in all water bodies (Figure 3.17).

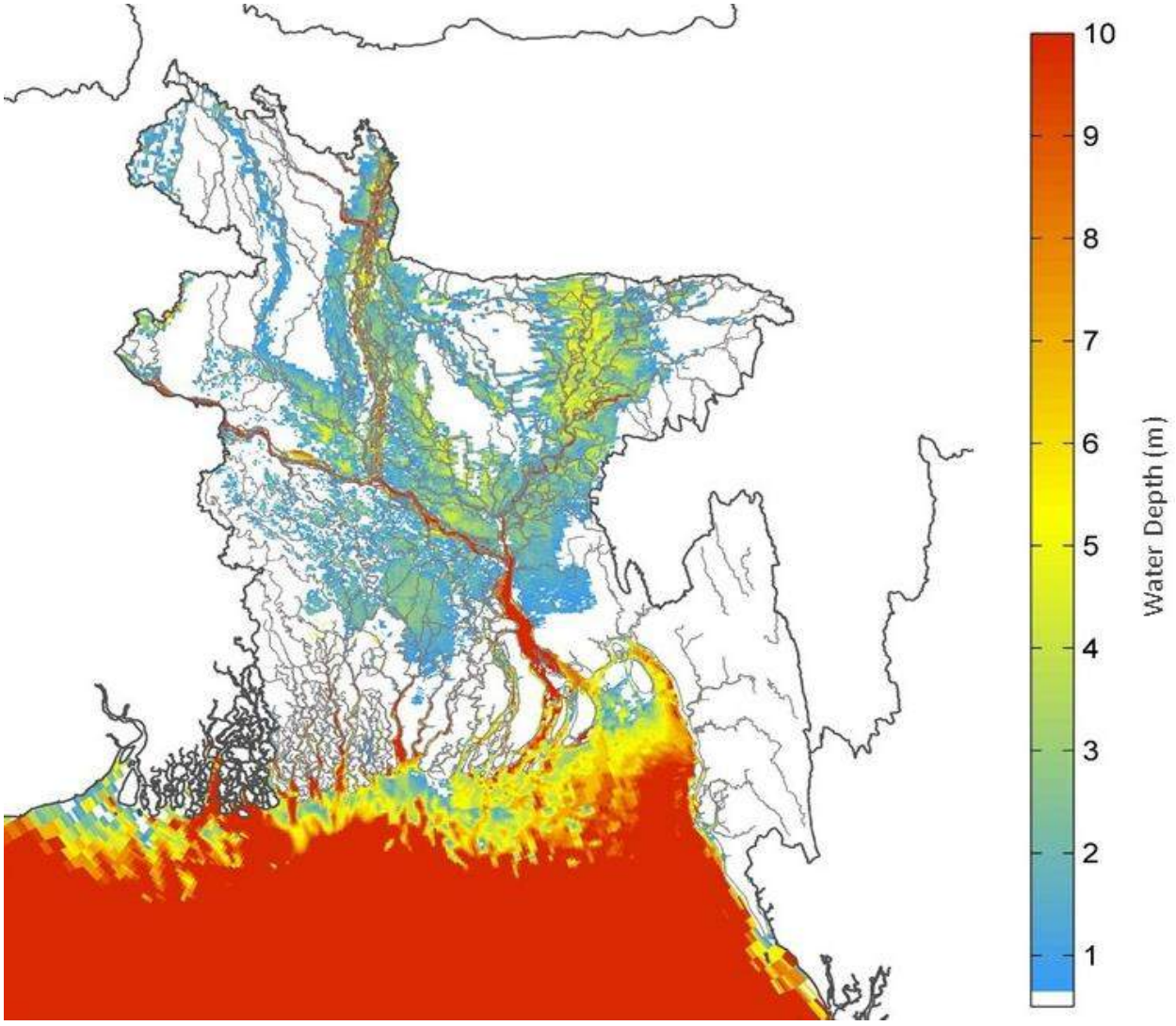

Figure 3.17: *Flood depth map for 1998 flood simulated by BDM. This map shows flood depths in land and in all water bodies – rivers, estuaries, ocean, haors, wetlands. The range of depth values shown in the figure is 0-10m.*

3.8 Sedimentation in Floodplains

Processes of sediment transport and flooding described in the previous sections determine the patterns and extent of floodplain sedimentation on the delta surface. On the other hand, floodplain sedimentation on the delta surface is an important determinant of delta sustainability against sea

level rise (Rogers and Overeem, 2017) and offsetting waterlogging created due to polders (WARPO and BUET, 2019). To understand the flooding and sedimentation processes in different flooding and intervened conditions, we performed four numerical experiments similar to what was done in WARPO and BUET (2019). But study area of WARPO and BUET (2019) was only the coastal zone. In this study, we did it for the entire GBM delta of Bangladesh part. The four numerical experiments performed are (1) Intervened stage in average flood condition (2) Intervened stage in extreme flood condition (3) Natural stage in average flood condition (4) Natural state in extreme flood condition. In intervened stage, we considered intervention by all the existing embankments in the delta including the 139 polders in the coast. In natural state, we removed all the 139 polders in the coast from the system but kept the other embankments in the non-coastal region of the delta (for example, Brahmaputra Right Embankment, Mujib Badh etc.). We did it because, coastal polders are believed to restrict most of the floodplain sedimentation and thus act against delta building process (Rogers and Overeem, 2017; WARPO and BUET, 2019). To determine average and extreme flood condition, we did frequency analysis using long term discharge data at Hardinge bridge of Ganges and Bahadurabad of Brahmaputra-Jamuna. As flood in the delta is dictated by discharge of Barhamaputa-Jamuna, frequency analysis result of Bahadurabad station is used to determine the flood condition. Average flood is defined as a flood with return period of 2.33 years and extreme flood is defined as the flood with a return period of 200 years. With these definitions, year 2000 is identified as an average flood year and year 1998 is identified as an extreme flood year.

3.8.1 Sedimentation in intervened state

Results of numerical experiments with intervened condition is shown in Figure 3.18. We can see the expected increase of inundation in intervened state when flood condition is changed from average to extreme (Figures 3.18a and 3.18b). Increased flooding is observed all over the country, but the impact is seen to be maximum in the south-central part of the coat where there is no polder. Floodplain sedimentation is caused by flooding in the floodplains. So, pattern of floodplain sedimentation follows the pattern of floodplain flooding (Figures 3.18c and 3.18d). During BDM simulations, total sediment inflows to the system increases from 400 million ton to 1,243 million ton when flood condition changes from average to extreme. Water inflows to the system also increases in average flood condition compared to extreme flood condition causing increased floodplain flooding (Figures 3.18a and 3.18b). The increased sediment flux causes increased floodplain sedimentation during extreme flood (Figures 3.18c and 3.18d). BDM simulations also show sedimentation thickness, sedimentation volume, and percentage of sedimentation volume with respect to total inflow sediments for seven hydrological region of the country – north-west, north-central, north-east, south-west, south-central, south-east, and eastern hill tracks. The figure also shows total floodplain sedimentation volume and percentage of this volume with respect to total inflow sediment volume. These values are summarized in Table 3.4.

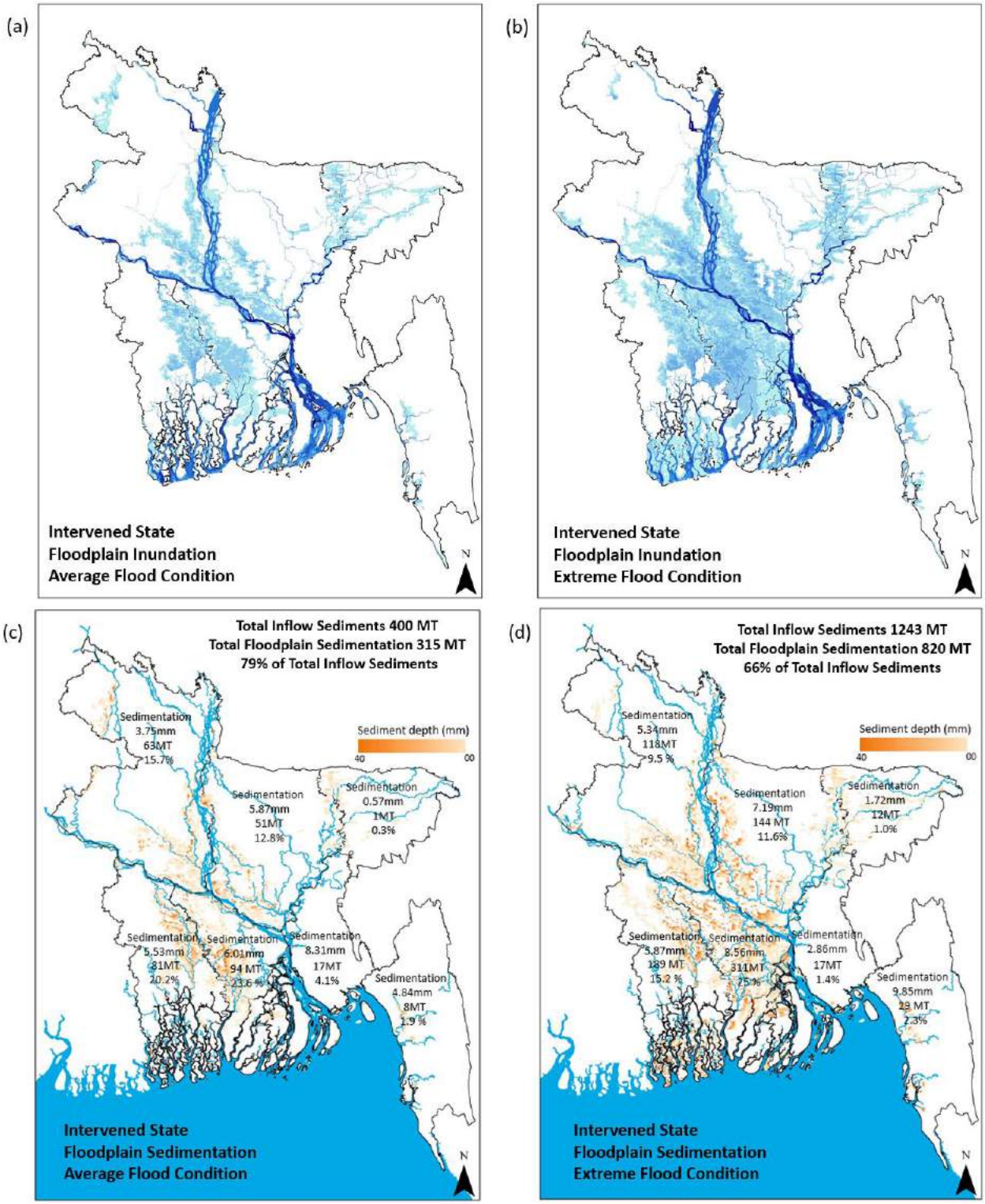

Figure 3.18: *BDM simulations showing flooding (a-b) and sedimentation (c-d) in intervened state during average flood and extreme flood conditions. The figures also show total and regional sedimentation depths on the delta surface.*

Table 3.4: Yearly distribution of sedimentations in intervened state for average flood and extreme flood conditions

Total Sediment Distribution in Intervened State					
Flood Condition	Total Inflow Sediments (Million Ton)	Total Delta Floodplain Sedimentation (Million Ton)	Coastal Floodplain Sedimentation (Million Ton)	Percent Retained in Total Delta Floodplains	Percent Retained in Coastal Floodplain
Average	400	315	192	79%	48%
Extreme	1243	820	517	66%	42%

Regional Sediment Distribution in Intervened State						
Region	Sedimentation Thickness (mm)		Sedimentation Volume (Million Ton)		Percentage of Sedimentation Volume w.r.t Total Inflow Sediments	
	Average	Extreme	Average	Extreme	Average	Extreme
NW	3.75	5.34	63	118	15.7%	9.5%
NC	5.87	7.19	51	144	12.8%	11.6%
NE	0.57	1.72	1	12	0.3%	1.0%
SW	5.53	5.87	81	189	20.2%	15.2%
SC	6.01	8.56	94	311	23.6%	25.0%
SE	8.31	2.86	17	17	4.1%	1.4%
EHT	4.84	9.85	8	29	1.9%	2.3%

[*] *Average Relative Sea Level Rise = 5.0mm / year (Brown and Nicholls, 2015; Becker et al., 2020)*

In Table 3.4, we can see that in the intervened state, due to increased sediment inflows in the system from 400 MT in average flood condition to 1243 MT in extreme flood condition, total retained sediment volume in the delta floodplain increases from 315 MT (79% of total inflow sediments) to 820 MT (66% of total inflow sediments). When sedimentation on the delta surface is considered, coastal floodplain gets special attention due to relatively low elevation of the coastal land which is susceptible to inundation due to sea level rise. We can see that sedimentation volume in the coastal floodplain increases from 192 MT (48% of total inflow sediments) in average flood condition to 517 MT (42% of total inflow sediments) in extreme flood condition. Here, for both total retained sediment volume and coastal floodplain retained volume, sediment volume increases in extreme flood condition compared to average flood condition. But its percentage share decreases due to relatively large increase of total sediment inflows in extreme flood condition.

The regional sediment distribution on the delta floodplains (Table 3.4) shows sedimentation depth, sedimentation volume, and percentage of sedimentation volume in different regions with respect to total inflow sediments. It is seen that sedimentation depth on the delta surface during intervened condition varies between 0.57mm to 9.85mm depending on the flood condition and floodplain location. It is found from the literature that the relative sea level rise (RSLR) in GBM delta is

approximately 5.0 mm/year by considering average yearly sea level rise and subsidence (Brown and Nicholls, 2015; Becker et al., 2020). We can see that in average flood condition, sedimentation depth on the delta surface is less than 5.0 mm/year only in NW, NE, and EHT regions, and in extreme flood condition only in NE and SE regions have sedimentation depth less than 5.0 mm (Table 3.4). For all other regions except these, sedimentation depth is greater than 5.0 mm/year showing potential sedimentation on the delta surface in the intervened state for all flood conditions which will offset the threat of inundation of GBM delta due to sea level rise. The 2 regions (NW and NE) are relatively higher elevation non-coastal regions which are not susceptible to inundation due to sea level rise. Although sedimentation rate in EHT region is relatively low during average flood condition (4.84mm), we can see a very high rate of sedimentation in this region for extreme flood condition (9.85mm). The maximum sedimentation depth on delta surface is found in SE region (8.31mm) during average flood condition and in SC region (8.56mm) during extreme flood condition (we are not considering high sedimentation in EHT region during extreme flood condition as mentionable, because the high value of sedimentation in this region occurs mainly along the low elevation mud flats along the coast). It should be noted here that in BDM simulations (Figures 3.18c and 3.18d), we found the sedimentation in SE region mainly in Urir Char-Sandwip zones. Urir Char-Sandwip region is situated in the turbidity maximum zone (Sarker et al., 2011) where BDM simulated sediment concentration is also high (see Figures 2.11e – 2.11i in Chapter Two). On the other hand, there is no polder in SC region which drives increased sediments in this region during extreme flood condition resulting increased sedimentation depth. When we consider percent share of sediment volume on the delta surface, we found that SC region (where there is no polder at present) always share the maximum percentage for all flood conditions (23.6% in average flood and 25.0% in extreme flood).

3.8.2 Sedimentation in natural state

In these numerical experiments, we have removed all the polders from the coastal region but retain all the embankments in non-coastal region (Figure 3.19). So, the increased inundated area for both the average flood and extreme flood conditions is mainly in the coastal region (Figures 3.19a and 3.19b). Similar to the intervened states, sedimentation in the natural states also follow the inundation pattern on the floodplains (Figures 3.18 and 3.19). With similar sediment inflow volumes for both the flooding conditions, increased inundated (and thus sedimented) areas cause increased sediment volumes on the delta surface. In average flood condition, sediment volume on the floodplains in the natural state increase to 342 MT compared to 315 MT in intervened state (about 9% increase). In extreme flood condition, this increase is 967 MT in natural state from 820 MT in intervened state (about 18% increase). This additional volumes of sediments on the delta surface are mainly in the coastal region and contributes to delta building process. When coastal floodplains are considered, we can see that in average flood condition, increase in natural state is 214 MT compared to 192 MT in intervened condition (about 12% increase). In extreme flood condition, these values are 626 MT in natural state from 517 MT in intervened state (about 21% increase). Different sedimentation parameters in natural state are summarized is Table 3.5.

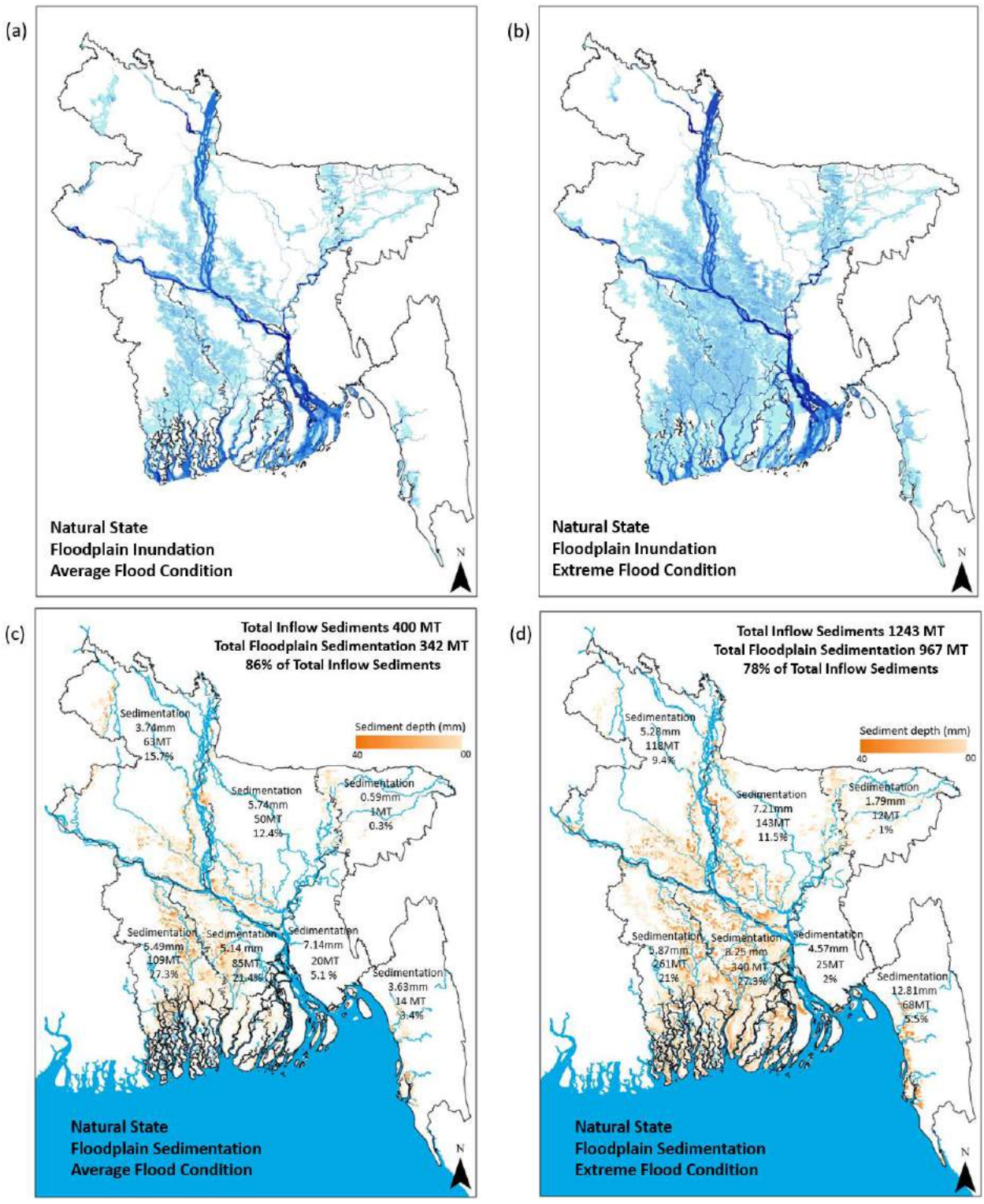

Figure 3.19: *BDM simulations showing flooding (a-b) and sedimentation (c-d) in natural state during average flood and extreme flood conditions. The figures also show total and regional sedimentation depths on the delta surface.*

Table 3.5: Yearly distribution of sedimentations in natural state for average flood and extreme flood conditions

Total Sediment Distribution in Natural State					
Flood Condition	Total Inflow Sediments (Million Ton)	Total Delta Floodplain Sedimentation (Million Ton)	Coastal Floodplain Sedimentation (Million Ton)	Percent Retained in Total Delta Floodplains	Percent Retained in Coastal Floodplain
Average	400	342	214	86%	54%
Extreme	1243	967	626	78%	50%

Regional Sediment Distribution in Natural State						
Region	Sedimentation Thickness (mm)		Sedimentation Volume (Million Ton)		Percentage of Sedimentation Volume w.r.t Total Inflow Sediments	
	Average	Extreme	Average	Extreme	Average	Extreme
NW	3.74	5.28	63	118	15.7%	9.4%
NC	5.74	7.21	50	143	12.4%	11.5%
NE	0.59	1.79	1	12	0.3%	1.0%
SW	5.49	5.87	109	261	27.3%	21.0%
SC	5.14	8.25	85	340	21.4%	27.3%
SE	7.14	4.57	20	25	5.1%	2.0%
EHT	3.63	12.81	14	68	3.4%	5.5%

[*] *Average Relative Sea Level Rise = 5.0mm / year (Brown and Nicholls, 2015; Becker et al., 2020)*

Except in SE region, sedimentation thickness for all other regions have increased in extreme flood condition compared to average flood condition. The sedimentation thickness shown in Table 3.5 (and in Table 3.4) represents average thickness of the region. This means if new sedimented area appears due to increased flooding with relatively lower depth, average sedimentation thickness decreases. So, the decreased sedimentation thickness does not mean that less sedimentation has occurred in that place. This is the reason of decreased sedimentation thickness in SE region due to increased flooding in extreme flood condition. We have earlier seen this incident for the same region (SE region) in the intervened state (Table 3.4). For average flood condition, the RSLR value of 5.0 mm/year (Brown and Nicholls, 2015; Becker et al., 2020) is seen to be lower in all the regions except NW, NE of the non-coastal region and EHT of the coastal region. Land elevations of NW and NE regions are relatively high, and these two regions are not susceptible to be inundated by sea level rise. The part of the EHT which is sedimented is low elevation mud flat. Although sedimentation is this part of EHT is relatively low (3.63 mm) in average flood condition, we can see a very high rate of sedimentation (12.81mm) during extreme flood condition. A similar pattern in EHT region was found for intervened condition (Table 3.4). Except EHT, we can see a high rate of increase of sedimentation in SC region in natural state when flood condition changes from

average to extreme (5.14mm is increased to 8.25mm). We also found similar trend in this region for intervened state also (Table 3.4, 6.01mm increased to 8.56mm). When sedimentation volume is considered, we can see increased sedimentation volume in all the regions when flood condition changes from average to extreme. This is obvious, because sediment inflow has increased from 400 MT in average flood condition to 1243 MT in extreme flood condition. Regarding percentage share of these sediments, we found SW region (Sundarban dependent region) has the maximum share (27.3%) in average flood condition, and SC region (non-poldered region in intervened state) has the maximum share (27.3%) in extreme flood condition.

3.8.3 Changes in sedimented area for changes in flood conditions and physical state of the system

We have calculated the total sedimented area in the entire country and the coast for all the four numerical experiments described above (Table 3.6). This gives us an idea about increased sedimented area due to change in flood condition and physical state of the system.

Table 3.6: Sedimented area for different flood conditions and different delta states.

Flood Condition	Sedimented area of the entire delta (km^2)			Sedimented area in the coastal zone (km^2)		
	Intervened State	Natural State	Increase for physical state	Intervened State	Natural State	Increase for physical state
Average	12,620	14,914	18%	6,310	8,232	30%
Extreme	23,120	27,365	19%	12,139	15,863	31%
Increase for flood condition	83%	84%		92%	93%	

We can see that change in physical state of the system from intervened state to natural state increase the sedimented area by 18-19% for entire delta and 30-31% for the coastal region, while change in flood condition from average to extreme condition increase the sedimented area by 83-84% for the entire delta and 92-93% for the coastal region. So, GBM delta in its present state (intervened state) is sufficiently capable to accommodate increased sedimented area only due to change in flood condition.

3.8.4 Change in sedimentation depth for changes in flood condition and physical state of the system

We have used Table 3.4 and Table 3.5 to calculate the change in sedimentation depth for all the four numerical experiments. This makes it possible to have an idea about the changes in sedimentation depth due to changes in flood condition and physical state of the system (Table 3.7). The results show that due to change in flood condition from average to extreme, average increase of sedimentation depth on delta surface for intervened state is 0.93mm and for natural state is

2.04mm. On the other hand, if we change the physical state of the system from intervened to natural keeping the flood condition same (and thus keeping the sediment inflow to the system same), average sedimentation depth on the delta surface decreases to 0.48mm in average flood but increases to 0.63mm in extreme flood conditions. The decrease of sedimentation depth is caused by extended sedimented area (see Table 3.6) while total sediment inflows remain the same (because flood condition is same but physical state is changed). These results show that in terms of sedimentation depth on the delta surface, we will get advantage by changing delta state form intervened state to natural state. In the previous section (section 3.8.3) we have seen to get advantage in terms of sedimented area when flood condition is changed from average to extreme. So, in terms of delta sustainability, maximum advantage will be achieved if flood condition is changed from average to extreme and physical state of delta is changed from intervened to natural.

Table 3.7: Change in sedimentation depth due to change in flood condition and physical state of the delta.

	Change in sedimentation depth due to change in flood condition from average to extreme (+ve for increase, -ve for decrease)		Change in sedimentation depth due to change in physical state of the system from intervened to natural (+ve for increase, -ve for decrease)	
Region	Intervened (mm)	Natural (mm)	Average (mm)	Extreme (mm)
NW	+1.59	+1.54	-0.01	-0.06
NC	+1.32	+1.47	-0.13	+0.02
NE	+1.15	+1.20	+0.02	+0.07
SW	+0.34	+0.38	-0.04	0.00
SC	+2.55	+3.11	-0.87	-0.31
SE	-5.45	-2.57	-1.14	+1.71
EHT	+5.01	+9.18	-1.21	+2.96
Average Sedimentation	+0.93	+2.04	-0.48	+0.63

**Average Relative Sea Level Rise = 5.0mm / year (Brown and Nicholls, 2015; Becker et al., 2020)*

3.8.5 Change in sedimented area and sedimentation depth for changes in sediment inflows and physical state of the system

To summarize the changes in sedimented area and sedimentation depth on the delta surface due to changes in flood condition and physical state of the system, we have used results of Tables 3.4, 3.5, 3.6, 3.7 to prepare Table 3.8 as shown below:

Table 3.8: Changes in sedimented area and sedimentation depth due to changes in flood condition and physical state of the system.

	Intervened State			Natural State		
Sediment Inflow (MT)	Average	400	Increase by 210%	Average	400	Increase by 210%
	Extreme	1,243		Extreme	1,243	
Sedimented area on the floodplains (km2)	Average	12,620	Increase by 83%	Average	14,914	Increase by 84%
	Extreme	23,120		Extreme	27,365	
Sediment volume on the floodplains (MT)	Average	315	Increase by 160%	Average	342	Increase by 183%
	Extreme	820		Extreme	967	
Sedimentation depth in non-tidal floodplains (mm)	Average	0.57–8.31	Increase by 1.15-1.54	Average	0.59–5.74	Increase by 4.28-7.07
	Extreme	1.72–9.85		Extreme	4.87–12.81	

[*] *Average Relative Sea Level Rise = 5.0mm / year (Brown and Nicholls, 2015; Becker et al., 2020)*

In our case, change in flood condition from average to extreme condition means increase in sediment inflows from 400 MT to 1243 MT (210%). Changing physical state of the system means removing the existing polders from the system. In intervened state, increasing sediment inflows by 210% increases the sedimented area on floodplains by 83%, sediment volume by 160%, and sedimentation depth on the delta surface by 1.15-1.54mm (Table 3.7). The corresponding increase for natural state is 84% for the sedimented area, 183% for sediment volume, and 4.28-7.07mm for sedimentation depth (Table 3.7). This shows that by increasing sediment inflows, sedimented area and volume on the floodplains can be largely increased. But we get comparatively little advantage in terms of sedimented area and volume by changing the physical state of the system from intervened to natural (83% & 160% in intervened state, and 84% & 183% in natural state, see Table 3.7). But for sedimentation depth, we can see remarkable increase for the similar increase of sediment inflows (1.15-1.54mm to 4.28-7.07mm).

Changing physical state of the system by removing all the polders from the system is not realistic and not implementable. But the similar impact can be achieved by adopting different sediment management practices (for example different form of controlled flooding including TRM). On the other hand, we can ensure sustained sediment inflows to the system in the delta through

transboundary negotiation and proper sediment management. So, delta sustainability can be ensured by ensuring required sediment inflows from outside of the delta and by appropriate sediment management inside of the delta.

3.8.6 Importance of SC region on delta sustainability

A special note should be mentioned about the SC region. At present there is no polder in the SC region. In all the previous discussions, we have seen that SC regions plays an important role when percentage of sediment retained on the floodplains, sedimentation volume, and sedimentation depth is considered (see Table 3.9).

Table 3.9: Contribution of SC region on delta sustainability

	Intervened		Natural	
Sediment retained on the floodplain	Average	23.6%	Average*	21.4%
	Extreme	25.0%	Extreme	27.3%
Sedimentation volume	Average	94 MT	Average*	85 MT
	Extreme	311 MT	Extreme	340 MT
Sedimentation depth in tidal floodplains	Average	6.01 mm	Average*	5.14 mm
	Extreme	8.56 mm	Extreme*	8.25 mm

**The decrease is due to dispersion of sediments in a wider area of sedimentation when the state of the system is changed from intervened state to natural state.*

Compared to the total GBM delta surface, the share of SC region is (Table 3.9): total inundated area which is also sedimented area is 9% (Table 3.1), sediment retained on the floodplain 21.4-27.3%, sediment volume retained 94-340 MT, and sedimentation depth 5.14-8.56mm. This shows overall importance of SC region compared to the entire delta when delta sustainability is considered. Any intervention (directly or indirectly) on SC region that restricts sedimentation in SC region will seriously affect the delta sustainability.

CHAPTER FOUR
Sediment Management Practices in the GBM Delta

4.1 Introduction

In Chapter One of the report (section 1.2), we have discussed that the present sediment management practices in the GBM delta are (1) TRM (2) Cross-dam and (3) Dredging. An example of locations in the coastal part of GBM delta of these sediment management practices are shown in Figure 4.1. The purpose of a sediment management practice is usually to solve a local problem. But we can term a sediment management practice as an effective option when it can solve the local problem and at the same time, can ensure the best use of sediment resource for delta building process and contribute to delta sustainability. In this chapter, we will assess impacts of sediment management practices from this viewpoint.

Figure 4.1: *Locations of few sediment management practices in the coastal part of GBM delta. The locations are seen for TRM, cross-dam, and dredging.*

All the past studies related to sediment management practices in GBM delta focused on these three options. Out of these three, there are large number of studies dealing with TRM (Amit et al., 2013; Khadim et al., 2013; Karim and Mondal, 2017; Gain et al., 2017; Al Masud and Islam, 2018; Hussain et al., 2018; Talchabhadel et al., 2018; Adnan et al., 2018; Seijgera et al., 2019; Gain et al., 2019; Islam et al., 2020; Islam et al., 2021a; Islam et al, 2021b). The reason is obvious. TRM was and is still believed to solve the long-lasting waterlogging problem in the south-west region of Bangladesh. Compared to TRM, there are relatively less studies on other two sediment management practices. Cross-dam is the most popular sediment management practice in this region as a land-reclamation method, and all the past studies focused on effectiveness of cross-dams (Jakobsen et al., 2002; EDP, 2007; Sarker et al., 2011; Rogers and Overeem, 2017; Angamuthu et al., 2018; Hale et al., 2019). We found very few studies in the past that deals with the dredging issue. The studies so far conducted on dredging either focused on dredging cost or effectiveness of dredging (Alim et al., 2016; Rahim et al., 2016; Rahman and Younus, 2016; WARPO and BUET, 2019; Rahman et al., 2021).

While discussing about sediment transport processes in the GBM delta (see Chapter Three), we have seen that sediment in the delta transports within a system that comprises rivers, estuaries, wetlands, haors, ocean, and delta floodplains. So, although all the three sediment management practices mentioned above are aimed to solve the local problems, its impact cannot be local. For example, impact of a cross dam in the coast or dredging of a river section in Brahmaputra-Jamuna must be felt on other part of the delta. But we did not see any study on this system impact of any of the sediment management practices in this delta.

As there are large number of studies available related TRM and TRM is also a type of natural dredging of the related river and sedimentation of the related floodplains, we decided to omit TRM from our study. In this study, we concentrated on two other sediment management practices in the region – cross-dam and dredging. Instead of studying local impacts of these two sediment management practices, we used a system approach by applying BDM (see Chapter Two) to study the system impact. In doing this, we will show the probable impact on the sediment transport processes (see Chapter Three) in the delta when any of these sediment management practices is implemented within the system. In this study, we will not propose any new sediment management practice in the delta. In our understanding, considering our present state of knowledge, it is much more important to rationalize the current popular sediment management practices by applying a system approach. A new sediment management practice (for example, controlled flooding or smart cross-dam or intelligent dredging without creating any adverse social and technical problems) may be a next step.

4.2 System Impacts of Cross-Dam

Cross-dam is a well-known sediment management practice which is used for land reclamation in the off-shore region (EDP, 2007). EDP proposed 18 probable cross dam locations in the coast (Figure 4.2). Out of these 18 probable locations, in this study, system impacts of 13 of these cross-dams are studied. In addition, system impact of Noakhali-Urir char cross-dam planned by BWDB

is also studied. We have applied BDM to study these system impacts. All the subsequent results are based on 1998 flood condition.

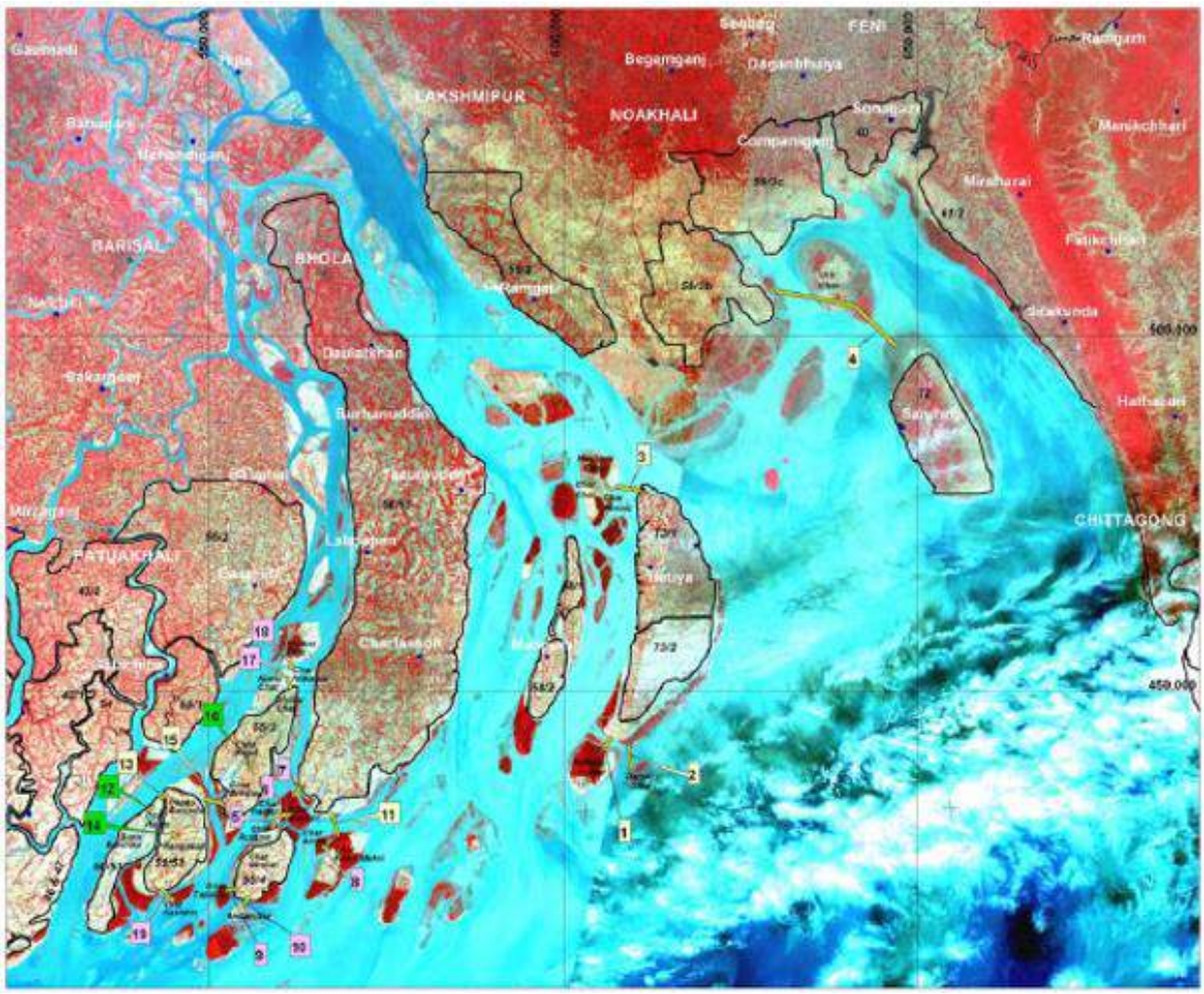

Figure 4.2: *Proposed cross-dam locations by EDP (source: EDP, 2007). We have used these base locations to select 13 cross-dams for which system impacts are studied.*

Before going to BDM application to study system impact of cross-dams, we did some image analysis to see the local impact of an already implemented cross-dam by BWDB. Figure 4.3 shows the location of the cross-dam (Figure 4.3a) which was implemented in 2010, planform in 1984 (16 years before construction of cross-dam, Figure 4.3b) and planform in 2018 (8 years after construction of cross-dam, Figure 4.3c). The green, blue, and yellow circles show where lands are reclaimed due to the cross-dam. The white circle shows the land which is eroded due to the impact of the cross-dam. This result show only the local impact but tells nothing what happens in other locations of the delta due to construction of this cross-dam.

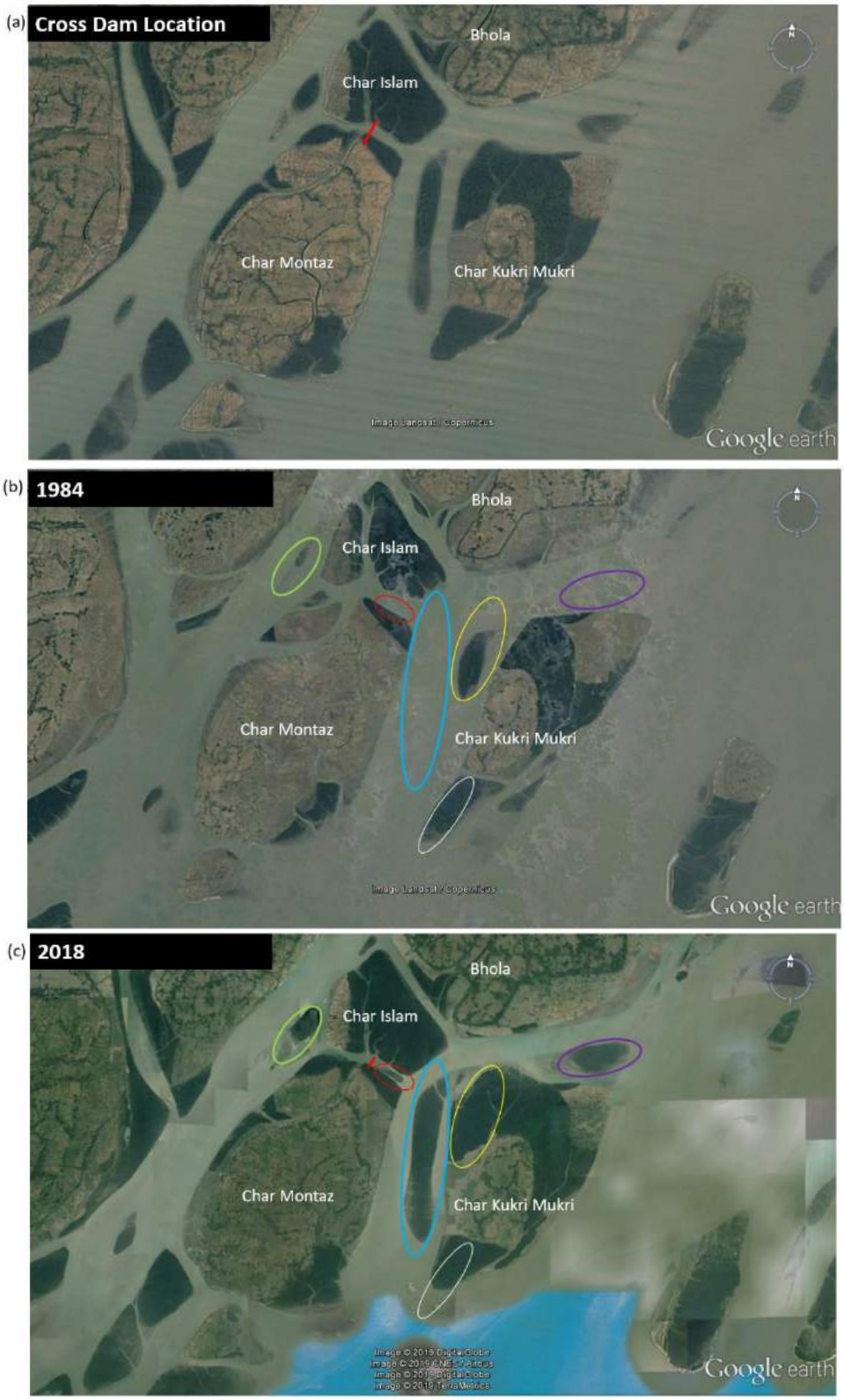

Figure 4.3: *Local impact of a cross-dam implemented by BWDB. (a) Location of the cross-dam (b) Planform of cross-dam location 16 years before the construction of the cross-dam (c) Planform changes of cross-dam location 8 years after construction of the cross-dam.*

4.2.1 System impacts of EDP proposed cross-dams

We found 5 of the small cross-dams proposed by EDP (2007) that can be merged into single cross-dam. With this assumption, the 13 selected cross-dam locations which are used in BDM application is shown in Figure 4.4. In the model application, we assumed all the cross-dams are implemented within the system. With this assumption, BDM is applied to study system impact of these cross-dams in the delta.

The indicators to assess the system impacts are: change in water level in selected locations, change in cross section in selected locations, change in inundation depth during peak monsoon in the delta, change in peak monsoon velocity in the delta, change in suspended sediment concentration in the delta, changes in sedimentation and erosion in the region, and change in sedimentation volume and depth on the delta surface.

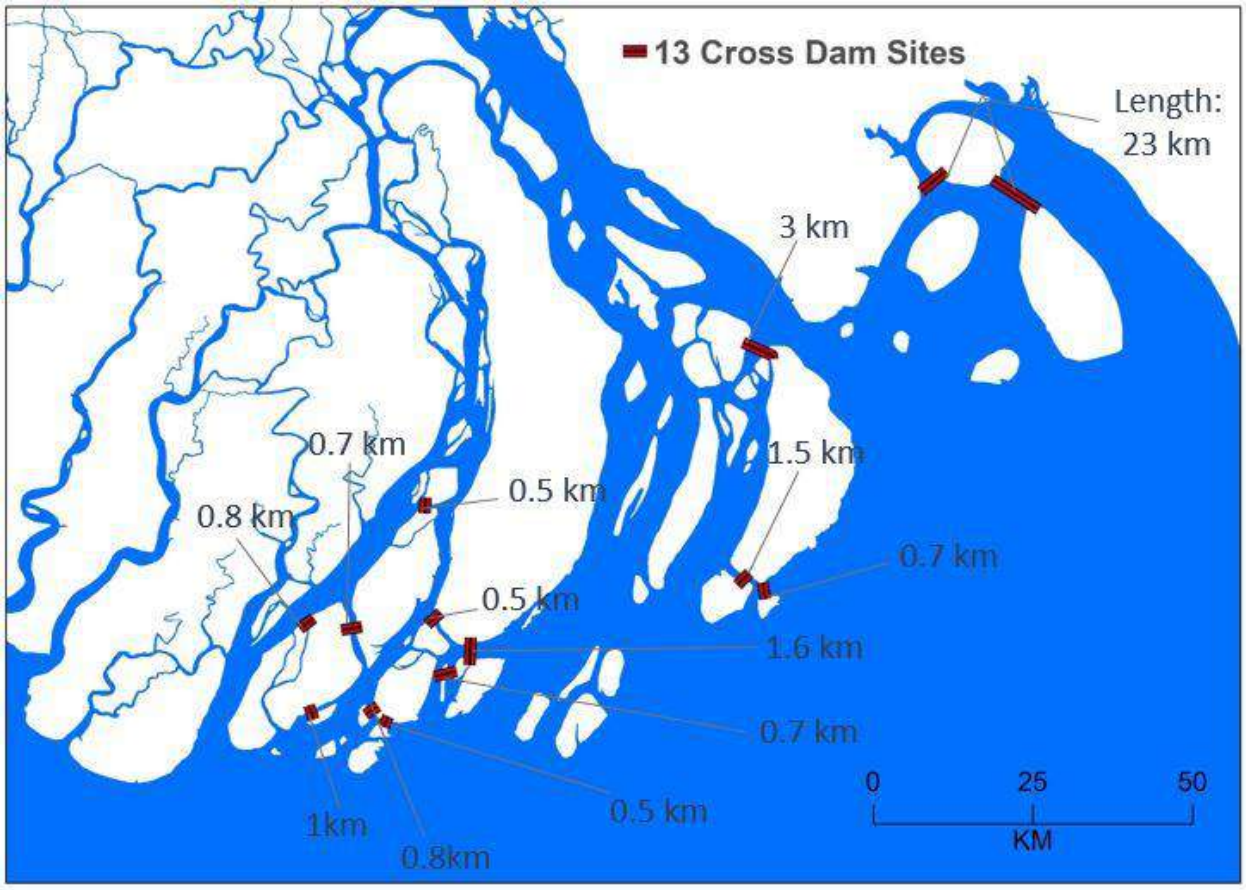

Figure 4.4: *Cross-dam locations used in BDM application. These 13 cross-dam locations are selected based on cross-dams shown in Figure 4.2. The length of each of the cross-dams are also shown.*

Change in water level

Impact on water level at the locations shown (Figure 4.5) due to construction 13 cross-dams shows changes in tidal amplitude along Meghna Estuary. We can see more impact close to Meghna Estuary mouth (location-2) compared to inside of the estuary (location-1). This change in tidal amplitude will change the tidal hydrodynamics of the system and may lead to a long-term hydro-morphodynamic change in the region. This aspect was also mentioned by Jakobsen et al. (2002).

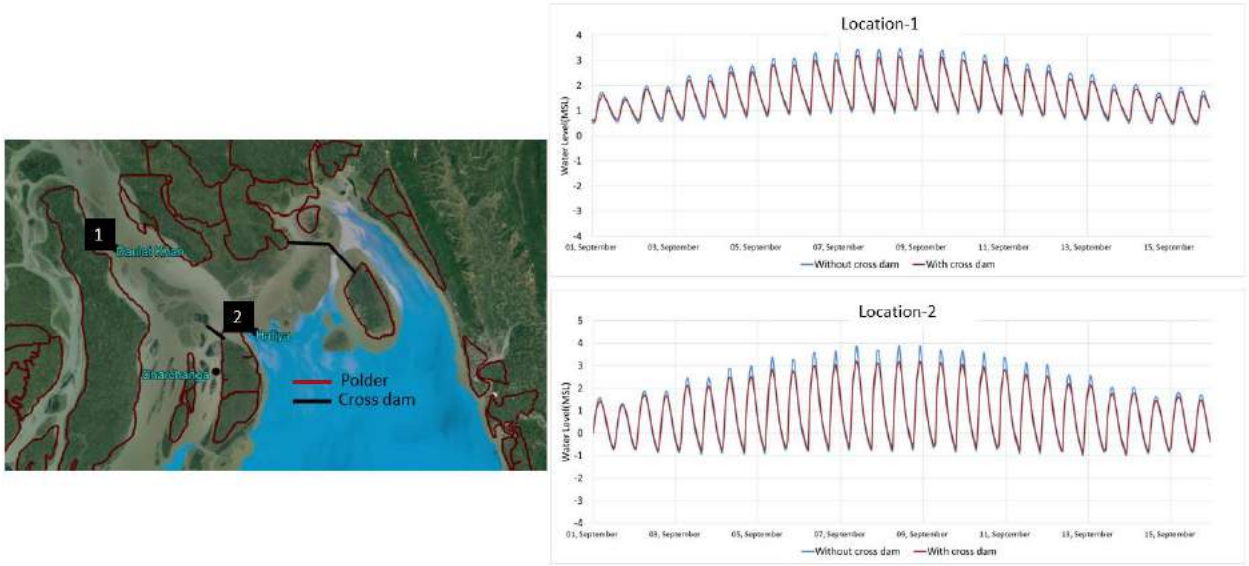

Figure 4.5: *Impact of 13 cross-dams on water level inside Meghna Estuary (location-1), and at Meghna mouth (location-2). The water level is plotted for September 1-15, 1998.*

Changes in cross section

We have examined yearly changes in cross-sections in locations – one in close proximity of the Sandwip-Urir Char cross-dam and the other in the Baleshwar River (Figure 4.6). As expected, sedimentation in the cross-dam location reclaims the land and reduces the cross-section area. On the other hand, due to riverbed erosion, cross-section area in Baleshwar River increases. Sandwip-Urir Char cross-dam is located in the zone of turbidity maximum (Sarker et al., 2011), whereas Baleshwar is located within the recirculation zone in the coast where sediments re-enter into the western estuarine systems (see Figure 3.12, Chapter Three). Due to trapped sediments in the cross-dam location, sediment supply from the zone of turbidity maximum decreases. This may lead to riverbed erosion in the western estuarine systems. This impact of cross-dam is significant. If cross-dam locations are intelligently selected, then reduced sediment supply (due to trapped sediment in cross-dam location) in the western estuarine systems may act positively to increase conveyance capacity of the rivers in the south-west region. This will act to reduce waterlogging problem in the region.

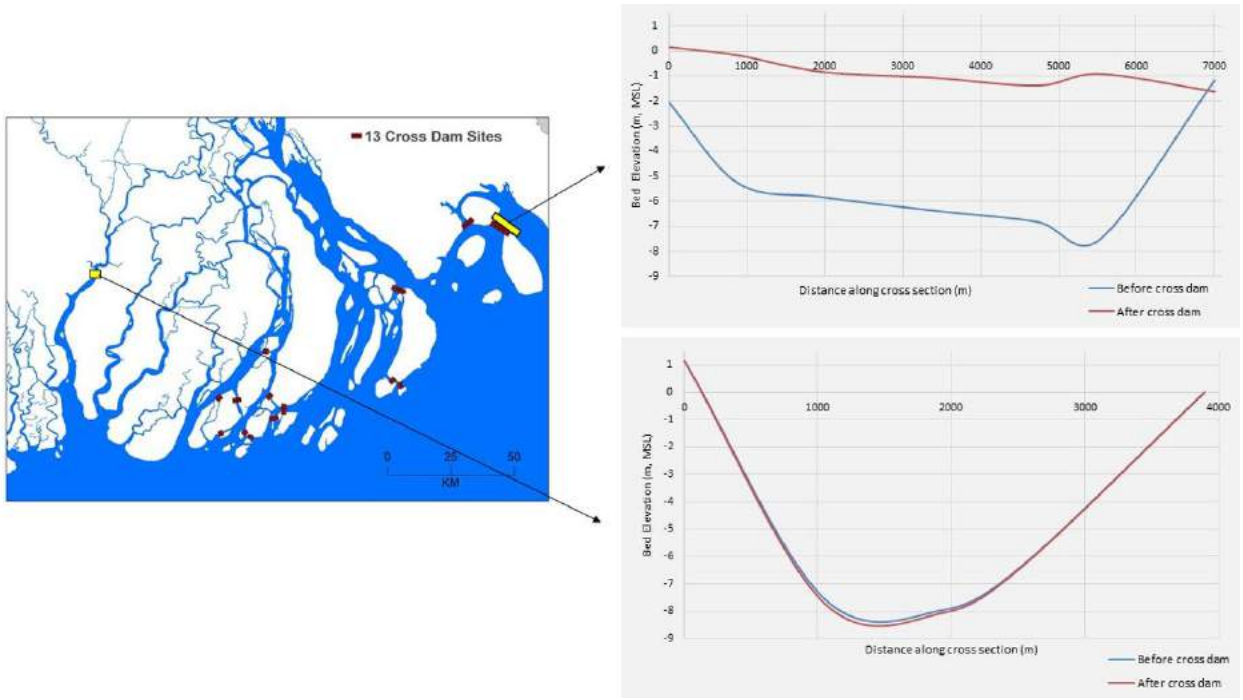

Figure 4.6: C*ross section at the cross-dam location (top) and at a location in the western estuarine system (bottom). The top section shows reduced cross-sectional area, and the bottom section shows the increased cross-sectional area*.

Changes in inundation depth

We have assessed impact on peak flood inundation depth in the delta due to construction of the 13 cross-dams (Figure 4.7). Cross-dam reduces the channel depth. Due to reduced channel depth, water level close to reclaimed land increases. This leads to increased flood inundation in locations close to the cross-dam locations. Due to construction of 13 cross-dams, we can see increased flooding in unprotected low-elevation intertidal mud flats in the EHT region. Increased flooding is also observed in the unprotected regions of Sandwip, Urir Char, Noakhali, Hatiya, Bhola, and surrounding island. This result shows importance of studying system impacts before taking any new cross-dam project.

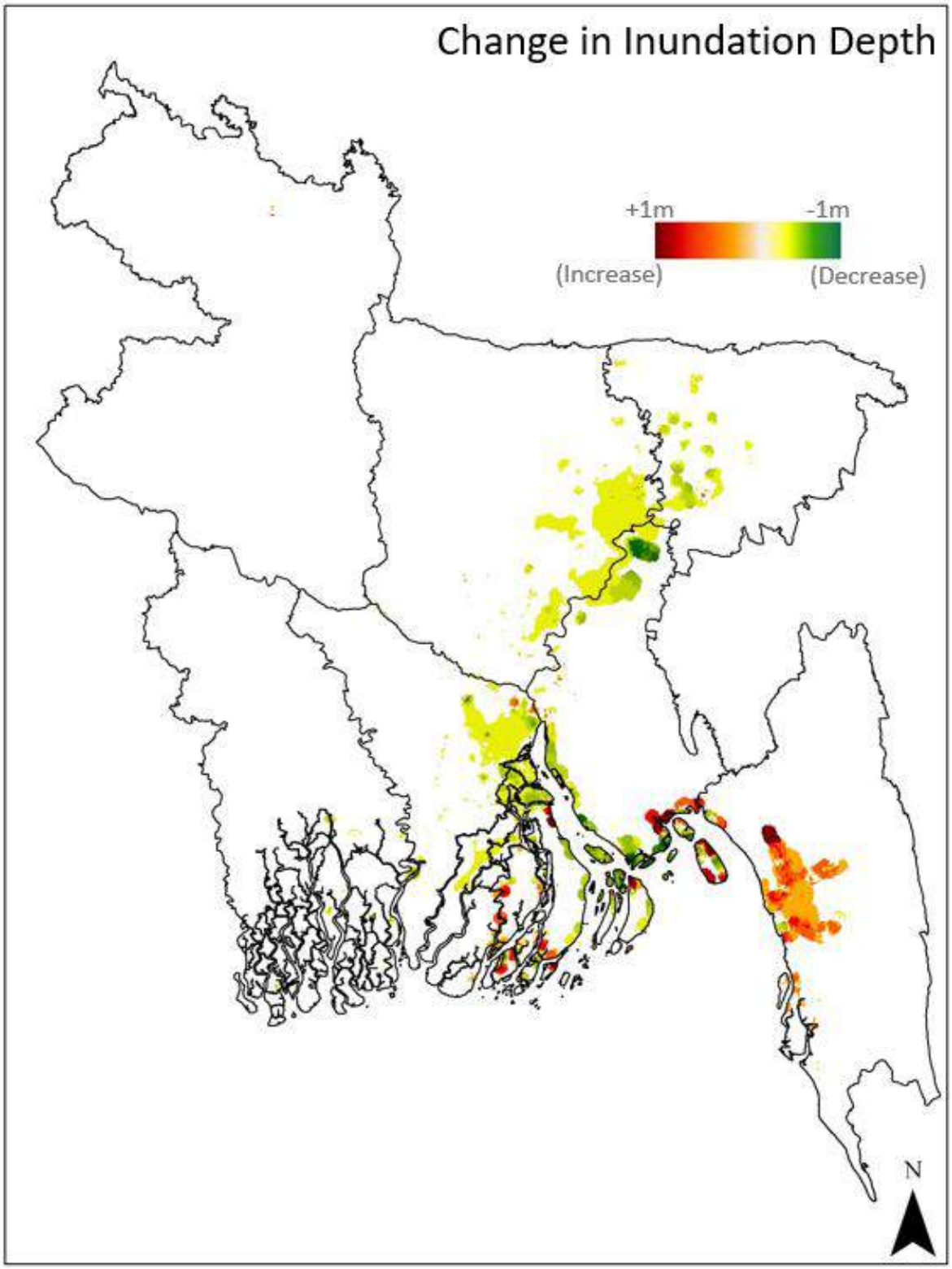

Figure 4.7: *Impact on peak inundation depth due to construction of 13 cross-dams. The red zones show increased inundation depth and green zones show decreased inundation depth compared to base inundation depth when no cross-dams were constructed.*

Change in peak monsoon velocity

Cross-dams decreases peak monsoon velocity in the vicinity of cross-dam locations (Figure 4.8). This reduces sediment transport capacity in these locations and cause increased sedimentation. This accelerates the process of land reclamation. But the at the same time, increases the increased inundation depth during peak monsoon (Figure 4.7). The decreased velocity zone is also observed along the Meghna Estuary and in the deep ocean region. This will increase unwanted sedimentation in these locations. However, there are few locations that includes Sandwip channel and downstream of the Meghna mouth where peak monsoon velocity will increase. This will increase sediment transport capacity in these regions. The entire processes of increased sedimentation and increased sediment transport will change the morpho-dynamic equilibrium of the system.

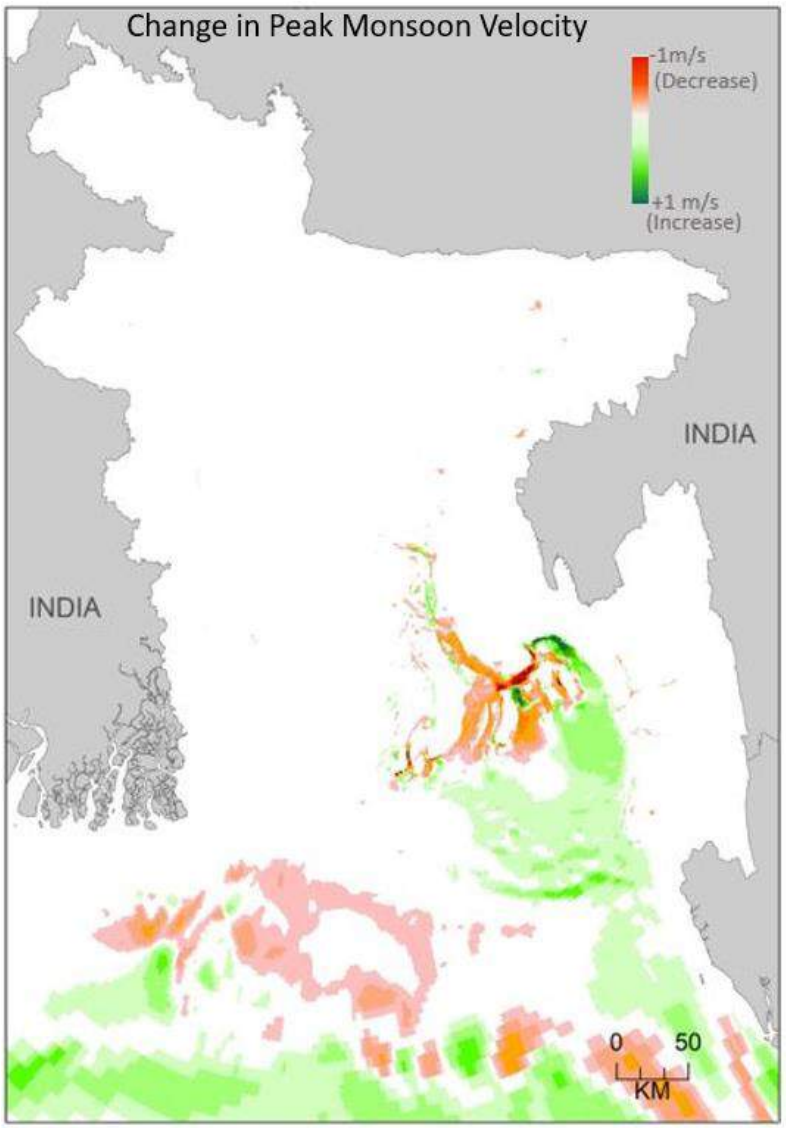

Figure 4.8: *Change in peak monsoon velocity due to construction of 13 cross-dams. The red zones show decrease in velocity and the green zone shows increase in velocity compared to the base velocity when no cross-dams were constructed.*

Change in suspended sediment concentration

We have computed change in suspended sediment concentration in the delta due to construction of 13 cross-dams. The result shows change in peak monsoon suspended sediment concentration (Figure 4.9). To smooth out the temporal fluctuation, we have made 7-days moving average as a representative value. The results show a drastic change in sediment concentration regime within the system due to these 13 cross-dams. We can see a decreased suspended sediment concentration not only close to the cross-dam locations, but also in the river and estuary systems. Decreased sediment concentration is indicative of reduced transport capacity which results increased sedimentation. On the other hand, increased sediment concentration is indicative of increased transport capacity which is associated with increased erosion. We can see decreased sediment concentration in the turbidity maximum region (Sarker et al., 2011) and increased sedimentation in the western estuarine systems. So, there is a possibility of increased bed erosion for the estuaries in the western region which will improve waterlogging problem in this region. But at the same time, may decrease the land building process. Combined operation of cross-dam and TRM may simultaneously accelerate improving the channel conveyance capacities and land building processes.

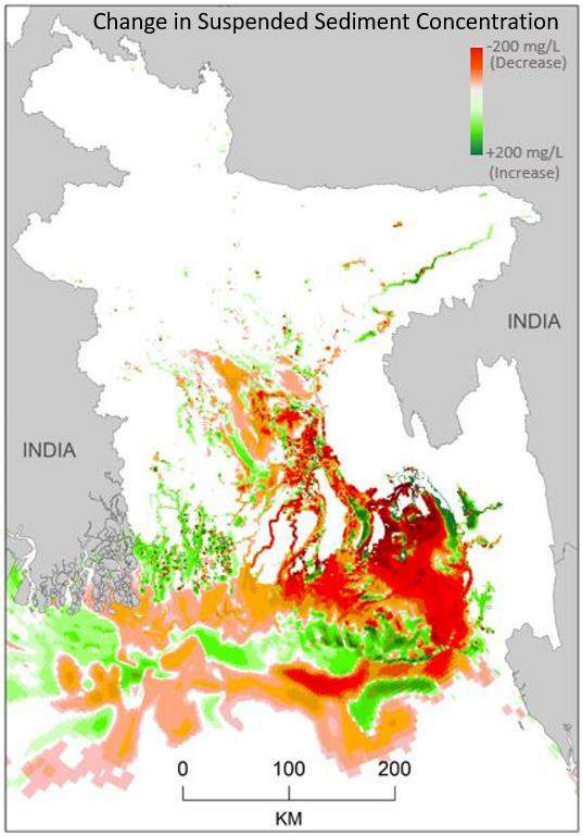

Figure 4.9: *Change in suspended sediment concentration due to construction of 13 cross-dams. The red zones show decrease sediment concentration, and the green zones show increased sediment concentration compared to the base sediment concentration when no cross-dam was constructed.*

Changes in sedimentation and erosion

We have computed change in yearly sedimentation and erosion for the delta due to construction of 13 cross-dams (Figure 4.10). Change in yearly sedimentation and erosion is the result of change in peak monsoon velocity indicative of transport capacity (Figure 4.8) and change in suspended sediment concentration due to change in transport capacity (Figure 4.9). We see the expected phenomena of sedimentation or erosion (green zone or red zone respectively in Figure 4.10) in the zones where both transport capacity and sediment concentration decrease or increase (red zones or green zones in Figures 4.8 and Figure 4.9). This again shows possible increase of conveyance capacities of the western estuaries due to construction of cross-dams which will contribute positively to solving waterlogging problems in the south-west region. We can see insignificant impacts of sedimentation and erosion in the delta surface (Figure 4.10) supported by less impact of changes of transport capacity (Figure 4.8) and suspended sediment concentration (Figure 4.9).

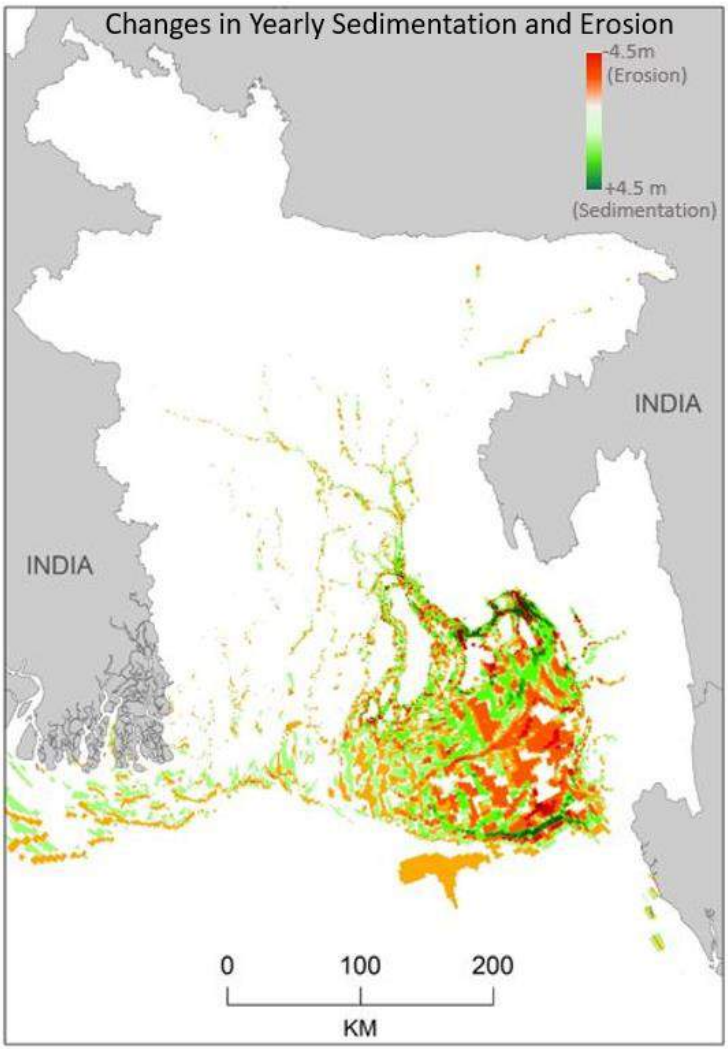

Figure 4.10: *Changes in yearly sedimentation and erosion in the delta due to construction of 13 cross-dams. The red zones show increased erosion, and the green zones show increased sedimentation compared to the condition when no cross-dams were constructed.*

Change in sedimentation volume and depth on the delta surface

Change in sedimentation volume and sedimentation depth on the delta surface due to construction of 13 cross-dams are shown in Figure 4.11 and is summarized in Table 4.1. We can see that there is almost no impact on the non-tidal delta surface. The maximum change is observed on the delta surface in the close vicinity of the cross-dam locations. As mentioned before, we calculated the changes based on sediment inflows of extreme flood condition.

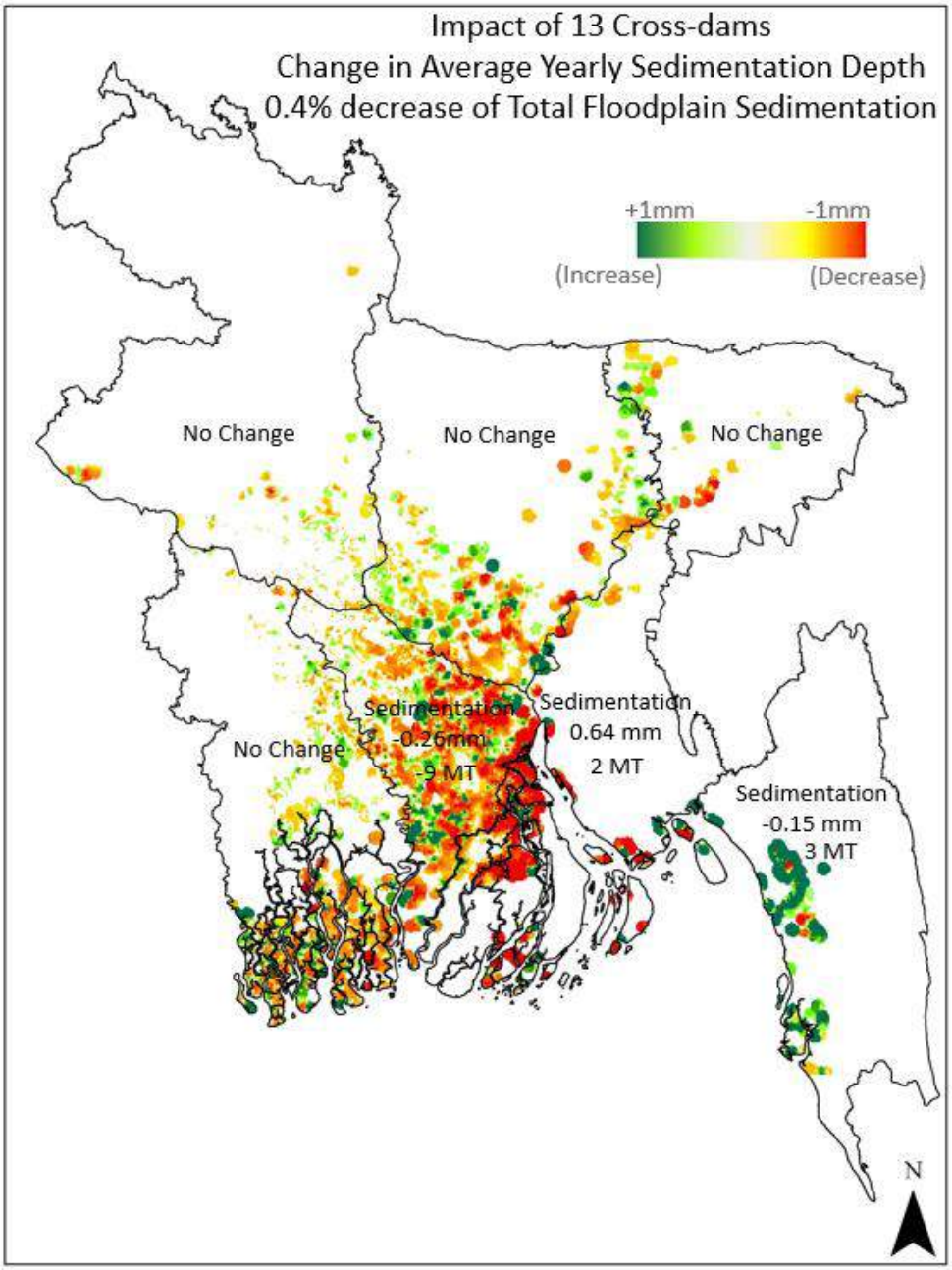

Figure 4.11: *Changes in yearly sedimentation depth on the delta surface due to construction of 13 cross-dams. The red zones show decrease, and the green zones show increase of sedimentation depth compared to the condition when no cross-dams were constructed.*

Table 4.1: Yearly distribution of change of sedimentation in GBM delta due to construction of 13 cross-dams.

Change in Total Sediment Distribution					
Flood Condition	Change in Inflow Sediments (Million Ton)	Change in Delta Floodplain Sedimentation (Million Ton)	Change in Coastal Floodplain Sedimentation (Million Ton)	Change in Percent Retained in Total Delta Floodplains	Change in Percent Retained in Coastal Floodplain
Extreme	No Change	-4	-4	-0.4%	-0.4%
Change in Regional Sediment Distribution					
Region	Change in Sedimentation Depth (mm)	Change in Sedimentation Volume (Million Ton)		Change in Percentage of Sedimentation Volume w.r.t Total Inflow Sediments	
NW	No Change	No Change		No Change	
NC	No Change	No Change		No Change	
NE	No Change	No Change		No Change	
SW	No Change	No Change		No Change	
SC	-0.26	-9		-0.70%	
SE	+0.64	+2		+0.10%	
EHT	-0.15	+3		+0.20%	

The changes of yearly distribution of sedimentation parameters shows that (Table 4.1) impact of 13 cross-dams do not affect the non-tidal part of the delta. Due to the trapped sediments as a result of 13 cross-dams, total retained sediments on the delta floodplain reduces by -0.4%. The maximum reduction occurs in SC region. Earlier we have seen that (see subsection 3.8.5 of Chapter Three) SC region plays an important role on delta sustainability. The impact of 13 cross-dams shows that due to construction of these cross-dams, sedimentation volume on SC region will decrease by 0.7% associated with a 0.26mm reduction of sedimentation depth. This will have a long-term negative impact on delta sustainability. We also see that these 13 cross-dams increase the retained sedimentation volume on SE and EHT regions with a corresponding increase of sedimentation depth of 0.64mm on SE region and decrease of 0.15mm on EHT region. Increase of sedimentation depth on SE region is concentrated in Sandwip-Urir Char and other cross-dam influenced region of the delta (see Figure 4.11). On the other hand, sedimentation depth on EHT decreases although the sedimentation volume is increased. This happens because larger area of EHT which is mainly low-elevation intertidal zone is sedimented with 0.2% increase of sedimentation volume.

4.2.2 System impacts of BWDB proposed Noakhali-Urir Char Cross-dam

BWDB Noakhali-Urir Char cross-dam (hereafter we will term it as Urir Char cross-dam) is one of the 13 EDP (2007) proposed cross-dams. The location of Urir Char cross-dam is shown in Figure 4.12.

Figure 4.12: *Location of BWDB planned Urir Char cross-dam. This is one of the 13 EDP proposed cross-dams.*

In this section, we will make a comparative analysis among the indicators (those we have earlier discussed about 13 cross-dams) between the 13 cross-dams and Urir Char cross-dam.

Change in water level

We have compared the change in water level between 13 cross-dams and Urir Char cross dam in two locations in Meghna Estuary region (Figure 4.13). There is no noticeable change in tidal range for Urir Char cross-dam compared to 13 cross-dam. Location-1 is located inside the Meghna Estuary and location-2 is located on the mouth of the Meghna Estuary.

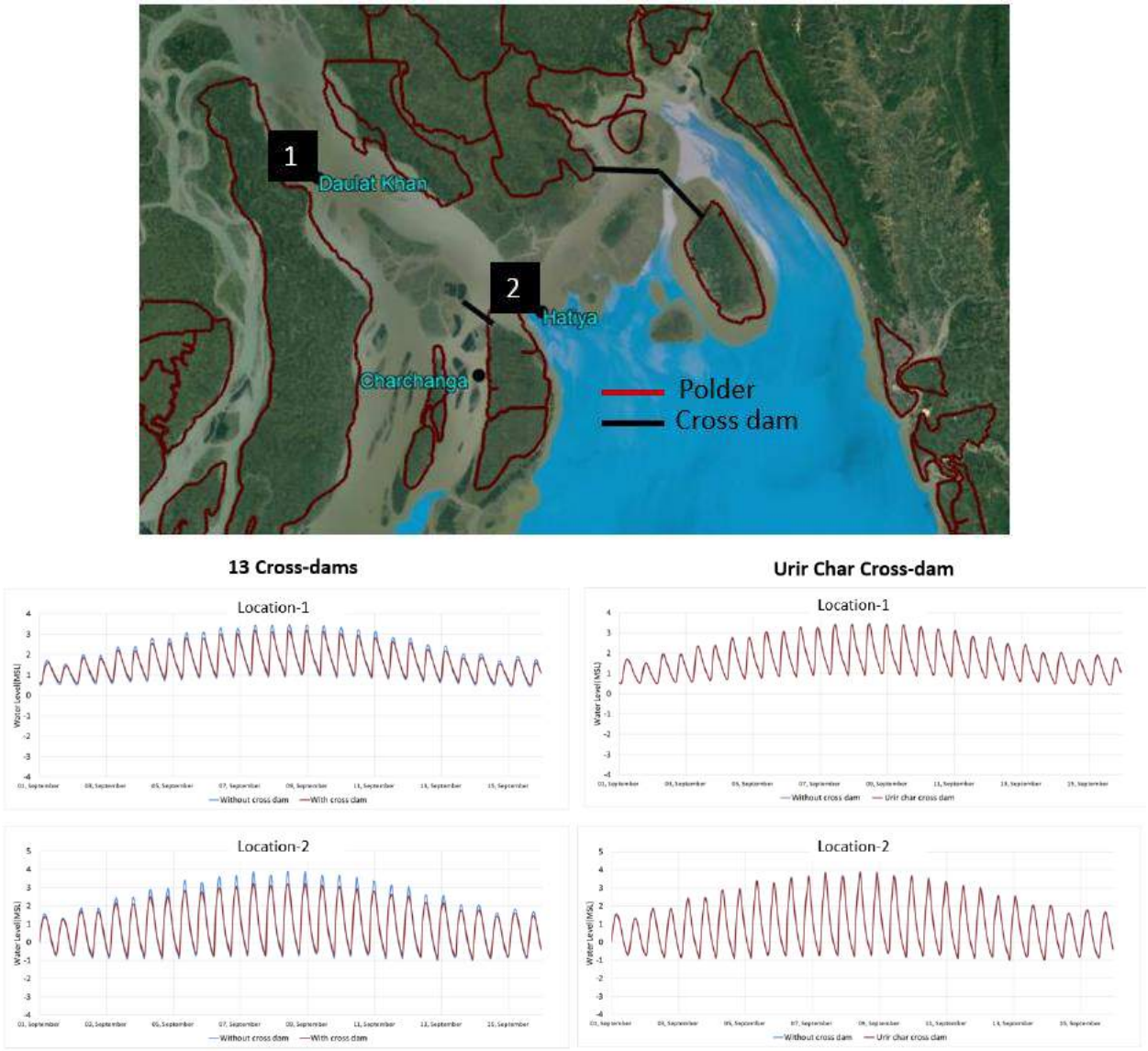

Figure 4.13: *Comparison of water level between 13 cross-dam and Urir Char cross-dam in two locations of Meghna Estuary.*

Changes in cross section

To compare the impact on cross sectional changes at the similar locations due to 13 cross-dams and Urir Char cross dam, cross sections at two locations along the coast are compared (Figure 4.14). Location-1 coincides with the cross-dam location for both the 13 cross-dams and Urir Char cross-dam. Location-2 is selected in the western estuary regions to see whether impacts are similar for both the cases in the regions where we are expecting increase of channel conveyance due to trapped sediments in cross-dam locations. We can see the expected land reclamation in cross-dam location for both the cases. But for the Urir Char cross-dam, we do not find any increased

conveyance in the western estuarine systems due to trapped sediments in the cross-dam location. This impact is visible for the 13 cross-dams.

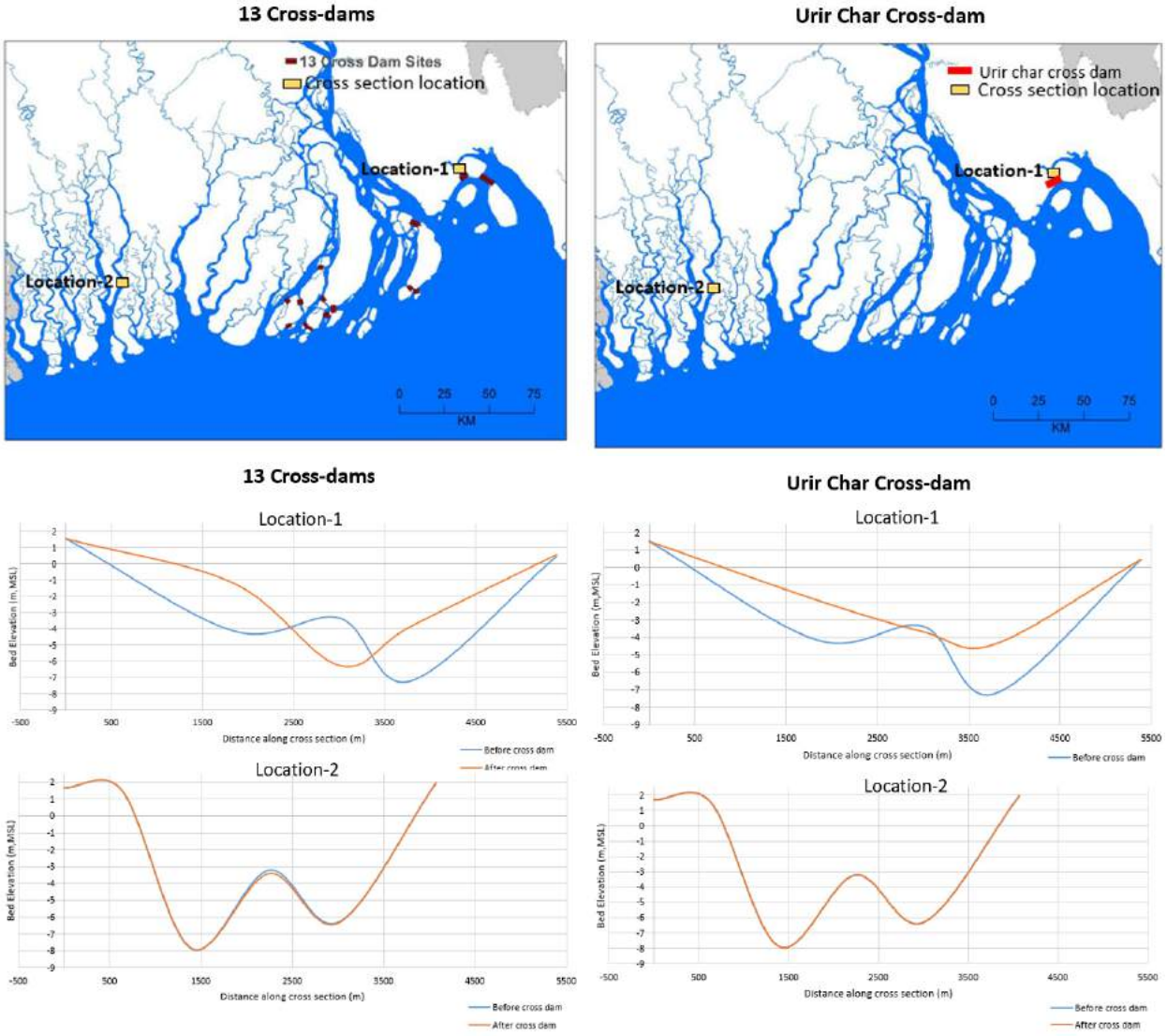

Figure 4.14: *Comparison of cross section between 13 cross-dam and Urir Char cross-dam in two locations along the coast.*

Changes in inundation depth

Comparison for changes in inundation depth between the 13 cross-dams and Urir Char cross-dam shows that inundation also occur due to Urir Char cross-dam, but as expected, its area extent is less than what is observed for the 13 cross-dams (Figure 4.15). For Urir Char cross-dam, increased inundation due to the cross-dam is restricted to Urir Char, Noakhali coast, and unprotected part of Hatiya. On the other hand, 13 cross-dams cause increased inundation in a wider area comprising Sandwip, Urir Char, Noakhali, Hatiya, Bhola, and surrounding island.

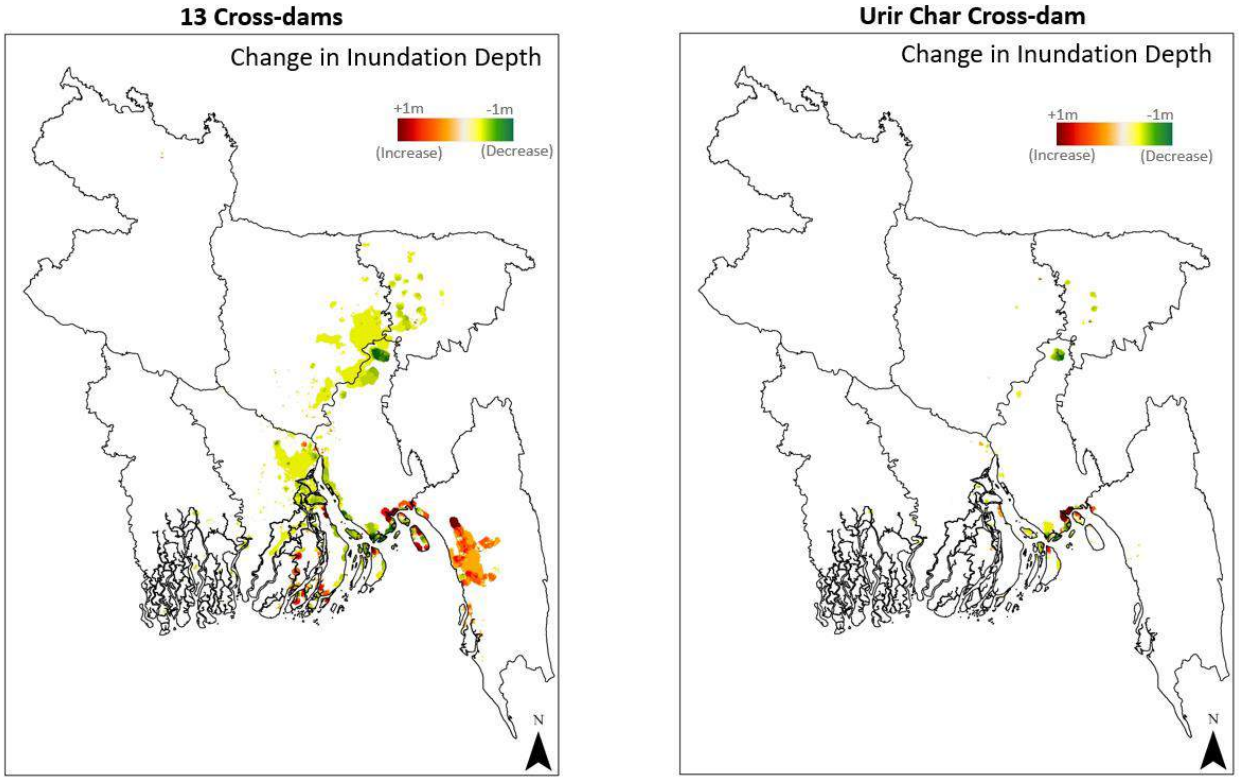

Figure 4.15: *Comparison of changed inundation between 13 cross-dams and Urir Char cross-dam. The red zones show increased inundation, the green zones show decreased inundation, and the yellow zones show insignificant changes.*

Change in peak monsoon velocity

Peak monsoon velocity can be used as an indicator of transport capacity of sediments. We have compared the change in peak monsoon velocity between the 13 cross-dam and Urir Char cross-dam (Figure 4.16). For this parameter, the impact of Urir Char cross-dam is very much local compared to 13 cross-dams. The decreased transport capacity which increases sedimentation near the Urir Char cross-dam is found only close to the cross-dam location. Unlike 13 cross-dams, we do not see any impact on the Meghna Estuary for the Urir Char cross-dam. However, similar to 13 cross-dams, transport capacity also increases in Sandwip channel for the Urir Char cross-dam.

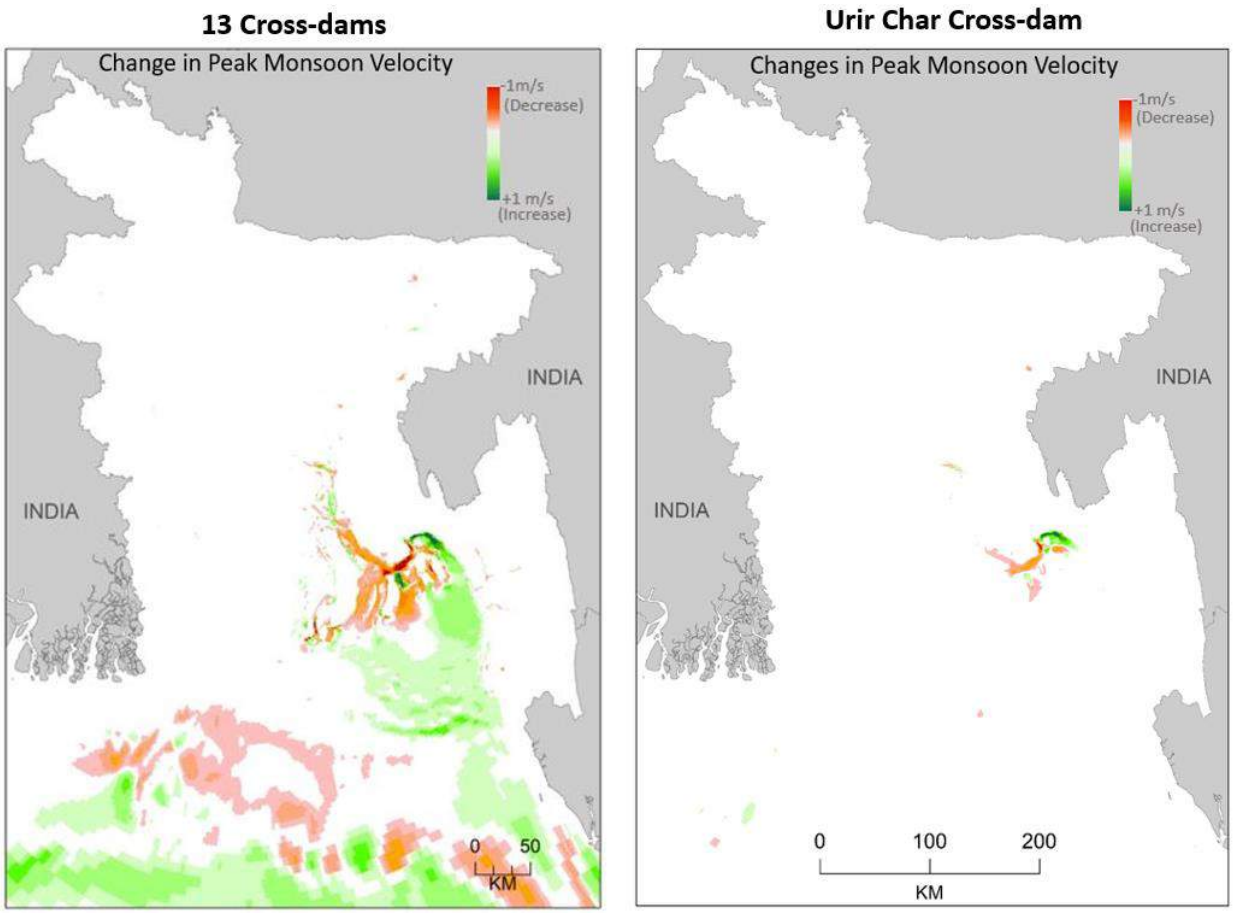

Figure 4.16: *Comparison of peak monsoon velocity between 13 cross-dam and Urir Char cross-dam. The red zone represents decrease, green zone represent increase, yellow zone represents insignificant change of peak monsoon velocity.*

Change in suspended sediment concentration

Comparison is made between the 13 cross-dam and Urir Char cross-dam for the change in suspended concentration due to construction of these cross-dams (Figure 4.17). Similar to 13 cross-dams, Urir Char cross-dam also decreases suspended sediment concentration in the turbidity maximum zone (Sarker et al., 2011), but with a less intensity. The increased sediment concentration which is indicative of increased channel bed erosion in the western estuarine system is very weak for Urir Char cross-dam compared to 13 cross-dams. So, we do not expect any increased channel conveyance in the western estuaries due to Urir Char cross-dam (see Figure 4.14).

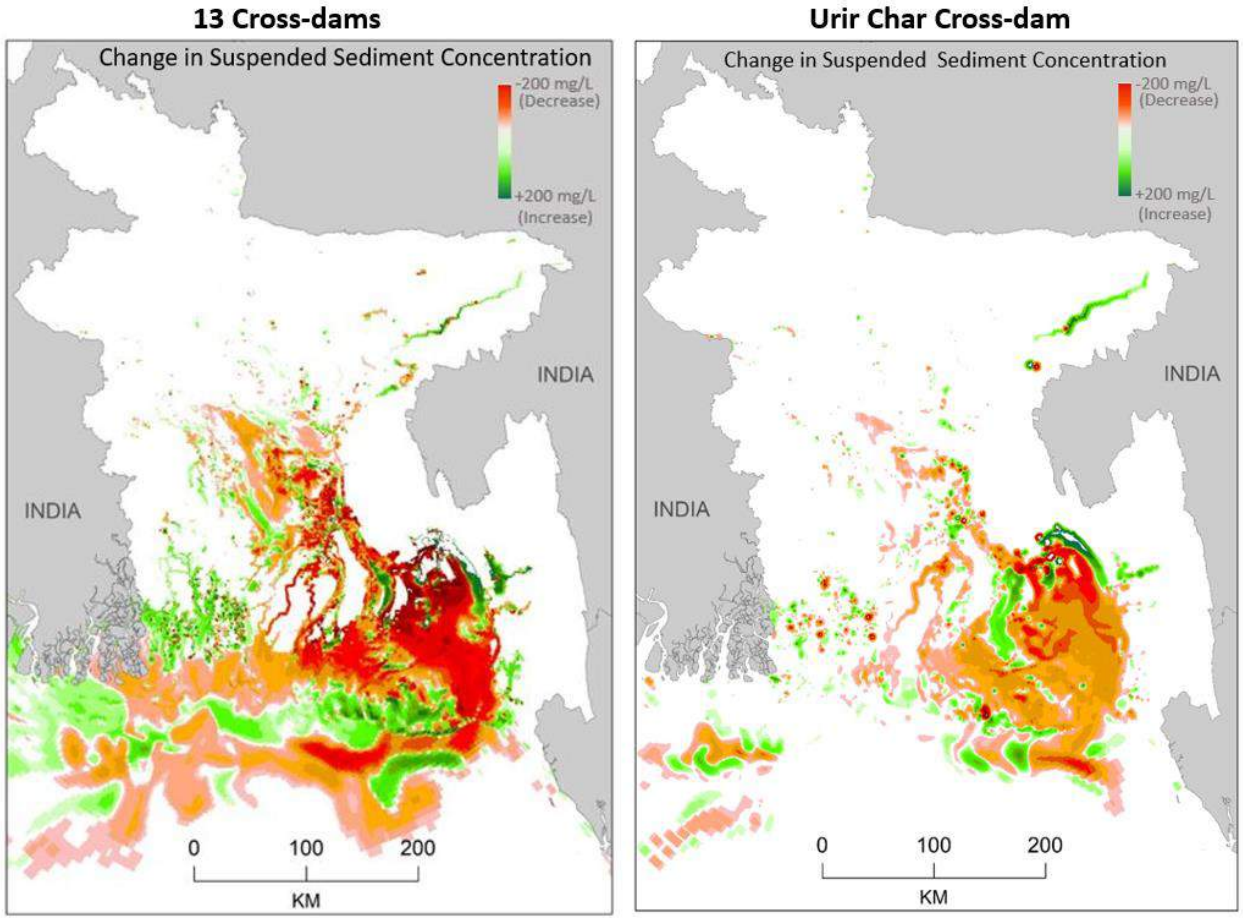

Figure 4.17: *Comparison of suspended sediment concentration between the 13 cross-dams and Urir Char cross-dam. The red zones show decreased sediment concentration, the green zone shows increased sediment concentration, and the yellow zone shows insignificant changes.*

Changes in sedimentation and erosion

Comparison is made between the 13 cross-dams and Urir Char cross-dam for changes in sedimentation and erosion (Figure 4.18). Similar to 13 cross-dams, the expected sedimentation zone is concentrated close to the cross-dam location for the Urir Char cross-dam also. The influence zone of Urir Char cross-dam is seen to be propagated in a wider zone of the ocean and coast. Unlike 13 cross-dams, we do not see any erosion zone in the western estuary system due to construction of Urir Char cross-dam only.

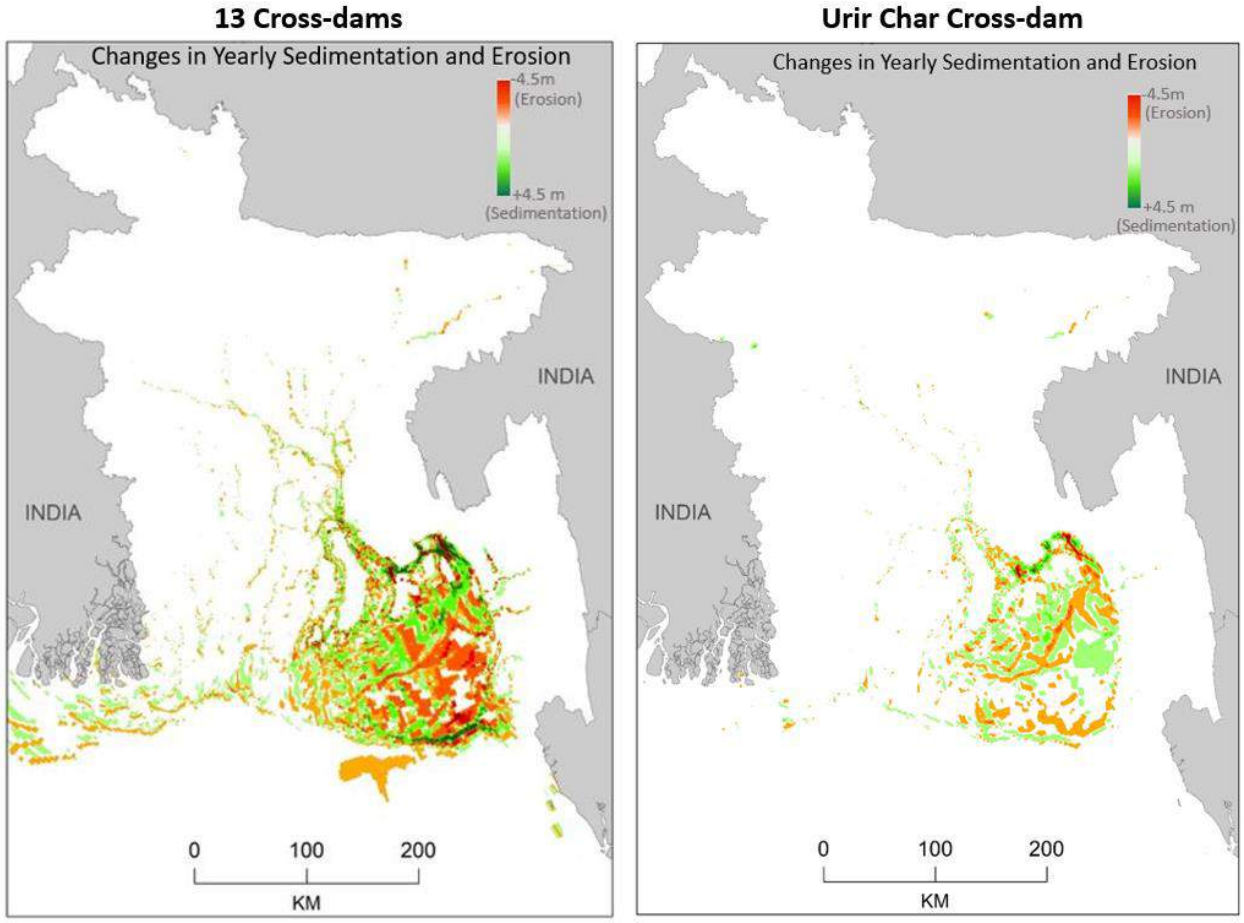

Figure 4.18: *Comparison between 13 cross-dams and Urir Char cross-dam for yearly sedimentation and erosion. The red zones show increased erosion, the green zone shows increased deposition, and the yellow zones show insignificant changes.*

Change in sedimentation volume and depth on the delta surface

Comparison is made between the 13 cross-dams and Urir Char cross-dam for the change in yearly sedimentation volume and sedimentation depth on the delta surface (Figure 4.19). As expected, the intensity and extent of impact of sedimentation on delta surface of Urir Char cross-dam is much less than 13 cross-dams. Contrary to the 13 cross-dam, we do not see any noticeable decrease of sedimentation depth in Sundarban region for the Urir Char cross-dam. Similar to 13 cross-dam, Urir Char cross-dam has no effect on non-tidal delta surface and also on SC region. Due to Urir Char cross-dam, sedimentation volume on the delta surface reduces to 0.1 MT which is 0.008% of the total inflow sediments. This value is insignificant compared to the 13 cross-dam (see Table 4.2). Similar to 13 cross-dams, we can see decrease of sedimentation volume in SC region due to Urir Char cross-dam also (decrease by 1.1 MT) which is 0.088% with respect to total inflow sediments. The sedimentation depth in the SC region also decreases by 0.20mm due to Urir Char cross-dam compared to 0.26mm decrease due to 13 cross-dams (Table 4.2). Although

sedimentation volume in SE region (the region where Urir Char is located) increases by 1 MT, sedimentation depth in SE region decreases by 0.18mm. This happens due to larger area of SE is sedimented due to construction of Urir Char cross-dam. This shows that sedimentation rate in Urir Char region will be higher if 13 cross-dams are constructed instead of Urir Char cross-dam only.

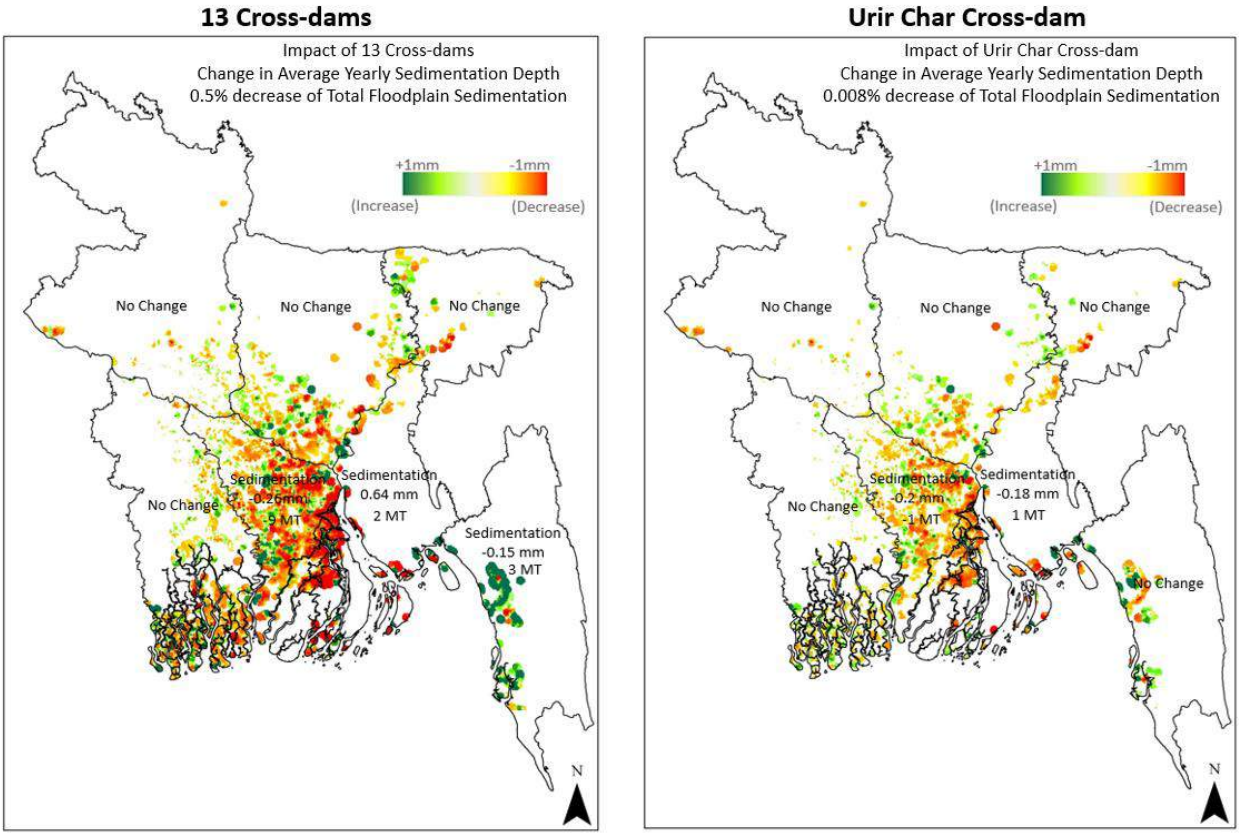

Figure 4.19: *Comparison between 13 cross-dams and Urir Char cross-dam for yearly sedimentation volume and sedimentation depth on the delta surface. The red zone shows decreased sedimentation depth, the green zones show increased sedimentation depth, and the yellow zones show insignificant changes.*

Table 4.2: Comparison of change of sedimentation in GBM delta between 13 cross-dams and Urir Char cross-dam.

Comparison of Change in Total Sediment Distribution					
Flood Condition	Change in Inflow Sediments (Million Ton)	13 Cross-dam Change in Delta Floodplain Sedimentation (Million Ton)	Urir Char Cross-dam Change in Delta Floodplain Sedimentation (Million Ton)	13 Cross-dam Change in Percent Retained in Total Delta Floodplains	Urir Char Cross-dam Change in Percent Retained in Total Delta Floodplains
Extreme	No Change	-4	-0.1	-0.4%	-0.008%
Comparison of Change in Regional Sediment Distribution					
Region	13 Cross-dam Change in Sedimentation Depth (mm)	Urir Char Cross-dam Change in Sedimentation Depth (mm)	13 Cross-dam Change in Sedimentation Volume (Million Ton)	Urir Char Cross-dam Change in Sedimentation Volume (Million Ton)	13 Cross-dam Change in Percentage of Sedimentation Volume w.r.t Total Inflow Sediments	Urir Char Cross-dam Change in Percentage of Sedimentation Volume w.r.t Total Inflow Sediments
NW	No Change	No Change	No Change	No Change	No Change	No Change
NC	No Change	No Change	No Change	No Change	No Change	No Change
NE	No Change	No Change	No Change	No Change	No Change	No Change
SW	No Change	No Change	No Change	No Change	No Change	No Change
SC	-0.26	-0.20	-9	-1.1	-0.70%	-0.088%
SE	+0.64	-0.18	+2	+1	+0.10%	+0.080%
EHT	-0.15	No Change	+3	No Change	+0.20%	No Change

4.2.3 Assessment of cross-dam as a sediment management practice

To assess overall performance of cross-dam as a sediment management practice, we should consider how effective a cross-dam is to serve its main purpose (which is mainly land reclamation and the effect is pre-dominantly local) and how it performs to contribute to the delta sustainability. From our previous discussions, we can summarize the positive and negative impacts of cross-dam which will make it possible for an overall assessment of performance of cross-dam as a sediment management practice. Positive impacts of cross-dam are: (1) reclaim land in the cross-dam location where sediment concertation is high (2) increase river conveyance in other regions caused by reduced sediment supply due to trapped sediments in the cross-dam location. If this region is within the zone of waterlogging, this will act positively to reduce waterlogging problem in the region. The negative impacts of cross-dam are (1) change the tidal amplitude in the influenced zone which may lead to a long-term hydro-morphodynamic change in the region (2) increases the inundation in the unprotected land close to the cross-dam (3) decreases sediment transport capacity in other regions which are within the influence zone of the cross-dam and causes unwanted sedimentation in those locations (4) reduces retained sediment volume and sedimentation depth on the delta

surface and act against delta sustainability. If we make a trade-off between positive impacts and negative impacts of cross-dam, we can see that in terms of effective use of sediment resource which will serve both local purpose and overall delta sustainability – cross-dam alone is not an effective sediment management practice.

4.3 System Impacts of Dredging

Dredging is the most common and frequently conducted sediment management practice in this region. Dredging is done mainly to improve channel conveyance for navigational purposes, to reduce flood extent, and to guide the river to an expected course (Rahman et al., 2021). Dredging is conducted in various rivers within the delta as a need basis. Dredging is frequently done in Brahmaputa-Jamuna River, Gorai River, and in Hari River. We found no past studies where system impact of dredging is made in GBM delta.

4.3.1 System impacts of dredging in major rivers

To study simultaneous system impacts of dredging on major river systems, we made numerical experiments by synthetically conducting dredging in two reaches of Jamuna-Brahmaputra River and two reaches of Ganges River. The dredging location of numerical experiment for Brahmaputra-Jamuna is selected based on the study of Musfequzzaman et al., (2016). For the Ganges, we selected the dredged section which will reduce flood extent for the Ganges dependent part of the system. The length and depth of two reaches of dredged section of Brahmaputra-Jamuna is shown in Figure 4.20:

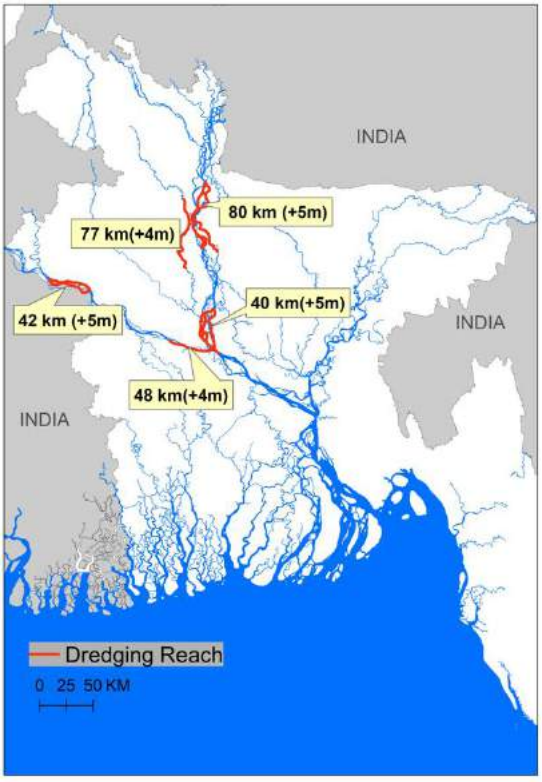

Figure 4.20: *Length and depth (shown in bracket) of dredged sections of the five reaches of Brahmaputra-Jamuna and Ganges rivers. The red mark shows the dredged reach.*

Effectiveness of dredging

To assess effectiveness of dredging, cross-section plot in a section of the dredged reach of Jamuna-Brahmaputra is studied (Figure 4.21a). The result shows response of the river section one year after dredging operation is performed. We can see that most part of the dredged section is filled within one year of dredging operation. Among the dredged reaches, the maximum filling rate (134% and 244%) of dredged depth is observed in the reaches of Brahmaputra-Jamuna River (Figure 4.21b). This rate is higher than the filling rate of the dredged reaches of the Ganges River (100% and 178%). This shows that the filling rate depends on the sediment flux of the dredged river.

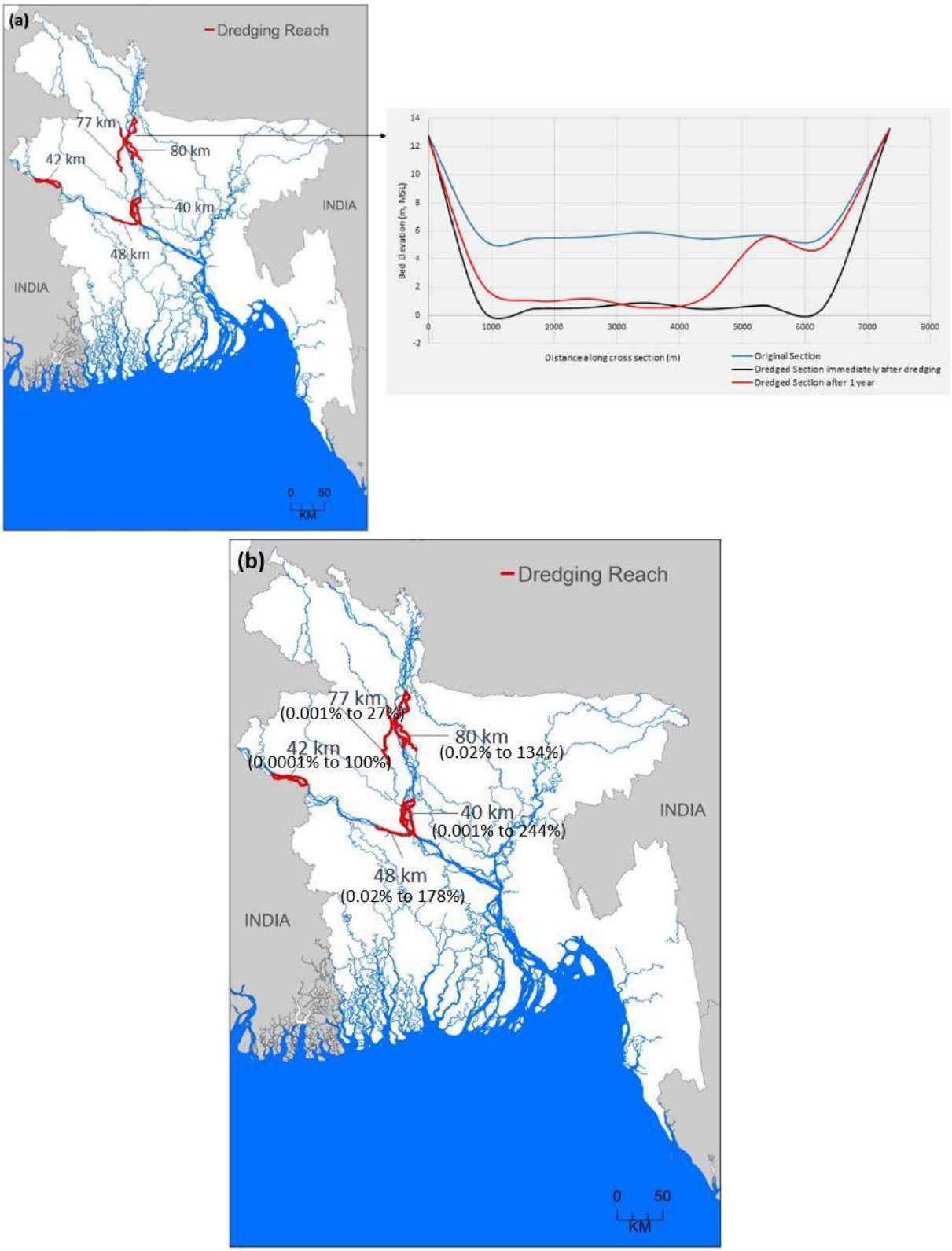

Figure 4.21: (a) *Response of a river section after dredging is performed. The figure shows the original river section, the dredged section, and the section of the river one year after the dredging.* (b) *Ranges of percent filling of depth of dredged sections.*

Changes in hydro-morphological parameters

Changes in 4 hydro-morphological parameters are assessed as indicators to measure system impacts due to dredging in the reaches shown in Figure 4.20. These parameters are: change in inundation depth, change in peak monsoon velocity, change in suspended sediment concentration, and change in yearly sedimentation and erosion.

The change in inundation depth (Figure 4.22) show that dredging reduces the flooding extent by decreasing flood depth in an extended region of the delta comprising Brahmaputra-Jamuna and Ganges floodplains. The impact is visible upto the SW region. A negative impact on inundation (increased inundation depth) is visible in the downstream reaches of the dredged section. Dredging reduces inundation depth in the floodplains. The water volume on these floodplains is carried by the increased conveyance of the dredged section. But when the same volume of water reaches at the downstream section, it overflows because the conveyance of the downstream reaches is inadequate to carry the extra volume of water coming from the floodplains. As expected, the water depths in the dredged reaches of the Brahmaputra-Jamuna and Ganges rivers increase. This result shows that dredging is indeed effective in reducing the inundation depth and flooding extent. But at the same time, adverse effect may result in the reaches where river conveyance is insufficient to carry the extra volume of water coming from the floodplains.

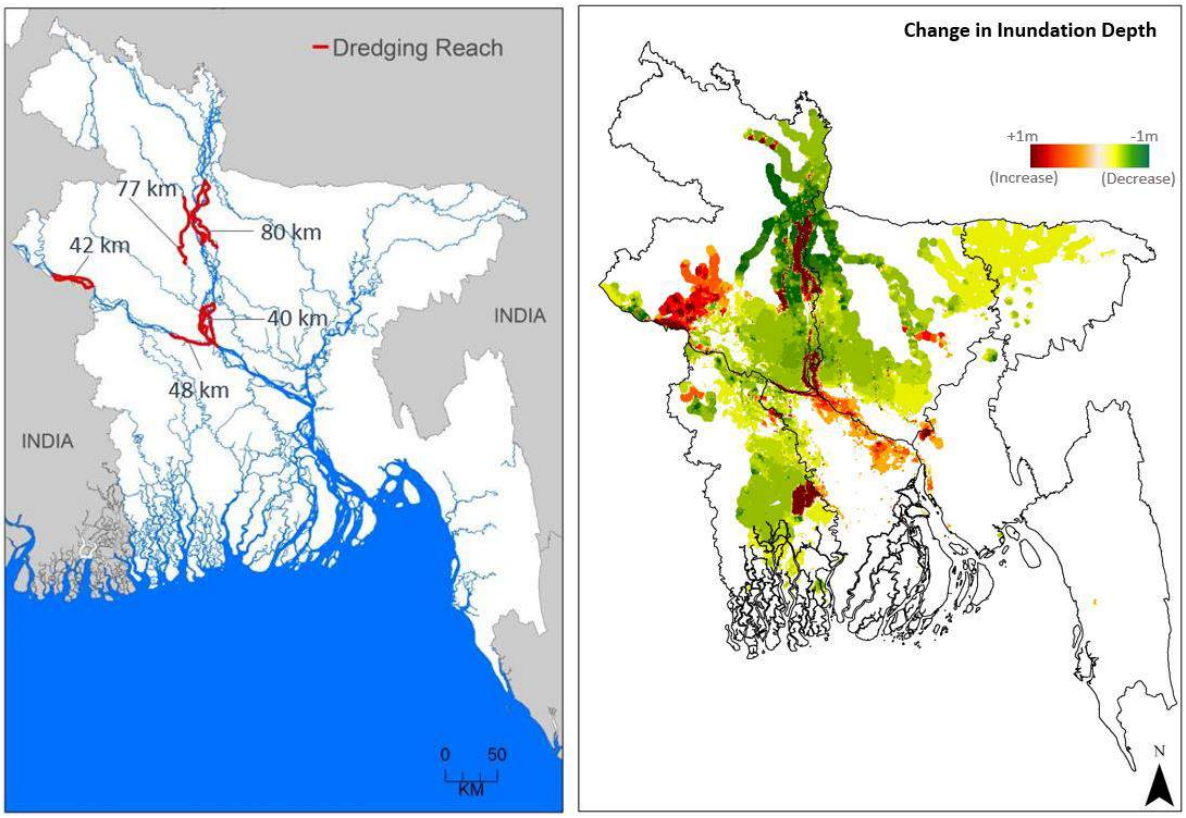

Figure 4.22: *Changes in inundation depth (right image) due to dredging in the dredged reaches of the rivers shown in the left image. The green zones show decrease in inundation depth, the red zones show in the increase in inundation depth, and the yellow zones show insignificant impact.*

The impacts on velocity magnitude (Figure 4.22) show that water velocity during the peak of monsoon decrease over the dredged river reaches. This means dredging reduces sediment transport capacity of the river in the dredged sections. As total inflow of sediment flux in the system remains unchanged, the reduced sediment transport capacity in the dredged section will cause sedimentation in the dredged reaches and new dredging is required to maintain the dredged depth. The velocity magnitude decreases in floodplain reaches where dredging also decreases the water depth. The impact of dredging is visible in a wider domain on the delta surface.

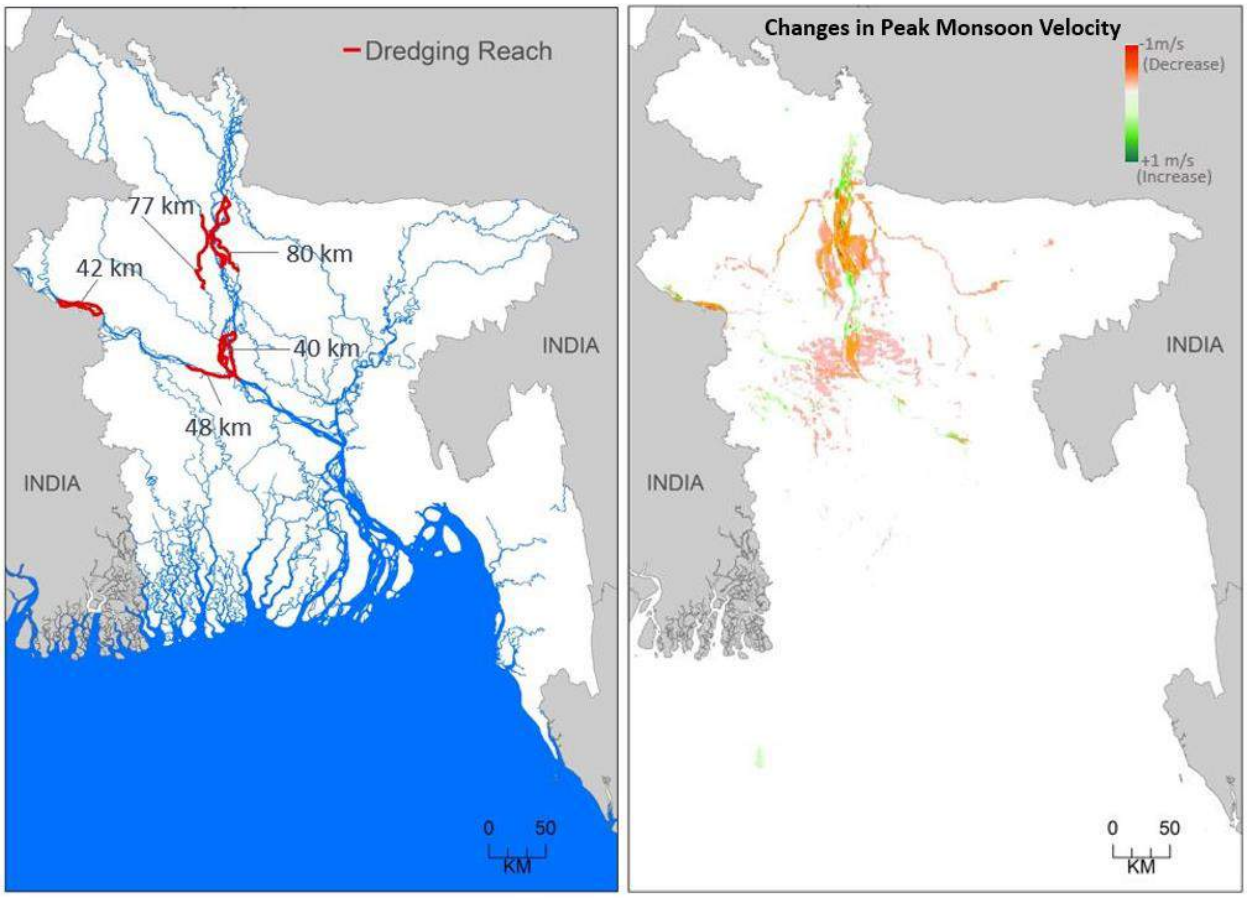

Figure 4.23: *Changes in peak monsoon velocity (right image) due to dredging in the dredged reaches of the rivers shown in the left image. The red zones show decrease in velocity magnitude, the green zones show the increase in velocity magnitude, and the yellow zones show insignificant impact.*

Due to reduced sediment transport capacity, suspended sediment concentration (SSC) decreases in the dredged reaches of the river (Figure 4.24). Figure 4.24 shows the scenario of 7-days average SSC during the peak flood of 1998. The averaging is made to filter the instantaneous variation of SSC due to fluvial flows and tides in the system. Increased suspended sediment concentration is observed in the downstream reaches of the dredged sections where increased velocity is also observed (Figure 4.23). As dredging reduces flooding extent in the floodplains, the sediments

which were supposed to be deposited over the floodplain are transported to the downstream reaches. These additional sediments, in addition to sediments coming from the river-bed due to increased bed shear stress in upstream and downstream reaches of dredged reaches, are responsible to increase the sediment concentration in the downstream reach of the dredged sections. The impact on sediment regime is seen to propagate in the entire river-estuary-floodplain systems (Figure 4.24). Due to reduced inundated extent, average sedimentation depth on the delta surface will reduce.

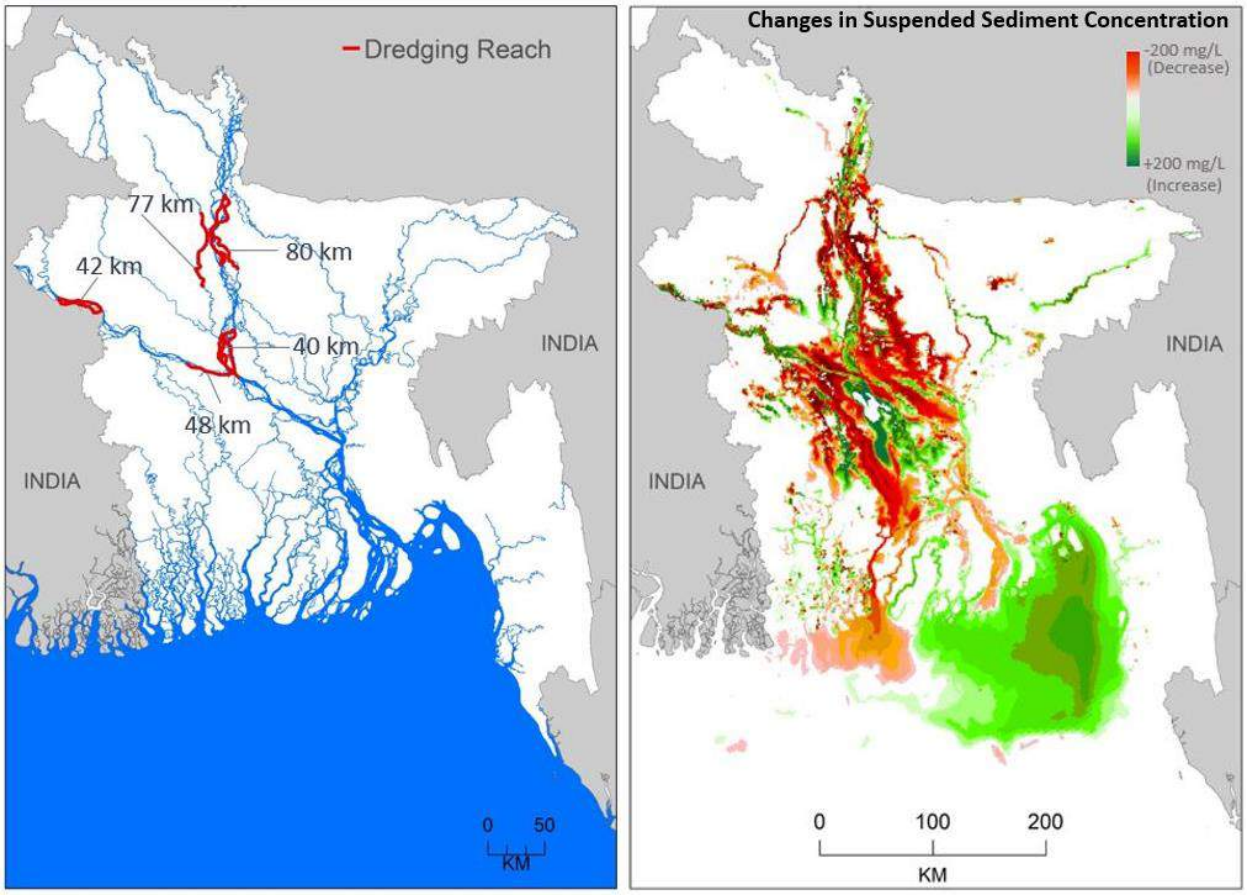

Figure 4.24: *Changes in suspended sediment concentration (right image) due to dredging in the dredged reaches of the rivers shown in the left image. The red zones show decrease in suspended sediment concentration, the green zones show the increase, and the yellow zones show insignificant impact.*

When changes in yearly sedimentation and erosion are concerned, it is found that dredged sections in the rivers reaches experience sedimentation (Figure 4.25). Few of the upstream and downstream reaches of the dredged sections experience riverbed erosion. The eroded sediments from the riverbed and excess sediments which were supposed to be deposited over the floodplains are now spread over the entire system.

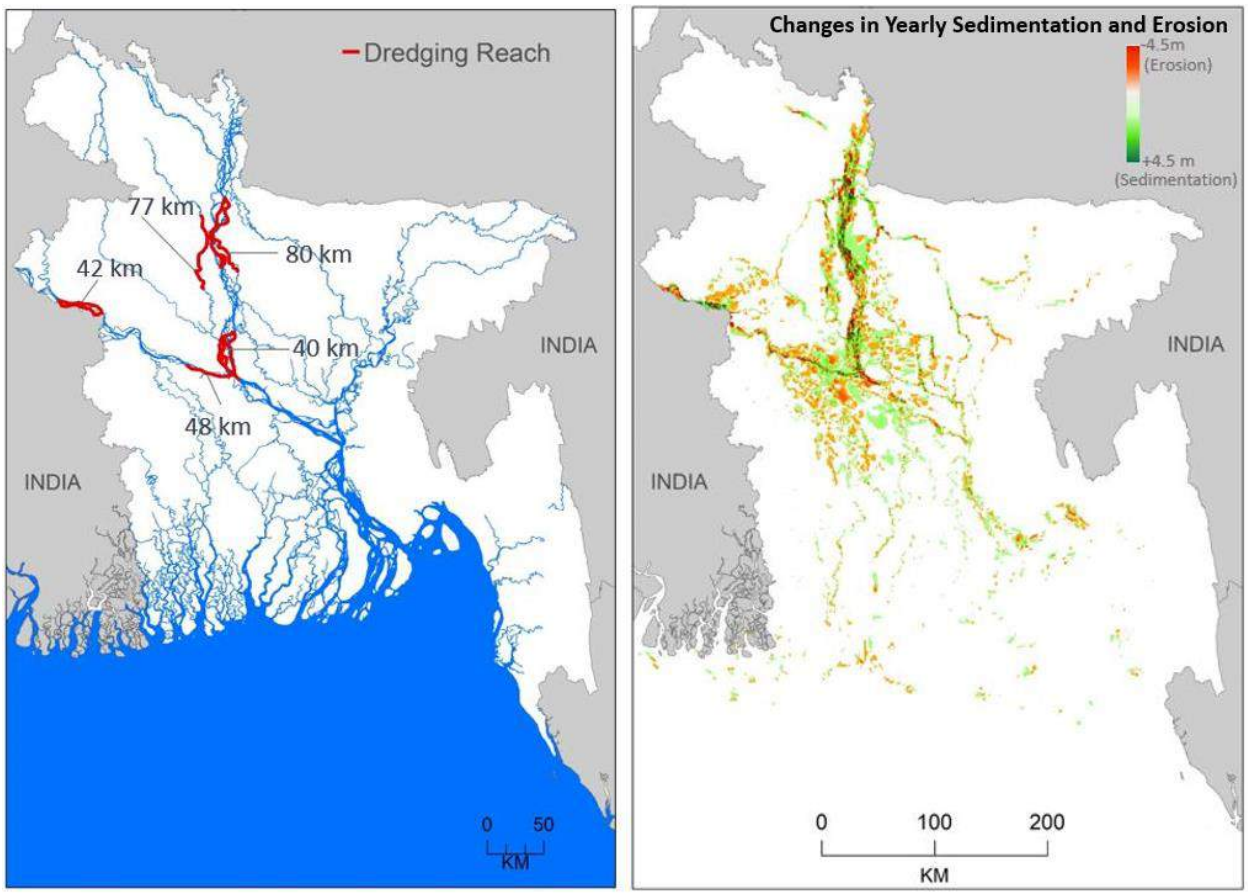

Figure 4.25: *Changes in yearly sedimentation and erosion (right image) due to dredging in the dredged reaches of the rivers shown in the left image. The green zones show increased sedimentation, the red zones show increased erosion, and the yellow zones show insignificant impact.*

We have tried to assess the impact of dredging on sediment dynamics (sedimentation / erosion) along the thalweg of the entire river reaches of Brahmaputra-Jamuna, Ganges, Padma, Lower Meghna and Gorai. A visible impact is seen all along the Brahmaputra-Jamuna River with increased sedimentation in the dredged reach (Figure 4.26a). A similar impact is seen along the Ganges River (Figures 4.26b to 4.26e) and upstream part of the Padma River (Figure 4.26f). The impacts slowly disappear toward the downstream part of the Padma River (Figures 4.26g and 4.26h). Although very insignificant, impacts are still visible along the Lower Meghna River (Figures 4.26i). We also found impact on a different river system – the Gorai River (Figure 4.26j). It appears that dredging impacts are visible long way out from the dredged sections. The impacts are dependent on the length and depth of the dredged sections. The dredged sections experience increased sedimentation within a short time period.

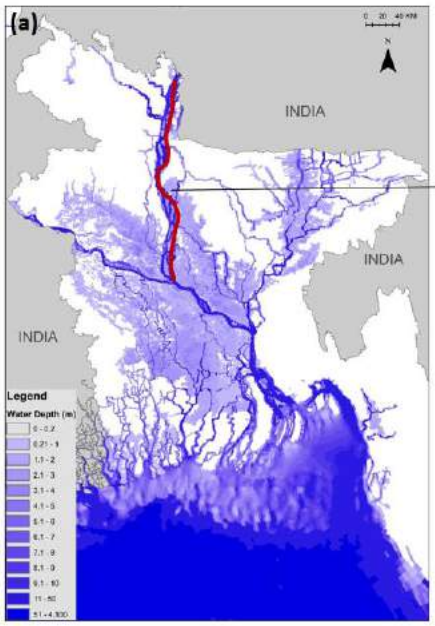
(a)
INDIA
INDIA
INDIA
Legend
Water Depth (m)

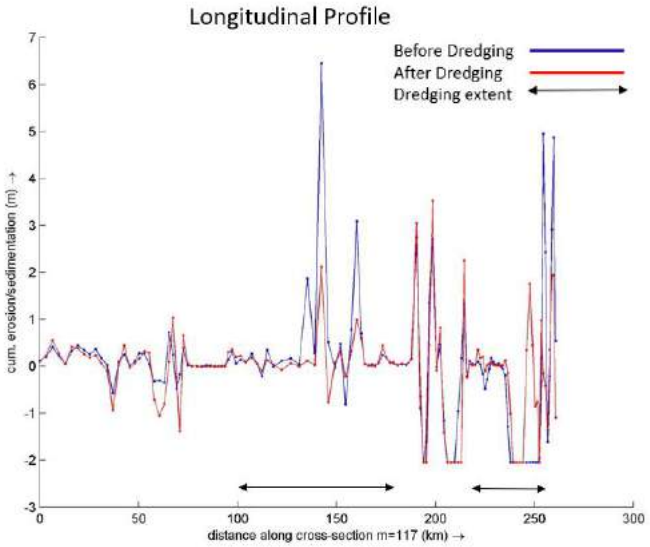
Longitudinal Profile
Before Dredging
After Dredging
Dredging extent
cum. erosion/sedimentation (m) →
distance along cross-section m=117 (km) →

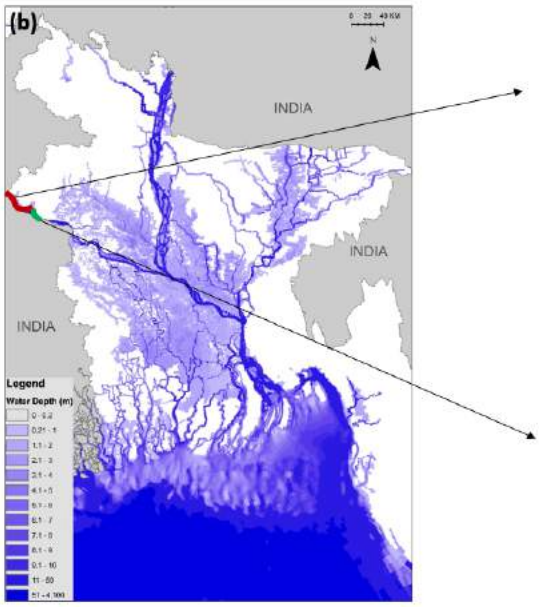
(b)
INDIA
INDIA
INDIA
Legend
Water Depth (m)

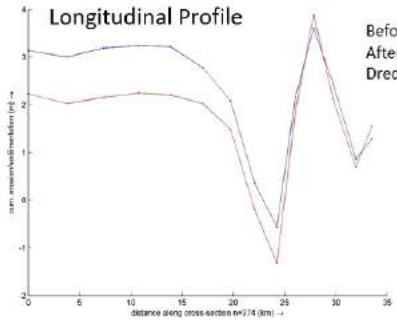
Longitudinal Profile
Before Dredging
After Dredging
Dredging extent

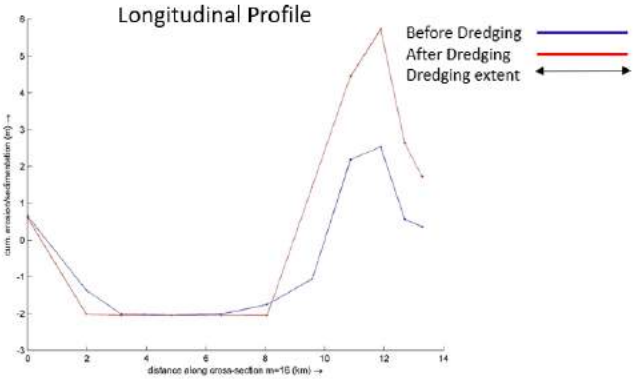
Longitudinal Profile
Before Dredging
After Dredging
Dredging extent
distance along cross-section m=16 (km) →

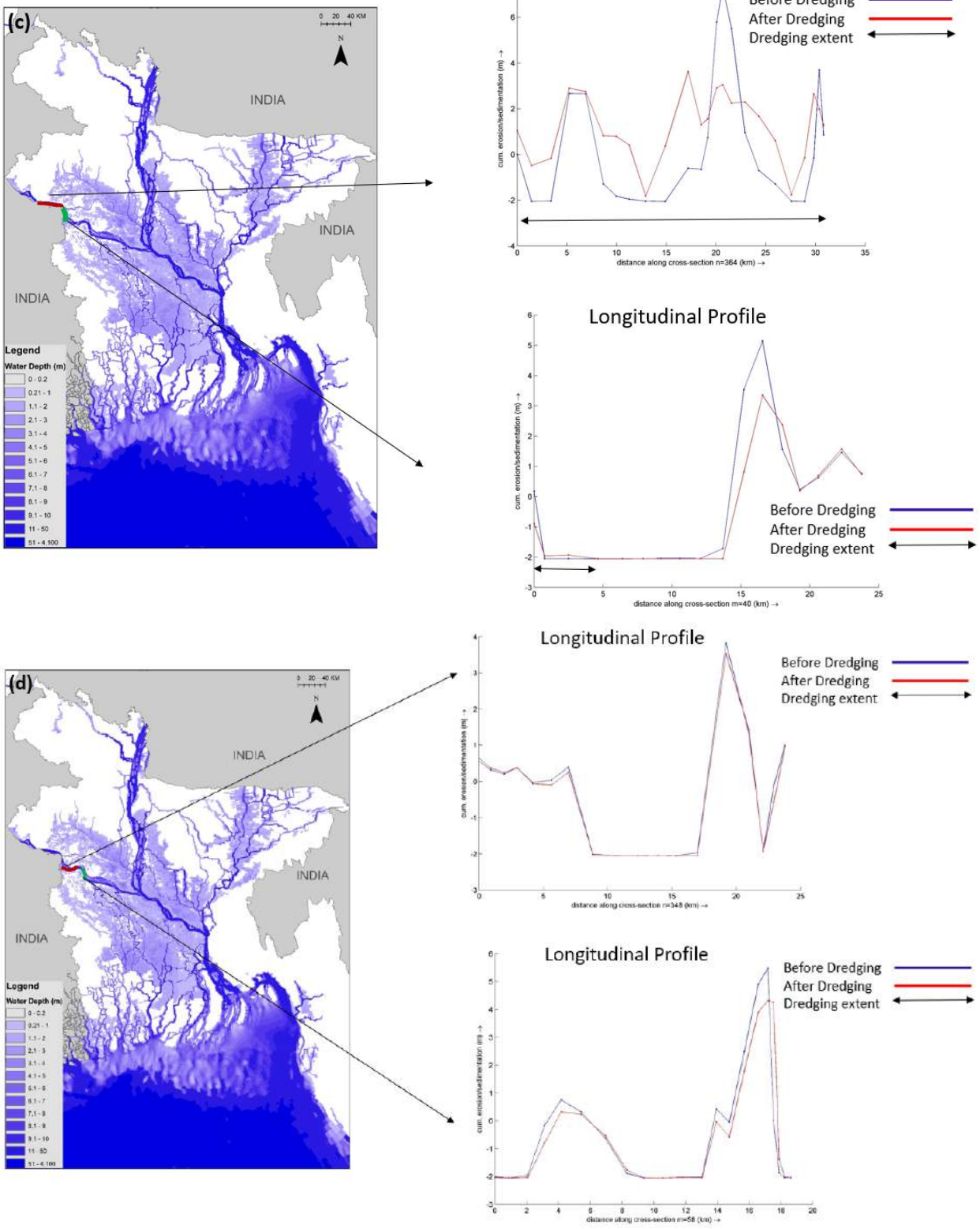
(c)
INDIA
INDIA
INDIA
Legend
Water Depth (m)
Longitudinal Profile
Before Dredging
After Dredging
Dredging extent
cum. erosion/sedimentation (m) →
distance along cross-section n=364 (km) →
Longitudinal Profile
Before Dredging
After Dredging
Dredging extent
cum. erosion/sedimentation (m) →
distance along cross-section m=40 (km) →
(d)
INDIA
INDIA
INDIA
Legend
Water Depth (m)
Longitudinal Profile
Before Dredging
After Dredging
Dredging extent
distance along cross-section n=348 (km) →
Longitudinal Profile
Before Dredging
After Dredging
Dredging extent

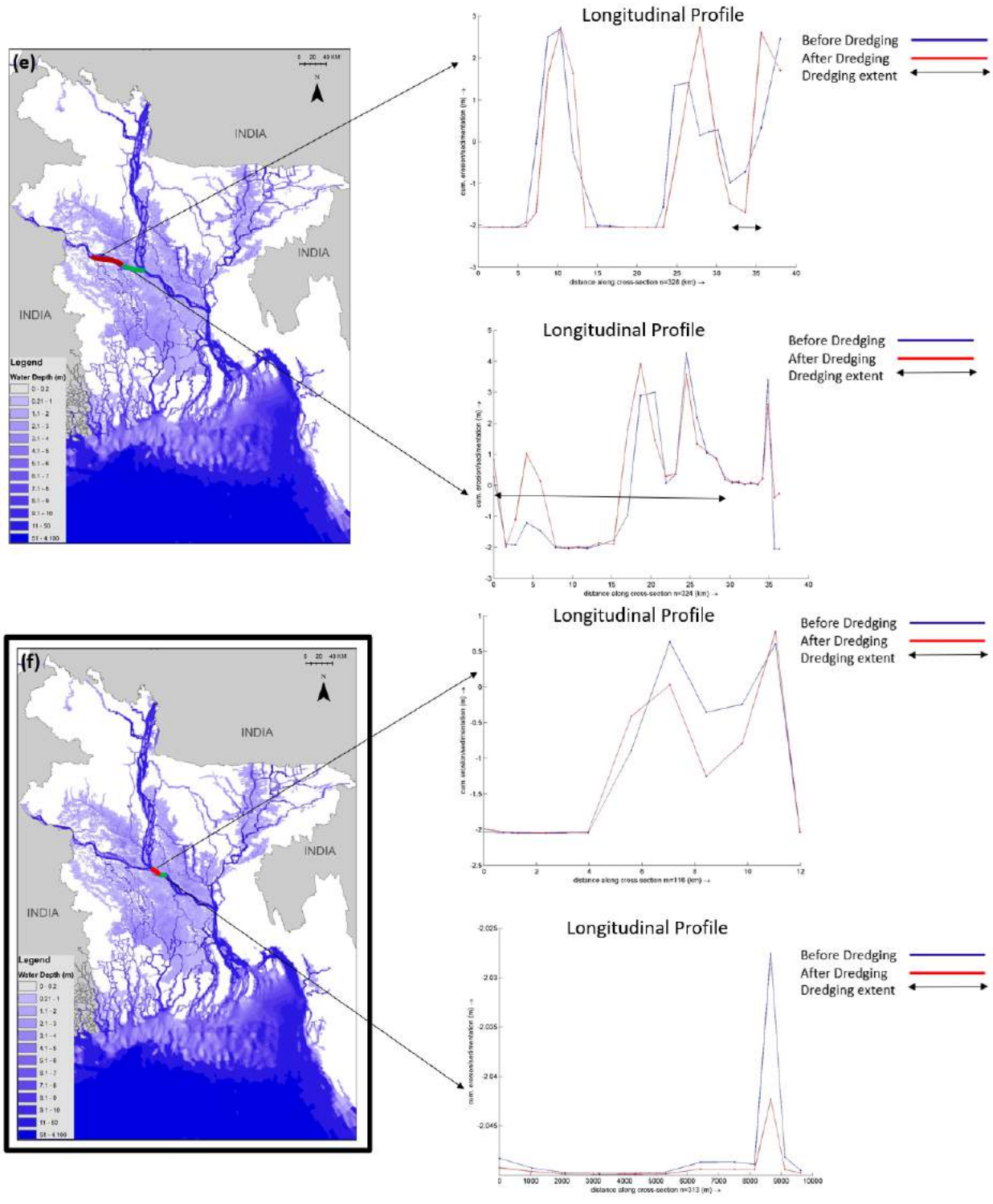
(e)
INDIA
INDIA
INDIA
Legend
Water Depth (m)
Longitudinal Profile
Before Dredging
After Dredging
Dredging extent
Longitudinal Profile
Before Dredging
After Dredging
Dredging extent
(f)
INDIA
INDIA
INDIA
Legend
Water Depth (m)
Longitudinal Profile
Before Dredging
After Dredging
Dredging extent
Longitudinal Profile
Before Dredging
After Dredging
Dredging extent

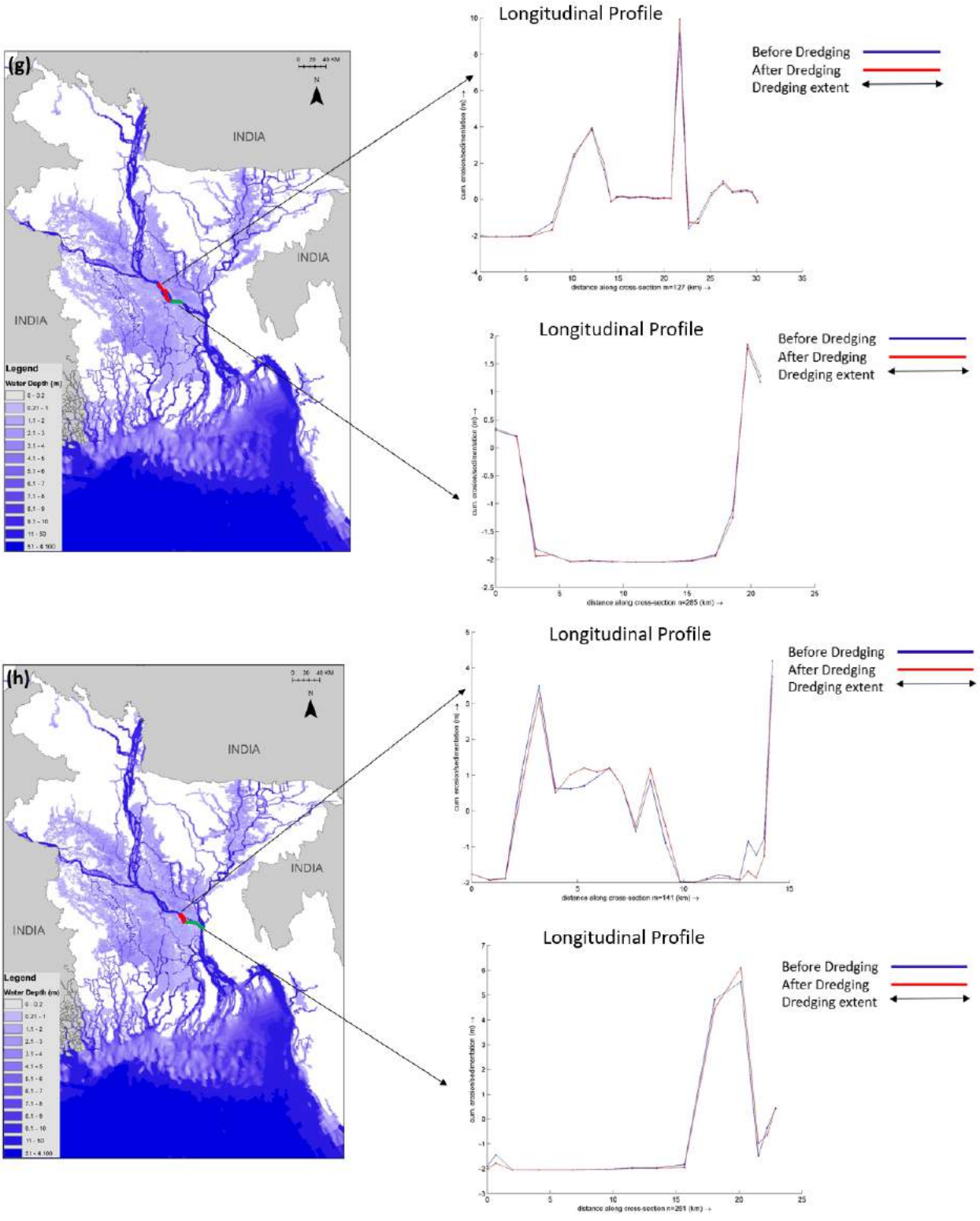
(g)
INDIA
INDIA
INDIA
Legend
Water Depth (m)
Longitudinal Profile
Before Dredging
After Dredging
Dredging extent
Longitudinal Profile
Before Dredging
After Dredging
Dredging extent
(h)
INDIA
INDIA
INDIA
Legend
Water Depth (m)
Longitudinal Profile
Before Dredging
After Dredging
Dredging extent
Longitudinal Profile
Before Dredging
After Dredging
Dredging extent

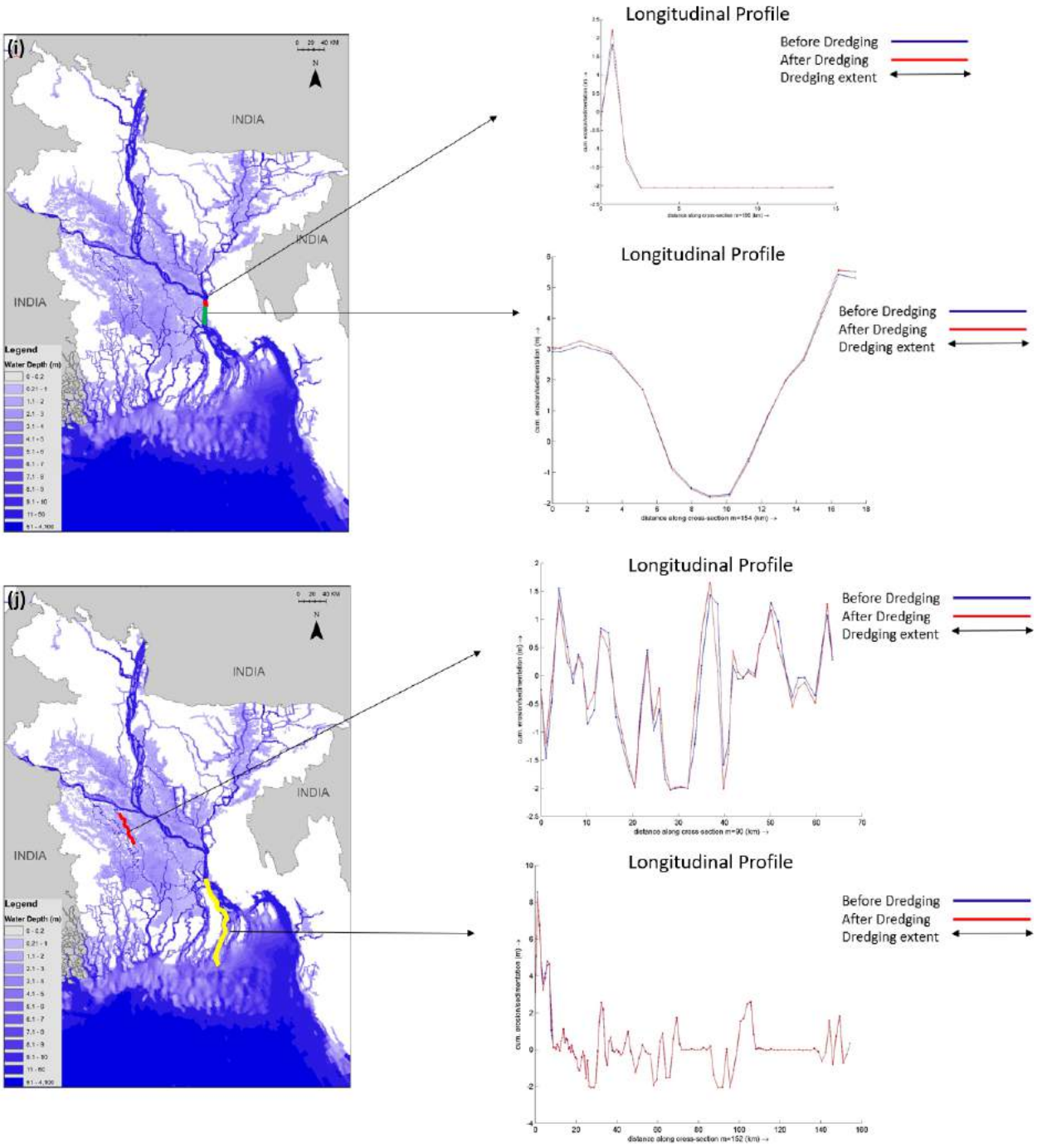

Figure 4.26: *Longitudinal profiles along different river reaches of the delta. The figure show shows reaches of the river (a) Brahmaputra-Jamuna (b-e) Ganges (f-h) Padma (i) Lower Meghna (j) Gorai.*

Change in sedimentation volume and depth on the delta surface

In our numerical experiment, we have removed the dredged material from the system so that the dredged material cannot re-enter into the system. This means the sediment volume which originally enters into the system remains the same, but due to the changed hydro-morphology of the system, the dynamics of sediment distribution reaches a new equilibrium. We will examine the change of this new system compared to the pre-dredged system. The inflow water and sediment are taken as extreme flood condition.

The changed yearly sedimentation depth on the delta surface (Figure 4.27) shows a decreased sedimentation depth on the delta floodplains from where we have earlier seen an improved inundation condition due to dredging (Figure 4.22). In these locations we have also seen decreased transport capacity (Figure 4.23) associated with decreased suspended sediment concentration (Figure 4.24). The increased conveyance of the dredged section decreases its transport capacity. The sediments which were supposed to be deposited over the floodplains are now deposited in the dredged section causing a rapid filling of the dredged section (Figure 4.21). This process eventually results a decreased sedimentation volume and sedimentation depth over the delta surface which are flood free due to dredging (Figure 4.27).

The change in sedimentation parameters due to this dredging show that (Table 4.3) 48 MT of sediment volume in the delta floodplain will be decreased which is 3.9% of total inflow sediment volume. In terms of sediment volume on the delta surface, change in coastal floodplain is positive which shows an increase of 4 MT of sediments on the delta surface (0.3% of total inflow sediments in the system). We can see maximum negative impacts on NE and NC regions. These regions are directly benefited in terms of inundation reduction. Sedimentation volume in the NE region is decreased by 20 MT (1.6% of total inflow volume) with a corresponding decrease of sedimentation depth of 1.0mm. For the NC region, these values are 33 MT (2.7% of total inflow sediments) and 0.3mm respectively. For the coastal region, the changes are positive. The maximum increase of sedimentation depth is for the SW region (0.9mm) followed by SC (0.2mm) and SE regions (0.3mm). The corresponding increase of sedimentation volume in SW region is 7 MT, and for the SE region it is 1 MT. In the SC region, the increase in sedimentation depth (0.2mm) is associated with a decrease of sedimentation volume of 4 MT. This means in the dredged state of delta, increased volume of sediments in the SC region is distributed in a reduced inundated area compared to the non-dredged state. The positive impact on the coastal region is due to the increased suspended sediments in the coastal ocean (Figure 4.24) which comes in the system from the excess sediments which were supposed to be deposited on the delta floodplains.

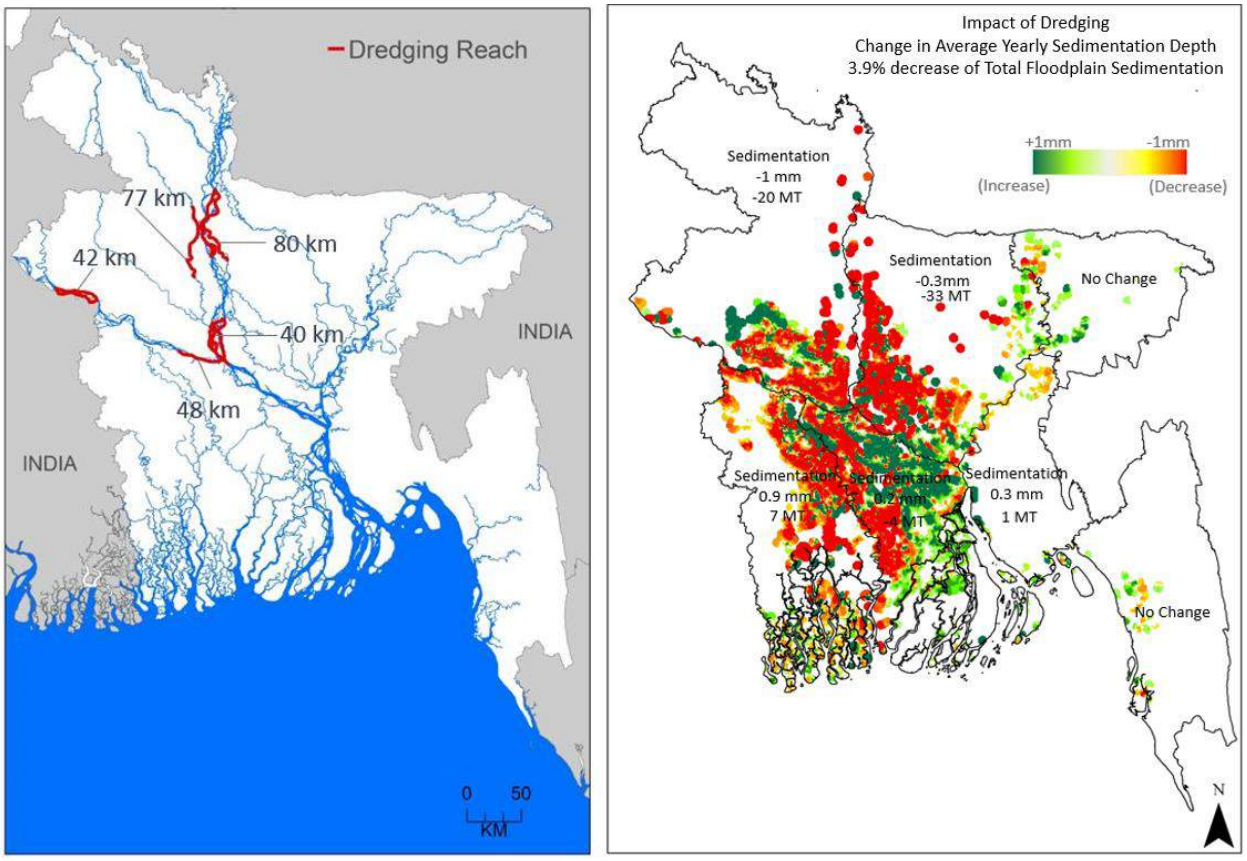

Figure 4.27: *Changes in average yearly sedimentation depth (right image) due to dredging in the dredged reaches of the rivers shown in the left image. The green zones show increased sedimentation depth, the red zones show decreased sedimentation depth, and the yellow zones show insignificant impact.*

Table 4.3: Yearly distribution of change of sedimentation in the GBM delta due to dredging in the river reaches of Brahmaputra-Jamuna and Ganges shown in Figure 4.20

Change in Total Sediment Distribution					
Flood Condition	Change in Inflow Sediments (Million Ton)	Change in Delta Floodplain Sedimentation (Million Ton)	Change in Coastal Floodplain Sedimentation (Million Ton)	Change in Percent Retained in Total Delta Floodplains	Change in Percent Retained in Coastal Floodplain
Extreme	No Change	-48	+4	-3.9%	+0.3%
Change in Regional Sediment Distribution					
Region	Change in Sedimentation Depth (mm)	Change in Sedimentation Volume (Million Ton)		Change in Percentage of Sedimentation Volume w.r.t Total Inflow Sediments	
NW	-1.0	-20		-1.6%	
NC	-0.3	-33		-2.7%	
NE	No Change	No Change		No Change	
SW	+0.9	+7		+0.7%	
SC	+0.2	-4		-0.3%	
SE	+0.3	+1		-0.08%	
EHT	No Change	No Change		No Change	

4.3.2 System impacts of dredging of Hari River

Hari River is situated in between Polder 24 and Polder 25 (Figure 4.28) and is believed to play a key role for waterlogging problem in the SW region. In addition to TRM (which is also a natural dredging process in addition to sedimentation in surrounding floodplains), there are several projects of BWDB for conducting dredging in the Hari River. Dredging in the Hari River increases the river conveyance and acts to temporarily reduce the waterlogging problem in the region. The difference between TRM and dredging in the Hari River is – dredging increases the conveyance of the Hari River which reduces the inundation on the floodplain, TRM does the same thing, but in addition, TRM also increases the sedimentation depth in the floodplains.

In this study, we have conducted synthetic dredging in the Hari River in a length of about 10km reach with the dredged depth of 3m.

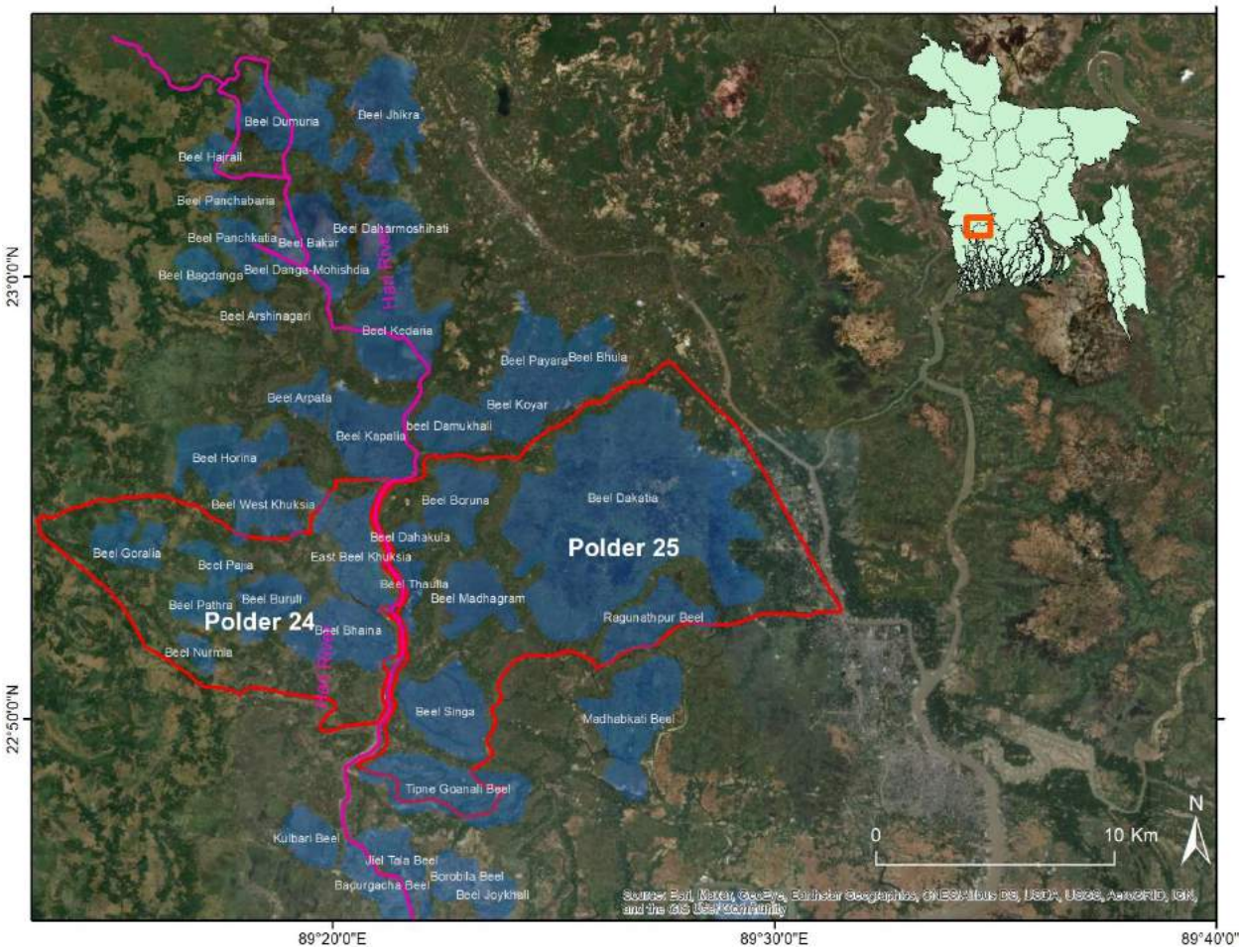

Figure 4.28: Location of the Hari River. Dredging in this river reduces waterlogging problem inside polders 24 and 25.

We investigated the changes of the sedimentation parameters in the entire system due to the dredging in Hari River (Figure 4.29 and Table 4.4). Hari River is located in the SW region (Figure 4.28). But the impact of dredging in the Hari River is seen to be felt in the entire coast except the EHT region. However, there is no impact in the non-tidal part of the delta. As mentioned before, when dredging reduces flood inundation in the floodplains, it also reduces sedimentation depth in the floodplain. On the other hand, TRM also reduces flood inundation, but at the same time increases the sedimentation depth in the connected beels. So, this will increase the average sedimentation depth in the floodplains. This is the advantage of TRM over dredging. Due to Hari River dredging, total sediment volume on the delta surface reduces by 0.2 MT which is 0.016% of total sediment inflow to the system. This reduction of sediment volume is entirely in the coastal zone. In the coastal zone, maximum reduction of sedimentation depth on the delta surface is for SC region (0.2mm) followed by SW and SE regions (0.1mm each). Corresponding sediment volume reductions are 0.1 MT for the SC region, and 0.05 MT each for the SW and SE region. We can see that dredging in the Hari River reduces the sedimentation depth in SW region where the

Hari River is located. This dredging also reduces sedimentation depth on the SC region which is an important region for the delta sustainability.

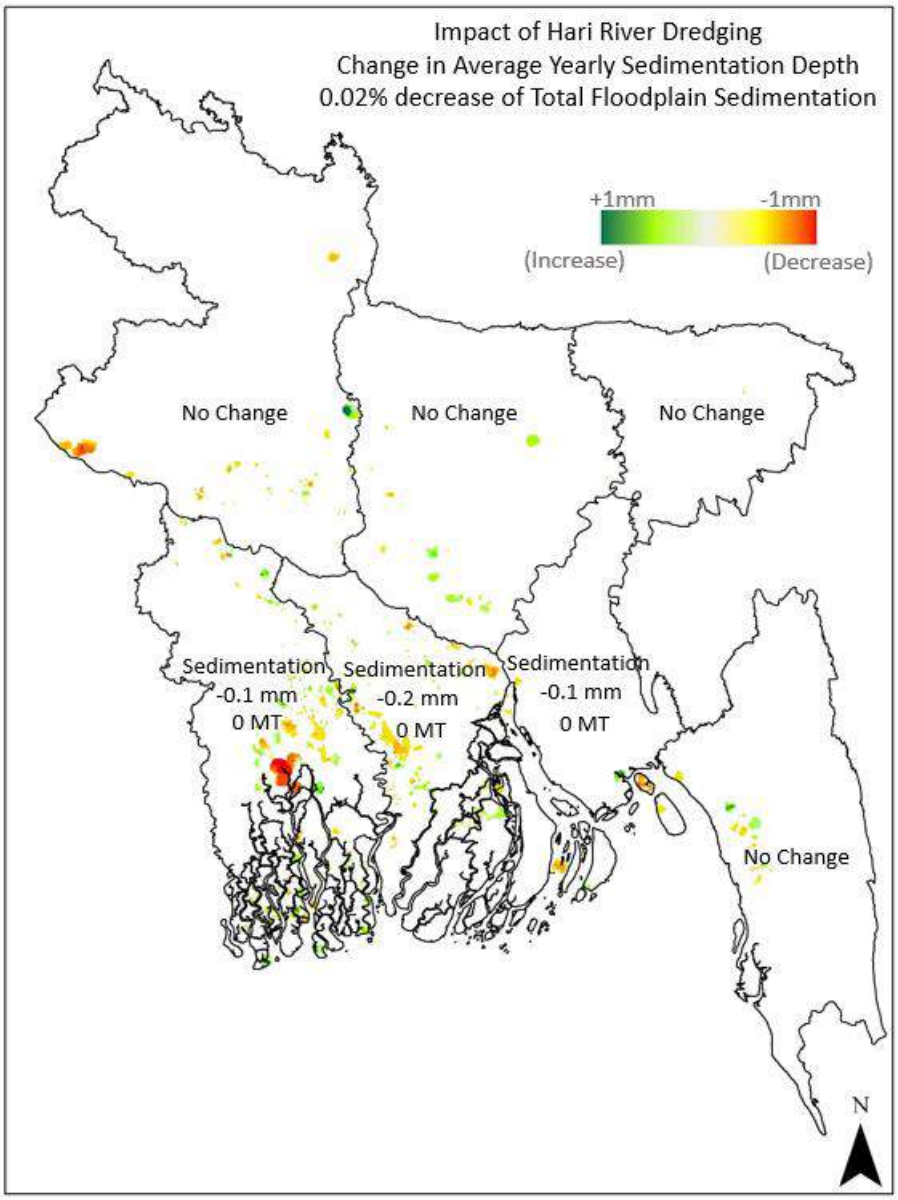

Figure 4.29: *Changes in average yearly sedimentation depth due to dredging in the Hari River. The green zones show increased sedimentation depth, the red zones show decreased sedimentation depth, and the yellow zones show insignificant impact.*

Table 4.4: Comparison of yearly distribution change of sedimentation in the GBM delta between Brahmaputra-Jamuna & Ganges (B-J-G) and Hari River due to dredging in the locations shown in Figures 4.20 and 4.28.

Comparison of Change in Total Sediment Distribution					
Flood Condition	Change in Inflow Sediments (Million Ton)	B-J-G Dredging Change in Delta Floodplain Sedimentation (Million Ton)	Hari River Dredging Change in Delta Floodplain Sedimentation (Million Ton)	B-J-G Dredging Change in Percent Retained in Total Delta Floodplains	Hari River Dredging Change in Percent Retained in Total Delta Floodplains
Extreme	No Change	-48	-0.2	-3.9%	-0.016%
Comparison of Change in Regional Sediment Distribution					
Region	B-J-G Dredging Change in Sedimentation Depth (mm)	Hari River Dredging Change in Sedimentation Depth (mm)	B-J-G Dredging Change in Sedimentation Volume (Million Ton)	Hari River Dredging Change in Sedimentation Volume (Million Ton)	B-J-G Dredging Change in Percentage of Sedimentation Volume w.r.t Total Inflow Sediments	Hari River Dredging Change in Percentage of Sedimentation Volume w.r.t Total Inflow Sediments
NW	-1.0	No Change	-20	No Change	-1.6%	No Change
NC	-0.3	No Change	-33	No Change	-2.7%	No Change
NE	No Change	No Change	No Change	No Change	No Change	No Change
SW	+0.9	-0.1	+7	-0.05	+0.7%	-0.004%
SC	+0.2	-0.2	-4	-0.10	-0.3%	-0.008%
SE	+0.3	-0.1	+1	-0.05	-0.08%	-0.004%
EHT	No Change	No Change	No Change	No Change	No Change	No Change

4.4 Dredging in the Payra Port Channel

Payra port is situated on the bank of Rabnabad channel in Kalapara upazila of Patiakhali district. Rabnabad channel is one of the largest estuaries in terms of sediment flux (Ahmed, 2017). Siltation of the navigation channel of the port is considered as one of the major issues about the operation of the port (Ahmed, 2017).

We have applied BDM to study the yearly sedimentation patterns in the navigation channel of Payra port. Before calculating the sedimentation volume, validation of BDM is performed with the available data at the Payra port navigation channel. This validation is in addition to the overall validation of BDM (See Chapter Two).

Figure 4.30 shows the location and approximate alignment of Payra port navigation channel. This is a long but narrow channel of approximately 70 km long and 200 m wide. To capture the details of this channel, a finer grid model is constructed within the main BDM framework (Figure 4.31).

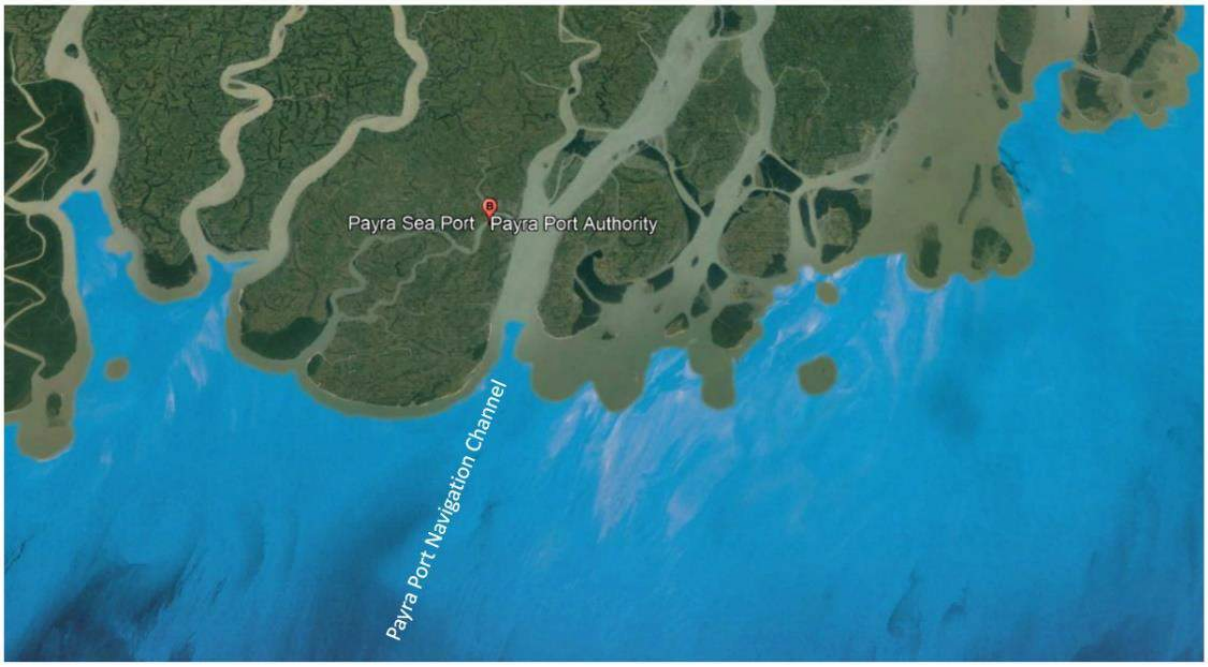

Figure 4.30: *Location of Payra port navigation channel. The figure shows the location of the port and the navigation channel.*

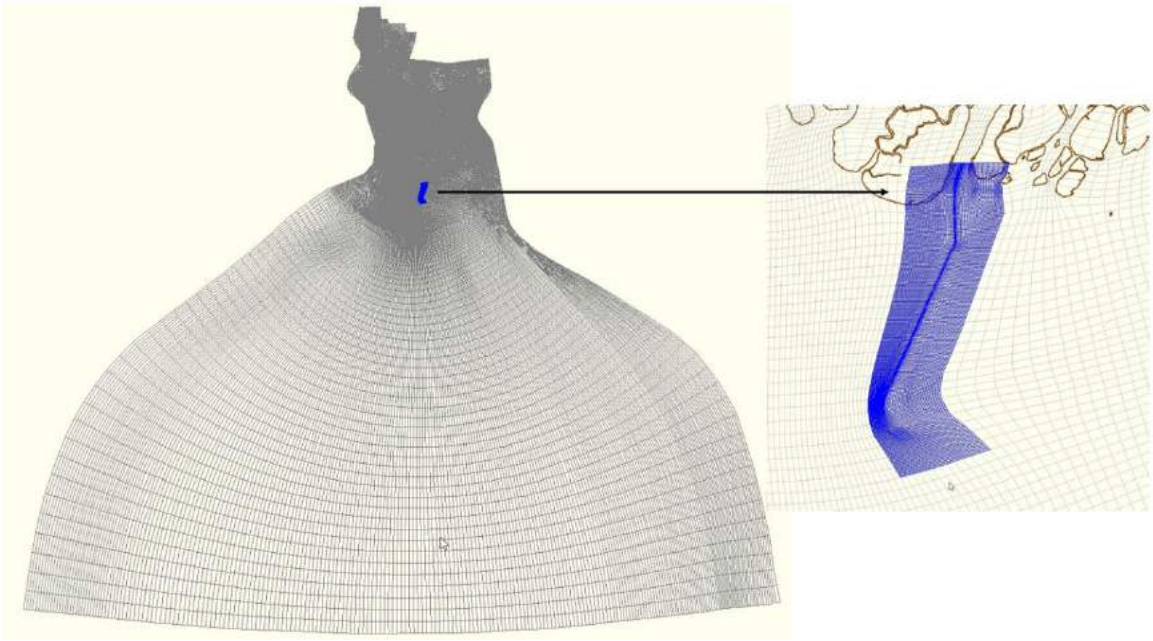

Figure 4.31: *Fine grid Payra Port navigation channel within BDM grid. The fine grid model works as a separate domain within the main BDM. This makes it possible to consider the impact of entire GBM systems in the sedimentation of the navigation channel.*

4.4.1 Validation for the Payra port navigation channel

Measured bed level data at the Payra port navigation channel is available for January 2020 and January 2021. On the other hand, complete calibration and validation of BDM is made for the years 2017 and 2018 respectively (Chapter Two). Large number of data required to validate BDM is not available for the measurement period of Payra port channel. Due to this, measured bed level for January 2020 and January 2021 is compared with the model bed level for January 2017 and January 2018. It is obvious that flow and sediment inflows for 2020-2021 is not same for 2017-2018. All the comparisons are made for -6.2mCD dredged channel. This is the existing channel depth for the Parya port navigation channel.

Bed level comparison for the entire channel length

Measured and model bed level for the entire channel for January 2020 is compared with the model bed level of January 2017 (Figure 4.32), and measured bed level for January 2021 is compared with the model bed level of January 2018 (Figure 4.33).

Comparison with Measured Data at Payra Port Channel
Bed Level (mCD)

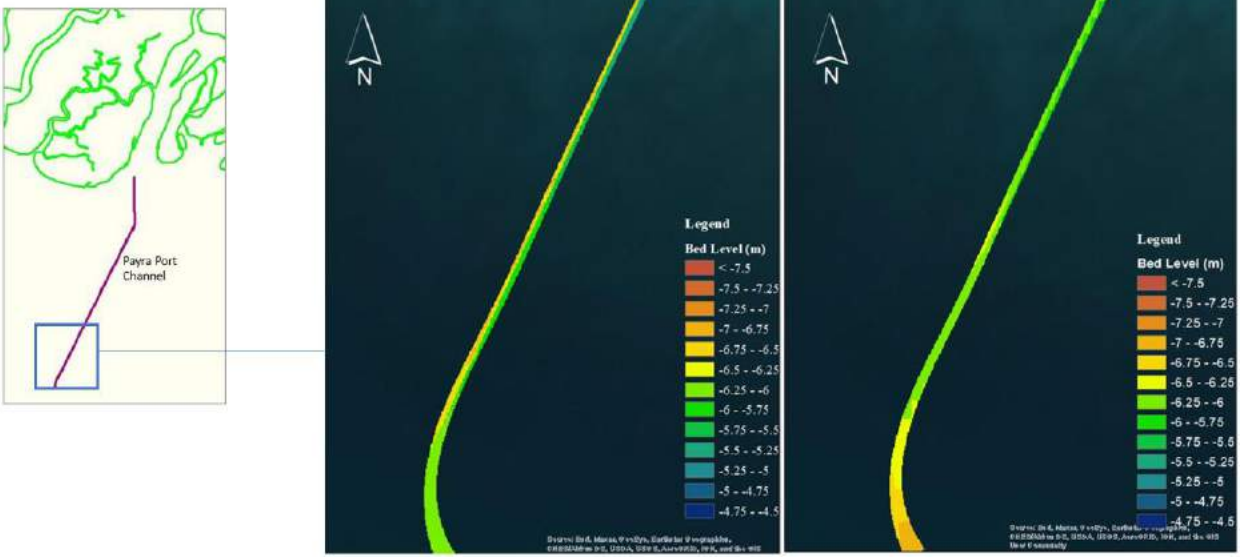

Comparison with Measured Data at Payra Port Channel
Bed Level (mCD)

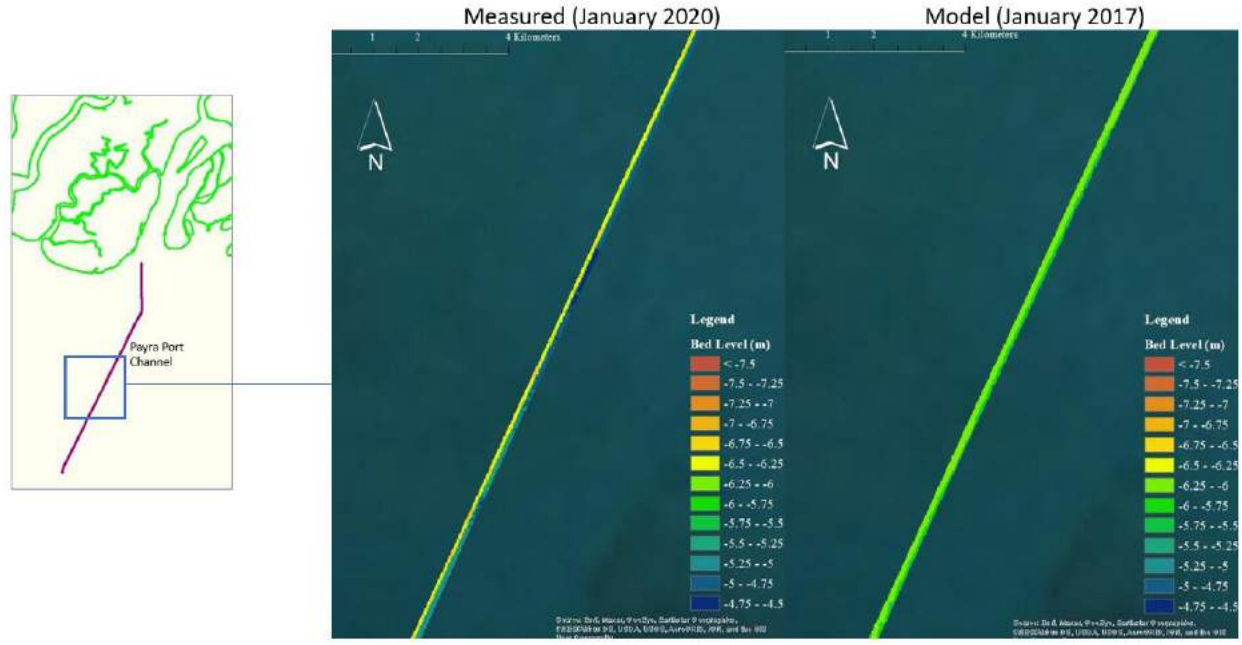

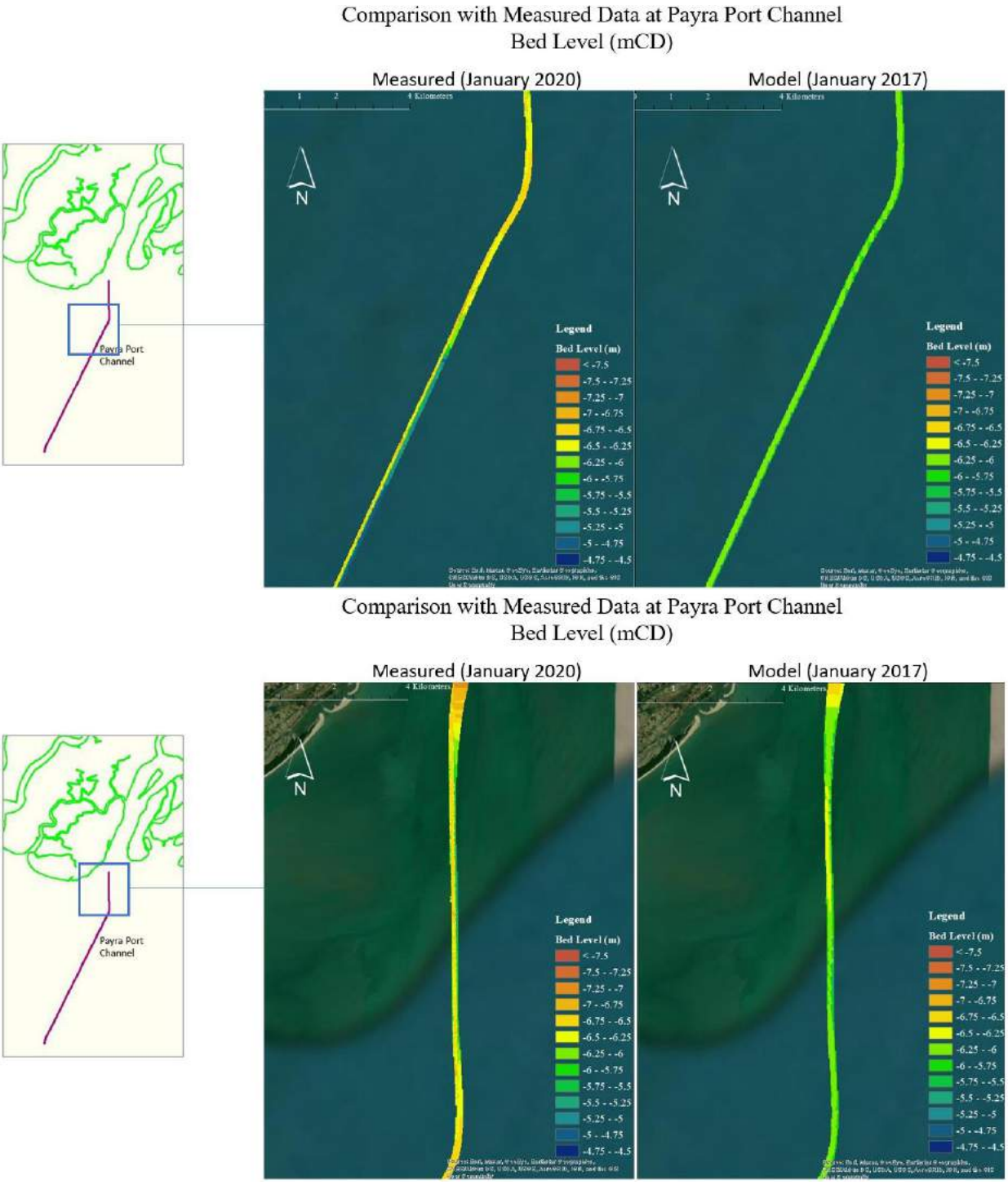

Figure 4.32: *Comparison between measured (January 2020) and model (January 2017) bed level for the Payra port navigation channel. Comparison is made for a dredged channel of -6.2mCD depth.*

Comparison with Measured Data at Payra Port Channel
Bed Level (mCD)

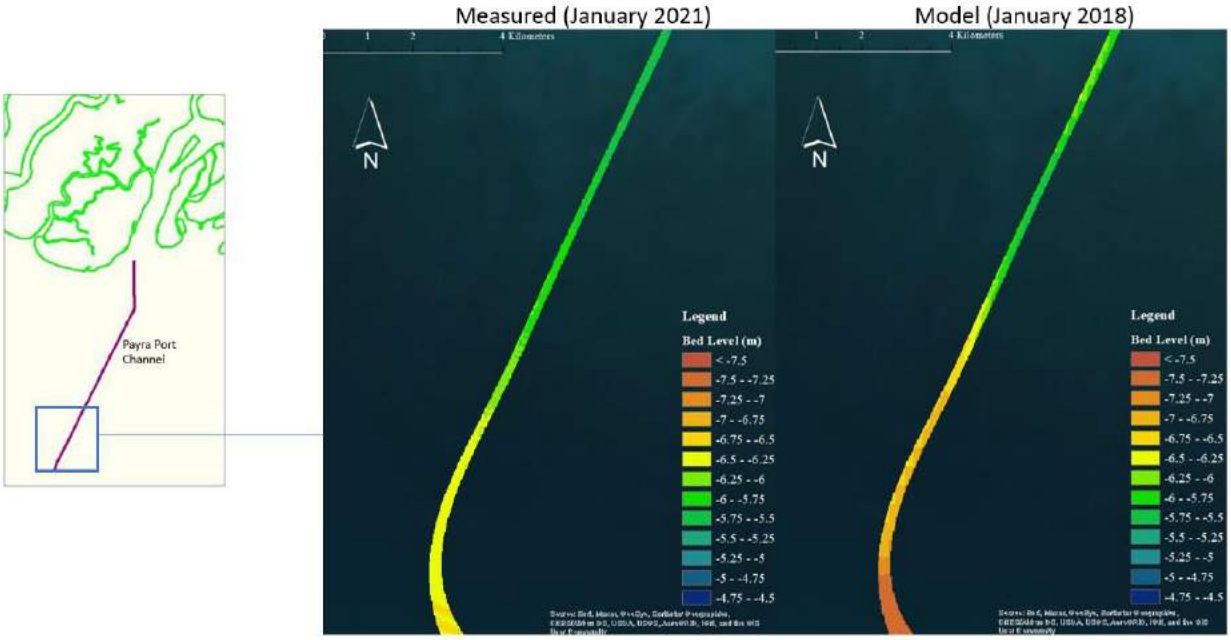

Comparison with Measured Data at Payra Port Channel
Bed Level (mCD)

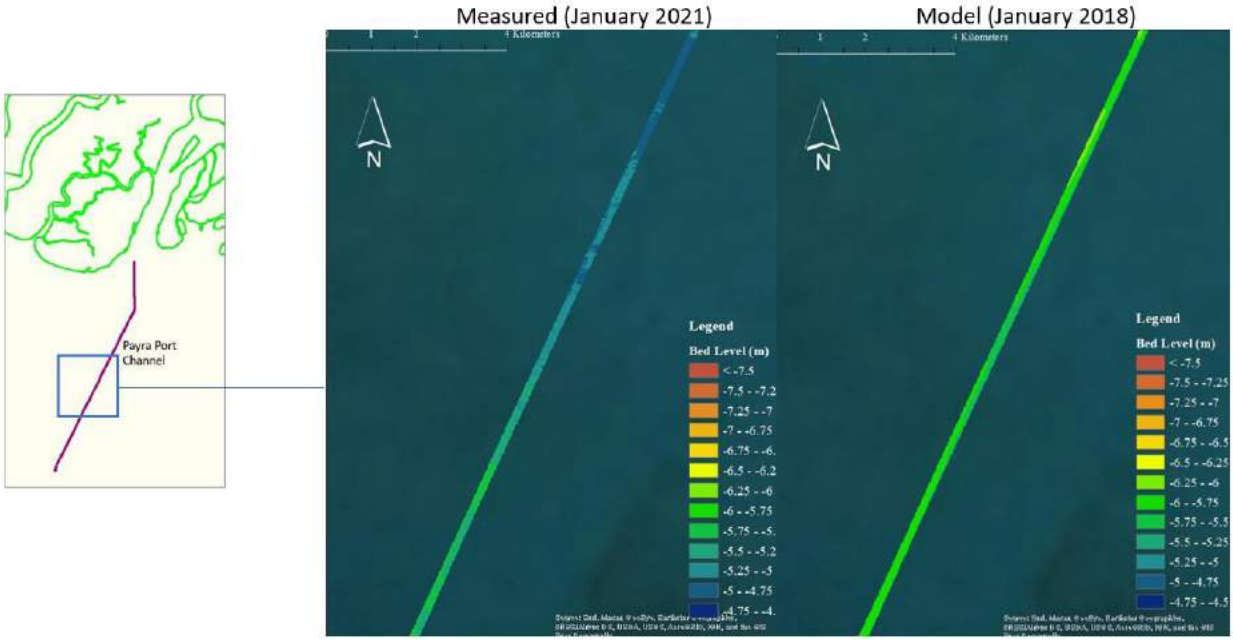

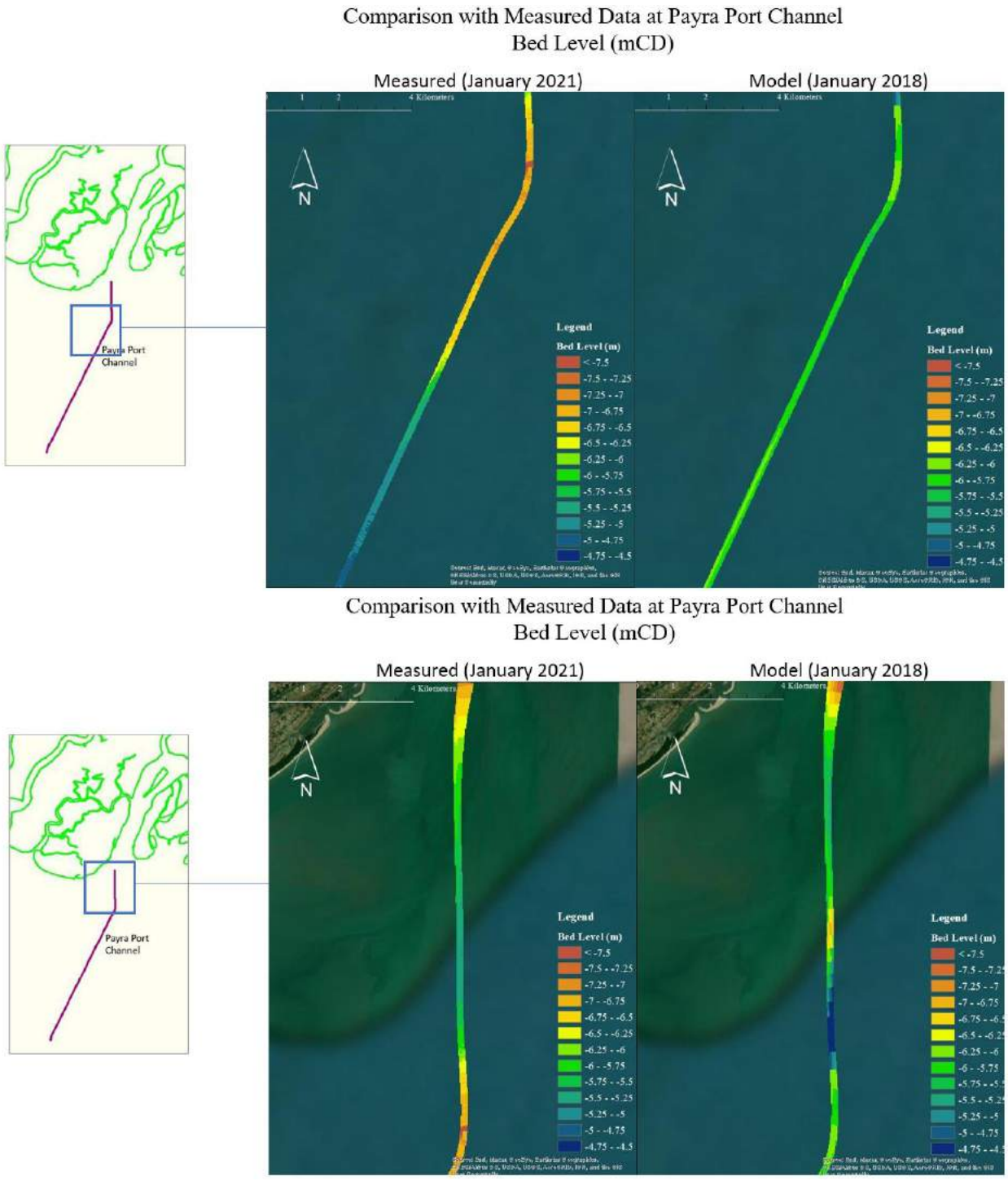

Figure 4.33: *Comparison between measured (January 2021) and model (January 2018) bed level for the Payra port navigation channel. Comparison is made for a dredged channel of -6.2mCD depth.*

Comparison of cross sections

Cross sections at different locations of the channel are compared between the measured data of January 2020 with the model result of January 2017 (Figure 4.34), and measured data of January 2021 with the model result of January 2018 (Figure 4.35).

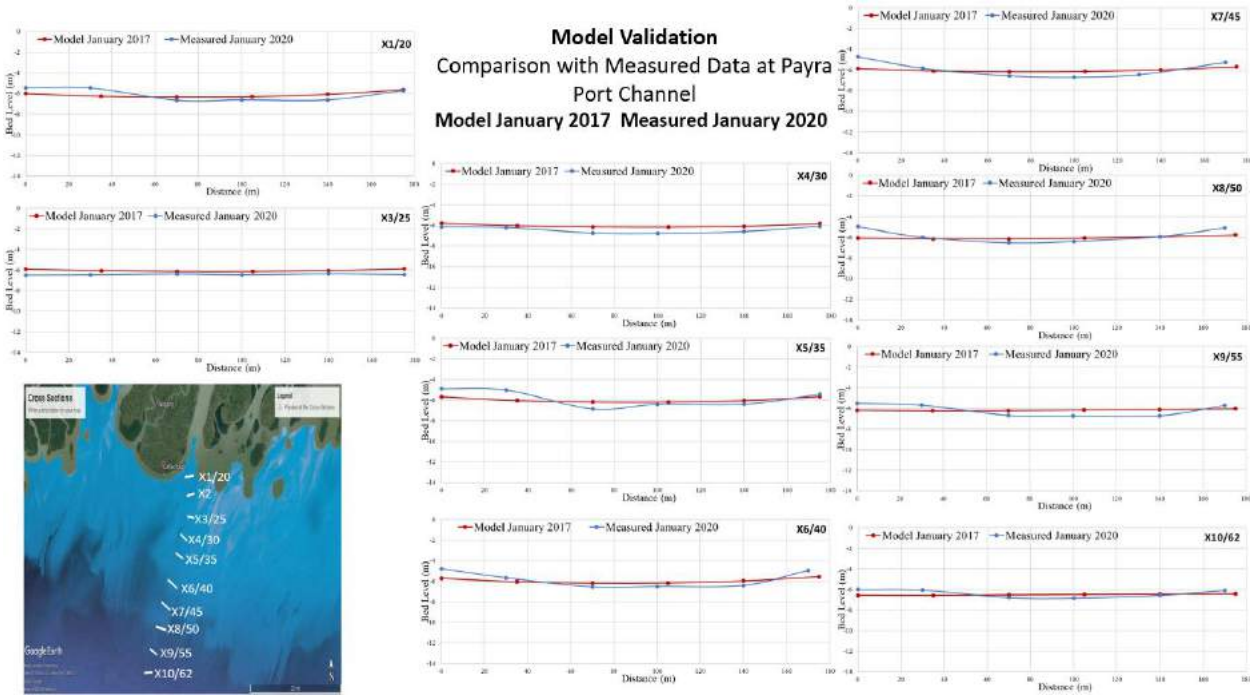

Figure 4.34: *Comparison between measured (January 2020) and model (January 2017) cross sections at different locations of the Payra port channel. Comparison is made for a dredged channel of -6.2mCD depth.*

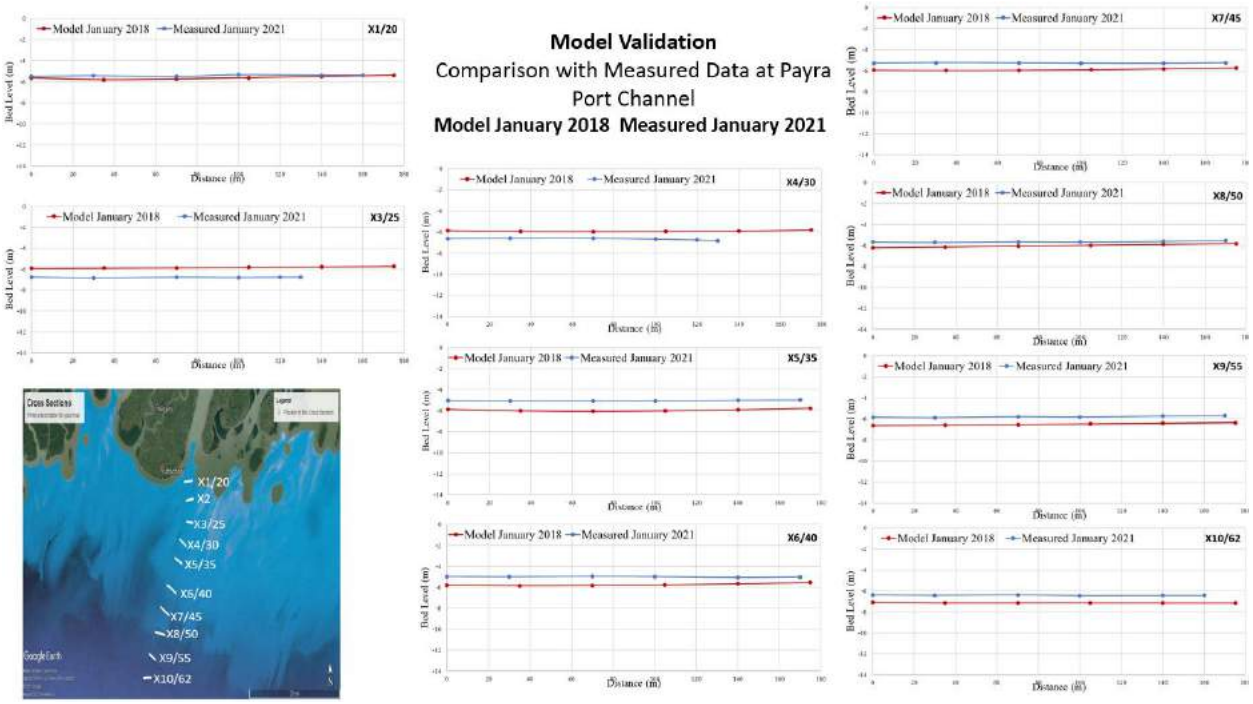

Figure 4.35: *Comparison between measured (January 2021) and model (January 2018) cross sections at different locations of the Payra port channel. Comparison is made for a dredged channel of -6.2mCD depth.*

4.4.2 Model simulations to generate sedimentation scenarios in the channel

Following physical and atmospheric conditions are considered to generate different sedimentation scenarios in the channel (Table 4.5).

Table 4.5: Physical and atmospheric conditions for different scenarios generated to study channel sedimentation patterns.

Channel depth	Natural -6.2mCD -10.5mCD
Inflow conditions	Low Medium High
Cyclones	Amphan Sidr

Regarding the channel depth, natural means a channel in the same alignment of navigation channel with its existing bathymetry. The two dredged depths -6.2mCD and -10.5mCD are selected based on different drafts of vessels that the navigation channel can allow. The three inflow conditions are selected based on 3 inflow river water discharges and sediment inflow conditions. During low inflow conditions, both the water discharge and sediment inflows through the major river systems (Ganges, Brahmaputra, Upper Meghna) are low. In this way, both the water discharge and sediment inflow in the major river systems increase from low to high inflow conditions. After frequency analysis, year 2000 is selected as the low inflow condition, year 2017 is selected as the medium inflow condition, and year 1998 is selected as the high inflow condition. As cyclones are believed to play a role in the sediment dynamics in the region (Kudrass et. Al., 2018), 2 cyclone scenarios are considered – Amphan and Sidr. Amphan is a recent cyclone in the region (May 2020) which is relatively weak compared to cyclone Sidr (November 2007). In addition to cyclone strength, the basic difference between cyclone Amphan and cyclone Sidr is – cyclone Amphan made landfall during pre-monsoon time (May 2020) whereas, cyclone Sidr made landfall during the post monsoon (November 2007). Sediment supply in the region is expected to be minimum during the pre-monsoon season and maximum during the post-monsoon season. There is one similarity between these two cyclones – the track of both the cyclones are on the left side of the navigation channel. So, impacts of both the cyclones are supposed to be high on the navigation channel.

The scenarios shown in Table 4.5 are used to generate yearly sedimentation patterns in the channel. Yearly cross-sectional change in different sections of the channel for all the scenarios described in Table 4.5 is shown in Figure 4.34.

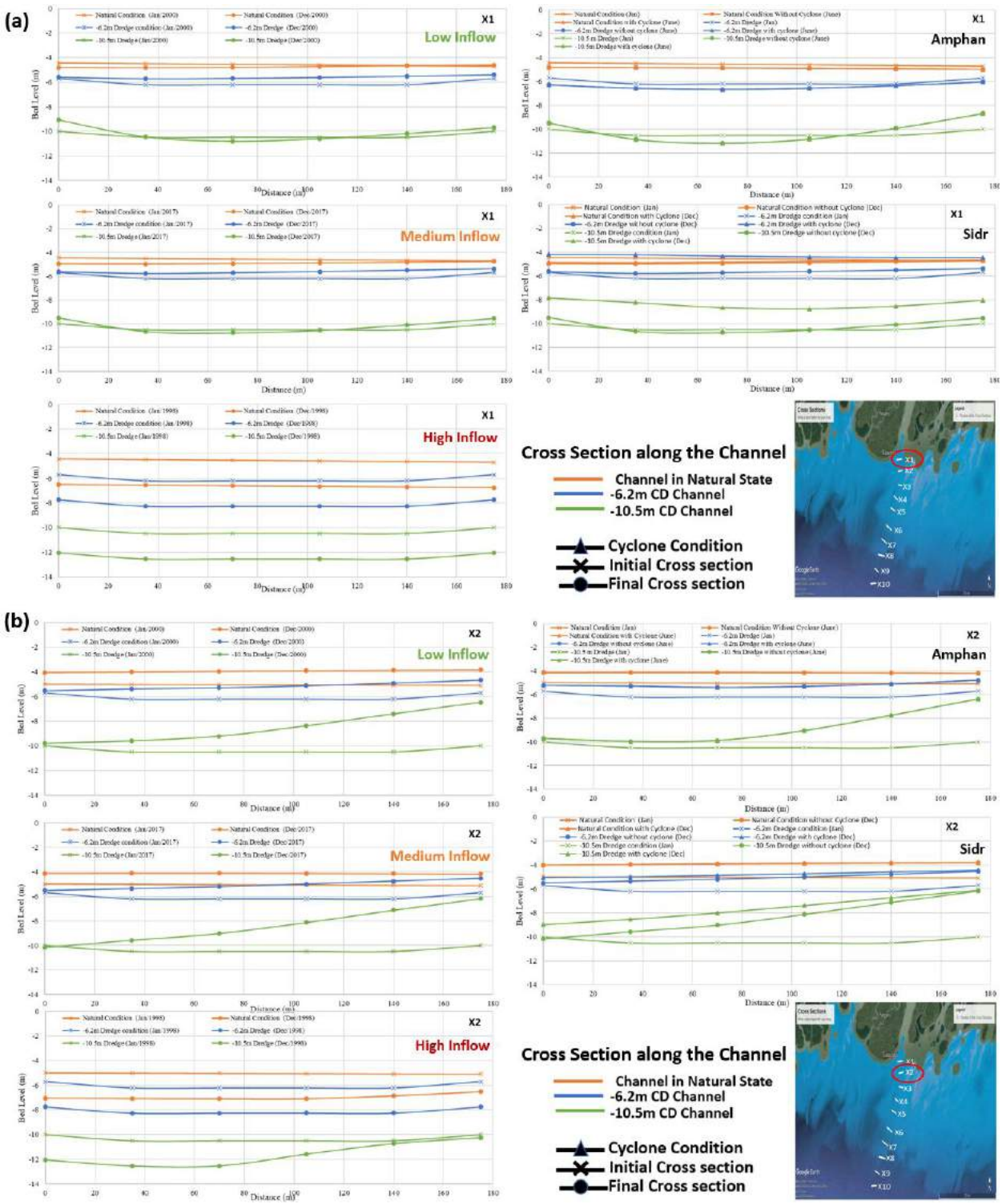
(a)
X1
Low Inflow
X1
Amphan
X1
Medium Inflow
X1
Sidr
X1
High Inflow
Cross Section along the Channel
Channel in Natural State
-6.2m CD Channel
-10.5m CD Channel
Cyclone Condition
Initial Cross section
Final Cross section
(b)
X2
Low Inflow
X2
Amphan
X2
Medium Inflow
X2
Sidr
X2
High Inflow
Cross Section along the Channel
Channel in Natural State
-6.2m CD Channel
-10.5m CD Channel
Cyclone Condition
Initial Cross section
Final Cross section

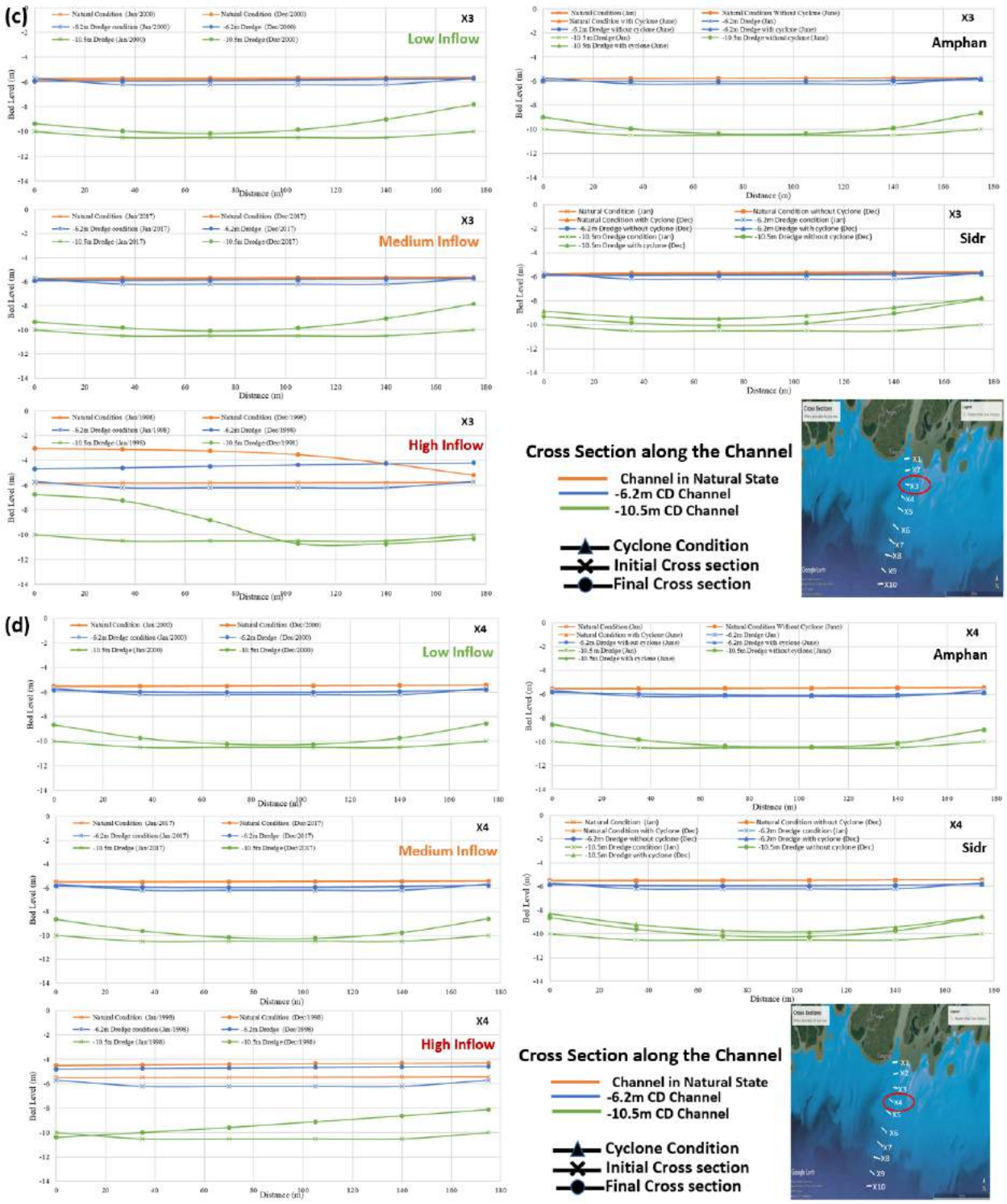
(c)
X3
Low Inflow
X3
Medium Inflow
X3
High Inflow
X3
Amphan
X3
Sidr
Cross Section along the Channel
Channel in Natural State
-6.2m CD Channel
-10.5m CD Channel
Cyclone Condition
Initial Cross section
Final Cross section
(d)
X4
Low Inflow
X4
Medium Inflow
X4
High Inflow
X4
Amphan
X4
Sidr
Cross Section along the Channel
Channel in Natural State
-6.2m CD Channel
-10.5m CD Channel
Cyclone Condition
Initial Cross section
Final Cross section

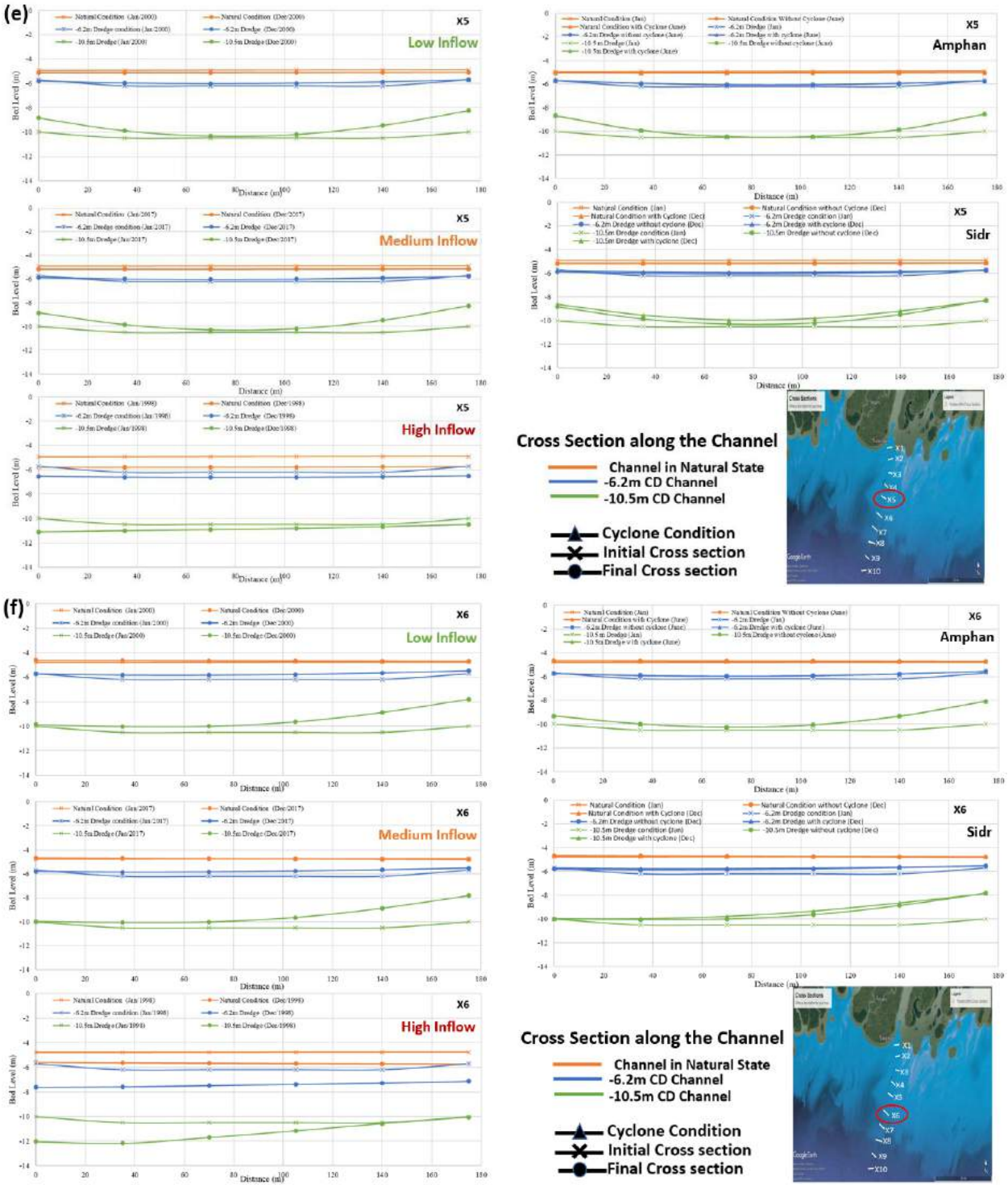
(e)
X5
Low Inflow
X5
Medium Inflow
X5
High Inflow
X5
Amphan
X5
Sidr
Cross Section along the Channel
Channel in Natural State
-6.2m CD Channel
-10.5m CD Channel
Cyclone Condition
Initial Cross section
Final Cross section
(f)
X6
Low Inflow
X6
Medium Inflow
X6
High Inflow
X6
Amphan
X6
Sidr
Cross Section along the Channel
Channel in Natural State
-6.2m CD Channel
-10.5m CD Channel
Cyclone Condition
Initial Cross section
Final Cross section

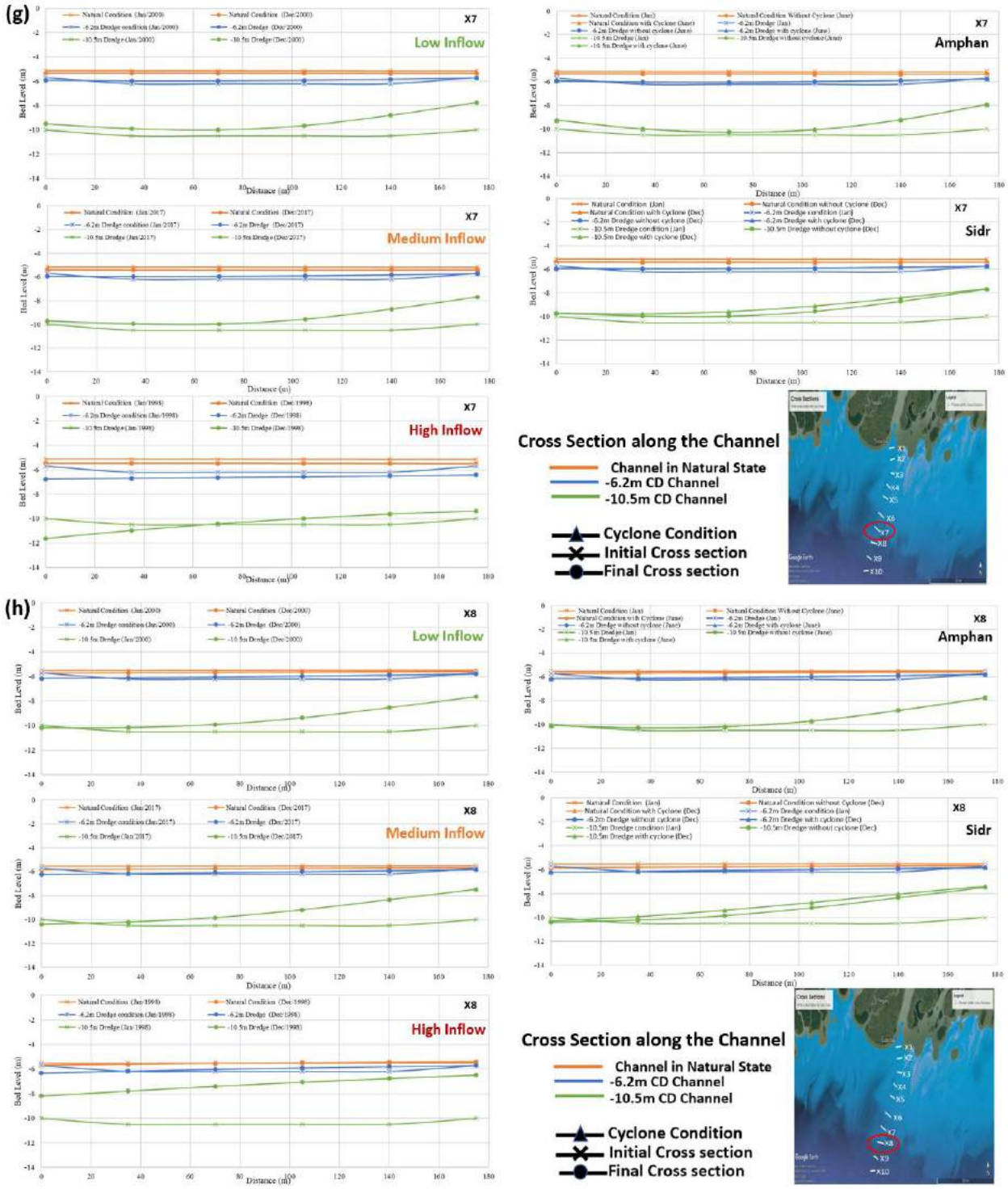
(g)
X7
Low Inflow
X7
Amphan
X7
Medium Inflow
X7
Sidr
X7
High Inflow
Cross Section along the Channel
Channel in Natural State
-6.2m CD Channel
-10.5m CD Channel
Cyclone Condition
Initial Cross section
Final Cross section
(h)
X8
Low Inflow
X8
Amphan
X8
Medium Inflow
X8
Sidr
X8
High Inflow
Cross Section along the Channel
Channel in Natural State
-6.2m CD Channel
-10.5m CD Channel
Cyclone Condition
Initial Cross section
Final Cross section

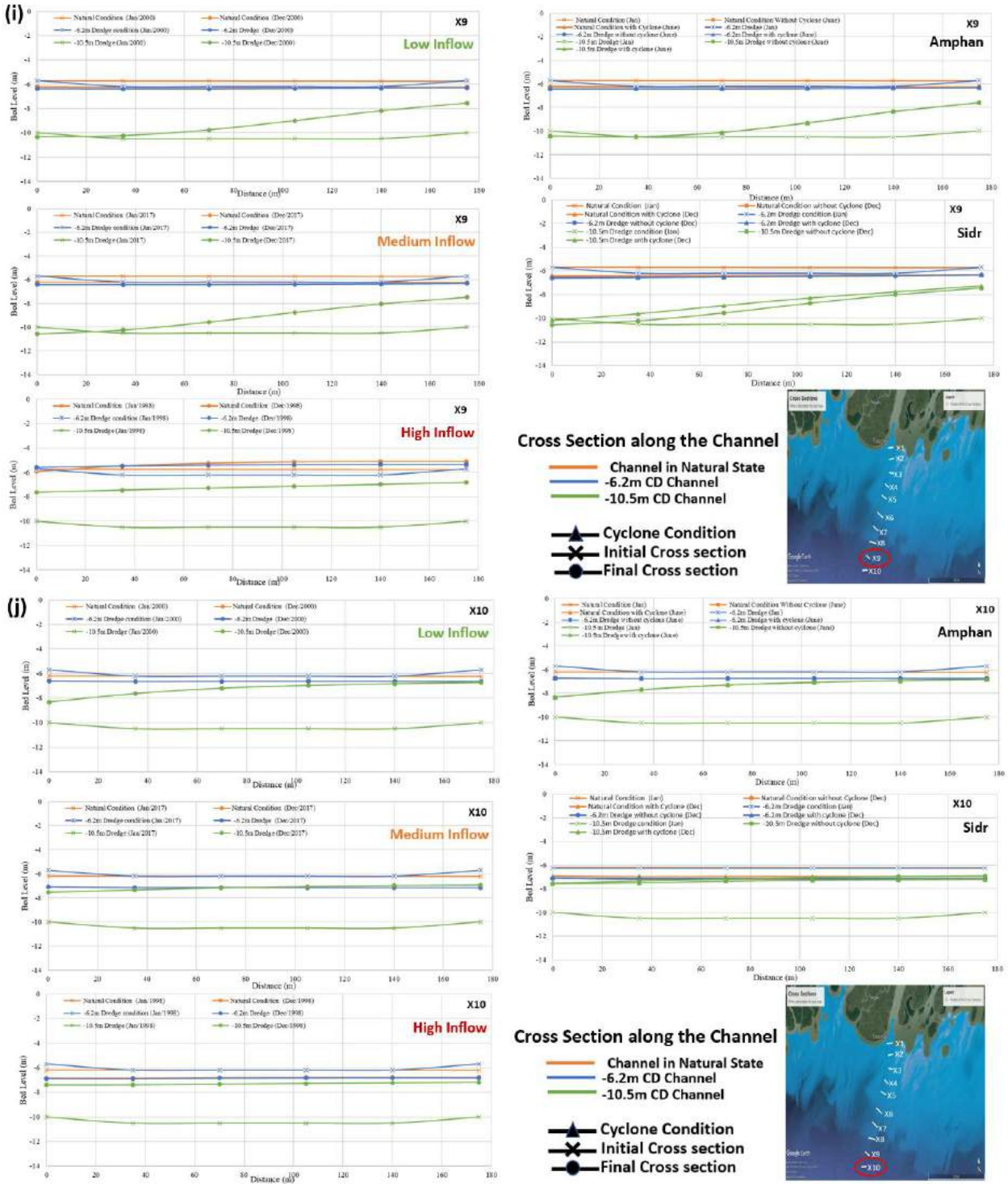

Figure 4.36: *Cross sections showing yearly sedimentation pattern at different locations of the channel for different scenarios of Table 4.5. Cross section locations are shown at the bottom right corner of each figure.*

When the channel is in natural state, there is hardly any change in channel section over a year with small yearly channel sedimentation (Figure 4.36). With increased amount of channel dredging (-6.2m CD and -10.5m CD depth), sedimentation starts increasing. For both the -6.2m CD and -10.5m CD channel, maximum sedimentation is observed in sections just at the outfall of the Rabnabad channel (section X2, Figure 4.36b) and the most offshore section (section X10, Figure 4.36j). Section X2 (Figure 4.36b) falls in the direct sediment outfall zone of Rabnabad channel and section X10 (Figure 4.36j) falls in the active re-circulation zone of sediments coming out from the Lower Meghna Estuary (see Chapter Three). Sedimentation pattern in the entire channel section (Figure 4.33) also shows that active sedimentation zone of the channel is at the outfall section of Rabnabad channel and on the path of re-circulation zone of sediments from Lower Meghna Estuary (see Chapter Three). Sedimentation in the channel depends on the inflow sediment volume. Increased inflow sediments from upstream river systems increase the sedimentation in the channel for all channel conditions.

It is generally believed that cyclonic events cause increased sedimentation in the region (Kudrass et. Al., 2018). To study the impacts of cyclone, two cyclonic scenarios are considered (Table 4.5). It is found that cyclone Amphan has no impact on sedimentation in the channel, but cyclone Sidr has considerable impact on channel sedimentation (Figure 4.36). Impact of cyclone Sidr is found to be maximum in the active sedimentation zone of region (sections X2 and X10, Figures 4.36b and 4.36j). As mentioned before, cyclone Amphan occurred during the pre-monsoon (May 2020) when sediment inflow in the region is minimum, and cyclone Sidr occurred during the post-monsoon (November 2007) when sediment inflow in the region is maximum.

Sedimentation in the dredged channel is significantly higher than the channel in natural state. With the increase of dredging depth, sedimentation increases at a faster rate. Sedimentation process in the Payra port channel depends on the upstream flow conditions of the riverine systems. Sediment supply from upstream depends on the sediment inflow during the monsoon. Increased sediment inflow from upstream generally increases the sedimentation in the channel. Although high flow from upstream also causes erosion of the channel at few sections. Depending on the sediment inflow pattern, sedimentation in a specific monsoon month can be higher than yearly sedimentation volume. Sedimentation patterns at different sections of channel are different. High strength cyclone during post-monsoon season that makes landfall at the west side of the channel (for example cyclone Sidr) cause additional sedimentation in the channel. A similar but low strength cyclone (for example cyclone Amphan) during pre-monsoon season has little impact on sedimentation in the channel.

4.4.3 Effectiveness of dredging

Effectiveness of dredging is calculated by calculating percent filling of the 70km dredged channel and maximum sedimentation depth within the 70km channel during different flow conditions (Table 4.6). The results show that ranges of yearly filling the -6.2mCD channel vary between 35%

to 50% depending on different flow conditions. The maximum yearly sedimentation depths of this channel for different flow conditions vary between 1.6m to 1.9m. This depth is calculated from the dredged channel. The maximum yearly sedimentation depths for the -10.5mCD channel is much higher than -6.2mCD channel and vary between 4.8m to 5.2m depending on different flow conditions. As initial volume of -10.5mCD channel is much higher than -6.2mCD channel, percent filling of this channel is relatively low compared to -6.2mCD channel (31% - 34% compared to 35% - 50% of the -6.2mCD channel).

Table 4.6: Effectiveness of dredging of the 70 km navigation channel of Payra port for different flow conditions

Flow Condition	Channel Depth	Yearly Percent Filling	Yearly Maximum Sedimentation Depth
High	-6.2 mCD	50%	1.9m
	-10.5 mCD	34%	5.2m
Medium	-6.2 mCD	39%	1.7m
	-10.5 mCD	32%	4.9m
Low	-6.2 mCD	35%	1.6m
	-10.5 mCD	31%	4.8m

Impacts of cyclones are assessed by calculating changes of percent filling of the channel and changes maximum sedimentation depths for cyclones Sidr and Amphan (Table 4.7).

Table 4.7: Effectiveness of dredging of the 70 km navigation channel of Payra port for different cyclone conditions

Flow Condition	Channel Depth	Change of Percent Filling due to Cyclone	Change of Maximum Depth due to Cyclone
Cyclone Sidr	-6.2 mCD	+28%	0.50m
	-10.5 mCD	+11%	0.90m
Cyclone Amphan	-6.2 mCD	+0.02%	No Change
	-10.5 mCD	No Change	No Change

Track, landfall location, and landfall time of cyclone Sidr was much favourable for sedimentation in the Payra port channel. This was not the case for cyclone Amphan. In terms of sedimentation depth, impact of cyclone is not very significant. We can see for cyclone Sidr maximum sedimentation depth of the -6.2mCD channel is 0.50m and for the -10.5mCD channel it is 0.90m (Table 4.7). But when we see the percent filling of the channel, we can see that due to cyclone Sidr, the extra filling of the channel varies between 11% - 28% (Table 4.7). This shows that although increase of sedimentation depth due to cyclone is not very significant, but its impact is uniformly distributed throughout the channel.

CHAPTER FIVE
Discussion and Conclusion

GBM delta has a complex integrated systems comprising inland river systems and its floodplains, coastal estuarine systems and associated coastal floodplains, wetlands, coastal and marine water bodies. Sediment management in this complex system should consider flow and sediment transport from the inland river systems, erosion-deposition in the inland rivers and floodplain, transport of these sediments in the estuaries and coastal floodplains, discharge of sediments to the ocean, deposition of sediment in marine environment, transport of sediment with the oceanic processes and re-entry of part of these sediments into the estuarine systems. A single integrated modeling framework is a pre-requisite to study water & sediment transport processes and sediment management options in GBM delta. In this study, an integrated modeling framework named Bangladesh Delta Model (BDM) is developed in Delft 3D numerical model background and applied to study sediment transport processes and sediment management options. Flow model of BDM is calibrated against time series measured data of the year 2017 in 29 water level stations (non-tidal and tidal), and morphology model is calibrated against measured time series data of the same year of suspended sediment concentration in 1 measuring station. Morphology model is also calibrated against satellite data of spatiotemporal suspended sediment concentration of 2017. The data domain of satellite images covers major rivers, the coast, and the ocean. The important feature of turbidity maximum zone in the ocean is well simulated by BDM. BDM is validated with measured water level (non-tidal and tidal) data for the year 2019 in 23 measuring stations. Flow model of BDM is also validated against areal extent of flood inundation for 1998 flood. Validation of morphology model of BDM is made by comparing model floodplain sedimentation depth with measurement from secondary data in 4 locations of Sundarban region.

BDM is applied to study the sediment transport processes in the GBM delta by using several proxy parameters. The entire processes of sediments entering in the system during fluvial flood, propagation within the river-estuary-floodplain systems, discharge into the ocean, re-entering into the system by the oceanic circulation, and deposition of these sediments on the delta floodplains are simulated with BDM. At the beginning of the ebb tide, BDM simulates a zone of stagnation which has significant impact on the sedimentation all along the estuary mouths in creating zone of turbidity maximum. It is found that the swatch of no ground acts like a separate channel on the ocean and due to this channel, sediments from the Lower Meghna system may be diverted and may not be able to directly deposit in the swatch of no ground. It is found that sediment concentration inside the swatch of no ground is very low during the normal tide condition. This condition may change during cyclones. Without cyclones, normal wind is found to have impacts on transport processes. South-westerly monsoon wind is observed to increase sediment flux mainly along Lower Meghna mouth. This is mainly due to large Meghna flow associated with wide estuary mouth. Wind impact of north-easterly wind is low except during cyclone times. The cyclone in this region creates a south-westerly current due to anticlockwise rotation of cyclone. This south-westerly current drives the sediments from the turbidity maximum region to the swatch of no ground and may be a probable cause of sediment accumulation inside the swatch of no ground.

But as cyclone is a short duration, season dependent but high intensity incident, cyclone generated sediment transport will not create a long-term impact on sedimentation in the region. When sediment concentration in the ocean is considered, it is found that high concentration sediments are confined within the continental shelf region. Deep ocean has very low sediment concentration. In the east coast, Lower Meghna sediments are dispersed till the Thailand coast and in the west coast, this dispersion is found all along the east coast of India. BDM simulation shows sediments from the Ganges-Brahmaputra-Meghna systems discharges into the Bay of Bengal through the Lower Meghna mouth, turn clockwise, part of the sediments deposit in the ocean and the rest of the sediments re-enter into the western estuarine systems. Sediment transport due to this re-circulation plays a dominant role in delta building process and accelerating sedimentation in the unprotected part of the delta.

Sedimentation in the floodplains is due to the inundation caused by monsoon flooding in the delta. During an extreme flood year with a return period of 200 years, the maximum inundated land area which is also the total floodplain area is found to be 27-29% of the total land area of the delta. When flood condition changes from average to extreme in intervened state of the delta, total sedimented area increases to 83% and sediment volume on the floodplain increases by 160%. In natural state, this increase is 84% for sedimented area and 183% for sediment volume on the floodplains. On the other hand, for the same flood condition (average or extreme), if physical state of delta changes from intervened state to natural state, the sedimented area increases by 18% (in average flood) to 19% (in extreme flood) and sediment volume on floodplains increase by 9% (in average flood) to 18% (in extreme flood). This shows that GBM delta in its present state (intervened state which is the present-day state of the delta) is sufficiently capable to accommodate increased sedimented area if sediment inflow to the system is increased. The sedimentation depths on the delta surface vary between 0.57mm/year to 9.85mm/year in intervened state and 0.69mm/year to 12.81mm/year in natural state. Considering magnitude of Relative Sea Level Rise (RSLR) of 5.0mm/year, it is found that the delta in intervened state (present state) is capable enough to combat against sea level rise. If the physical state of the delta is changed to natural state, the combat strength of the delta is increased. So, delta sustainability can be ensured by ensuring required sediment inflows from outside of the delta and by appropriate sediment management inside of the delta.

SC region plays an important role on overall sedimentation in the delta. The maximum inundation area which is also the sedimented area in SC region is 9% of the total land area. Depending on the flood condition and physical state of the delta, sediment retained on the SC region varies 21.4-27.3%, sediment volume varies 94-340 MT, and sedimentation depth varies 5.14-8.56mm. This shows that SC region plays an important role in determining delta sustainability.

In GBM delta, the widely practiced sediment management options in GBM delta are: TRM, cross-dam, and dredging. A sediment management practice can be termed effective when it can solve the local problem and at the same time can utilize the sediment resource for delta building process.

Cross-dams are constructed for land reclamation. Local impact of cross-dam is sedimentation in the cross-dam location. Both the local impact and extent of system level impacts (positive or

negative) of cross-dam depends on location, size, and number of cross-dams. Positive impacts of cross-dam are: (1) reclaim land in the cross-dam location where sediment concertation is high (2) increase river conveyance in other regions caused by reduced sediment supply due to trapped sediments in the cross-dam location. The negative impacts of cross-dam are (1) change the tidal amplitude in the influenced zone which may lead to a long-term hydro-morphodynamic change in the region (2) increases the inundation in the unprotected land close to the cross-dam (3) decreases sediment transport capacity in other regions which are within the influence zone of the cross-dam and causes unwanted sedimentation in those locations (4) reduces retained sediment volume and sedimentation depth on the delta surface and act against delta sustainability. In terms of effective use of sediment resource which will serve both local purpose and overall delta sustainability – cross-dam alone is not an effective sediment management practice.

Dredging is done to improve channel conveyance for navigational purposes, to reduce flood extent, and to guide the river to an expected course. Dredging reduces the transport capacity in the dredged section. As inflow sediments remain the same, decreased sediment transport capacity causes rapid sedimentation in the dredged section. The sedimentation rate in the dredged section depends on the sediment flux of the river where dredging is performed. Dredging reduces inundation in the floodplain due to increased conveyance of dredged section and the sediments which were supposed to be deposited over those floodplains are transported to the downstream reaches. Positive impacts of dredging include (1) increased conveyance of the dredged zone (2) reduced inundation depth within the influence zone of the dredged reach (3) dredging in the upstream rivers increases sediment volume and sedimentation depths in the coastal floodplains and thus contribute to the delta building processes. Negative impacts of dredging are (1) dredged sections are quickly filled up (2) increased inundation in the downstream reaches of the dredged section (3) dredging in the upstream river reaches decreases sediment volume and sedimentation depths in non-tidal floodplains. Calculating the trade-off between positive impact and negative impact of dredging shows that dredging is an effective sediment management practice provided dredging sections are selected by considering both local impact and system impacts. When Hari River dredging is considered to reduce waterlogging problem in the south-west region, it is found that controlled flooding is a better option for Hari River, because this will cause decrease of inundation and increase of sedimentation depth on the floodplains. But dredging decreases the sedimentation depth along with decreased inundation. When dredging of Payra port navigation channel is considered, it is found that sedimentation depth is higher for the deeper channel compared to shallow channel. Higher inflow sediments from upstream fills the channel quickly. The channel filling rate for the shallow channel varies 35% - 50% with sedimentation depths 1.6m – 1.9m. For deeper channel, these values are 31% - 34% and 4.8m – 5.2m. There is a visible impact of cyclone when sedimentation of the channel is considered. Strong, post-monsoon cyclone which makes landfall on the left side of the channel creates the maximum impact. Depending on the dredged channel depth, a strong cyclone can cause extra filling of the channel by 11% - 28% with sedimentation depths 0.50m – 0.90m.

The delta in intervened state (present state) is capable enough to combat against sea level rise. If the physical state of the delta is changed to near natural state, the combat strength of the delta is increased. Delta sustainability can be ensured by ensuring required sediment inflows from outside of the delta (through transboundary negotiation) and by appropriate sediment management inside of the delta. SC regions plays an important role on overall delta sedimentation. Any intervention on SC region that restricts sedimentation in SC region will seriously affect the delta sustainability. In terms of effective use of sediment resource which will serve both local purpose and overall delta sustainability – cross-dam alone is not an effective sediment management practice. Dredging is an effective sediment management practice provided dredging sections are selected by considering both local impact and system impacts. A combination of cross-dam and dredging in appropriate locations of the delta may be a better option to solve the both the local problems and ensure delta sustainability, but this needs further study.

References

Adnan M.S.G., R. Talchabhadel, H. Nakagawa, et al. (2018), How much of the south western delta of Bangladesh can be restored with Tidal River Management (TRM)?, Science of the Total Environment (2018), https://doi.org/10.1016/ j.scitotenv.2020.138747.

Ahsan Quamrul and Anisul Haque (2020), Dead Zone in the Bay of Bengal, The Financial Express, November 14 2020, Published online https://thefinancialexpress.com.bd/views/dead-zone-in-the-bay-of-bengal-1605365324

Angamuthu B, Darby SE, Nicholls RJ. (2018), Impacts of natural and human drivers on the multi-decadal morphological evolution of tidally-influenced deltas. Proc. R. Soc.A 474: 20180396. http://dx.doi.org/10.1098/rspa.2018.0396

Akter Jakia, Dano Roelvink, Mick van der Wegen (2021), Process-based modeling deriving a long-term sediment budget for the Ganges-Brahmaputra-Meghna Delta, Bangladesh, Estuarine, Coastal and Shelf Science 260 (2021) 107509, https://doi.org/10.1016/j.ecss.2021.107509.

Akter, R., Asik, T.Z., Sakib, M., Akter, M., Sakib,. M.N., Al Azad, A.S.M., Maruf, M., Haque, A. and Rahman, M. (2019), The dominant climate change event for salinity intrusion in the GBM delta, Climate, 2019, 7, 69, doi: 10.3390 / cli7050069, https://www.mdpi.com/2225-1154/7/5/69/pdf

Al Azad, A.S.M.A., Mita, K.S., Zaman, M.W., Akter, M., Asik, T.Z., Haque, A., Hussain, M.A., Rahman, M.M. (2018), Impact of tidal phase on inundation and thrust force due to storm surge, Journal of Marine Science and Engineering, 2018, 6, 110; doi:10.3390/jmse6040110.

Al Masud, M. M., & Islam, A. K. A. M. S. (2018). The Challenges of Sediment Management in Tidal Basin: Application of Indigenous Knowledge for Tidal River Management in the Southwest Coastal Bangladesh.

Alim Md. Samiul, Chowdhury Quamruzzaman, Md. Momenur Rahim, Md. Khairul Bashar Swapan, Mohammad Tofael Ahmed & A S Daiyan Ahmed (2016), Dredging Design and Estimation of Annual Net Growth of Paturia-Daulatdia Ferry Ghat, Bangladesh, International Journal of Scientific & Engineering Research, Volume 7, Issue 5, May-2016, ISSN 2229-5518.

Amir, S.I.I., et al., (2013). River Sediment Management–A Case Study in Southwestern Bangladesh, International Journal of Geological and Environmental Engineering, Vol.7 (3), pp 175-184, 2013.

Becker et al., (2020). Water level changes, subsidence, and sea level rise in the Ganges–Brahmaputra–Meghna delta, 117 (4) 1867-1876; first published January 6, 2020; https://doi.org/10.1073/pnas.1912921117.

Bennett, V. C., Mulligan, R. P., & Hapke, C. J. (2018). A numerical model investigation of the impacts of Hurricane Sandy on water level variability in Great South Bay, New York. *Continental Shelf Research, 161*, 1-11.

Brown, S. and Nicholls, R.J. (2015). Subsidence and human influences in mega deltas: the case of the Ganges–Brahmaputra–Meghna. Science of the Total Environment, 527, pp.362-374.

BWDB (2011), Bangladesher Nod Nodi, BWDB, August 2011.

BWDB (1998), Annual flood report. Flood Forecasting and Warning Centre.

Coleman, J. M. (1969). Brahmaputra River: channel processes and sedimentation. Sedimentary geology, 3(2-3), 129-239.

del Ninno Carlo, Paul A. Dorosh, Lisa C. Smith, and Dilip K. Roy (2001), The 1998 floods in Bangladesh : disaster impacts, household coping strategies, and response, International Food Policy Research Institute, HV610 1998.B3 A19, WASHINGTON, D.C.

Dietrich M., K.B. Best, J.L. Raff, et al. (2020), A first-order geochemical budget for suspended sediment discharge to the Bay of Bengal from the Ganges-Brahmaputra river system, Science of the Total Environment (2020), https://doi.org/10.1016/j.scitotenv.2020.138667
Duda PB, Hummel PR, Donigian Jr AS, Imhoff JC (2012), BASINS/HSPF: Model use, calibration, and validation. Trans ASABE 55:1523–1547.

Duti Bushra Monowar, M. Monowar Hossain, Fahad Khan Khadim, Ahmmed Zulfiqar Rahaman, and D. A. Quadir (2017), Mapping Floods in Bangladesh using Satellite Data: An Overview, The Journal of NOAMI, 34(1): 57-68 (June 2017).

EDP (2007), Estuary Development Programme, Technical Note EDP-01, DHV-Haskoning, May 2007.

Gain Animesh K., Md. Ashik-Ur-Rahman, David Benson (2019), Exploring institutional structures for Tidal River Management in the Ganges-Brahmaputra Delta in Bangladesh**,** Journal of the Geographical Society of Berlin**,** Vol. 150, No. 3, Research article.

Gain Animesh K., David Bensonb, Rezaur Rahmanc, Dilip Kumar Dattad, Josselin J. Rouillarde (2017), Tidal river management in the south west Ganges-Brahmaputra delta in Bangladesh: Moving towards a transdisciplinary approach? Environmental Science and Policy 75 (2017) 111–120, http://dx.doi.org/10.1016/j.envsci.2017.05.020.

Goodbred, S.L. and Kuehl, S.A., (2000), The significant of large sediment supply, active tectonism, and estuary on margin sequence development: Late Quaternary stratigraphy and evolution of the Ganges-Brahmaputra delta, Sediment. Geol, 133, 227-248.

Hale Richard , Rachel Bain , Steven Goodbred Jr. , and Jim Best (2019), Observations and scaling of tidal mass transport across the lower Ganges–Brahmaputra delta plain: implications for delta

management and sustainability, Earth Surf. Dynam., 7, 231–245, 2019, https://doi.org/10.5194/esurf-7-231-2019.

Haque, A**.,** Sumaiya and Rahman, M.M. (2016), Flow distribution and sediment transport mechanism in the estuarine systems of Ganges-Brahmaputra-Meghna delta, International Journal of Environmental Science and Development, Vol.7, No.1, January 2016.

Haque, A., and Nichols, R.J. (2018). Floods and the Ganges-Brahmaputra-Meghna delta, Ecosystem Services for Well-Being in Deltas, R. J. Nicholls et al. (eds.), Palgrave Macmillan, UK, London, Springer Nature, https://doi.org/10.1007/978-3-319-71093-8_8.

Haque, A., Kay, S. and Nichols, R.J. (2018), Present and future fluvial, tidal and storm surge flooding in coastal Bangladesh, Ecosystem Services for Well-Being in Deltas, R. J. Nicholls et al. (eds.), Palgrave Macmillan, UK, London, Springer Nature, https://doi.org/10.1007/978-3-319-71093-8_8.

Hu, K., Chen, Q., Wang, H., Hartig, E. K., & Orton, P. M. (2018). Numerical modeling of salt marsh morphological change induced by Hurricane Sandy. *Coastal Engineering*, *132*, 63-81.

Hussain, N., Islam, M. H., & Firdaus, F. (2018). Impact of Tidal River Management (TRM) for Water Logging: A Geospatial Case Study on Coastal Zone of Bangladesh. Journal of Geoscience and Environment Protection, 6, 122-132.

Islam Md Feroz, Hans Middelkoop, Paul P. Schot, Stefan C. Dekker, Jasper Griffioen (2021a), Spatial and seasonal variability of sediment accumulation potential through controlled flooding of the beels located in the polders of the Ganges-Brahmaputra-Meghna delta of Southwest Bangladesh, Hydrological Processes. 2021;35:e14119, https://doi.org/10.1002/hyp.14119.

Islam Md Feroz, Paul P. Schot, Stefan C. Dekker, Jasper Griffioen and Hans Middelkoop (2021b), Physical controls and a priori estimation of raising land surface elevation across the southwestern Bangladesh delta using Tidal River Management, Hydrology and Earth System Science, https://doi.org/10.5194/hess-2021-300.

Islam Md Feroz, Hans Middelkoop, Paul P. Schot, Stefan C. Dekker, Jasper Griffioena (2020), Enhancing effectiveness of tidal river management in southwest Bangladesh polders by improving sedimentation and shortening inundation time, Journal of Hydrology 590 (2020) 125228.

IWM (2009), Use Existing Data on Available Digital Elevation Models to Prepare Useable Tsunami and Storm Surge Inundation Risk Maps for the Entire Coastal Region, Volume-II: DEM, Landuse and Geo-morphology Maps. Institute of Water Modelling & Bangladesh Institute of Social Research, April 2009.

Jakobsen F., M. H. Azam and M. Mahboob-ul-Kabir (2002), Residual Flow in the Meghna Estuary on the Coastline of Bangladesh, Estuarine, Coastal and Shelf Science (2002) 55, 587–597, doi:10.1006/ecss.2001.0929, available online at http://www.idealibrary.com

Karim Rezaul, Rakhee Mondal (2017), Local Stakeholder Analysis of Tidal River Management (TRM) at Beel Kapalia and the Implication of TRM as a Disaster Management Approach, Hydrology. Vol. 5, No. 1, 2017, pp. 1-6. doi: 10.11648/j.hyd.20170501.11.

Khadim Fahad Khan, Kanak Kanti Kar, Pronab Kumar Halder, Md. Atiqur Rahman, A.K.M. Mostafa Morshed (2013), Integrated Water Resources Management (IWRM) Impacts in South West Coastal Zone of Bangladesh and Fact-Finding on Tidal River Management (TRM), Journal of Water Resource and Protection, 2013, 5, 953-961, http://dx.doi.org/10.4236/jwarp.2013.510098.

Kudrass Hermann R, Björn Machalett, Luisa Palamenghi, Inka Meyer, Wenyan Zhang (2018), Sediment transport by tropical cyclones recorded in a submarine canyon off Bangladesh, Geo-Marine Letters (2018) 38:481–496, https://doi.org/10.1007/s00367-018-0550-x.

Li, X., Plater, A., & Leonardi, N. (2018). Modelling the transport and export of sediments in macrotidal estuaries with eroding salt marsh. *Estuaries and coasts*, *41*(6), 1551-1564.

Milliman, J. D. (1991). Flux and fate of fluvial sediment and water in coastal seas. RFC Mantoura, 69-89.

Moriasi DN, Arnold JG, Van Liew MW, et al (2007), Model evaluation guidelines for systematic quantification of accuracy in watershed simulations. Trans ASABE 50:885–900. https://doi.org/10.13031/2013.23153.

Musfequzzaman Md., Md. Abdul Matin and Fahmida Noor (2016), River response in the selected reach of Jamuna river due to dredging, Tech. J. River Res. Inst. 13(1): 102-110, 2016 (October), ISSN: 1606-9277.

Brown S. and R.J. Nicholls (2015), Subsidence and human influences in mega deltas: The case of the Ganges–Brahmaputra–Meghna, Science of the Total Environment 527–528 (2015) 362–374.

Nicholls, R.J., Hutton, C.W., Adger, W.N., Hanson, S.E., Rahman, M.M. and Salehin, M. (2018), Integrative Analysis for the Ganges-Brahmaputra-Meghna Delta, Bangladesh. In *Ecosystem Services for Well-Being in Deltas* (pp. 71-90). Palgrave Macmillan, Cham.

Rahman Afeefa, Anika Yunus (2016), Hydrodynamic and Morphological Response to Dredging: Analysis on Gorai River of Bangladesh, International Journal of Innovative Research in Science, Engineering and Technology, Vol. 5, Issue 8, August 2016.

Rahman, M., Dustegir, M., Karim, R., Haque, A., Nichols, R.J., Darby, S.E., Nakagawa, H., Hossain, M., Dunn, F.E. and Akter, M. (2018), Recent sediment flux to the Ganges-BrahmaputraMeghna delta system, Science of the Total Environment 643 (2018) 1054–1064, https://doi.org/10.1016/j.scitotenv.2018.06.147.

Rahaman Md Hafijur Khan, Jianguo Liu, Shengfa Liu, Jingrui Li, Li Cao, and Ananna Rahman (2020), Anthropogenic effect on heavy metal contents in surface sediments of the Bengal Basin

river system, Bangladesh, Environmental Science and Pollution Research (2020) 27:19688–19702 https://doi.org/10.1007/s11356-020-08470-4.

Rahman Md Mosiur, Md Sazadul Hasan, Moniruzzaman Khan Eusufzai, Md Munsur Rahman (2021), Impacts of Dredging on Fluvial Geomorphology in the Jamuna River, Bangladesh, Journal of Geoscience and Environment Protection, 2021, 9, 1-20, https://www.scirp.org/journal/gep

Rahim Md. Momenur, Chowdhury Quamruzzaman, Md. Samiul Alim, Khairul Bashar Swapan, Mohammad Tofael Ahmed, Sadia Gazi Antora, Md. Badrul Alam (2016), Proposal for Dredging of a Ferry Route in Mawa-Kaorakandi with Proper Protection System Due to Sedimentation, International Journal of Emerging Technology and Advanced Engineering, Volume 6, Issue 7, July 2016.

Rogers, K.G., Goodbred Jr, S.L. and Mondal, D.R. (2013), Monsoon sedimentation on the 'abandoned' tide-influenced Ganges–Brahmaputra delta plain. Estuarine, Coastal and Shelf Science, 131, pp.297-309.

Rogers, K. and Overeem, I. (2017), Doomed to drown? sediment dynamics in the human-controlled floodplains of the active Bengal Delta. Elementa Science of the Anthropocene, 5(65).

Salehi, M. (2018). Storm surge and wave impact of low-probability hurricanes on the lower delaware bay—Calibration and application. *Journal of Marine Science and Engineering*, *6*(2), 54.

Sandbach, S. D., Nicholas, A. P., Ashworth, P. J., Best, J. L., Keevil, C. E., Parsons, D. R., & Simpson, C. J. (2018). Hydrodynamic modelling of tidal-fluvial flows in a large river estuary. *Estuarine, Coastal and Shelf Science*, *212*, 176-188.

Sarker Maminul Haque, Jakia Akter, Md Ruknul Ferdous & Fahmida Noor (2011), Sediment dispersal processes and management in coping with climate change in the Meghna Estuary, Bangladesh, IAHS Publ. 349, 2011.

Seijgera Chris, Dilip Kumar Dattab, Wim Douvena, Gerardo van Halsemac and Malik Fida Khand (2019), Rethinking sediments, tidal rivers and delta livelihoods: tidal river management as a strategic innovation in Bangladesh, Water Policy 21 (2019) 108–126.

Sridevi B. and Sharma VVSS (2020), A revisit to the regulation of oxygen minimum zone in the Bay of Bengal, J. Earth Syst. Sci. (2020)129 107, Academy of Sciences https://doi.org/10.1007/s12040-020-1376-2.

Talchabhadel Rocky, Hajime Nakagawa, and Kenji Kawaike (2018), Sediment management in tidal river: A case study of East Beel Khuksia, Bangladesh, E3S Web of Conferences 40, 02050 (2018), River Flow 2018, https://doi.org/10.1051/e3sconf/20184002050.

Thanh, V. Q., Reyns, J., Van, S. P., Anh, D. T., Dang, T. D., & Roelvink, D. (2019). Sediment transport and morphodynamical modeling on the estuaries and coastal zone of the Vietnamese Mekong Delta. *Continental Shelf Research*, *186*, 64-76.

WARPO and IWM, (2016), Sediment Transport in Rivers, Technical Report Volume 4, Comprehensive report on Assessment of State of Water Resources: Sediment Transport in Rivers (4.8s). WARPO, Ministry of Water Resources.

WARPO and BUET (2019), Research on the Morphological processes under Climate Changes, Sea Level Rise and Anthropogenic Intervention in the Coastal Zone, Final Report, IWFM, BUET, March 2019.

Zhong-hua Tan, Chen Han-bao, Xu Ya-nan, Guan Ning (2021), Analysis of hydrodynamics and sediment conditions around East Coast Sea Area in Bay of Bengal, IOP Conf. Ser.: Earth Environ. Sci. 621 012081.

APPENDIX

Sediment Management Manual for the GBM Delta

Introduction

This manual on sediment management is prepared based on the results of the study which are presented in the main report. Like other similar manual (Xiaoqing, 2003), the structure of this manual is different. There are no generalized sediment transport equations nor any generalized method of sediment management in this manual. This manual is applicable only for the GBM delta. User of this manual will get the idea of sediment transport processes and will have some quantification on sedimentation for the GBM delta. This will be helpful to have a pre-assessment about the possible impacts of implementation of sediment management options. The two sediment management options considered in this manual is – cross-dam and dredging.

Sediment Inflow in the Delta

Total sediment inflows in the GBM delta varies between 400 MT to 1200 MT. Once entered the river systems, these sediments ultimately transport to the ocean after depositing/eroding in the river-estuary-floodplain systems. The clockwise oceanic circulation of these sediments causes re-entry of sediments through the mouths of large number of western estuaries in the south-west region. This circulation is impacted by frequent cyclones in the region and may drive these sediments inside the swatch of no ground. Polders in the coastal area restricts the floodplain deposition inside the poldered area causing the reduced elevation of land in these areas compared to riverbed level which ultimately results waterlogging. However, there is enough potential of existing sedimentation on the delta surface to combat against waterlogging, subsidence, and sea level rise.

Sediment Transport with Fluvial Flow

During the dry season, there is almost no sediment supply from the upstream systems. Rising stage of flood in the delta is generally June. During the rising stage of flood, sediment laden water starts to enter from the inflow river systems inside the delta. The eastern haor system is normally flooded before June. This system is not flooded with the major river systems which carry the bulk volume of sediment inflows. During peak monsoon, the delta floodplains are inundated. This flood water transports the sediments in the entire river-estuary-floodplain systems. The inundation in the coastal zone is caused by compound flooding driven by fluvial and tidal processes. Inundation in the coastal zone starts during the peak monsoon season and continues till the recession stage. So, fluvial sediments start to transport in the coastal zone from the peak monsoon. The sediments which enter the floodplains during the peak flood starts to deposit on the floodplain during the recession stage. Marine sediments are normally transported to the coastal zone (mainly in the Sundarban region) during the recession stage of the flood and during early dry season when sediments from the ‘turbidity maximum’ zone re-enters into the system by oceanic re-circulation through the estuary mouths. Flooding in the monsoon also cause erosion in the sedimented part of the delta surface mainly due to the high flow velocity during the recession phase of the flood when sediment concentration in the flood water decreases. Erosion also occurs in the coastal region during the ebb phase of the tide in the dry season when tidal range increases due to decreased upstream flow.

Sediment Transport with Tidal Flow

Tide is a regular phenomenon with short term (daily) and long term (fortnightly and above) variability. Sediments after discharged into the ocean from the riverine-estuarine systems encounter this tide. The oceanic phase of the sediment transport and overall sedimentation in the delta is affected by the tides. High tide generated in the deep ocean propagates all along the Bay of Bengal and reaches to west and east coast almost at the same time. At the time when high tide reaches the coast, low tide starts its journey and eventually reaches the coast. The process repeats itself to generate daily variation of tide. Tides arrive almost at the same time along the west and east coasts. Flood tide current slows down along the Lower Meghna estuary due to the impact of freshwater. Relatively higher current along the mouth of the estuaries of the western coast during the flood tide causes ocean sediments to enter inside the western estuarine systems. Sources of these ocean sediments are Lower Meghna estuary which propagates along the continental shelf during the ebb tide and later re-enter into the system during the flood tide. Just at the beginning of the ebb tide in the ocean, there is a flow disaggregation line, and a zone of stagnation occurs. This zone has significant impact on the sedimentation all along the estuary mouths in creating zone of turbidity maximum.

Impacts of Wind on Sediment Transport

In the Bay of Bengal, south-westerly monsoon wind blows with a speed of 4-5 m/s during June to September, and north-easterly wind of 1.5-3 m/s blows during December to February. South-westerly wind increases the tidal current during the flood phase of the tide which increases the sediment flux along the coast. Wind impact is visible along the Lower Meghna mouth, but not along the other locations of the coast. In this region, the normal wind direction in November is north-easterly which means towards the ocean. So, this wind creates flux in a direction away from the coast and will not drive additional sediments to enter in the estuary. Wind speed during this time of the year is low compared to south-westerly monsoon wind.

Impacts of Cyclone on Sediment Transport

Cyclone wind speed is several times stronger than the normal wind speed, is always directed toward the coast, and accordingly increase the volume of sediment flux toward the coast. Cyclonic wind suddenly increases the flood flow velocity (hydrodynamic shock) compared to without cyclone scenario. As sediment flux is related to water velocity, increased water velocity creates increased sediment flux for the same sediment concentration. So, for a similar sediment regime, cyclonic event creates increased sediment flux. This will drive increased volume of sediments to re-enter into the estuarine systems through increased flood flow velocity created by cyclone. The cyclone in this region creates a south-westerly current due to anticlockwise rotation of cyclone. This south-westerly current will drive the sediments from the turbidity maximum region to the swatch of no ground and may be a probable cause of sediment accumulation inside the swatch of no ground. The location and amount of sediment flux depends on the cyclone landfall location, cyclone time (pre- or post-monsoon), and cyclone strength. As cyclone is a short duration, season dependent but high intensity incident, cyclone generated sediment transport will not create a long-term impact on sedimentation in the region.

Sediment Dispersion in the Ocean

High concentration sediments are confined within the continental shelf. Sediments from the Lower Meghna estuary is mainly distributed within this zone. Deep ocean has very low sediment concentration. This means that sediment concentration in the deep ocean is low. In between the high sediment concentration zone and low sediment concentration, there is a narrow middle zone with medium sediment concentration where transition between high and low sediment concentration occurs. In the east coast, sediments from Lower Meghna propagates a long distance up to the coast of Thailand. In the west coast, sediments are propagated along the east coast of India.

Sediments in the Swatch of No Ground

Vertical distribution of sediment concentration close to the coast shows that high sediment concentration is confined within the first 50m depth of the ocean from MSL of the ocean surface. Deeper part of the swatch of no ground is within low sediment concentration zone. This shows in normal tidal environment (not cyclonic condition), sediments from either the eastern or the western oceanic circulations do not enter deep into the submarine canyon.

Sediment Re-circulation in the Ocean

The sediment movement path shows that the sediments from the Ganges-Brahmaputra-Meghna systems discharges into the Bay of Bengal through the Lower Meghna mouth, turn clockwise, part of the sediments deposit in the ocean and the rest of the sediments re-enter into the western estuarine systems. On the swatch of no ground sediment movement path is deflected and by-passed the swatch of no ground region. This shows that in normal tide condition, sediments from the Lower Meghna system may not be directly depositing inside the canyon. This situation will prevail for tide & wind condition also but may change during tide & cyclone condition depending on the cyclone track and strength. The driving force behind this recirculation is fluvial flow from upstream rivers, tide in the ocean, and Coriolis force due to earth rotation. Wind (normal wind and cyclonic wind) creates an additional force behind this re-circulation. In terms of sedimentation in the GBM delta, this re-circulation plays a very important role. Most of the sediments in the western estuarine systems and its related floodplains are re-entering into the system due to this re-circulation. The upstream freshwater connectivity of these systems is severely restricted due to flow reduction in Ganges during dry season as a result of Farakka barrage in the Indian part of the delta. This re-circulation drives the sediments to the western system from the turbidity maximum zone in the Lower Meghna Estuary. Sediment transport due to this re-circulation plays a dominant role in delta building process and accelerating sedimentation in the unprotected part of the delta.

Flooding in the Delta

Flooding in the delta brings the sediments on the floodplains and thus cause floodplain sedimentation. During an extreme flood condition, 27% - 29% of the delta surface is inundated with respect to total land area of the delta. Out of 7 hydrological regions, maximum land inundation of 9% occurs in the south-west region in the coast. BWDB reported ‘two-third of the country is

flooded during extreme flood' considers all the riverine and rainfall generated flooded land, rivers, estuaries, haors, and all other wetlands.

Floodplain Sedimentation

Floodplain sedimentation on the delta surface is an important determinant of delta sustainability against sea level rise and offsetting waterlogging created due to polders. Floodplain sedimentation is quantified for two flood conditions and two physical states of the delta. The two flood conditions are – average flood and extreme flood. Average flood is the flood with a return period of 2.33 years and extreme flood is the flood with 200 years return period. The two physical state of the delta are – intervened state and natural state. Intervened state is defined as the physical state when the delta is in its present-day condition. Natural state is defined as the physical state when all polders from the coastal region is removed from the system but other embankments in the non-tidal part of the delta remain. Following tables (Tables 1-6) give some quantifications about sedimentation on GBM delta floodplains. These tables are useful for any sediment management practices in the delta.

Yearly distribution of sediments in intervened state for average flood and extreme flood conditions are shown in Table 1:

Table 1: Yearly distribution of sedimentations in intervened state for average flood and extreme flood conditions

Total Sediment Distribution in Intervened State					
Flood Condition	Total Inflow Sediments (Million Ton)	Total Delta Floodplain Sedimentation (Million Ton)	Coastal Floodplain Sedimentation (Million Ton)	Percent Retained in Total Delta Floodplains	Percent Retained in Coastal Floodplain
Average	400	315	192	79%	48%
Extreme	1243	820	517	66%	42%

Regional Sediment Distribution in Intervened State						
Region	Sedimentation Thickness (mm)		Sedimentation Volume (Million Ton)		Percentage of Sedimentation Volume w.r.t Total Inflow Sediments	
	Average	Extreme	Average	Extreme	Average	Extreme
NW	3.75	5.34	63	118	15.7%	9.5%
NC	5.87	7.19	51	144	12.8%	11.6%
NE	0.57	1.72	1	12	0.3%	1.0%
SW	5.53	5.87	81	189	20.2%	15.2%
SC	6.01	8.56	94	311	23.6%	25.0%
SE	8.31	2.86	17	17	4.1%	1.4%
EHT	4.84	9.85	8	29	1.9%	2.3%

[*] *Average Relative Sea Level Rise = 5.0mm / year (Brown and Nicholls, 2015; Becker et al., 2020)*

Yearly distribution of sediments in natural state for average flood and extreme flood conditions are shown in Table 2:

Table 2: Yearly distribution of sedimentations in natural state for average flood and extreme flood conditions

Total Sediment Distribution in Natural State					
Flood Condition	Total Inflow Sediments (Million Ton)	Total Delta Floodplain Sedimentation (Million Ton)	Coastal Floodplain Sedimentation (Million Ton)	Percent Retained in Total Delta Floodplains	Percent Retained in Coastal Floodplain
Average	400	342	214	86%	54%
Extreme	1243	967	626	78%	50%

Regional Sediment Distribution in Natural State						
Region	Sedimentation Thickness (mm)		Sedimentation Volume (Million Ton)		Percentage of Sedimentation Volume w.r.t Total Inflow Sediments	
	Average	Extreme	Average	Extreme	Average	Extreme
NW	3.74	5.28	63	118	15.7%	9.4%
NC	5.74	7.21	50	143	12.4%	11.5%
NE	0.59	1.79	1	12	0.3%	1.0%
SW	5.49	5.87	109	261	27.3%	21.0%
SC	5.14	8.25	85	340	21.4%	27.3%
SE	7.14	4.57	20	25	5.1%	2.0%
EHT	3.63	12.81	14	68	3.4%	5.5%

[*] *Average Relative Sea Level Rise = 5.0mm / year (Brown and Nicholls, 2015; Becker et al., 2020)*

Sedimented area for different flood conditions and different delta states are shown in Table 3:

Table 3: Sedimented area for different flood conditions and different delta states.

	Sedimented area of the entire delta (km^2)			Sedimented area in the coastal zone (km^2)		
Flood Condition	Intervened State	Natural State	Increase for physical state	Intervened State	Natural State	Increase for physical state
Average	12,620	14,914	18%	6,310	8,232	30%
Extreme	23,120	27,365	19%	12,139	15,863	31%
Increase for flood condition	83%	84%		92%	93%	

Changes in sedimentation depths for different flood conditions and different states of the delta are shown in Table 4. Changes in sedimented area and sedimentation depths for different flood conditions and different physical states of the delta is shown in Table 5.

Table 4: Change in sedimentation depth due to change in flood condition and delta physical state.

	Change in sedimentation depth due to change in flood condition from average to extreme (+ve for increase, -ve for decrease)		Change in sedimentation depth due to change in physical state of the system from intervened to natural (+ve for increase, -ve for decrease)	
Region	Intervened (mm)	Natural (mm)	Average (mm)	Extreme (mm)
NW	+1.59	+1.54	-0.01	-0.06
NC	+1.32	+1.47	-0.13	+0.02
NE	+1.15	+1.20	+0.02	+0.07
SW	+0.34	+0.38	-0.04	0.00
SC	+2.55	+3.11	-0.87	-0.31
SE	-5.45	-2.57	-1.14	+1.71
EHT	+5.01	+9.18	-1.21	+2.96
Average Sedimentation	+0.93	+2.04	-0.48	+0.63

**Average Relative Sea Level Rise = 5.0mm / year (Brown and Nicholls, 2015; Becker et al., 2020)*

Table 5: Changes in sedimented area and sedimentation depth due to changes in flood condition and physical state of the system.

	Intervened State			Natural State		
Sediment Inflow (MT)	Average	400	Increase by 210%	Average	400	Increase by 210%
	Extreme	1,243		Extreme	1,243	
Sedimented area on the floodplains (km2)	Average	12,620	Increase by 83%	Average	14,914	Increase by 84%
	Extreme	23,120		Extreme	27,365	
Sediment volume on the floodplains (MT)	Average	315	Increase by 160%	Average	342	Increase by 183%
	Extreme	820		Extreme	967	
Sedimentation depth in non-tidal floodplains (mm)	Average	0.57–8.31	Increase by 1.15-1.54	Average	0.59–5.74	Increase by 4.28-7.07
	Extreme	1.72–9.85		Extreme	4.87–12.81	

**Average Relative Sea Level Rise = 5.0mm / year (Brown and Nicholls, 2015; Becker et al., 2020)*

SC region of the coast plays an important role on delta sustainability. Table 6 shows percent of sediment retained, sedimentation volume, and sedimentation depth in SC region.

Table 6: percent of sediment retained, sedimentation volume, and sedimentation depth in SC region.

	Intervened		Natural	
Sediment retained on the floodplain	Average	23.6%	Average*	21.4%
	Extreme	25.0%	Extreme	27.3%
Sedimentation volume	Average	94 MT	Average*	85 MT
	Extreme	311 MT	Extreme	340 MT
Sedimentation depth in tidal floodplains	Average	6.01 mm	Average*	5.14 mm
	Extreme	8.56 mm	Extreme*	8.25 mm

**The decrease is due to dispersion of sediments in a wider area of sedimentation when the state of the system is changed from intervened state to natural state.*

Sediment Management Practices in the GBM Delta

Present sediment management practices in the GBM delta are (1) TRM (2) Cross-dam and (3) Dredging. The purpose of a sediment management practice is usually to solve a local problem. But we can term a sediment management practice as an effective option when it can solve the local problem and at the same time, can ensure the best use of sediment resources for delta building process and contribute to delta sustainability.

Cross-dam as a Sediment Management Practice

Cross-dam is used for land reclamation in the off-shore region of the delta. Cross-dam reduces the tidal range close to the cross-dam location. Reduced sediment supply from the cross-dam location (due to trapped sediments by cross-dam) cause riverbed erosion in other location of the delta which receives these sediments. Cross-dam increases the flood inundation close to the cross-dam location. Cross-dam decreases sediment transport capacity in other regions which are within the influence zone of the cross-dam and causes unwanted sedimentation in those locations. In terms of effective use of sediment resource which will serve both local purpose and overall delta sustainability – cross-dam alone is not an effective sediment management practice.

Impacts of EDP (2007) proposed 13 cross-dams on delta sedimentation are presented in Table 7 and comparison with these 13 cross-dams with BWDB planned Urir Char cross-dam is presented

in Table 8. These two tables can be consulted before implementing any cross-dam project within the GBM delta. Locations of the 13 cross-dams and Urir Char cross-dam is shown in Figure 1.

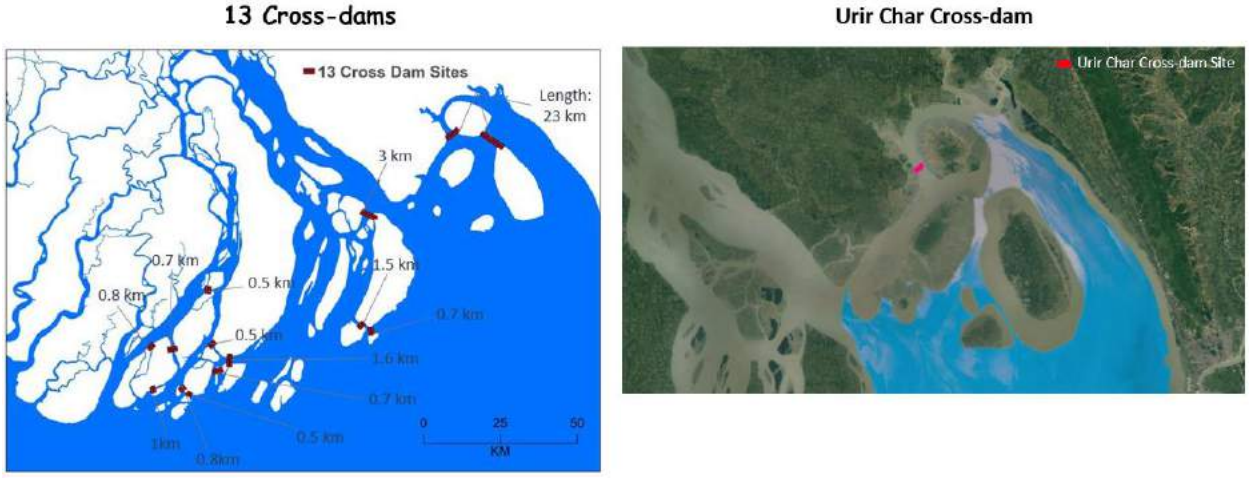

Figure 1: Locations of EDP proposed 13 cross-dams and BWDB planned Urir Char cross-dam sites. Tables 7 and 8 are prepared based on the cross-dams in these locations.

Table 7: Yearly distribution of change of sedimentation in GBM delta due to construction of 13 cross-dams.

Change in Total Sediment Distribution					
Flood Condition	Change in Inflow Sediments (Million Ton)	Change in Delta Floodplain Sedimentation (Million Ton)	Change in Coastal Floodplain Sedimentation (Million Ton)	Change in Percent Retained in Total Delta Floodplains	Change in Percent Retained in Coastal Floodplain
Extreme	No Change	-4	-4	-0.4%	-0.4%
Change in Regional Sediment Distribution					
Region	Change in Sedimentation Depth (mm)	Change in Sedimentation Volume (Million Ton)		Change in Percentage of Sedimentation Volume w.r.t Total Inflow Sediments	
NW	No Change	No Change		No Change	
NC	No Change	No Change		No Change	
NE	No Change	No Change		No Change	
SW	No Change	No Change		No Change	
SC	-0.26	-9		-0.70%	
SE	+0.64	+2		+0.10%	
EHT	-0.15	+3		+0.20%	

Table 8: Comparison of change of sedimentation in GBM delta between 13 cross-dams and Urir Char cross-dam.

Comparison of Change in Total Sediment Distribution						
Flood Condition	Change in Inflow Sediments (Million Ton)	13 Cross-dam Change in Delta Floodplain Sedimentation (Million Ton)		Urir Char Cross-dam Change in Delta Floodplain Sedimentation (Million Ton)	13 Cross-dam Change in Percent Retained in Total Delta Floodplains	Urir Char Cross-dam Change in Percent Retained in Total Delta Floodplains
Extreme	No Change	-4		-0.1	-0.4%	-0.008%
Comparison of Change in Regional Sediment Distribution						
Region	13 Cross-dam Change in Sedimentation Depth (mm)	Urir Char Cross-dam Change in Sedimentation Depth (mm)	13 Cross-dam Change in Sedimentation Volume (Million Ton)	Urir Char Cross-dam Change in Sedimentation Volume (Million Ton)	13 Cross-dam Change in Percentage of Sedimentation Volume w.r.t Total Inflow Sediments	Urir Char Cross-dam Change in Percentage of Sedimentation Volume w.r.t Total Inflow Sediments
NW	No Change	No Change	No Change	No Change	No Change	No Change
NC	No Change	No Change	No Change	No Change	No Change	No Change
NE	No Change	No Change	No Change	No Change	No Change	No Change
SW	No Change	No Change	No Change	No Change	No Change	No Change
SC	-0.26	-0.20	-9	-1.1	-0.70%	-0.088%
SE	+0.64	-0.18	+2	+1	+0.10%	+0.080%
EHT	-0.15	No Change	+3	No Change	+0.20%	No Change

Dredging as a Sediment Management Practice

Dredging is done mainly to improve channel conveyance for navigational purposes, to reduce flood extent, and to guide the river to an expected course. Dredging is conducted in various rivers within the delta as a need basis. Dredging reduces sediment transport capacity of the river in the dredged sections. As total inflow of sediment flux in the system remains unchanged, the reduced sediment transport capacity in the dredged section will cause sedimentation in the dredged reaches and new dredging is required to maintain the dredged depth. Depending on the inflow sediment condition, most part of a dredged section is quickly filled. Dredging reduces the flooding extent by decreasing flood depth. If conveyance of the downstream reaches of the dredged section is inadequate, excess water from the dredged region will cause inundation. As dredging reduces flooding extent in the floodplains, the sediments which were supposed to be deposited over the floodplain are transported to the downstream reaches. These additional sediments, in addition to sediments coming from the river-bed due to increased bed shear stress in upstream and downstream reaches of dredged reaches increase the sediment concentration in the downstream

reach of the dredged sections. Dredging is an effective sediment management practice provided dredging sections are selected by considering both local impact and system impacts.

Impacts of dredging in two reaches of Brahmaputra-Jamuna and Ganges are presented in Table 9 and comparison with these dredging with Hari River dredging is presented in Table 10. These two tables can be consulted before implementing any dredging operation within the GBM delta. Locations of the dredged reaches of Brahmaputra-Jamuna & Ganges and Hari River is shown in Figure 2.

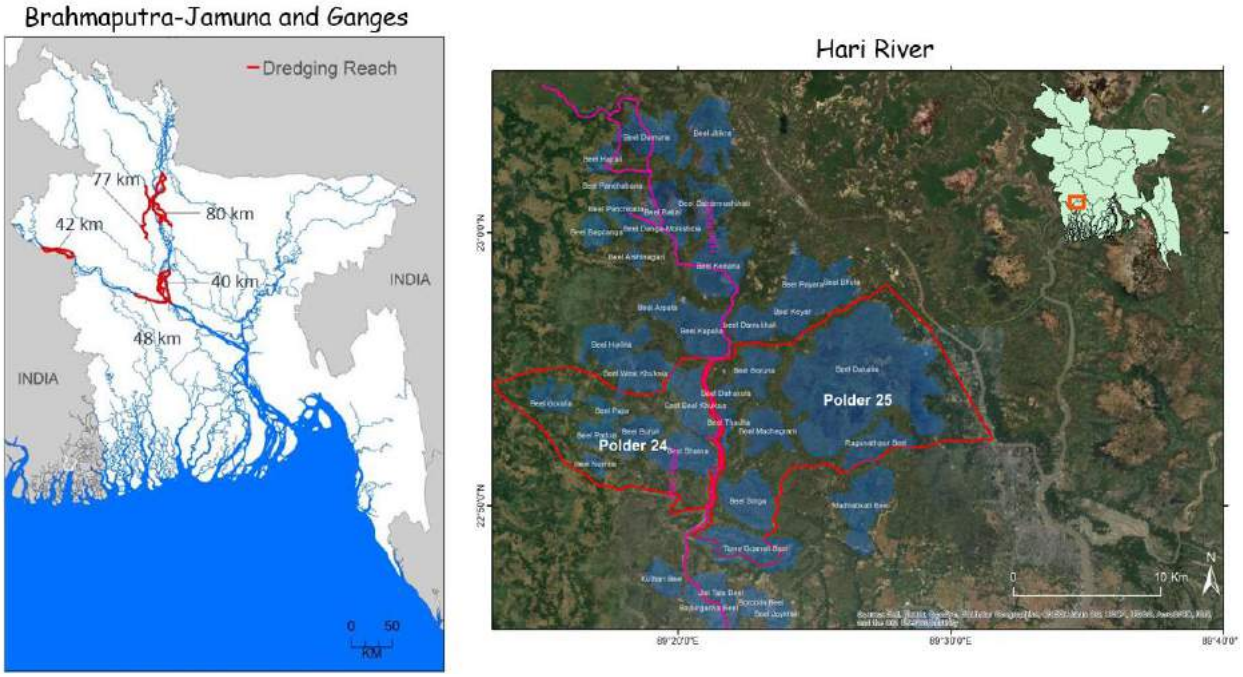

Figure 2: Locations of dredged reaches of Brahmaputra-Jamuna and Hari River. Tables 9 and 10 are prepared based on the dredging in these locations.

Table 9: Yearly distribution of change of sedimentation in the GBM delta due to dredging in the river reaches of Brahmaputra-Jamuna and Ganges as shown in Figure 2.

Change in Total Sediment Distribution					
Flood Condition	Change in Inflow Sediments (Million Ton)	Change in Delta Floodplain Sedimentation (Million Ton)	Change in Coastal Floodplain Sedimentation (Million Ton)	Change in Percent Retained in Total Delta Floodplains	Change in Percent Retained in Coastal Floodplain
Extreme	No Change	-48	+4	-3.9%	+0.3%
Change in Regional Sediment Distribution					
Region	Change in Sedimentation Depth (mm)	Change in Sedimentation Volume (Million Ton)		Change in Percentage of Sedimentation Volume w.r.t Total Inflow Sediments	
NW	-1.0	-20		-1.6%	
NC	-0.3	-33		-2.7%	
NE	No Change	No Change		No Change	
SW	+0.9	+7		+0.7%	
SC	+0.2	-4		-0.3%	
SE	+0.3	+1		-0.08%	
EHT	No Change	No Change		No Change	

Table 10: Comparison of yearly distribution change of sedimentation in the GBM delta between Brahmaputra-Jamuna & Ganges (B-J-G) and Hari River due to dredging in the locations as shown in Figure 2.

Comparison of Change in Total Sediment Distribution					
Flood Condition	Change in Inflow Sediments (Million Ton)	B-J-G Dredging Change in Delta Floodplain Sedimentation (Million Ton)	Hari River Dredging Change in Delta Floodplain Sedimentation (Million Ton)	B-J-G Dredging Change in Percent Retained in Total Delta Floodplains	Hari River Dredging Change in Percent Retained in Total Delta Floodplains
Extreme	No Change	-48	-0.2	-3.9%	-0.016%
Comparison of Change in Regional Sediment Distribution					
Region	B-J-G Dredging Change in Sedimentation Depth (mm)	Hari River Dredging Change in Sedimentation Depth (mm)	B-J-G Dredging Change in Sedimentation Volume (Million Ton)	Hari River Dredging Change in Sedimentation Volume (Million Ton)	B-J-G Dredging Change in Percentage of Sedimentation Volume w.r.t Total Inflow Sediments	Hari River Dredging Change in Percentage of Sedimentation Volume w.r.t Total Inflow Sediments
NW	-1.0	No Change	-20	No Change	-1.6%	No Change
NC	-0.3	No Change	-33	No Change	-2.7%	No Change
NE	No Change	No Change	No Change	No Change	No Change	No Change
SW	+0.9	-0.1	+7	-0.05	+0.7%	-0.004%
SC	+0.2	-0.2	-4	-0.10	-0.3%	-0.008%
SE	+0.3	-0.1	+1	-0.05	-0.08%	-0.004%
EHT	No Change	No Change	No Change	No Change	No Change	No Change

Dredging in Marine Environment

As an example of effectiveness of dredging in marine environment, navigation channel of Payra port is selected. Payra port navigation is in the Meghna Estuary region within the zone of turbidity maximum (Sarker et al., 2011) as shown in Figure 3.

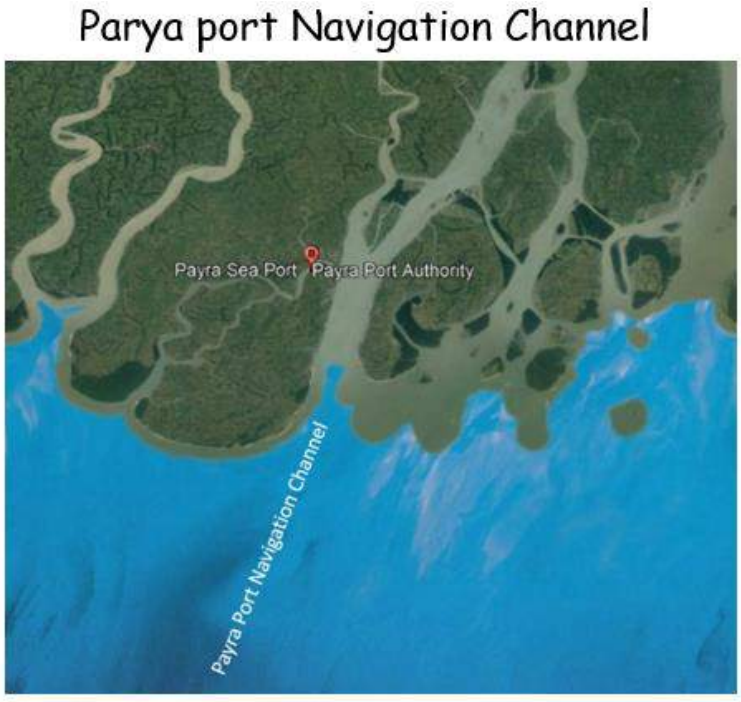

Figure 3: Location of Payra port navigation channel in the Meghna Estuary region. This zone is within the zone of turbidity maximum (Sarker et al., 2011).

Sedimentation in the dredged channel of Payra port navigation channel is significantly higher than the channel in natural state. With the increase of dredging depth, sedimentation increases at a faster rate. Sedimentation process in the Payra port channel depends on the upstream flow conditions of the riverine systems. Sediment supply from upstream depends on the sediment inflow during the monsoon. Increased sediment inflow from upstream generally increases the sedimentation in the channel. Although high flow from upstream also causes erosion of the channel at few sections. Depending on the sediment inflow pattern, sedimentation in a specific monsoon month can be higher than yearly sedimentation volume. High strength cyclone during post-monsoon season that makes landfall at the west side of the channel (for example cyclone Sidr) cause additional sedimentation in the channel. A similar but low strength cyclone (for example cyclone Amphan) during pre-monsoon season has little impact on sedimentation in the channel. The channel filling rate for different channel depths, different flow conditions, and different cyclone conditions are shown in Table 11 and Table 12.

Table 11: Channel filling rates for different channel depths and for different flow conditions.

Flow Condition	Channel Depth	Yearly Percent Filling	Yearly Maximum Sedimentation Depth
High	-6.2 mCD	50%	1.9m
	-10.5 mCD	34%	5.2m
Medium	-6.2 mCD	39%	1.7m
	-10.5 mCD	32%	4.9m
Low	-6.2 mCD	35%	1.6m
	-10.5 mCD	31%	4.8m

Table 12: Channel filling rates for different channel depths and for different cyclone conditions.

Flow Condition	Channel Depth	Change of Percent Filling due to Cyclone	Change of Maximum Depth due to Cyclone
Cyclone Sidr	-6.2 mCD	+28%	0.50m
	-10.5 mCD	+11%	0.90m
Cyclone Amphan	-6.2 mCD	+0.02%	No Change
	-10.5 mCD	No Change	No Change

References

EDP (2007), Estuary Development Programme, Technical Note EDP-01, DHV-Haskoning, May 2007.

Sarker Maminul Haque, Jakia Akter, Md Ruknul Ferdous & Fahmida Noor (2011), Sediment dispersal processes and management in coping with climate change in the Meghna Estuary, Bangladesh, IAHS Publ. 349, 2011.

Xiaoqing Yang (2003), Manual on Sediment Management and Measurement, World Meteorological Organization, Operational Hydrology Report No. 47, WMO-No. 948, Secretariat of the World Meteorological Organization – Geneva – Switzerland.